Graves' orbitopathy in a novel preclinical model

Moshkelgosha, Sajad

Awarding institution:
King's College London

Take down policy

If you believe that this document breaches copyright please contact librarypure@kcl.ac.uk providing details, and we will remove access to the work immediately and investigate your claim.

Graves' orbitopathy in a novel preclinical model

Sajad Moshkelgosha

Thesis submitted to King's College London in candidature

of

Doctor of Philosophy (PhD)

School of Medicine

London
October 2014

Abstract

Background: Graves' disease is an autoimmune disorder characterised by goitre, hyperthyroidism and Graves' orbitopathy (GO). The hyperthyroidism is caused by thyroid hypertrophy and stimulation of function, resulting from anti-TSHR antibodies. Moreover, for pathophysiology of GO, there is compelling evidence on the role of antibodies to insulin-like growth factor 1 receptor (IGF-1R). However, the precise pathogenesis of GO remains unresolved, hampered by lack of an animal model. Our laboratory has previously shown that genetic immunisation leads to development of Graves' disease. In addition, there were signs of orbital inflammation in some immune animals.

Aims: The objective of my thesis was to modify and evaluate new regimes in the genetic delivery in order to develop a preclinical GO model. The new model would be characterised immunologically and by thyroid function studies. Furthermore, procedures would be developed to characterise the orbital tissue by histopathology, to allow better anatomical evaluation in correlation with MRI. In addition, study into the pathophysiology of the disease was another objective of this project.

Results: Modifications in the immunisation scheme with hTSHR A-subunit plasmid *in vivo* electroporation were successfully established leading to induction of anti-TSHR response, thyroid dysfunction, and extensive remodelling of the orbital tissue. The orbital manifestations were characterised by infiltration of inflammatory cells including CD3$^+$/CD4$^+$ T cells, F4/80$^+$ macrophages and mast cells, as well as hypertrophy of extraorbital muscles together with accumulation of glycosaminoglycan. In addition, orbital heterogeneity was apparent, where some immune mice (10%) showed

2

extensive adipogenesis. Furthermore, other immune animals showed an intense CD3^{+} T cells infiltrate surrounding the optic nerve. A striking finding that underpins the experimental model was the *in vivo* MRI of mouse orbital region that provided a clear and quantifiable evidence of extraorbital muscle hypertrophy with orbital protrusion (proptosis). In addition, some animals exhibited congested eyelid manifestation of chemosis, which was characterised histologically as dilated orbital blood vessels and oedema. Immunisation with control plasmids failed to show any orbital pathology.

High level of antibodies to hTSHR were present in sera of animals challenged with hTSHR A-subunit plasmid with predominantly TSH blocking antibodies, which led to profound hypothyroidism. Although, these findings support TSHR as the pathogenic antigen in GO, the enigmatic role of antibodies to IGF-1R in GO remains unclear. This study describes a significant response to IGF-1R in some animals immunised with hTSHR A-subunit plasmid. A definite way to study the nature of the anti-IGF-1R antibody response following challenge with a different immunogen (hTSHR A-subunit) is by development of monoclonal antibodies to IGF-1R induced in the model, attempts of which are also reported in the thesis.

Conclusion: We successfully developed an experimental model that recapitulates orbital pathology in GO patients. The development of a new preclinical model for GO will facilitate molecular investigations into pathophysiology of the disease and evaluation of new therapeutic interventions.

Claims of Originality

The work described in this thesis was carried out in School of Medicine, King's College London. Unless stated, the experiments were carried out by the author.

The thesis entitled 'Grave's orbitopathy in a new preclinical animal model' has not been submitted for degree or other qualification at any other university.

Sajad Moshkelgosha

October 2014

Acknowledgments

Dedication

I dedicate my dissertation work to my loving parents, Dr Saied Moshkelgosha and Mrs Zeinab Kaviani whose unlimited supports made this work happen. I also, dedicate this work with very special thanks to my wife, Mrs Hadiseh Khalili for being there for me throughout the entire doctorate program.

Table of Contents

13

Figures and Tables

Abbreviations

AITD	Autoimmune thyroid disease
APC	Antigen presenting cell
BSA	Bovine serum albumin
bTSH	Bovine TSH
cAMP	Cyclic adenosine monophosphate
CTLA4	Cytotoxic T lymphocyte antigen 4
ELISA	Enzyme-linked immunosorbent assay
EOM	Extraorbital muscles
ER	Endoplasmic reticulum
EUGOGO	European group on Graves' orbitopathy
FCS	Foetal calf serum
Foxp3	Forkhead box P3
FOV	Field of view
FSE	Fast-spin-echo
GAGs	Glycosaminoglycans
GO	Grave's orbitopathy
GWAS	Genome-wide association studies
H_2O_2	Hydrogen peroxide
HBSS	Hanks' buffered saline solution
HLA	Human leukocyte antigen
hTSHR	Human thyroid-stimulating hormone receptor

IBMX	3-isobutyl-1-methylxanthine
IFN-γ	Interferon gamma
IGF-1	Insulin-like growth factor-1
IGF-1R	Insulin-like growth factor-1 receptor
Ig	Immunoglobulin
IgG	Immunoglobulin G
IHC	Immunohistochemistry
IL-1	Interleukin1
IL-6	Interleukin6
KO	knockout
LATS	Long-acting thyroid stimulator
Lumi-IGF-1	Chemiluminescent labelled IGF-1
mAb	Monoclonal Antibody
MFI	Mean fluorescence intensity
MHC	Major histocompatibility complex
mIGF-1R	mouse IFG-1R
MTC	Masson's trichrome
mTECs	Medullary thymic epithelial cells
NIS	Sodium-iodide symporter
PBS	Phosphate buffer solution
PPAR-γ	Peroxisome proliferator-activated receptor γ
PRR	Pattern recognition receptor

PTPN22	Protein tyrosine phosphatase
RAI	Radioactive iodine
rhIGF-1	Recombinant human insulin-like growth factor-1
RORγ	RAR-related orphan receptor gamma
SDS-PAGE	Sodium dodecyl sulphate polyacrylamide gel electrophoresis
STAT4	Signal transducer and activator of transcription 4
T_3	Triiodothyronine
T_4	Thyroxine
TCRs	T cell receptors
TE	Echo time
Tfh	T follicular helper
Tg	Thyroglobulin
TGF-β	Transforming growth factor beta
TNF	Tumour necrosis factor
TPO	Thyroid peroxidise
TR	Repetition time
Tregs	Regulatory T cells
TSAbs	Thyroid stimulation antibodies
TSBAbs	Thyroid stimulation blocking antibodies
TSH	Thyroid-stimulating hormone
TSHR	Thyroid-stimulating hormone receptor

Chapter One

General Introduction

1.1 Autoimmunity

The most important aspect of the immune response is to distinguish between self/host tissues and infection. However, in some cases, the immune system is inappropriately targeted to host tissues; i.e. causes autoimmunity. Generally, autoimmunity results from a failure of self-tolerance, which may lead to an imbalance between lymphocyte activation and regulation. However, it is very unlikely that self-reactive lymphocytes that have escaped central and peripheral tolerance mechanisms are able to cause autoimmunity unless activated APCs present autoantigens to those lymphocytes (Abbas et al., 2012). Two main players have been implicated in autoimmune diseases: $CD4^+$ T cells and MHC molecules. In the last few years, many studies have shed light on the emerging role of different $CD4^+$ T subsets in autoimmunity, including Tregs, Th17 cells and Th22 cells.

As mentioned earlier, regulatory T cells play a fundamental role in the suppression of self-reactive lymphocytes in the periphery. Tregs are also responsible for the regulation of the inflammatory process to prevent extensive tissue injury. There are two suppression mechanisms proposed for the action of Tregs, inhibitory cytokine release and a contact-mediated effect on APCs (Caridade et al., 2013). Regulatory T cells inhibit the ability of APCs to stimulate T cells. Tregs mediate this mechanism through the inhibition of binding of T cells and APCs by CTLA-4 (Romo-Tena et al., 2013). CTLA-4 of Tregs bind to B7 molecules which reduces the availability of B7 and prevents adequate co-stimulation required for the immune response.

In addition, regulatory T cells produce IL-10 and TGF-β, both of which inhibit immune responses (Zhou et al., 2011). TGF-β regulates the differentiation of functionally

distinct subsets of T cells. As described before, the development of peripheral FoxP3+ regulatory T cells depends on TGF-β. However, in combination with IL-1 and IL-6, TGF-β promotes the development of the Th17 subset of CD4$^+$ T cells by virtue of its ability to induce the transcription factor RORγt.

TH17 cells are activated to eliminate extracellular bacteria and fungi (Zelante et al., 2007). Moreover, Th17 cells have been implicated in the development of autoimmune diseases [reviewed in (Miossec et al., 2009, Wilke et al., 2011, Maddur et al., 2012)]. Th17 cells are characterised by the secretion of major cytokines such as IL-17A, IL-17F, and IL-22 (Liang et al., 2006). In addition to those major cytokines, Th17 cells also produce other effector cytokines, including IL-6, IL-9, IL-23, IL-26, and TNFα. Evidence suggests that Th17 cells are closely related to TH1 cells, as they may express T-bet in addition to RORγt. Th17 also induce IFN-γ in the presence of IL-12 (Basu et al., 2013) (**Fig1.1**).

Tregs and Th17 cells are two important CD4$^+$ T cell subsets, which have important roles in peripheral immune responses, so that an imbalance in their relative activities can lead to the development of tissue inflammation and autoimmune diseases (Li et al., 2007). An imbalance between Th17 cells and nTregs in rheumatoid arthritis has been described (Niu et al., 2010). However, skewed balance toward Th17 is not necessarily a fundamental part of autoimmune disease, particularly in MS (Haas et al., 2005, Feger et al., 2007, Saresella et al., 2008, Jadidi-Niaragh and Mirshafiey, 2011). Recently, other studies have focused on an unusual potency of Th17 cells, and of plasticity of Tregs. Th17 cells, in contrast to Th1 and Th2 cells, possess a tendency for developmental flexibility or plasticity (Lee et al., 2009, Murphy and Stockinger, 2010). Moreover, there is evidence in support of an early developmental overlap in Th17 and

iTregs, as both require a common developmental factor, TGF-β (Bettelli et al., 2006, Weaver et al., 2006, Mangan et al., 2006). Similarly, iTregs, but not thymically derived natural Tregs, also retain substantial developmental plasticity (**Fig1.1**).
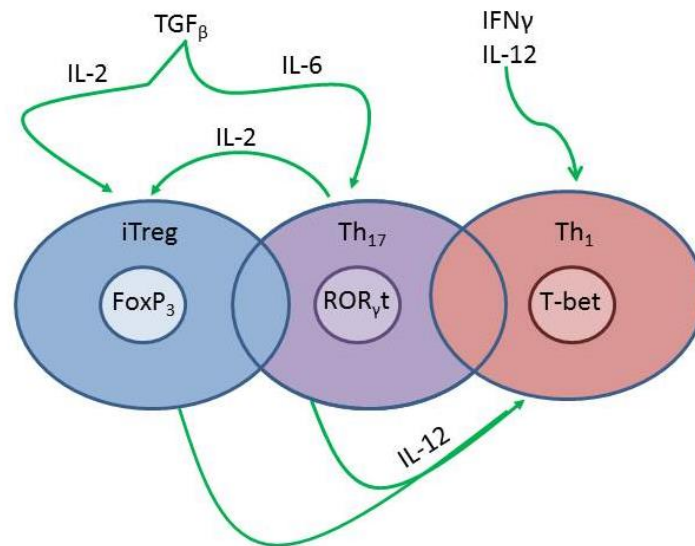
Fig 1.1 Overlap of the Th17, iTreg, and TH1 cells axes of differentiation
Developmentally, the Th17 lineage overlaps the iTreg pathway early and Th1 pathway late. Adapted from Basu et al., 2013, revised and re-drawn by applicant.

Therefore, in a new immunological perspective, Tregs and Th17 cells may be considered to orchestrate the pathogenesis of autoimmunity. While Tregs suppress the autoreactive responses in various autoimmune diseases, Th17 cells exacerbate these diseases through induction of various pro-inflammatory mediators. So the regulation of the relative activity of these cells may assign the fate of autoimmune diseases (Wright et al., 2011). More recently, it was postulated that TGF-β, retinoic acid and lipid mediators are potential mediators in establishing the balance between Tregs and Th17 cells (Haak et al., 2009, Maddur et al., 2012) (**Fig 1.2**).
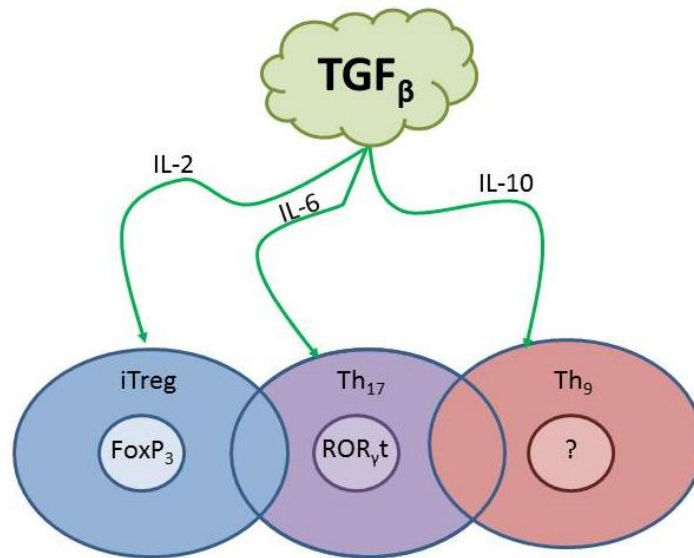
Fig 1.2 Putative model for balance regulation between Treg and Th17 cells

This model suggests that balance between Treg and Th17 cells orchestrated by TGF-β. Adapted from Jadidi-Niaragh, 2012, revised and re-drawn by applicant.

The aetiology and pathogenesis of autoimmune diseases remain largely unknown. The major factors that contribute to the development of autoimmunity are genetic susceptibility and environmental triggers. The higher concordance of autoimmune diseases in monozygotic twins, compared to dizygotic or sibling pairs, supports a role for genetic susceptibility. For instance, type 1 diabetes shows a concordance of close to 50% in monozygotic twins and 5% to 6% in dizygotic twins (Lo et al., 1991, Bach, 2002). There are similar observations in systemic lupus erythematosus (Block et al., 1975) and autoimmune thyroid disease (Brix et al., 1998, Brix et al., 2001, Brix and Hegedus, 2011, Brix et al., 2011) (it will be discussed on more detail in this chapter). However, there are differences in type 1 diabetes incidence among genetically similar groups that live in dissimilar environmental conditions, with the incidence often

following local incidence trends (Bach, 2002). Thus, autoimmune diseases are characterised as complex or multifactorial disease (Selmi et al., 2012).

Most autoimmune diseases are complex polygenic traits, in which affected individuals inherit multiple genetic polymorphisms that contribute to disease susceptibility (Stankov et al., 2013). Some of these polymorphisms are genes representing the susceptibility alleles shared amongst different, clinically unrelated autoimmune diseases, such as MHC (Tsai and Santamaria, 2013), STAT4 (Glas et al., 2010, Ji et al., 2010) and IL-12A receptor (Bossini-Castillo et al., 2012, Zhang et al., 2012). Other loci are associated with particular diseases, suggesting that they may affect organ damage. The technique of genome-wide association studies has greatly extended the analysis of the genetic basis of complex diseases, and we now know of many genes that are associated with autoimmune diseases (Barrett et al., 2009). Among the genes that are associated with autoimmunity, the strongest associations are with MHC genes. In fact, in many autoimmune diseases, the MHC locus alone contributes half or more of the genetic susceptibility. However, the mechanisms underlying the association of particular MHC alleles with various autoimmune diseases are still not clear. Amongst the non-MHC genes associated with autoimmunity, the protein tyrosine phosphatase PTPN22 is associated with several autoimmune diseases such as rheumatoid arthritis, type 1 diabetes, autoimmune thyroiditis, and systemic lupus erythematosus (Fousteri et al., 2013).

Evidence continues to accumulate supporting a role for the environment in autoimmunity (Hemminki et al., 2010, Selmi et al., 2012, Miller et al., 2012). Among environmental factors implicated, the most important factor is infection (Root-Bernstein and Fairweather, 2014). A number of theories have been proposed to

explain how infections could cause autoimmune diseases. These include exposure of the immune system to a cryptic antigen, epitope spread, molecular mimicry and bystander effect (Rose, 2012, Getts et al., 2013, Mangalam et al., 2013, Rigante et al., 2014). The theory of cryptic antigen is one of the oldest theories explaining the role of infection in autoimmunity. It is based on the idea that self reactive antigens are "cryptic" the checkpoints of central and peripheral tolerance. Thus, infection triggers to release the cryptic antigens. Epitope spreading is an alternative to the cryptic antigen theory. The epitope spread theory originated following observations of changes in the major epitopes recognised during progression of autoimmune disease (Lehmann et al., 1992). Epitope spread occurs as part of the normal immune response to infections. Initially, in encountering to infection, the immune system reacts to a dominant epitope, but when it later re-encounters the same pathogen, it produces an immune response against different epitopes of the pathogen, so that the immune system improves its ability to clear the pathogen.

The idea that molecular mimicry could drive autoimmunity originated after the observation of close sequence homology between microbial and human proteins (Fujinami et al., 1983). Over the last three decades, experimental evidence demonstrated cross-reactivity between pathogens and self antigens (Cunningham, 2012, Christen et al., 2012, Smyk et al., 2012) . However, a mechanism involving molecular mimicry in the induction of autoimmunity has recently been challenged (Tandon et al., 2013, Root-Bernstein and Fairweather, 2014). Another popular theory to explain role of infection in autoimmune diseases is the "bystander effect", which proposes that proinflammatory cytokines are released by innate immune cells in response to infections, which can then activate autoreactive T lymphocytes (Owens

and Bennett, 2012). It has been suggested that the bystander effect is crucial for the induction of autoimmunity (Mangalam et al., 2013). This would explain the need for adjuvants in animal models of autoimmune disease.

An underlying assumption of most of these theories is that autoimmunity is the consequence of a defect in the immune response (Mills, 2011, Blander et al., 2012, Cusick et al., 2012). However, recent studies hypothesise that self-reactivity is part of normal regeneration and healing processes (Galli et al., 2012). A major problem in defining the connection between infection and autoimmunity is that the detection of infectious microorganisms in the individual at the time when autoimmunity develops is not easy to achieve. The lesions that result in autoimmunity are probably not due to the infectious agent itself but result from host immune responses that may be triggered or dysregulated by the microbe.

1.1 Thyroid gland

The thyroid gland is the largest endocrine gland in humans. The main function of thyroid gland is the synthesis and secretion of thyroid hormones, thyroxine (T4) and triiodothyronine (T3). Thyroid hormones regulate a wide range of normal physiological processes including metabolism, growth, development and reproduction. The gland is composed of closely packed spherical units, which are called follicles. On cross-section, follicles consisting of single layer of thyroid cells surrounding a lumen (**Fig 1.3 A**). On the apical side of thyroid follicular cells, there are numerous microvilli extended into the colloid where secretion of hormone occurs (**Fig 1.3 B**).
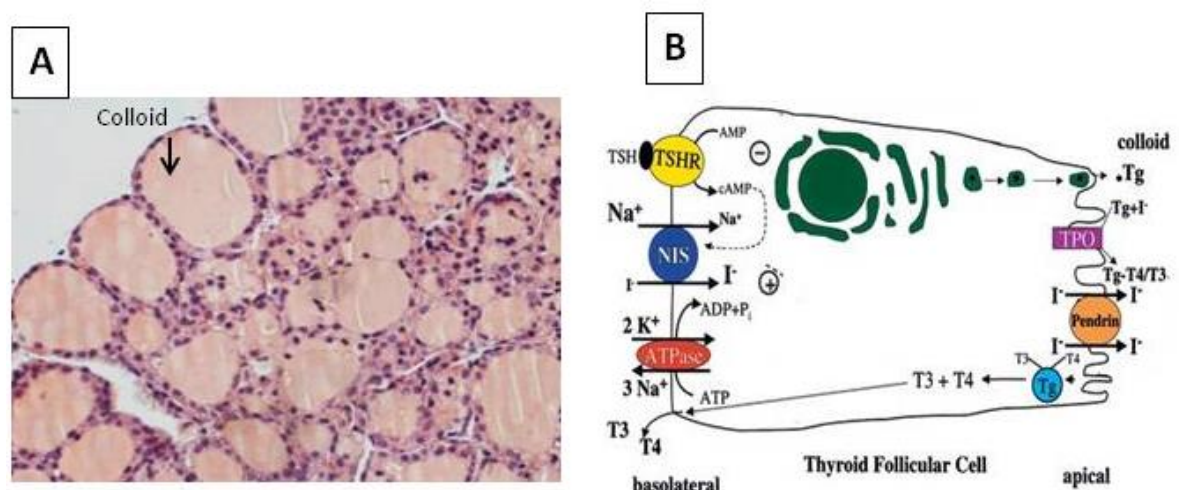
Fig 1.3 Thyroid gland and thyroid follicular cells
(A) Cross-section of thyroid gland from a normal mouse thyroid, 100X.
(B) Schematic presentation of thyroid follicular cells and hormone synthesis.

Thyroid follicular cells synthesise thyroglobulin (Tg) and thyroid peroxidase (TPO). While Tg is transported to the colloid by exocytosis, TPO is anchored to the apical cell membrane. At this membrane, oxidation of iodide occurs by iodination of tyrosyl

residues in the large Tg molecule to monoiodotyrosine and diiodotyrosine. Iodination takes place in the colloid in the presence of TPO and hydrogen peroxide (H_2O_2). One molecule of T4 is made by coupling two diiodotyrosines in the Tg molecule. In the same way T3 is made from monoiodotyrosine and diiodotyrosine. At the thyroid follicular cell apical membrane, colloid is taken up into vesicles by pinocytosis and absorbed into the cell. Lysosomes containing proteolytic enzymes then fuse with the colloid vesicle. This releases T4 and T3, as well as inactive iodotyrosines. Although T4 is the major hormone secreted by the thyroid gland, it is not biologically active. T4 is converted to the active T3 in peripheral tissues by iodothyronine deiodinases.

Iodine, which is acquired from the diet, is an indispensable component of thyroid hormones. Iodine is reduced to iodide and taken up throughout the small intestine via the mucous membrane to the blood. It is then concentrated into the thyroid follicular cell by a specialised symporter, the sodium-iodide symporter (NIS). Thyroid stimulating hormone (TSH) regulates both the synthesis and the function of NIS. Intact NIS in the basal cell membrane is a necessary for accumulation of iodine in the thyroid. Once iodide is transported across the basal membrane by NIS, it passes via passive diffusion in the cytoplasm to the apical membrane. In the apical membrane pendrin, the anion transporter, transfers iodide across the apical membrane by exchanging chloride ions for iodide to the lumen where thyroid hormone synthesis takes place.

1.1.1 Pathophysiology of thyroid gland

Thyroiditis is a common name for several inflammatory conditions in the thyroid. Thyroid autoimmune diseases and multi-nodular goitre are the most common

conditions affecting the thyroid gland. The goitre is the thyroid condition in which iodine deficiency, in most cases, leads to enlargement of the thyroid. Apart from iodine deficiency, the main cause of goitre is multi-nodular nontoxic benign goitre. Pathogenesis of goitre occurs because of focal follicle cell hyperplasia at one or more sites in the thyroid gland. Multi-nodular goitre can develop to a toxic phase from a nontoxic multi-nodular goitre. In this case, the growing goitre can be toxic with increasing synthesis and release of hormone. Although thyroid nodules are common, thyroid cancer is a relatively rare condition. A thyroid tumour is normally derived from thyroid follicle cells and in rare cases from C cells, which lie between follicle cells in the connective tissue. The most common thyroid tumours are classified into follicular adenoma, follicular cancer, papillary cancer and medullary thyroid cancer.

1.1.2 Autoimmune thyroid diseases

Intriguingly, thyroid autoimmunity consists of two opposing clinical syndromes, Hashimoto's (destructive) thyroiditis and Graves' (hyperthyroidism) disease. In this section, a brief description of thyroid autoimmunity in general is provided and more detail of each condition will be   discussed in subsequent sections.

Autoimmune thyroid disease (AITD) is the most common organ-specific autoimmune disorder affecting Caucasians in the Western world, with an incidence 1–2% of the population (Jacobson et al., 1997, Hollowell et al., 2002). The disease incidence rate is up to 10 times higher in women than men (Gessl et al., 2012). It is also postulated that there is an association between pregnancy in women and AITD. During pregnancy, the serum concentrations of thyroid Abs decrease due to generation of maternal Tregs

that maintain tolerance to the foetus (Weetman, 2010, Weetman, 2012). After delivery, there is a rebound with a transient rise in thyroid Abs. The postpartum period carries a risk of onset of Graves' disease; although, the risk might have been overestimated (Rotondi et al., 2008). Furthermore, evidence from different studies confirmed that skewed X-chromosome inactivation is associated with an increased risk of developing AITD in women (Brix et al., 2005, Simmonds et al., 2014). AITD is also an age-related condition and mostly occurs at ages between 35 and 60; although, there are cases of younger age (Hollowell et al., 2002, Gastaldi et al., 2014, Diana et al., 2014, Levy-Shraga et al., 2014).

Infiltration of the thyroid gland by lymphocytes and production of thyroid autoantibodies are the main characteristics of autoimmune thyroid diseases. In Hashimoto's thyroiditis, the immunological process is dominated by lymphocyte-mediated cell-damaging processes, leading to destruction of follicular cells. However, in Graves' disease, immune reactivity is dominated by synthesis and release of Abs. AITD is a multifactorial disease where both genetic and environmental factors contribute to pathogenesis of the disease and its severity.

Genetic factors and environmental factors associated with AITD are reviewed in (Tomer, 2010) and (Menconi et al., 2011) respectively. Twin studies confirmed that AITD has a major genetic contribution (Brix et al., 1998, Brix et al., 2001, Brix and Hegedus, 2011, Brix et al., 2011). Thus, different groups attempted to find an association between disease incidence and susceptible genes. According to recent reviews, three gene loci are most associated with autoimmune thyroid disease; (i) MHC region, (ii) CTLA4 and (iii) PTPN22 (Weetman, 2009, Brand and Gough, 2010). In addition, for hyperthyroid AITD patients, there is one thyroid specific susceptibility

locus which is TSHR (Dechairo et al., 2005, Brand et al., 2009) (these genes will be discussed in more detail in section 1.3.7). Moreover, SNP in the Kozak sequence of CD40 is associated with Graves' disease in Caucasians and Koreans, but not in Taiwanese (Jacobson and Tomer, 2007, Hsiao et al., 2008). The genetic and epigenetic factors that may increase the risk of AITD are still not fully defined (Tomer, 2014). Although, twin studies have convincingly demonstrated that genetic factors contribute about 70% to the development of AITD (Brix and Hegedus, 2012), the interaction of environmental factors with genetic susceptibility is required for breakdown of self-tolerance leading to AITD (Effraimidis and Wiersinga, 2014).

1.1.3 Hashimoto's thyroiditis

Hashimoto's thyroiditis is the most common thyroid autoimmune condition in man. The condition was first reported by Hakaru Hashimoto in 1912. Similar to many other autoimmune diseases, Hashimoto's disease is more common in females and is age-related; usually occurring after the age of 30. Hashimoto's thyroiditis is characterised by destruction of the thyroid tissues due to autoimmune reactivity. The hallmark of Hashimoto's disease is the presence of Abs against Tg and TPO in patients' sera. However, destruction of thyroid follicular cells is mostly associated with cellular rather than humoral immunity (Quaratino et al., 2004). At disease onset, secretion of thyroid hormone may be increased due to release of stored hormone from the lumen into the periphery. Subsequently, as a result of damage to thyrocytes, thyroid hormone production decreases, which leads to hypothyroidism.

As mentioned earlier, both genetic and environmental factors are considered to be involved in Hashimoto's thyroiditis. The relative contribution of each is not clearly

defined and may vary from patient to patient. High intake of iodine is demonstrated to play an important role as an environmental factor (Laurberg et al., 2010). Evidence shows that the destruction of thyroid follicles occurs by the apoptotic mechanisms (Wang et al., 2004).

1.2   Graves' disease

Clinical features of Graves' disease were described in late 1700s by Caleb Parry. However, Robert James Graves, an Irish physician, published in 1835 case reports of patients with goitre and palpitation with one case of exophthalmos. At the same time, Karl von Basedow also well documented case reports and suggested mineral water containing iodide as a treatment. Different aetiologies were described for Graves' disease until the early 19th century including cardiac, neurological and hyper-secretion from ductless glands. After the identification of TSH in the 1930s, it was suggested that an excess of TSH caused Graves' disease. However, it was demonstrated that TSH levels remain constant in Graves' patients and may be lower than in controls. Subsequently, in 1962, long-acting thyroid stimulator (LATS) was described. With the activity found in the gamma-globulin fraction of patients' sera (McKenzie, 1962). Finally, in 1964, the autoimmune basis of Graves' disease was established by describing the immunoglobulin nature of LATS (Kriss et al., 1964).

In contrast to Hashimoto's thyroiditis, patients with Graves' disease mostly show hyperthyroidism. Excessive circulating thyroid hormone leads to an increase in metabolic rate and cell proliferation. The most common symptoms of hyperthyroidism are weight loss, nervousness and heat intolerance. Hyperthyroidism results from

activating Abs to TSHR on thyroid follicular cells, which are able to emulate the actions of TSH. Stimulation of TSHR by Abs makes the negative feedback regulation inoperative, as the stimulating Abs are persistently activating the thyroid gland. In addition to hyperthyroidism and thyroid enlargement, which are the classical symptoms, the well-known complication of Graves' disease is Graves' orbitopathy (GO). There are also other rare extrathyroidal signs on Graves' patients including pretibial myxoedema, skin changes (thyroid dermopathy) and, more rarely, fingertip and nail abnormalities (thyroid acropachy) (Fatourechi, 2012).

Graves' disease is the most common cause of hyperthyroidism in areas with sufficient iodine intake, with a prevalence of about 0.5% (Brent, 2008) and incidences around 21 per 100,000 per year (Nystrom et al., 2013). Individuals of any age can be affected, but women aged 40–60 years have the highest risk of developing the disease (Weetman, 2000). Genetic factors account for up to 80% of the risk of developing Graves' disease (Brix et al., 2001, Brand and Gough, 2010); the other 20% represent environmental risk factors, such as cigarette smoking, sex hormones, pregnancy, stress, infections and adequate iodine intake (Brand and Gough, 2010, Morshed et al., 2012, Effraimidis and Wiersinga, 2014). These factors contribute to the onset of Graves' disease in genetically predisposed individuals. In different population studies, smoking is negatively associated with both progressing and *de novo* development of thyroid autoantibodies (Strieder et al., 2003, Asvold et al., 2007, Pedersen et al., 2008). Furthermore, a prospective study reported a transient increase in the risk of autoimmune thyroid disease after cessation of smoking (Effraimidis et al., 2009).

Unlike Hashimoto's thyroiditis, in Graves' disease, immune reactivity is dominated by synthesis and release of antibodies [reviewed in (Prabhakar et al., 2003, Weetman,

2003)]. The antibodies consist of two opposite types in terms of pathophysiological activities, thyroid stimulating antibodies and thyroid blocking antibodies, which will be described in more detail later. Although infiltration and inflammation occur in the thyroid in the disease, it is rare to see destruction of thyroid tissue in Graves' patients.

1.2.1 Autoantigens in thyroid autoimmunity

Although, the aetiology of autoimmune thyroid diseases remains unclear, auto-antigens and their roles in pathogenesis of the disease are well studied. TPO, Tg, and TSHR are three well-known antigens that are targeted in autoimmune thyroid disease (details of each antigen will be discussed in next sub-sections). In addition, there is contradictory evidence of autoantibodies against other receptors such as sodium-iodide symporter (NIS) and pendrin. Since 1996, when NIS was successfully cloned (Dai et al., 1996), a possible role for NIS as an autoantigen was postulated (Ajjan et al., 1998a, Ajjan et al., 1998b). NIS has only a small ectodomain attached to 13 membrane-spanning segments. Early studies detected autoantibodies in serum from patients with thyroid autoimmune disease that bound to NIS and inhibited its iodide transport function (Raspe et al., 1995, Ajjan et al., 2000). In contrast, other data did not provide support for NIS as a major autoantigen (Seissler et al., 2000, Heufelder et al., 2001). Furthermore, a potential role of pendrin, another thyroidal iodide transporter, in AITD pathogenesis has been suggested (Czarnocka, 2011), but a recent study has excluded pendrin from being a major thyroid autoantigen (Kemp et al., 2013). A recent twin study shows that, although pendrin and NIS antibodies are absent in healthy individuals, autoantibodies are rare in diseased twin pairs too (Brix et al., 2014).

1.2.2 TSH receptor (TSHR)

The TSHR is a member of G protein–coupled receptor family with 7–transmembrane domains. TSHR gene (**Fig 1.5 A**) was cloned and sequenced completely for the first time at 1989 and 1990 by three independent groups (Libert et al., 1989, Misrahi et al., 1990, Frazier et al., 1990). This 764-aa protein is coded by a single gene on chromosome 14 (14q3). TSHR is comprised of three main parts, starting with residues 1 to 21, which form the signal peptide of TSHR. There is a large glycosylated ectodomain with 394-aminoacid encoded by 9 exons. The last is the 7–transmembrane domain and cytoplasmic tail of 350 amino acids which is encoded by one single exon. The transmembrane region is comprised of 281 amino acids with the cytoplasmic region 69 residues. The highly glycosylated ectodomain consists of two smaller domains of ten leucine rich regions (LRR, amino acids 22 - 316) and the "cleavage" or the "hinge" region (amino acids 316 to 366). The LRR interacts with the ligand TSH and with antibodies to TSHR. Glycosylation is important for binding to cell surface mannose receptors on APCs and their subsequent internalisation (Stahl and Gordon, 1982), a process that markedly enhances the efficacy of T-cell responses (Engering et al., 1997). Intramolecular cleavage within the hinge region represented by residues 316-366 (Tanaka et al., 1999b) divides TSHR into two distinct subunits. The secretory region is known as the A-subunit, whilst the B-subunit consists of the rest of the protein including the hinge region, a short membrane-anchored region and the intracellular portion (**Fig 1.5 B**) (Kajita et al., 1985, Loosfelt et al., 1992, Misrahi et al., 1994). Evidence from thyrocyte culture shows that the A-subunit is shed into the medium (Couet et al., 1996b, Tanaka et al., 1999a). The mechanism of A-subunit shedding is still

uncertain. Dissociation disulfide bonds by protein disulfide isomerase (PDI) (Couet et al., 1996a) is one of the most accepted concepts. Importantly, it was demonstrated that TSHR antibodies interact with TSHR A-subunit more strongly than to holoreceptor expressed on the cell surface (Chazenbalk et al., 2002, Nagayama et al., 2002)

TSH binding to the TSHR induces proliferation in thyrocytes through a cAMP-dependent signalling pathway. However, in the absence of ligand, TSHR is still able to generate a signal (Van Sande et al., 1995). This phenomenon is called constitutive activity. Studies showed increased constitutive activity following removal of the entire TSHR ECD (Zhang et al., 2000). Consequently the TSHR ectodomain can be regarded as a tethered, inverse agonist (Vlaeminck-Guillem et al., 2002). Binding of TSH to the ectodomain converts it to surrogate ligand (Vlaeminck-Guillem et al., 2002). So, it is the ectodomain, not TSH, which directly interacts with the transmembrane domain. Development of a mAb (CS17) that can block TSHR constitutive activity has been reported (Chen et al., 2007). The recent findings of G protein–coupled receptor structure after successful crystallography has provided insight into critical aspects of binding of endogenous ligands leading to activation of the receptor (Audet and Bouvier, 2012). It is suggested the important role of particular sites of transmembrane domains in receptor signalling. Site directed mutagenesis revealed that constitutive signalling activity can be silenced by mutation in the allosteric ligand binding site (Haas et al., 2011). These allosteric binding sites are independent of TSH binding and, therefore, have evolved much greater diversity than orthosteric sites (Davies et al., 2014).
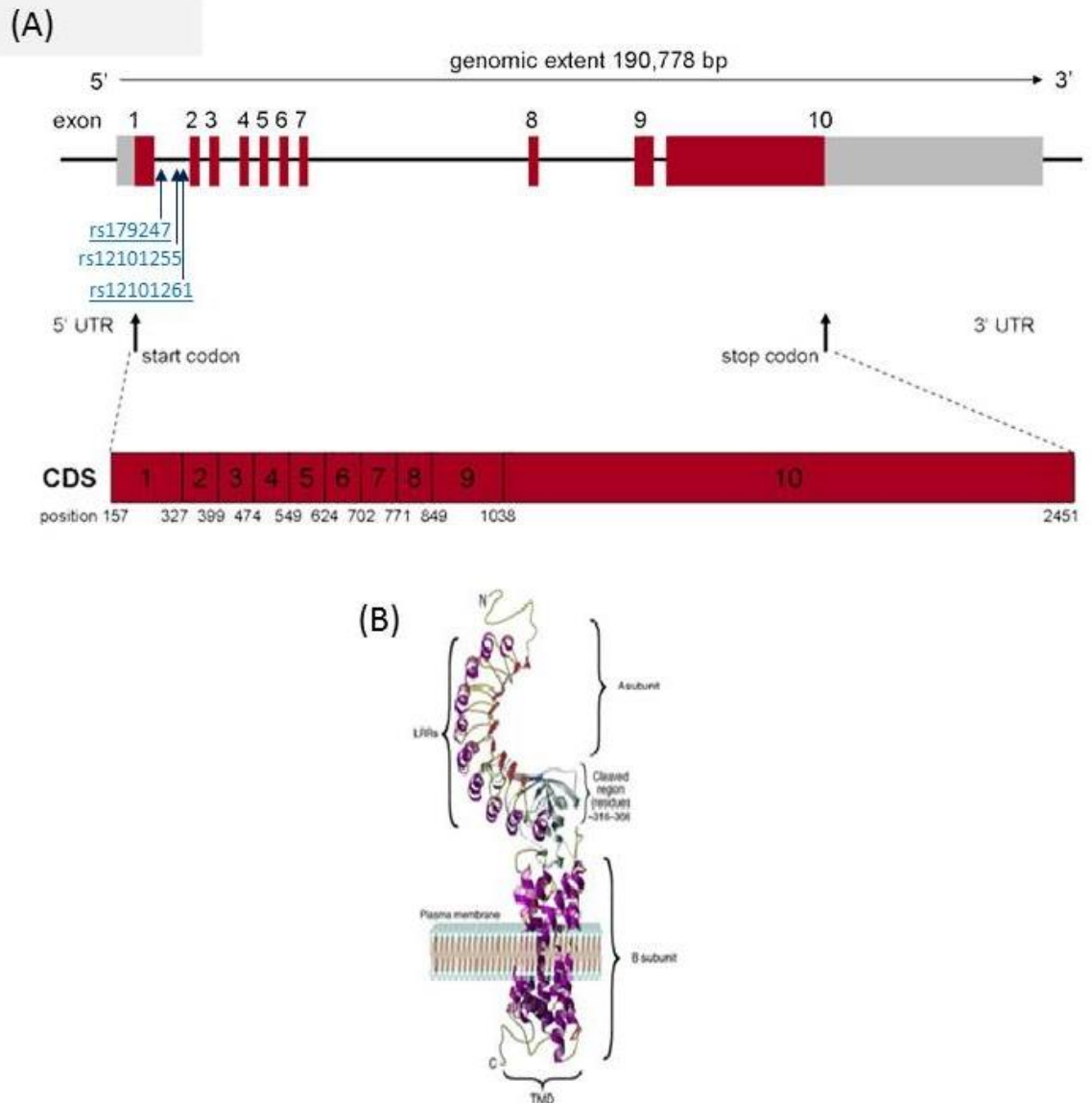
Fig 1.5 Schematic view TSHR gene and protein

(A) Structure of the TSHR gene and coding sequence (CDS). Boxes represent exons numbered 1 to 10 and proportional to length, red representing the coding sequence, grey representing untranslated regions (UTR); the horizontal line joining exons represents introns. Positions below the CDS are numbered relative to the transcription start. Three vertical arrows in Intron 1 represent common SNPs (rs179247, rs12101255, and rs12101261) susceptible for developing Graves' disease. Adapted from NCBI website, drawn by applicant.

(B) Schematic of TSHR protein showing A-subunit, B-subunit, hinge region (cleavage region), leucine rich domains (LRRs) are indicated. Adapted from Morshed et al. 2012 with permission from Prof T.F. Davies.

The TSHR is the master regulator of the thyroid gland and controls cell differentiation and hormone secretion. As TSHR affects different functions of the thyroid, it has been implicated in a wide range of thyroid diseases. Certain TSHR mutations lead to hyperthyroidism by over-activity of thyroid cells; in contrast, other deficiencies have resulted in receptor inactivation, which may lead to hypothyroidism. The TSHR is the major target auto antigen in Graves' disease, but, interestingly, thyrocytes are not the only cells that express TSHR.

1.2.3 Extrathyroidal expression of TSHR

In the late 1970s, different investigators showed functional expression of TSHR in fat cells (Mullin et al., 1976) and retrobulbar adipose tissue (Davies, 1978). It is also shown that, in the pretibial skin of patients with thyroid exophthalmos, the level of TSHR is elevated (Daumerie et al., 2002). A low abundance of TSHR in other tissues has also been reported, including skin, adrenal gland, kidney, and thymus (Endo et al., 1993, Feliciello et al., 1993, Paschke et al., 1994, Dutton et al., 1997). However, it seems that TSHR is detectable only at the transcriptional level (Paschke et al., 1994). The presence of the TSHR protein in extrathyroidal tissue, where functional receptor expression is more abundant, appears to be the cause of pathology in extrathyroidal tissue in Graves' disease. This idea is supported by findings that orbital tissue from patients suffering from an orbital condition of Graves' disease have more abundant expression of TSHR in comparison with normal orbital tissue (Bahn et al., 1998, Starkey et al., 2003).

1.2.4 Graves' disease and antibodies to TSHR

The interaction of TSHR with its ligands is very complex. For instance, TSH is considered to have more than 52 amino acids interacting with the receptor: 33 from the TSH A-subunit and 19 residues from the TSH B-subunit. Each of those binding sites contributes differently to binding affinity (Nunez Miguel et al., 2009).

The antibodies to TSHR comprise three different subtypes, thyroid stimulating antibodies (TSAbs), thyroid blocking antibodies (TSBAbs) and neutral antibodies (Rees Smith et al., 1988). TSAbs mimic the actions of TSH and initiate the TSHR signalling cascade leading to hyperthyroidism. In contrast, TSBAbs inhibit TSHR stimulation by TSH leading to a decrease of thyroid hormone secretion (Rees Smith et al., 1988, Jaume et al., 1997). The binding site for stimulating antibodies is represented by all 10 LRRs. TSH is not able to bind to a receptor that is already occupied by TSAbs (Jeffreys et al., 2002). The binding site for TSHR blocking antibodies is different to that of stimulating Abs (Oda et al., 2000); TSBAbs also inhibit the binding of TSH to receptor but are not able to induce cAMP production (**Fig 1.6 A,B**). On the other hand, neutral TSHR antibodies neither block TSH binding nor stimulate the receptor and they do not induce cAMP generation (Morshed et al., 2010).

The study of the interaction between the TSHR and antibodies in disease is difficult because of the very low serum concentration in patients (de Forteza et al., 1994, Jaume et al., 1997). However, in last decade, two major approaches have advanced our understanding of TSHR Abs and their roles in Graves' disease. These are (i) isolation of monoclonal antibodies (mAbs) to TSHR and (ii) development of animal

41

models. The isolation of TSHR mAb helped to characterise Graves' disease. The first real success was achieved in 2002 when hamster and mouse monoclonal antibodies to the TSHR were produced (Ando et al., 2002, Sanders et al., 2002, Costagliola et al., 2002). One year later, a human thyroid stimulating mAb, M22, was generated from Graves' patient samples (Sanders et al., 2003). Human blocking mAbs (5C9) have also been isolated (Sanders et al., 2005). There is also evidence that patient sera contain a mixture of stimulating and blocking type TSHR autoantibodies (Rees Smith et al., 1988, Watanabe et al., 1997). More recently, the isolation of a blocking type TSHR mAb (K1-70) and a stimulating type TSHR mAb (K1-18) from a single patient has been reported (Evans et al., 2010). The crystal structure of the A-subunit of TSHR with the Fab fragment of the human thyroid stimulating mAb M22 has been determined at 2.55Å resolution (Sanders et al., 2007) and the crystal structure of the A-subunit of TSHR with the Fab human thyroid blocking mAb, K1-70 at 1.9Å resolution (Sanders et al., 2011). Both M22 and K1-70 bind to the concave surface of the TSHR LRR; however the interactions of the K1-70 involve regions located more towards the N-terminus of the LRR than the M22. In particular, K1-70 interacts with TSHR leucine rich repeats 1 to 8, while M22 binds to entire 10 LRR (Sanders et al., 2007, Nunez Miguel et al., 2009, Sanders et al., 2011) (**Fig 1.6 A,B**).
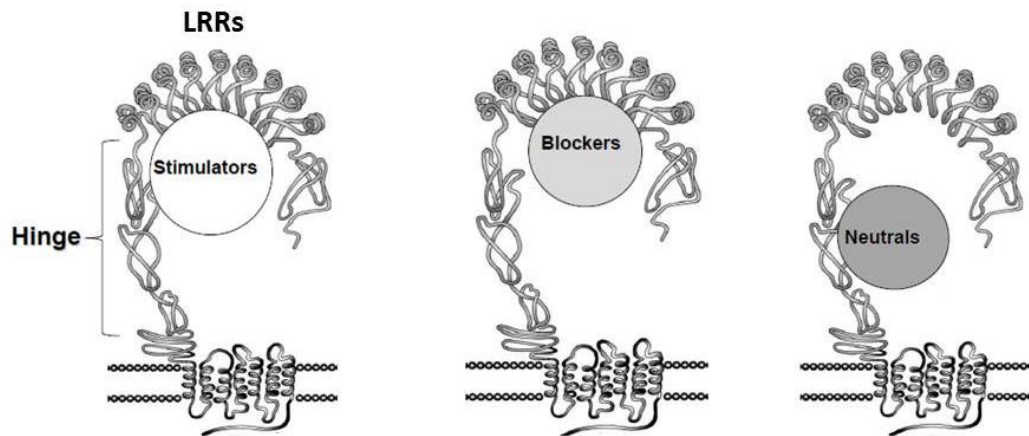
Fig 1.6 TSHR and its stimulating and blocking mAbs binding sites
Schematic view of differences in binding sites of TSAbs, TSBAbs and neutral Abs in TSHR structure. Adapted from Morshed et al. 2012 with permission from Prof T.F. Davies.

1.2.5 Genetic basis for Graves' disease

As already mentioned there is a strong evidence for genetic basis of autoimmune thyroid diseases based on the finding that 50% of patients have family members with Graves' disease and that siblings from Graves' patients have a risk of 33% to develop an autoimmune thyroid disorder themselves (Simmonds and Gough, 2004, Tomer, 2010). Moreover, concordance rates for Graves' disease are 35% in monozygotic twins, while this is only 3% in dizygotic twins (Brix et al., 2001, Brix and Hegedus, 2012). Statistical modelling estimates that 79% of the predisposition to Graves' disease is determined by genetic factors, while environmental factors account for the other 21% (Brix and Hegedus, 2012).

Moreover, current advances in genomics, including the identification of more than a million common SNPs ,the creation of accurate linkage disequilibrium maps of these SNPs and more recently genome wide association study (GWAS) approach have revealed a novel set of susceptible genes for AITD as well as other autoimmune diseases (Cho and Gregersen, 2011, Simmonds, 2013). Genetic studies, however, before existence of such advance methods have been performed using candidate gene case–control studies involving screening variants SNPs within genes of interest. These studies led to three susceptible loci; HLA class II region, CTLA-4 and PTPN22 (Simmonds and Gough, 2011). In early years of 21st century, newly developed fluorescence-based genotyping uncovered association of CD25 and HLA class I region in AITD, and TSHR in Graves' disease specifically (Simmonds and Gough, 2011). Afterwards, GWAS study in large cohorts (more than 1000 patients and 1000 controls) has been used to identify new susceptible loci (Simmonds, 2013). The first AITD GWAS was performed in 2011 in

a Chinese cohort and confirmed association of several known Graves' disease susceptibility loci including the HLA region, TSHR and CTLA4, along with two novel susceptibility loci at chromosome positions 6q27 and 4p14 (Chu et al., 2011). Another GWAS was undertaken in primarily European ancestry and supported association between PTPN22, the HLA class I region, CTLA4 and hypothyroidism (Eriksson et al., 2012). More recently, strong association for seven additional loci was also found, including MMEL1, TRIB2, LPP, BACH2, chromosome 11q21, PRICKLE1 and ITGAM by Immunochip project in the UK (Cooper et al., 2012).

Intriguingly, there are several susceptible genes in common between both AITDs, while some genes are unique for each of these pathologically distinct syndromes (**Fig 1.7**) (Tomer, 2014). Generally, the genes associated with AITDs and particularly with Graves' disease are divided into two different groups; immune response related genes and thyroid function associated genes. Here we briefly discuss the role of well-studied genes in pathology of the disease while the novel identified loci need further investigations.
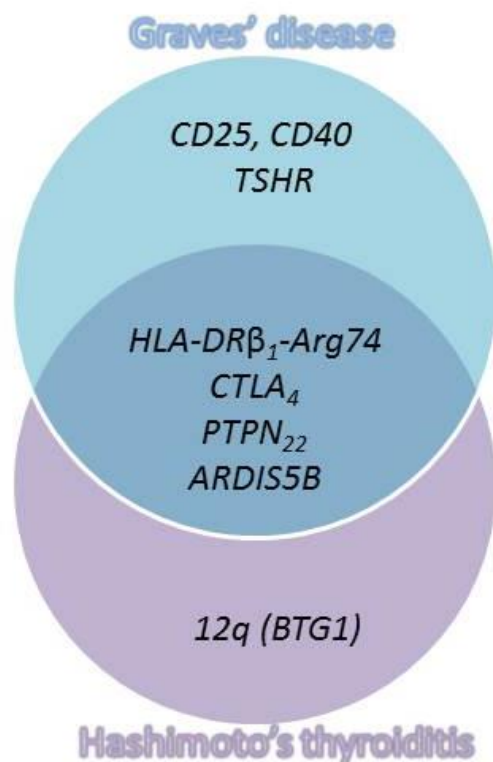
Fig 1.7 Susceptible genes for Graves' disease and Hashimoto's thyroiditis.
Adapted from Tomer, 2014, revised and re-drawn by applicant.

MHC

Early studies showed an association between MHC regions and the development of Graves' disease (Jacobson et al., 2008). MHC regions encode for the human leukocyte antigen proteins which are essential for peptide presentation to immune cells. Initially it was thought that a HLA class I molecule, HLA-B8, accounted for the association between HLA and the development of Graves' disease in Caucasians (Bech et al., 1977), but later studies revealed that this association is due to a HLA class II molecule, HLA-DR3 (Boehm et al., 1992). Recently, it is shown that HLADRβ1-Arg74 is critical for the development of AITD (Ban et al., 2004, Menconi et al., 2008). An arginine at

position 74 has similar effect on development of type 1 diabetes (Menconi et al., 2010). Interestingly, replacement of arginine by glutamine at that position plays a protective role (Menconi et al., 2008). Further studies confirmed the previous associations and also showed positive associations between Graves' disease and HLA-DRB1, HLA-DQA1 and HLA-DQB1 (Tomer, 2010, Chu et al., 2011). In contrast, some HLA molecules, such as HLA-DR5, have a protective effect on the development of Graves' disease (Uno et al., 1981).

CTLA4

The CTLA4 gene encodes the cytotoxic T-lymphocyte-associated serine esterase-4 protein that suppresses T-cell activation and subsequent T-cell driven immune responses. The CTLA-4 protein is not expressed by resting, naive T cells, but is expressed upon T-cell receptor - HLA interaction (Teft et al., 2006). The CTLA4 gene is a highly polymorphic gene and specific polymorphisms have been associated with various autoimmune diseases, such as type I diabetes mellitus, autoimmune hypothyroidism, celiac disease, primary biliary sclerosis, systemic lupus erythematosus, multiple sclerosis and rheumatoid arthritis (Gough et al., 2005). Four different polymorphisms have been consistently linked to the development of Graves' disease across different ethnic groups (Allahabadia et al., 2001, Kavvoura et al., 2007). Together with the HLA genes, polymorphisms in CTLA4 have been predicted to account for 50% of the genetic predisposition for Graves' disease (Jacobson and Tomer, 2007, Tomer, 2010).

CD40

CD40 plays a key role in the cross talk between APCs and T cells. Importantly, on B cells, CD40 provides a crucial signal for proliferating, differentiating, and switching to the production of immunoglobulin G (Jacobson and Tomer, 2007). Therefore, CD40 is among the susceptible genes for number of autoimmune diseases (Peters et al., 2009) including Graves' disease (Jacobson et al., 2007). A C/T polymorphism was detected in the Kozak sequence of the CD40 gene of which the CC genotype is strongly associated with Graves' disease (Ban et al., 2006, Kavvoura et al., 2007, Jacobson et al., 2007), although there is contradictory evidence in different ethnicity (Hsiao et al., 2008). The C-allele of this polymorphism is associated with increased CD40 expression on B cells and antigen presenting cells, which may result in higher activity of auto-reactive B cells. In addition, increased CD40 expression on thyroid cells enhances thyroid proinflammatory functions, thereby perpetuating the inflammatory process (Jacobson et al., 2005, Jacobson et al., 2007, Tomer, 2014). More recently by using a Graves' mouse model, it is shown that upregulation of CD40 accelerates disease by activating IL-6 (Huber et al., 2012).

PTPN22

The PTPN22 gene encodes the lymphoid tyrosine phosphatase (LYP) protein. This protein regulate the T cell receptor signalling pathway which is like CTLA4 has a powerful inhibitory effect (Burn et al., 2011). There is an evidence that replacement of arginine by tryptophan at amino acid 620 of LYP (R620W) due to a SNP at position 1858 in PTPN22 is associated with Graves' disease (Velaga et al., 2004). It is hypothesised that the LypR620W variant loses its function and influence on immune

responses, which increases the risk for autoimmune disease (Davies et al., 2012). However, it is shown that LypR620W allele is a gain-of function variant that suppresses T cell receptor signalling. It is unclear how such suppression predisposes to autoimmunity, but some have suggested that it allows escape from central tolerance in the thymus (Vang et al., 2007). Interestingly, this association seems specific for Caucasians and was not found in the Japanese GD population (Jacobson and Tomer, 2007).

CD25

As already mentioned in section 1.1.1, Tregs are divided into nTregs and iTregs. Natural Tregs is formed in the thymus and is characterised by the expression of the FoxP3, high expression of CD25 and low CD127 expression. They migrate peripherally and affect the immune system through the production of anti-inflammatory cytokines and direct cell-to-cell interactions, performing suppressive and protective functions. However, iTregs are formed peripherally out of $CD4^+$ $CD25^-$ stimulated by TGFβ, transforming into the phenotype $CD4^+CD25^+CTLA4^+$ and FoxP3 (Ohkura and Sakaguchi, 2010). The role of Tregs in the pathogenesis and development of different autoimmune disorders are well studied (Chavele and Ehrenstein, 2011, Szypowska et al., 2012). However, only few studies have been conducted on the role of Tregs in AITD and Graves' disease (Fountoulakis et al., 2008, Pan et al., 2009, Bossowski et al., 2013). One of the recent study by analysis of Tregs in newly diagnosed patients with Graves' disease revealed a reduction in the $CD4^+$ FoxP3 and $CD4^+$ $CD25^{high}$ lymphocytes compared to the control group (Bossowski et al., 2013). Moreover, an earlier study showed that in AITD it is not the number of Tregs but the incomplete suppressive function of Tregs in peripheral

blood that may lead to autoimmune process (Marazuela et al., 2006). Furthermore, it is confirmed that polymorphism in CD25 gene is associated with Graves' disease (Brand et al., 2007). More recently, similar study has shown the association between FoxP$_3$ polymorphism and Graves' disease in Chinese Han population (Zheng et al., 2015).

In addition to genes encoding proteins associated with immunological functions that have been mentioned above (Cooper et al., 2012), polymorphisms in genes encoding cytokines such as interleukin 1 receptor antagonist, tumour necrosis factor (TNF)-α, interferon (IFN)-γ, IL-4 as well as the vitamin D receptor gene have shown to be associated with Graves' disease (Hunt et al., 2000), but need to be validated in other and larger patient cohorts.

Thyroid-specific genes

Of the three thyroid main autoantigens which were explained in earlier sections, Tg and TSHR have been shown to be associated to Graves' disease. However, a very recent GWAS meta-analysis provided some evidence that TPO gene is also associated at least with the production of TPO Abs (Medici et al., 2014). TSHR gene association and its possible mechanisms will be discussed in detailed in this section.

TSHR

Prior to the completion of the human genome project and the availability of detailed SNP maps, three common germline SNPs of the TSHR have been examined for association with Graves' disease (Tonacchera and Pinchera, 2000). The first two SNPs are located in the extracellular domain at positions 36 and 52, an aspartic acid to

histidine substitution (D36H), and a proline to threonine substitution (P52T). The third SNP is a substitution of glutamic acid for aspartic acid (D727E) within the intracellular domain of the receptor. However, for a long time there was no consistent evidence between Graves' disease and above polymorphisms by studying in different ethnical populations (Tomer and Davies, 2003). More recent evidence suggested association between Graves' disease and non-coding (intronic) SNPs, most consistently with an intron 1 SNP **(Fig 1.5 A)** (Hiratani et al., 2005, Yin et al., 2008, Tomer and Huber, 2009, Ploski et al., 2010, Tomer et al., 2013).

In last few years, there have been different attempts to explain the mechanisms by which SNPs in intron 1 TSHR predisposes to Graves' disease (Colobran et al., 2011, Stefan et al., 2014). Two explanatory mechanisms have being postulated;

i) It is shown that the intronic TSHR polymorphisms could influence the splicing of exons coding the extracellular domain of the protein (Hiratani et al., 2005). There is also evidence indicating that the risk alleles of TSHR SNPs (rs179247 and rs12101255) were associated with production of the soluble A-subunit (Brand et al., 2009). As already mentioned in Section 1.3.4, the production of soluble form of TSHR would favour the generation of an autoimmune response to the receptor.

ii) An evidence on association between the risk alleles and a lower TSHR expression in the thymus (Colobran et al., 2011) proposed that the escape of more TSHR reactive T cells might related to induction of Graves' disease. Recent study supported this mechanism by demonstrating that IFNα interacts through chromatin remodelling with an SNP in intron 1 of the TSHR gene (rs12101261) to reduce thymic TSHR expression (Stefan et al., 2014). If TSHR expression in the thymus were reduced by the intron 1

variants, that would enable autoreactive T cells that target the TSHR to escape deletion in the thymus and thereby trigger disease later in life (Colobran et al., 2011, Tomer, 2014, Stefan et al., 2014, Gimenez-Barcons et al., 2015, Pujol-Borrell et al., 2015).

1.2.6 Environmental factors of Graves' disease

Besides genetic factors, environmental factors have also been implicated in the development of Graves' disease and are estimated to account for 21 % of the predisposition for Graves' disease (Brix et al., 2001).

Smoking

Smoking is considered as highly associated socio-environmental risk factor to Graves' disease development (Vestergaard et al., 2002). There is also evidence to show smoking increase the chance of relapse as well as its negative effects on the remission of disease following treatments (Glinoer et al., 2001, Kimball et al., 2002). A dose dependent association exists between smoking and the risk to develop Graves' disease, but effect of smoking is mostly studied in GO (Tanda et al., 2009, Hemminki et al., 2010, Miller et al., 2012, Wiersinga, 2013) which will be discussed in more detail later.

Iodine

Iodine is required for the synthesis of thyroid hormones and a clear relationship exists between the amount of iodine intake and the occurrence of thyroid hormone disorders (Brent, 2010). Hyperthyroidism is more common in geographical areas with sufficient iodine intake, in contrast to hypothyroidism which is more prevalent in iodine-deficient areas (Laurberg et al., 2000, Laurberg et al., 2010). Increased iodine

intake normally leads to a reduction of thyroid hormone production (the Wolff-Chaikoff effect). However, in patients having areas of autonomous thyroid hormone production in their thyroid, this may lead to increased thyroid hormone production (the Jod-Basedow effect). Usually these effects resolve within a few days, but when persisting, they may lead to thyroid damage and autoimmune activation (Zimmermann and Boelaert, 2015). Apart from this, iodine can also influence thyroid autoimmunity via direct activating effects on immune cells or by highly iodinated and therefore immunogenic Tg (Papanastasiou et al., 2007).

Selenium

Selenium is an important trace mineral which is an essential nutrient for selenocysteine synthesis that influences thyroid hormone production (Duntas, 2010). Selenium deficiency has been associated with an increased thyroid gland volume and echogenicity. Oxidative stress plays a role in GD and selenium also functions as an anti-oxidant. Besides this, selenium exerts other immunomodulatory effects, such as the reduction of macrophage migration and a decreased T-cell proliferation (Duntas, 2010). Selenium supplementation results in a decrease of TPO antibody levels in hypothyroid patients and improves the clinical signs of moderate-to-severe GO (Marcocci et al., 2011).

Infections

Differences in the occurrence of GD between seasons and geographic locations, together with serological evidence for recently encountered infections in Graves' patients, support the association between specific infections and Graves' disease

(Tanda et al., 2009, Hemminki et al., 2010). For instance *Borrelia burgdorferi* and especially *Yersinia enterocolitica* infections have been associated with Graves' disease. The association between Graves' disease and B. burgdorferi is merely based on shared genetic homologies between *B. burgdorferi* and thyroid antigens, but experimental evidence is limited to a case study (Benvenga et al., 2006). The association between *Y. enterocolitica* infections and Graves' disease is supported by the increased frequency of *Y. enterocolitica* specific antibodies in Graves' patients (Corapcioglu et al., 2002). Moreover, our laboratory recently provided evidence on cross-reactivity of *Y. enterocolitica* outer membrane porin with TSHR using strong stimulating TSHR mAb (Hargreaves et al., 2013). Molecular mimicry between certain *Y. enterocolitica* peptides and TSHR epitopes has been shown to play a role herein. More recently, Prof Pujol-Borrell and colleagues suggested that continuous stimulation of thymocytes by low affinity antibacterial Abs such as *Y. enterocolitica,* that cross-react with TSHR eventually leading to high affinity TSAbs (Gimenez-Barcons et al., 2015). Despite these data, a prospective studies showed that *Y. enterocolitica* antibodies are independent from the occurrence of Graves' disease and that no causal or pathogenic role exists for *Y. enterocolitica* in Graves' disease (Effraimidis et al., 2011).

Viral infections (especially hepatitis C infections) have also been associated with Graves' disease. Increased frequencies of thyroid disorders or thyroid autoantibodies were found in patients infected with the hepatitis C virus, but conflicting data exist and the exact mechanism by which hepatitis C infections contribute to Graves' disease development is still unknown (Menconi et al., 2011).

1.2.7 Autoimmune processes in Graves' disease

Genetic, environmental and endogenous factors contribute to a break-down of self tolerance and the formation of autoantibodies against the TSHR. A complex interplay between dendritic cells, Treg, T cells, B cells and thyrocytes plays a role in the development of Graves' disease (Mao et al., 2011). DCs have been found elevated in the thyroid and peripheral blood from Graves' patients (Quadbeck et al., 2002). DCs within the thyroid initially display an immature phenotype and are predominantly found in close contact with thyroid follicular cells (Quadbeck et al., 2002). Following the uptake of thyroid antigens, the DCs mature and obtain a phenotype that is well-equipped for antigen presentation. Thyroid antigen presentation to lymphocytes may take place in the thyroid and the draining lymph nodes which leads to selective activation of T cells that express a T cell receptor recognising thyroid antigens (Quadbeck et al., 2002). T cells that infiltrate the thyroid gland of Graves' patients are predominantly CD4^{+} T cells and, together with B cells, they form germinal centre-like structures (Ben-Skowronek et al., 2009). In contrast to Hashimoto's thyroiditis, Graves' disease is characterised by a mild lymphocytic infiltration and only little glandular destruction, indicating that destructive T cell mediated reactions are hardly involved in Graves' disease (Ben-Skowronek et al., 2009). Therefore, although T cells in Graves' patients recognise multiple epitopes of TSHR receptor and may target the TSHR directly (Ben-Skowronek et al., 2009), it is more likely that the DC activated T cells are involved in providing the essential co-stimulatory signals to B cells for the initiation of efficient autoantibody responses (i.e. B-cell maturation, antibody class switching) to thyroid antigens.

High expression of Fas and Fas ligand molecules on thyrocytes, DCs, and activated T cells may also contribute to Treg apoptosis. Tregs are potent suppressors of autoreactive T cell proliferation, antibody production by B cells and DC maturation (Nakamura et al., 2004). The decreased numbers of Treg in Graves' patients may lead to high numbers of naive and autoreactive T cells in the thyroid gland (Mao et al., 2011). The importance of Treg in the development of Graves' disease is further illustrated by studies showing that Treg depletion by anti-CD25 exacerbates disease onset in animal model in BALB/c and C57BL/6 mice (Saitoh et al., 2007, Nagayama et al., 2007).

Activated T cells, B cells and DC produce various inflammatory cytokines, which amplify the inflammatory process. The thyroidal inflammatory environment of Graves' disease is dominated by Th2 related cytokines, including IL-4, IL-5, IL-10 and IL-13 (Gianoukakis et al., 2008). Thyrocytes play a central role in the maintenance and perpetuation of the autoimmune inflammatory process in the thyroid gland. This is reflected by their increased expression of adhesion molecules, such as ICAM-1, and production of cytokines/chemokines including IL-6, IL-8, CCL5, IL-16 and CXCL10 (Gianoukakis et al., 2008).

1.3 Graves' orbitopathy (GO)

Various terms have been used to describe the eye complications associated with thyroid disease including "Graves' eye disease" or "Graves' ophthalmopathy", because it commonly presents in Graves' disease, however it has also been referred to as "thyroid associated eye disease" or "thyroid associated ophthalmopathy" because it

may also present in other thyroid diseases such as Hashimoto's thyroiditis (Bahn, 2010). The term "Graves' orbitopathy" will be used in this thesis in accordance with the recommendation of European group on Graves' orbitopathy (EUGOGO), a multidisciplinary consortium of clinicians who have special clinical and research interests in Graves' orbitopathy. The ,annual incidence of GO is approximately 16 per 100,000 and 3 per 100,000 for women and men, respectively (Garrity and Bahn, 2006).

Graves' orbitopathy is a common chronic extrathyroidal manifestation of Graves' disease. GO is characterised by an increase in orbital adipose tissue and an accumulation of glycosaminoglycans (GAGs); in other cases there is also expansion of extraorbital muscles causing increased volumes of orbital tissue (Weetman, 2003). Proptosis, periorbital swelling and extraocular muscle dysfunction are clinical symptoms of GO that can be explained by volume expansion in the bony orbital structure. CT scans show enlargement of both the orbital connective tissue and the extraorbital muscles in GO cases, but others appear to have involvement of only one eye (Garrity and Bahn, 2006). Some Graves' patients experience mild ocular discomfort and only 5% have severe orbitopathy; however almost all patients with Graves' disease have subclinical signs of orbitopathy (Piantanida et al., 2013, Tanda et al., 2013). The severity of proptosis is governed more by the expansion of orbital adipose and connective tissue volume than to increased muscle volume (Peyster et al., 1986). Common GO symptoms include ocular discomfort from dry eyes, excessive lacrimation, diplopia and photophobia. Patients with overt Graves' orbitopathy frequently present with upper eyelid retraction, proptosis and oedema and erythema of the periorbital tissues and conjunctivae (Bahn, 2010). In most cases, the onset of GO

is concomitant with the onset of hyperthyroidism, but orbital complication may present prior to, or following, the presentation of hyperthyroidism (Wiersinga and Bartalena, 2002).

To find the connection between thyroid and orbital tissue in Graves' orbitopathy, different theories have been proposed. A contribution of immunity was suggested a few years after the discovery of the autoimmune nature of Graves' disease (Kriss et al., 1964, Kriss et al., 1967). The detection of antibodies to striated muscle cells in sera of Graves' patients in the 1970s led to the proposal that muscle proteins express a candidate autoantigen for the disease; however antibodies to striated muscle cells have been found in many other conditions in which muscle cells are destroyed. These antibodies are now considered as a consequence, rather than cause, of inflammatory reaction in extra orbital muscles (Mizokami et al., 2004). Studies into the expression of functional TSHR on fibroblasts led to the concept of Abs to TSHR as the link between thyroidal and extrathyroidal tissue (Rotella et al., 1987). Meanwhile, evidence was emerging for a second potential autoantigen in Graves' orbitopathy. Weightman et al. showed that IGF-1R as a potential target for the "ophthalmopathy inducing antibodies" (Weightman et al., 1993). A few years later, studies demonstrated heterogeneity of orbital fibroblast which were led to understand the special role of orbital fibroblast in GO, reviewed in (Smith et al., 2002). In the last decade, investigators have attempted to understand in more detail the pathogenesis of the disease, including attempts to develop animal models (Weetman, 2000, Garrity and Bahn, 2006, Bahn, 2010, Bahn, 2013).

1.3.1 Clinical aspects of GO

An increase in orbital connective and/or muscle tissue within the relatively fixed space constraint of the bony orbit leads to protrusion of the eye and subsequent ocular symptoms such as upper eyelid retraction, oedema, erythema of the periorbital tissues and conjunctivae, proptosis and strabismus (Bahn, 2010). The expansion of orbital connective and muscle tissue is the result of a pathophysiological process to which several cell types and mediators contribute. The pathophysiology of GO includes at least one of the process below;

i)   Inflammation: infiltration of inflammatory cells into retrobulbar tissue

ii)   Excessive extracellular matrix, mostly GAGs, deposition by orbital fibroblasts

iii)   Expansion of the adipose tissue within the connective tissue of orbits.

Based on clinical features and imaging, GO patients can be classified as type I, which is associated with predominantly fat compartment enlargement, or type II, which is associated with predominantly extraorbital muscles enlargement (El-Kaissi et al., 2004, Kuriyan et al., 2013). In most GO patients however, a variable mixture of muscle enlargement (due to inflammation and deposition of extracellular matrix) and adipose expansion can be observed (Orgiazzi and Ludgate, 2010). There is evidence to show that the type of orbital pathology is age-dependant as expansion of adipose tissue has been more described in patients below 40 years of age and older individuals with GO predominantly show enlargement of extraorbital muscles (Eckstein et al., 2009). In case of extraorbital muscle enlargement, the most affected muscles are inferior rectus and medial rectus while the other muscles often not being involved (Kvetny et al.,

2006). It is also clear from orbital region imaging in GO patients that only the belly part of the muscles is affected, and the tendons remain unchanged, which differentiates GO from extraocular myositis (Orgiazzi and Ludgate, 2010). The orbital muscle enlargement is not associated with direct damage to the muscle cells, but is caused by infiltration of orbital fibroblasts and massive accumulation of ECM components between the muscle fibres (Eckstein et al., 2009).

The diagnosis of GO is usually made clinically. The signs and symptoms of active GO include lid retraction, proptosis, chemosis, diplopia, and corneal ulceration (Naik et al., 2010). In the chronic fibrotic phase, lid retraction, proptosis and restrictive strabismus are the most common findings. Patients with GO pose few diagnostic difficulties when these characteristic ocular findings occur concomitantly with the thyroid disease. However, when unilateral or inconclusive ocular features occur in the absence of objective evidence of thyroid dysfunction, GO can be difficult to diagnose (Feldon, 1990). Although the diagnosis of GO is based primarily on clinical signs and laboratory test results of thyroid dysfunction and autoimmunity, imaging studies, such as computed tomography (CT), magnetic resonance imaging (MRI), ultrasonography (US) and colour Doppler imaging (CDI), can also be extremely important in both the diagnosis and clinical or surgical and drug treatment follow-up (Kirsch et al., 2010). Imaging studies can verify possible extraocular muscle involvement as part of the diagnostic workup and may help distinguish the early acute inflammatory stage from the fibrotic, inactive stage of the disease (Kirsch et al., 2009). Finally, imaging studies of patients prone to develop dysthyroid optic neuropathy make the timely diagnosis and

treatment of the condition possible, avoiding permanent visual loss (Goncalves et al., 2012). More detail of imaging modalities will be discussed in Chapter 4.

The typical clinical course of GO in patients not receiving any treatment for their orbital complaints was first described and depicted by Rundle in 1957 (**Fig 1.8**) (Rundle, 1957). Generally, patients suffer an initial phase of progressive disease, the 'active' phase which is characterised by active inflammation, orbital infiltration of immune cells, ECM production and oedema. This may last several months and then the activity subsides and progresses to a phase of slow spontaneous recovery. This chronic 'inactive' phase may take months to years and is associated with fibrotic changes in the orbital tissue. The fibrosis is largely responsible for residual disease features such as adipose tissue expansion, proptosis and chronic eye movement dysfunction and determines the 'severity' of the disease (Perros and Kendall-Taylor, 1998). Assessment of the natural course of non-treated patients with mild-to-moderate GO revealed that 22% of patients showed definite improvement, 43% showed minor improvement 21% had no improvement and 14% got worse (Perros and Kendall-Taylor, 1998). Although GO is predominantly a mono-phasic disease; around 5% of GO patients experience a new flare up (Selva et al., 2004)
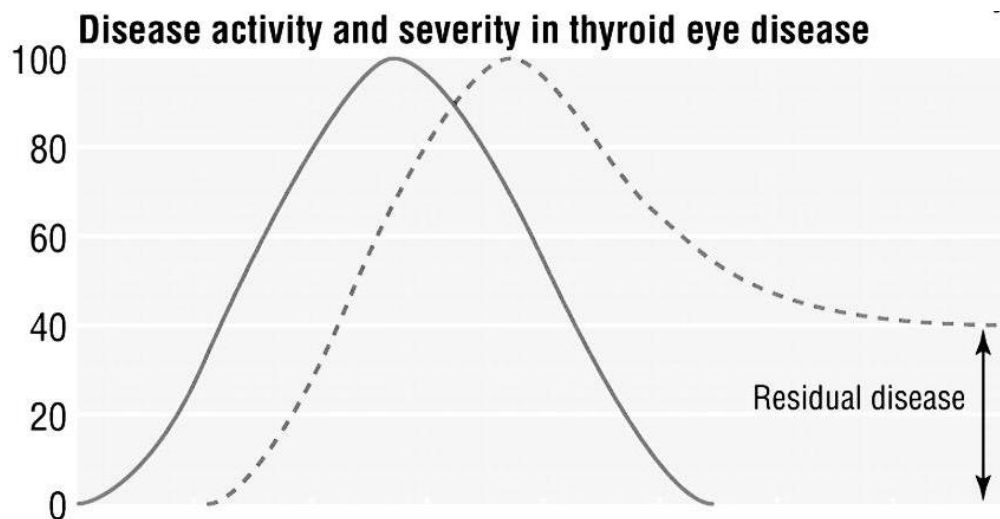
Fig 1.8 Rundle curve of activity and severity of GO.
The graph for showing the activity (line) and severity (dotted line) of orbital manifestation in GO patients known as Rundle curve. Adapted from Rundle 1957 and Cawood et al. 2004, revised and re-drawn by applicant.

1.3.2 Determinants in the development of GO

Comparable to other autoimmune diseases, women have a higher risk to develop GO. Male patients do however tend to develop a more severe phenotype. Furthermore, the prevalence increases from Asian to Caucasian to African populations (Stan and Bahn, 2010). Although this difference may be genetically determined, culture and life-style variations likely also contribute, as both endogenous (genetic factors, higher age, male sex) and exogenous (smoking, hypo/hyperthyroidism, iodine treatment) factors contribute to the development and the severity of GO (Stan and Bahn, 2010). The presence of such risk factors is important for the development of GO, as the presence of GD is necessary, but not required for the development of GO.

Genetics

Genetic predisposition for GO development largely parallels that of Graves' disease (as already discussed in section 1.3.7). The most important genes in which specific variations predispose for GO are those encoding CTLA4, PTPN22, CD40, TSHR (Eckstein et al., 2009, Stan and Bahn, 2010). In addition, HLA-DR3 is also associated with pre-disposition for GO. Several studies using relatively small patient cohorts also revealed associations between GO and polymorphisms in genes encoding Toll –like receptor-9 (Liao et al., 2010), CD86 (Liao et al., 2011) , transforming growth factor β (TGF-β), IL-4, IL-10 , IL-1α, IL-1 Ra , IL-12, IFN-γ, TNF-α (Khalilzadeh et al., 2009, Khalilzadeh et al., 2010, Anvari et al., 2010), intercellular adhesion molecule (ICAM)-1 (Kretowski et al., 2003), IL-23R (Huber et al., 2008) and IL-23 (Jia et al., 2015). The reported associations however vary considerably between different populations and the majority of these studies lack numbers and power to detect associations with the occurrence and severity of GO. Thus, although variations in genes, especially those encoding immunological factors, have been associated with GO, large and well-controlled studies are awaited before the exact contribution of specific gene variations can be determined. However, considering the clinical heterogeneity of GO, the relatively high number of genetic candidates possibly involved, and especially the low relative risks of these genetic factors, environmental factors are likely as important determinants as gene polymorphisms in GO development and its severity.

Smoking

Smoking is the best-known and strongest risk factor for the development and deterioration of GO. A dose-dependent relation exists between the number of pack years and the development of GO, with current smokers having a higher risk than past

smokers (Hegedius et al., 2004, Wiersinga, 2013). Smoking also increases the likelihood of GO progression after radioiodine therapy and delays or decreases the responsiveness to treatment with steroids or orbital irradiation (Eckstein et al., 2003). The detrimental effect of smoking on GO is considered to be due to induction of hypoxia (Cawood et al., 2007, Regensburg et al., 2011). Hypoxia modulates cytokine networks and enhances HLA-DR expression on fibroblasts (Cawood et al., 2007). Moreover, in vitro models have shown that cigarette smoke extract enhances adipogenesis and glycosaminoglycan production by orbital fibroblasts (Regensburg et al., 2011, Chng et al., 2014).

Mechanical factors

Swelling of tissues within the inextensible bony orbital cavity leads to an increase in intra orbital pressure by 3-8 folds in severe cases (Riemann et al., 1999b, Berthout et al., 2010) of normal orbital pressure, 4mmHg (Riemann et al., 1999a). This has mechanical consequences which account for most of the signs and symptoms of GO (Orgiazzi and Ludgate, 2010). Orbital tissue expansion impairs the venous and lymphatic outflow of the orbit, which subsequently leads to chemosis, periorbital oedema and inflammation. The importance of mechanical factors in the course of GO is further illustrated by the rapid alleviation of clinical symptoms after decompressive surgery (Eckstein et al., 2009). Recent *in vitro* study provided an evidence on the molecular mechanism of mechanical factors on progression of GO (Li et al., 2014). It was already shown that tissue tension modulates stem cell to differentiate particularly into adipocytes (McBeath et al., 2004). Dr Ezra and colleagues developed a novel *in vitro* 3D culture model as a platform for testing contractile effect on orbital fibroblasts. By using this 3D model environment, they also showed that orbital fibroblast from GO

patients, but not controls, can undergo adipogenesis without chemical stimulation (Li et al., 2014).

Thyroid hormone levels

Thyroid hormone level fluctuations, predominantly those associated with the occurrence of hypothyroidism after treatment of hyperthyroidism, is another important risk factor for the development of GO. Clearly, early and adequate stabilisation of thyroid hormone levels decreases the risk and severity of orbitopathy in GO patients (Kung et al., 1994). In addition, TSHR stimulating antibody levels correlate positively with the clinical activity and severity of GO and also decrease and stabilise upon adequate treatment of the hyperthyroidism (Ponto et al., 2011). This may be related to the stimulatory effects that TSHR stimulating antibodies exert on orbital fibroblasts.

1.3.3 The pathophysiology of GO

The pathophysiology of GO comprises various cells that interact with each other and as such contribute to orbital inflammation and tissue expansion, either via direct cell -cell contact or via secreted factors. The immune cells involved in GO include at least T cells, B cells, monocytes, macrophages and mast cells (Weetman et al., 1989, Kahaly et al., 1994, Pappa et al., 2000, Eckstein et al., 2004, Boschi et al., 2005, Morshed et al., 2012). Furthermore, orbital fibroblast is considered to fulfil a central role in GO (will be discussed in next section).

T cells

Infiltration of T cells into thyroid tissue (Davies et al., 1991, Davies et al., 1992) and their reactivity to TSHR antigen (Dayan et al., 1991, Martin et al., 1997) has been well described. As already mentioned above, there is also strong evidence on infiltration of T cells into orbital tissue of GO patients (Weetman et al., 1989, Kahaly et al., 1994, Pappa et al., 2000, Eckstein et al., 2004, Boschi et al., 2005). Studying retrobulbar tissue sample from GO patients revealed the cytokine and chemokine profile including very late antigen (VLA)-4, lymphocyte function associated protein (LFA-1), ICAM-I, vascular cell adhesion molecule (VCAM-1), and CD44 that play a key role in tissue inflammation (Heufelder and Bahn, 1992, Heufelder and Bahn, 1993a, Heufelder and Bahn, 1993b, Heufelder, 2000).

The TCR repertoire is restricted in early GO orbital tissue, suggesting orbit-antigen specific recruitment and expansion. T cells in orbital tissue from later stages of GO exhibit a much broader TCR repertoire (Heufelder et al., 1995a, Heufelder et al., 1995b, Heufelder et al., 1996b, Heufelder et al., 1996a). The infiltrated T cells communicate with target cells such as orbital fibroblasts via the secretion of soluble mediators (cytokines) or via direct cell-cell contact. In early GO, T cells predominantly produce Th1 cytokines (e.g. IL-2, IFN-γ, TNF-α), which shifts towards the production of Th2 cytokines (e.g. IL-4, IL-5, IL-10) in late GO (Aniszewski et al., 2000, Hiromatsu et al., 2000, Wakelkamp et al., 2003). A predominance of Th2 cytokines is linked to tissue remodelling and fibrosis (Barron and Wynn, 2011), which typically occurs during the later stages of GO.

T cells from GO patients specifically recognise autologous orbital fibroblasts (Grubeck-Loebenstein et al., 1994, Otto et al., 1996), a process in which TCR interaction with certain TSHR epitopes expressed on orbital fibroblasts can be involved (Arnold et al., 1994). In addition, cellular interaction between CD154 (also called CD40-Ligand) expressed by T cells and CD40 expressed by orbital fibroblasts also leads to production of various inflammatory mediators by orbital fibroblasts (Hwang et al., 2009, Zhao et al., 2010). This data suggests that orbital fibroblasts are prime targets of the T cell response in GO (Feldon et al., 2005, Feldon et al., 2006). Besides the effects of T cells on orbital fibroblasts, the CD40-CD154 co-stimulatory signal together with HLA class II - TCR interactions between B and T cells are essential to elicit a proper humoral immune response by B cells, which is evidently involved in Graves' disease and GO (Lehmann et al., 2008).

B cells

Only few B cells are present in orbital tissue from GO patients (Pappa et al., 2000, Kahaly et al., 1994). Despite this, the concomitant occurrence of GO and Graves' hyperthyroidism suggests that TSHR stimulating antibodies play an important role in the development of GO. This is further supported by the positive correlation of the clinical activity of GO with TSHR autoantibody levels and the elevated expression of TSHR in GO orbital tissues (Boschi et al., 2005, Khoo and Bahn, 2007).

Mast cells

The presence of mast cells in orbital tissues from GO patients has already been noticed for a long time (Wegelius et al., 1957). The importance of mast cells in GO is underscored by the improvement of tearing, itching and dryness of the eyes in a small

cohort of GO patients treated with the mast cell stabilising drugs montelukast and cetirizine (Lauer et al., 2008). Despite this, the exact role that mast cells fulfil in the pathophysiology of GO is largely unknown. In GO orbital tissue mast cells are mostly located in close proximity to adipocytes or fibroblasts and show features of degranulation (Boschi et al., 2005). This suggests that they might regulate orbital fibroblast and adipocyte activity. So far, however, only a limited number of in vitro studies explored the effect of mast cells on orbital fibroblast behaviour. These studies revealed that mast cells stimulate the production of hyaluronan and prostaglandin E2 (PGE2) by orbital fibroblasts (Guo et al., 2010, Smith and Parikh, 1999), processes in which mast cell-derived prostaglandin D2 (PGD2) (Guo et al., 2010), and CD40 - CD154 ligation between orbital fibroblasts and mast cells are involved (Zhao et al., 2010)

The reason of the increased mast cell numbers in GO orbital tissue is unknown, but stem cell factor (SCF, a growth factor for mast cells) is increased in serum from GD patients and may facilitate mast cell accumulation (Yamada et al., 1998). Serum levels of IgE can be increased in GD patients and correlations between elevated serum IgE levels and the presence of GO have been described (Molnar et al., 1996, Sato et al., 1999). In addition to this, immunohistochemical studies revealed the presence of IgE in GO orbital tissue (Raikow et al., 1990). IgE binds FcRE on mast cells and upon interaction with antigen, FcRE cross-linking causes degranulation of mast cells (Theoharides et al., 2007). Some investigators found IgE molecules that specifically recognised TSHR in GO patients (Metcalfe et al., 2002) which may possibly be involved in regulating mast cell recruitment and degranulation in GO. Although these data

indicate an important role for mast cells in GO, further studies are required to delineate the exact contribution of mast cells to the pathophysiology of GO.

1.3.4 Roles of orbital fibroblast

Studies on patients who suffer from Graves' orbitopathy have suggested that the extraorbital muscles remain intact early in the disease (Garrity and Bahn, 2006). But intense infiltration of T lymphocytes, mast cells and more abundant macrophages in connective/preadipocyte tissue indicate that they might be the primary target tissue (Bahn, 2003). Orbital fibroblast presence in orbital connective tissue as well as surrounding the extraorbital muscles (Garrity and Bahn, 2006). It has been demonstrated that orbital fibroblast express TSH receptor at both the mRNA and protein level (Feliciello et al., 1993, Heufelder et al., 1993, Mengistu et al., 1994, Hiromatsu et al., 1996, Valyasevi et al., 1999) and more abundant so in GO patients than in controls (Bahn et al., 1998, Starkey et al., 2003, Kumar et al., 2004). Investigators also showed expression of IGF-1 receptor in orbital fibroblasts (Weightman et al., 1993). Moreover, orbital fibroblasts seem to be very special for the synthesis and regulation of hydrophilic glycosaminoglycan (Smith et al., 1991, Smith et al., 1995b) and show particularly strong responses to proinflammatory cytokines (Young et al., 1998).

Importantly, orbital fibroblasts differ from other anatomic regions in that they have high proportions of CD90^{-} (Thy-1 negative) cells, up to 35%, in comparison to other fibroblasts (Smith et al., 1995a, Koumas et al., 2002). CD90 is well-known as a classical T cell marker (Rege and Hagood, 2006). Heterogeneity of orbital fibroblasts in terms of

CD90, make them specific in response to different cytokine stimulators. CD90⁻ orbital fibroblasts differentiate into mature adipocytes (adipogenesis) when treated with peroxisome proliferator-activated receptor γ (PPAR-γ) agonists (Smith et al., 2002) as well as with cAMP-enhancing agents (Valyasevi et al., 1999, Crisp et al., 2000).

On the other hand, CD90$^+$ orbital fibroblasts, which are more abundant in extraorbital muscles, are particularly capable of producing IL-6 and prostaglandin E2 (Koumas et al., 2002). Those cells that express CD90 are not able to differentiate to adipocytes; although, they express PPAR-γ in common with CD90⁻ fibroblasts (Smith et al., 2002). CD90$^+$ orbital fibroblasts are able to differentiate to myofibroblasts instead of adipocytes (Koumas et al., 2003). The heterogeneic nature of orbital fibroblast is summarised in (**Fig 1.9**). Both subsets of orbital fibroblasts produce IL-6 after stimulation with IL-1 through the CD40 pathway. CD90$^+$ orbital fibroblasts produce higher levels of prostanoids and display higher CD40 levels than CD90⁻, whereas CD90⁻ orbital fibroblasts produce more IL-8 (Koumas et al., 2002, Hwang et al., 2009).
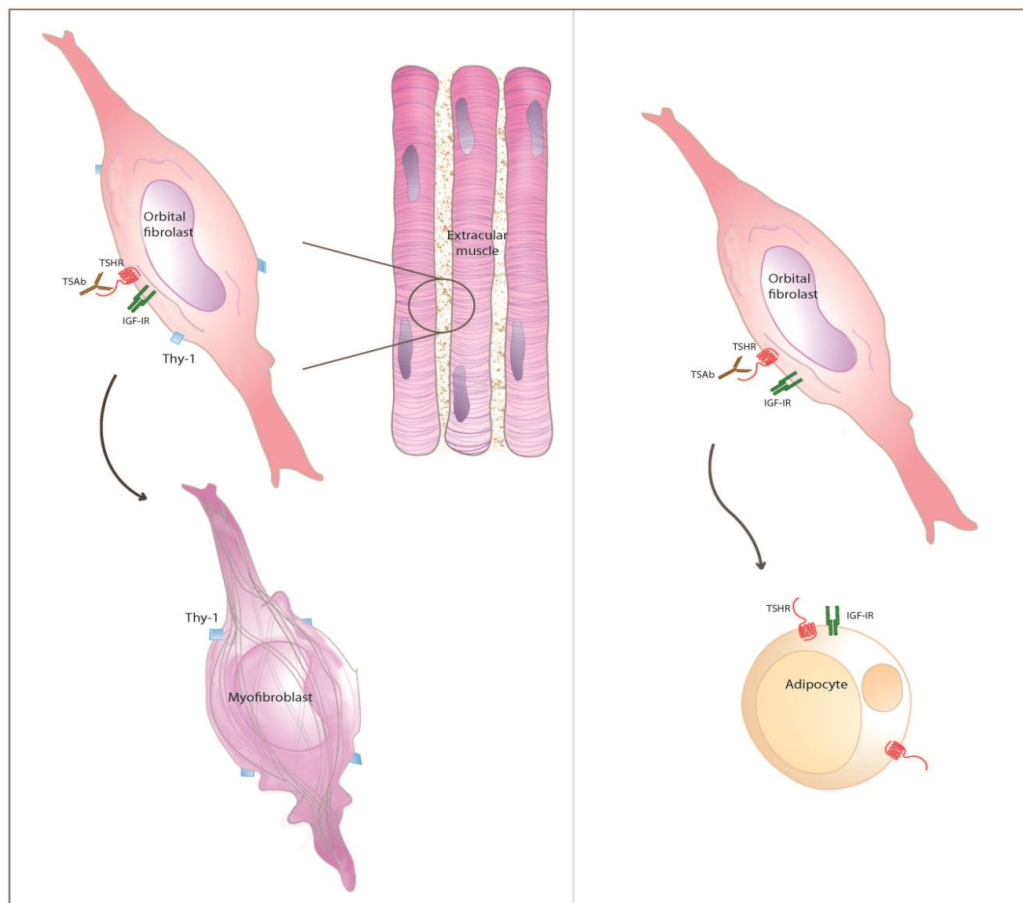
Fig 1.9 Schematic view of heterogeneity of orbital fibroblast

Orbital fibroblast expressing CD90 (Thy-1) differentiate to myofibroblasts after stimulation with TSAbs (left panel), while CD90$^-$ orbital fibroblasts undergo adipogenesis (right panel).

1.3.5 Hyaluronan production from orbital fibroblasts

Evidence shows that orbital fibroblasts are able to synthesise hydrophilic glycosaminoglycans (GAGs), particularly hyaluronan (Smith et al., 1991, Smith et al., 1995b). Hyaluronan is an abundant non-sulphated GAG and is an important component of the extracellular matrix in orbital tissue. Production of hyaluronan from orbital fibroblast occurs regardless of CD90 expression. The accumulation of

hyaluronan secreted from CD90⁻ orbital fibroblastss within the adipose tissue may cause a greater expansion of the fat compartment. Likewise, in the perimysial connective tissues within the extraorbital muscles, hyaluronan secretion from CD90^{+} cells causes an increase in the size of muscle bundles. Hyaluronan accumulation in both tissues results in the enlargement of the orbital compartment and subsequently proptosis.

Orbital fibroblasts derived from patients with GO, in contrast to orbital fibroblasts from healthy donors, respond to cytokines such as IL-1β and CD40 ligand (CD154) by increasing production of hyaluronan (Pritchard et al., 2003). Hyaluronan production is also inducible by GD-IgG in differentiated orbital fibroblast from patients who suffer GO (Smith and Hoa, 2004, van Zeijl et al., 2011), but not in non-differentiated orbital fibroblasts from GO patients (van Zeijl et al., 2010). Although, it has been proposed in some studies that hyaluronan secretion is mediated through the cAMP pathway (Imai et al., 1994, Zhang et al., 2009), evidence from a more recent study indicates that TSHR-mediated cAMP signalling is not a major pathway for hyaluronan synthesis (van Zeijl et al., 2011). In addition to TSHR-mediated signalling pathway, different groups showed that an IGF-1R blocking mAb can inhibit hyaluronan secretion from orbital fibroblast derived from GO patients (Smith and Hoa, 2004, Kumar et al., 2012).

1.3.6 Adipogenesis

Increased levels of adipogenic markers such as leptin, adiponectin and PPAR-y found in GO orbital tissue, which indicates the accumulation of adipose tissue in GO (Kumar et al., 2004, Kumar et al., 2005). Orbital fibroblasts have the capacity to differentiate into adipocytes and increase adipogenesis of orbital fibroblasts is a characteristic of GO.

Orbital fibroblasts that undergo adipogenic differentiation accumulate lipid vacuoles, and increase their TSHR expression and cytokine production (Valyasevi et al., 1999, Koumas et al., 2002). Especially Thy-1⁻ orbital fibroblasts differentiate in mature adipocytes when cultured under serum-free conditions in the presence of dexamethasone and isobutylmethylxanthine (IBMX) (Valyasevi et al., 1999, Koumas et al., 2002). Possibly, differences in the size of the Thy-1⁻ orbital fibroblast pool may be related to differences in adipose tissue expansion between GO patients (Khoo and Bahn, 2007).

Various factors stimulate adipogenic differentiation of orbital fibroblasts including IL-1β (Cawood et al., 2007), IL-6 (Jyonouchi et al., 2001), PGD2 (Guo et al., 2010) , TSH (Kumar et al., 2011) and TSHR stimulating antibodies (Kumar et al., 2010). Also the physical interaction between orbital fibroblasts and autologous T cells (Feldon et al., 2006) and cigarette smoke constituents (Cawood et al., 2007, Cawood et al., 2006) promote adipogenesis by orbital fibroblasts. Remarkably, Th1 cytokines such as TNF-α and IFNγ inhibit adipogenesis by orbital fibroblasts. (Valyasevi et al., 2001, Cawood et al., 2006). This fits in their role in early inflammation rather than in the later tissue expanding processes, although the Th2 related factor TGF-β also inhibits the adipogenesis by orbital fibroblasts (Valyasevi et al., 2001).

PPAR-γ is a nuclear transcription factor that is involved in cellular metabolism. Activation of PPAR-γ with thiazolidinediones such as pioglitazone or rosiglitazone is used as a treatment for type 2 diabetes as it increases lipid metabolism (Lehmann et al., 2008). GO patients who were treated with these drugs for type 2 diabetes sometimes encounter orbital deterioration due to PPAR-γ activation (Valyasevi et al.,

2002, Smith et al., 2002, Starkey et al., 2003). Besides their stimulating effect on adipogenesis, PPAR-γ agonists may also inhibit orbital inflammation and remodelling (Guo et al., 2011). Therefore, PPAR-y may be an important regulatory factor in GO and a well balanced PPAR-y activity may be beneficial in GO (Lehmann et al., 2008).

1.3.7 Insulin like growth factor 1 receptor (IGF-1R) as an autoantigen in GO

Insulin like growth factor receptor type 1 (IGF-1R) consists of 1368 amino acids and belongs to a family of relatively large transmembrane tyrosine kinase receptors. IGF-1R and insulin receptor (IR) have considerable similarities in their structure. IGF-1R is synthesised from a single mRNA and the translated protein is cleaved at residues 708 and 710 by furin enzyme. Two polypeptide subunits, α and β, are generated as a result of this cleavage. The α-subunit includes the extracellular domain and the β-subunit consists of a transmembrane domain, a tyrosine kinase domain and the C terminus. The α-subunit is subdivided into six protein domains as shown in (**Fig 1.10 A**). IGF-1Rα and IGF-1Rβ are linked together by disulfide bonds (**Fig 1.10 B**). The structure of the first three domains was revealed in 2001 (Ward et al., 2001) and subsequently, in 2009, the crystal structure of ECD has been resolved (Whitten et al., 2009).

The pathogenic role of IGF-1R in GO has been proposed after the following observations. A case study in 1986 demonstrated that IGF-1 expression was significantly increased in a retrobulbar biopsy specimen of GO patients in comparison to controls and also other tissues from the same GO patients (Hansson et al., 1986). They also reported the specificity of the increase in IGF-1, but not of other closely related family members such as insulin and IGF-II (Hansson, 1989). The same results

were also shown in thyroid tissue, but not specifically in Graves' disease (Minuto et al., 1989). In 1986, Kohn and colleagues showed that antibodies from Graves' patients are able to immunoprecipitate the tyrosine kinase domain of IGF-1R (Kohn et al., 1986). The results from these studies, in addition to evidence that showed an effect of IgG from GO patients in orbital fibroblast (Rotella et al., 1986) and extraorbital muscles (Perros and Kendall-Taylor, 1992), support a pathogenic role of IGF-1R antibodies in GO.
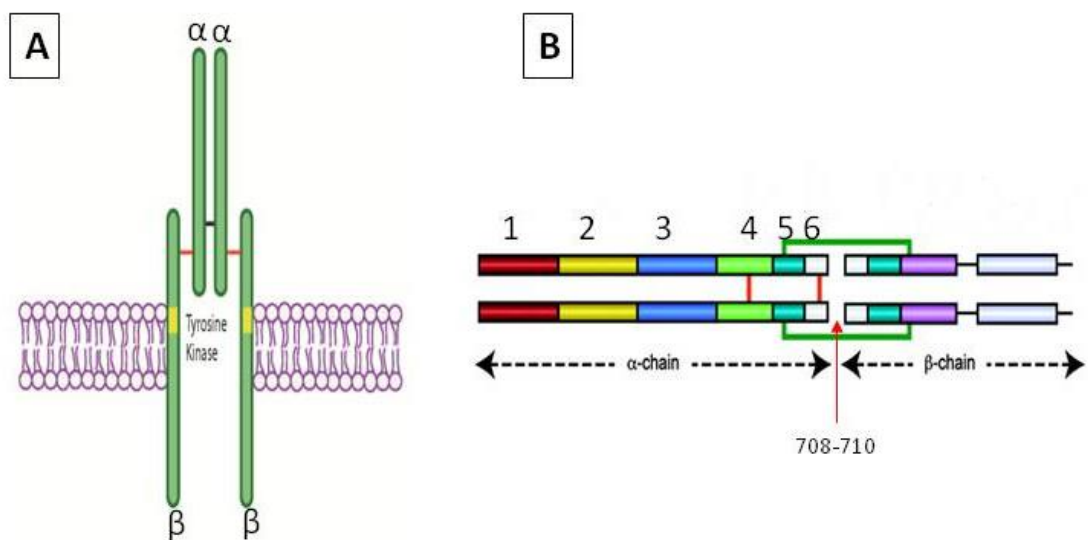
Fig 1.10 Schematic view of IGF-1R
(A) Homodimeric structure of IGF-1Rα and IGF-1Rβ subunits (including tyrosine kinase) **(B)** Six domains of IGF-1R α subunit (numbered) and IGF-1R cleavage site to yield IGF-1R α-subunit.

The key to early *in vitro* findings on association between IGF-1R and TSHR was the realisation that rat clonal thyroid epithelial cell line, FRTL-5, respond higher to TSH

stimulation in the presence of IGF-1 (Tramontano et al., 1986, Tramontano et al., 1987, Tramontano et al., 1988a, Tramontano et al., 1988b). Briefly, Ingbar's group reported that stimulation by not only TSH but also IGF-1 is able to increase cell proliferation and DNA synthesis in FRTL-5 cells (Tramontano et al., 1986, Tramontano et al., 1987). However, the results of their studies indicated that stimulation by IGF-1 does not activate cAMP signalling pathway (Tramontano et al., 1988a, Tramontano et al., 1988b).

In 1993, for the first time it was shown that immunoglobulin from Graves' patients, but not controls, can displace radiolabeled IGF-1 from orbital fibroblasts (Weightman et al., 1993). A decade later, Professor Smith's laboratory demonstrated that GD-IgG from Graves' patients can induce IL-16 and RANTES (Pritchard et al., 2003) and hyaluronan (Smith and Hoa, 2004) in orbital fibroblast. More importantly, this induction of cytokines and hyaluronan can be inhibited by a blocking IGF-1R mAb (1H7 mAb). In addition, the same group showed that TSHR and IGF-1R were co-localised on orbital fibroblast plasma membranes, forming a functional complex by both receptors (Tsui et al., 2008). More recently, functional studies in orbital fibroblasts have shown the close inter-relationship at the functional level between TSHR and IGF-1R (van Zeijl et al., 2010, van Zeijl et al., 2011). M22, the powerful stimulatory TSHR mAb, is able to enhance phosphorylation of Akt, but this is inhibited by the 1H7 mAb (Kumar et al., 2010, Kumar et al., 2012).

In other intriguing studies, IGF-1R expression has been shown in T cells and B cells derived from the peripheral blood of Graves' disease patients, whereas expression is absent in healthy controls (Douglas et al., 2007). In the T cell population, the up-regulation of IGF-1R was specifically present in the CD45RO subpopulation of memory

T cells. It was postulated that this may be related to inhibition of Fas-mediated apoptosis of T cells. On the contrary, up-regulation of IGF-1 expression by B cells in peripheral blood, orbit, and bone marrow is probably related to the increased expansion of B cells in Graves' patients (Douglas et al., 2008). IGF-1R expression by T and B cells is well documented, showing that there is no correlation of IGF-1R expression by lymphocytes and genetic determinants by twin studies (Douglas et al., 2009). The expression of IGF-1R on T and B cells will likely aggravate immune reactions directed against orbital fibroblast. The role of IGF-1R Abs in the pathogenesis of GO was reviewed in (Smith et al., 2012, Smith, 2013, Wang and Smith, 2014, Shan and Douglas, 2014) and will be discussed in more detail in Chapter 5 of this thesis.

1.3.8 Recent findings on the role of fibrocytes in GO

Although, much progress has been made over the past few years in understanding the dysregulation of the immune response in autoimmunity and the role of the target autoantigens (Kuchroo et al., 2012), the relationship between the thyroid and the extrathyroidal manifestations in GO is still not clear. Recent studies suggested the potential role for fibrocytes in GO (Smith, 2010b, Douglas et al., 2010, Gillespie et al., 2012). It is already known that fibrocytes are monocyte lineage derived from the bone marrow that have been implicated in many aspects of wound healing, tissue remodelling, and immune function (Chesney et al., 1997, Chesney et al., 1998). It is shown that fibrocytes express CXCR4, which is the receptor for CXCL12, in addition to expressing collagen-I and CD34 (Barth and Westhoff, 2007, Quan et al., 2004). The

CD34$^+$ population of fibrocytes are able to differentiate into adipocytes when treated with PPAR-γ and into myofibroblasts in response to TGF-β (Hong et al., 2007).

Fibrocytes are extremely rare (less than 1% of mononuclear cells) in the circulation of healthy individuals. However, in certain condition such as extensive tissue injury the abundance of fibrocytes increases dramatically (Moeller et al., 2009). Similarly, the laboratory of Prof Smith showed that CD34$^+$ fibrocytes are far more frequent component of PBMCs in Graves' patients compared to healthy controls (Douglas et al., 2010, Smith, 2015). In addition, numerous fibrocytes accumulate in the orbital connective tissue of patients with GO, an observation not seen in controls. Interestingly, they showed that infiltrated fibrocytes into orbital tissue of GO patients express high levels of both TSHR and IGF-1R (Douglas et al., 2010, Fernando et al., 2012). The level of surface expression of the TSHR seem to be equivalent on fibrocytes and thyroid epithelial cells and are substantially higher than those found on orbital fibroblasts (Smith, 2015). In addition, they were able to confirm functionality of expressing TSHR in fibrocytes by releasing proinflammatory cytokines in response to TSH or M22 (Gillespie et al., 2012). Besides TSHR, other thyroid-specific protein, such as Tg (Fernando et al., 2012) NIS and TPO (Fernando et al., 2014) are also expressed by cultured fibrocytes.

These data confirm that fibrocytes resemble orbital fibroblast function in Graves' patients (Koumas et al., 2002, Smith et al., 2002, Smith, 2010b, Douglas et al., 2010). Prof Smith and his colleges suggested a potential mechanism for involvement of fibrocytes in the pathogenesis of GO which is infiltration of fibrocytes with high level expression of TSHR and IGF-1R into orbital tissue and inducing cytokine secretion in response to TSHR Abs.   . Subsequently, inflammation and fibrosis process occurs. The

suggested mechanism clearly needs improvement as it does not cover how fibrocytes infiltrate into orbital tissue in the first place. Moreover, although the first paper in the potential role of fibrocytes on GO by this laboratory was published in 2010 (Douglas et al., 2010) and followed by number of publications (Fernando et al., 2012, Gillespie et al., 2012, Chen et al., 2014, Fernando et al., 2014, Smith, 2015), it is remained to be verified by an independent group.

1.3.9 Proposed model for pathogenesis of GO

Orbital fibroblasts begin to differentiate into adipocytes when activated by TSHR Abs, which results in increased expression of TSHR (Sorisky et al., 1996, Smith et al., 2002). Similarly, stimulation of IGF-1R results in the secretion of hyaluronan as well as chemokines including IL-16 and RANTES. These chemokines enhance the recruitment of activated T cells and other mononuclear immune cells into the orbit (**Fig 1.11**). Consequently, stimulation of orbital fibroblasts with cytokines, including interferon-γ and TNF, leads to increased hyaluronan secretion (Valyasevi et al., 1999, Starkey et al., 2003). Accumulation of hyaluronan between intact extraocular muscle fibres and within the orbital adipose tissues, results in enlargement of the orbital tissues. The expression of CD40 in orbital fibroblasts, and CD40 ligand (CD40L or CD154) in T cells, allows the direct interaction between orbital fibroblasts and T cells. Adipocytes and fibroblasts produce IL-6, which increases B cell maturation and increases the production of local TSHR Abs by plasma cells within the orbit (Weetman, 2000, Weetman, 2001, Weetman, 2003, Garrity and Bahn, 2006, Bahn, 2010, Iyer and Bahn, 2012, Smith et al., 2012, Smith, 2013).
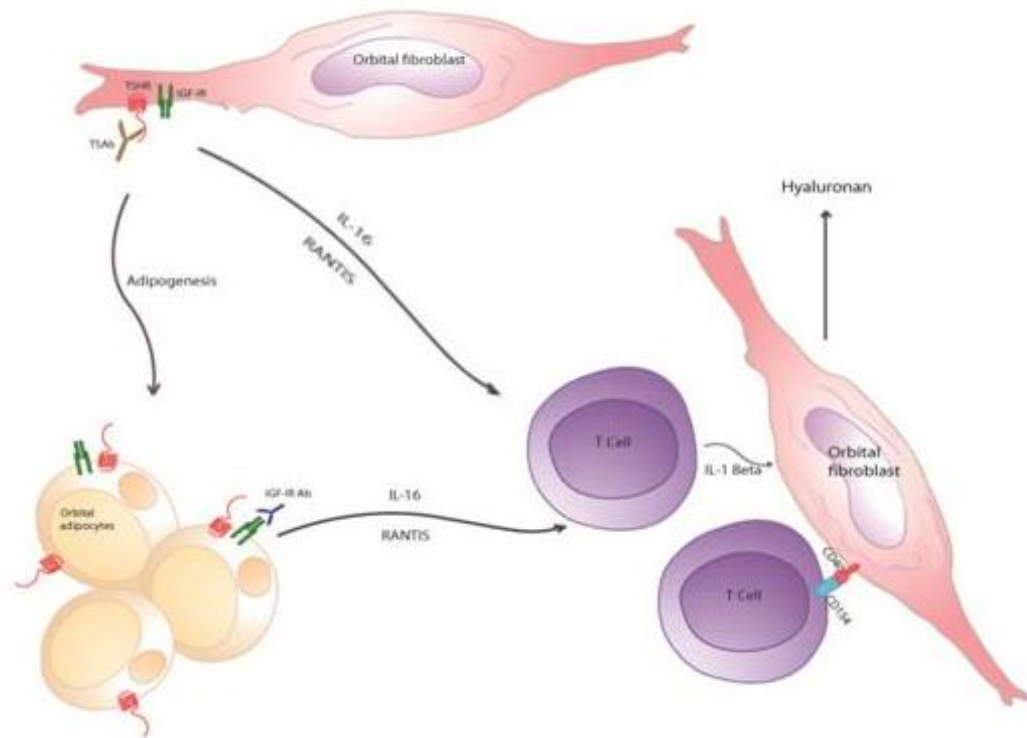
Fig 1.11 Proposed model for pathogenesis of GO

Abs to TSHR results in activation of orbital fibroblast to differentiate to adipocytes. Stimulation of the IGF-1R results in the secretion of IL-16 and RANTES which enhances recruitment of activated T cells and other mononuclear immune cells into the orbit. Figure is drawn by applicant.

1.3.10   Treatments for Graves' disease and orbital conditions

The ideal treatment for Graves' disease should restore normal thyroid function, prevent hypothyroidism and any recurrence of hyperthyroidism (Bartalena, 2013). Although various pharmacological therapies that aim to target the disease process are currently under investigation (Bahn, 2012b), management of Graves' disease still relies on three classical therapeutic methods which have been used for several decades (Hegedus, 2009): pharmacological treatment with antithyroid drugs, ^{131}I-radiotherapy and thyroidectomy (Bahn et al., 2011, Bartalena, 2013).

The approved antithyroid drugs are usually derived from thionamide components including methimazole, carbimazole and propylthiouracil. The main mode of action of this set of drugs is to decrease excess thyroid hormone synthesis by inhibiting TPO, thereby reducing the production of T3 and T4. In addition, these drugs can have immunosuppressive effects directly or through normalisation of thyroid status (Weetman, 1992, Cooper, 2005). Antithyroid drug therapy is suggested to be the first line of treatment for Graves' patients in European countries. The major drawback of antithyroid drug therapy is the high rate of recurrence, between 30% and 70% (Vitti et al., 1997, Allahabadia et al., 2000).

The ^{131}I therapy causes gradual necrosis of thyroid cells and can be effectively used for treatment of Graves' disease (Ross, 2011). The loss of functional thyroid tissue eventually results in hypothyroidism in most patients who receive ^{131}I-radiotherapy (Vaidya et al., 2008). There are two main concerns in ^{131}I-radiotherapy, apart from lifelong hypothyroidism: 1) radiation exposure and 2) possible progression or *de novo* occurrence of GO. Different studies show progression in pre-existing mild GO or even *de novo* occurrence as a result of ^{131}I-radiotherapy (Tallstedt et al., 1992, Bartalena et al., 1998, Traisk et al., 2009). The ^{131}I-radiotherapy can cause or progress orbitopathy in up to 20% of patients (Acharya et al., 2008), particularly in smokers (Traisk et al., 2009).

Surgery is a valid and definitive treatment for Graves' disease (Annerbo et al., 2012, Al-Adhami et al., 2012, Genovese et al., 2013) but is used less often than ^{131}I-radiotherapy. Patient preferences have a major role in the choice of surgery or [131]I-

radiotherapy. Thyroidectomy is clearly indicated in patients with relapse of hyperthyroidism after antithyroid drug treatment and in those with large goitres.

Similar to management of Graves' disease, the treatment for the orbital condition has also not changed for several decades (Stiebel-Kalish et al., 2009). Basically, the treatment of GO is limited to three options including local, oral or intravenous glucocorticoids, orbital radiotherapy and orbital decompression surgery. The available treatment options for GO are dependent on the severity of disease, based on the consensus statement of EUGOGO (Bartalena et al., 2008).

Glucocorticoid therapy, in comparison with other treatments, shows a favourable response in about 33–63% of patients, based on the open trials or randomised studies (Marcocci et al., 2001, Kahaly et al., 2005). Local (retrobulbar or subconjuctival) application of glucocorticoids therapy is less effective than oral form (Marcocci et al., 1987). The evidence also shows that i.v. glucocorticoids therapy is more effective than oral administration (Marcocci et al., 2001, Perros and Dickinson, 2005, Kahaly et al., 2005, Ng et al., 2005). However, i.v. glucocorticoids increase the risk of acute liver damage in association with very high cumulative doses (Weissel and Hauff, 2000, Marino et al., 2004). Glucocorticoids are the first line of treatment in patients with moderate to severe GO with active condition (Bartalena et al., 2008).

Orbital radiotherapy is shown to be effective in about 60% of GO patients by open trials (Prummel et al., 1989). It is also demonstrated that a combination of orbital radiotherapy with glucocorticoids (either orally or locally) is more effective than either treatment alone (Bartalena et al., 1983, Marcocci et al., 1991). Although, the main

concern about orbital radiotherapy is radiation exposure, studies on long-term safety are reassuring (Marquez et al., 2001, Marcocci et al., 2003, Wakelkamp et al., 2004).

Since anti-inflammatory treatment and orbital radiotherapy of GO rarely results in a complete resolution of symptoms, surgical treatment is very important for patients well-being. So the aims of surgical treatment in Graves' orbitopathy are improvement of function and appearance. Rehabilitative surgery includes orbital decompression, squint correction, lid lengthening and blepharoplasty (Eckstein et al., 2012). Surgery is usually performed in the inactive stage of disease with a minimum of 6 months of stable inactive orbitopathy (Rosen and Ben Simon, 2010). Additionally, sight-threatening GO is an indication for emergency surgery. Sight-threatening GO refers to either compressive optic neuropathy, which has to be treated immediately if there is no improvement after 2 weeks of i.v. steroid application (Bartalena et al., 2008).

A novel approach for optimal treatment of Graves' disease and its extrathyroidal complications has focused on both systemic dampening of the immune response dysregulation and antagonising excessive TSHR signalling (Bahn, 2012a). The studies on both the strategies are carried out via targeted biological agents including mAbs and small molecular ligands (SMLs). The rationale behind the targeted biological therapy is that antibody to TSHR is the key player in pathogenesis of Graves' disease (Iyer and Bahn, 2012). So, the disease can be managed by blocking or reducing the generation of pathogenic antibodies (Bahn, 2012b).

Studies showing a beneficial effect of B-cell depletion in other autoimmune diseases has led to the suggestion that B lymphocyte depletion may also be effective in patients with Graves' disease (El Fassi et al., 2006, Salvi et al., 2006). Rituximab (RTX), a

humanised chimeric mAb that targets CD20 on B cells, is one of the well-studied biological agents in Graves' disease (El Fassi et al., 2007, Salvi et al., 2007, Heemstra et al., 2008, El Fassi et al., 2009, Salvi et al., 2013). RTX inhibits the activation and differentiation of B lymphocytes by lysing these cells. More importantly, RTX also inhibits the ability of B cells to act as antigen-presenting cells and impairs T cell activation, thereby decreasing levels of both T and B cell derived cytokines. Despite the significant effect in the activity and severity of GO (Salvi et al., 2013), the high rate of side effects and poor cost-effectiveness (Hegedus et al., 2011) prohibit RTX as a standard therapeutic tool in GO. More recently, two randomised control trials of the RTX effects on GO patients have been performed, one in the USA and one in Europe. Although, two trials were designed comparable in terms of number and condition of recruited patients and RTX dosage, surprisingly the reported results completely contradict each other. The laboratory of Prof Bahn reported no additional benefit from RTX over placebo for their GO patients (Stan et al., 2015). On the other hand, Dr Salvi and his colleagues found RTX an effective disease-modifying treatment for moderate to severe GO patients (Salvi et al., 2015). The latter group mentioned slight differences in the baseline parameters of recruited patients may account for the discrepant outcome of the two studies (Salvi et al., 2015).

Furthermore, the idea of neutralising inflammation in autoimmune diseases either by blocking proinflammatory cytokines (Cho and Feldman, 2015) including anti-TNF agents (Feldmann, 2002), anti-IL-1 receptor agents (Dinarello, 2000), anti-IL-6 receptor agents (Nishimoto and Kishimoto, 2006) and anti-IL-12/ IL-23 (Teng et al., 2015) or

cellular immunity interaction (Keymeulen et al., 2005) has emerged a potential therapy in GO (Tan et al., 1996, Durrani et al., 2005, Paridaens et al., 2005).

As mentioned earlier, another potential therapy, apart from systemic dampening of the immune response, is antagonising excessive TSHR signalling. Although, the strong blocking TSHR mAbs (e.g. 5C9 mAb and 1-70 mAb) are available to compete with TSAbs for receptor binding (Sanders et al., 2008, Sanders et al., 2011), limitations to mAbs therapy include the risk of toxicity and unexpected immune reactions that have prevented their application in GO patients. Recently, the generation of small molecule ligands (SMLs) that antagonise TSHR signalling by two different laboratories tackled the limitations of mAb therapy (Neumann et al., 2011, van Zeijl et al., 2012). These high affinity and high potency molecules act as allosteric modulators of TSHR signalling without competing for extracellular ligand-binding sites (van Koppen et al., 2012). The *in vitro* studies in primary thyroid follicular cells and GO orbital fibroblasts confirmed the inhibition of TSHR signalling (van Zeijl et al., 2012, Turcu et al., 2013). In addition, an *in vivo* study in an animal model showed reduction in thyroid hormone by applying TSHR antagonist SMLs (Neumann et al., 2014), despite the criticisms of the animal model (Davies et al., 2014). Moreover, an *in vitro* study by another laboratory into PI3K inhibition in orbital fibroblast showed reduction of hyaluronan accumulation and adipogenesis (Zhang et al., 2014).

1.4   Experimental animal models

There are two types of animal models of autoimmunity used for *in vivo* studies on disease, induced models and spontaneous models. For example, non-obese diabetes

(NOD) mouse model, which develop type 1 diabetes, is very well known for spontaneous model. NOD mice that survive the onset of type 1 diabetes develop autoimmune thyroid disease characterised by thyroiditis later in life. Without immunisation, thyroiditis develops spontaneously in Biobreeding rats (Allen et al., 1986), NOD mice (Bernard et al., 1992) and NOD.H2h4 mice, only if given iodine in their drinking water. Unlike the occurrence of thyroiditis in nonhuman species, neither TSHR antibodies nor Graves' hyperthyroidism develop spontaneously in animals. Recent investigations into whether species more closely related to humans, i.e. the great apes, develop Graves' like syndromes have also proved negative (McLachlan et al., 2011, Aliesky et al., 2013). However, in last decade, a number of induced experimental models have been developed for Graves' disease, details of which are outlined below.

1.4.1 Graves' disease

As already explained, like other autoimmune diseases, one of the main approaches to define the pathogenesis of Graves' disease and Graves' orbitopathy is the development of animal models. In spite of difficulties to develop an animal model for Graves' disease, and specifically for extrathyroidal conditions, four successful animal models developed so far which will be outlined below. A number of reviews on animal models for Graves' disease have been published in the last few years (Ludgate, 2000, McLachlan et al., 2005, Nagayama, 2005, Dağdelen et al., 2009, Wiesweg et al., 2013). Although there were many attempts to develop animal models for Graves' disease (Volpe et al., 1993, Soliman et al., 1995), there were no significant successes in terms of development of reproducible animals model with high level of TSAbs until 1996

(Shimojo et al., 1996). After cloning of the human TSHR (Libert et al., 1989, Misrahi et al., 1990, Frazier et al., 1990), immunisation of mice with recombinant TSHR led to induction of TSHR antibody activity in different studies, but none demonstrated hyperthyroidism activity because of a lack of stimulating Abs (Marion et al., 1994, Wagle et al., 1994, Carayanniotis et al., 1995, Costagliola et al., 1995, Wang et al., 1998). Only one reported study, using a soluble, secreted ECD of human TSHR in female BALB/c mice, reported induction of stimulating antibodies and hyperthyroidism (Kaithamana et al., 1999), but this has not been reproduced in any other laboratory, including that of Professor Banga (Wang et al., 1998).

The first successful animal model for Graves' disease is known as Shimojo model (Shimojo et al., 1996). The rationale behind this model was based on the study in 1983 that showed induction of MHC II-expressing thyrocytes led to autoimmunity (Bottazzo et al., 1983). Thus, Shimojo and colleagues used transfected fibroblast cell lines (L-cells) that expressing both human TSHR and MHC class II antigens for injection to animals (Shimojo et al., 1996). The model relied on multiple injections of AKR/N mice because these mice have the same class I and a homologous class II to transfected fibroblasts. Disease incidence in this model was 10-15%. The following studies by same laboratory revealed more details of the model (Yamaguchi et al., 1997, Kikuoka et al., 1998). The Shimojo model was reproduced by other groups with some improvement when adjuvant is incorporated in the injection (Kita et al., 1999, McLachlan and Rapoport, 2004). Due to limitations of the model including nonspecific immune reactivity, low rate of disease incidence and lack of TSAbs (Rao et al., 2003, McLachlan and Rapoport, 2004), further studies on the model have not been reported.

Because of difficulties associated with immunisation of cells, most attention has been paid to genetic immunisation. Outbred mice were injected with plasmid vector coding the human TSHR and this led to autoimmune hyperthyroidism, but the disease incidence continued to be very low at around 15% (Costagliola et al., 1998), and not very different from that seen in the Shimojo model. Furthermore, success seemed to be restricted to outbred mice and inbred strains were resistant (Costagliola et al., 2000). Nevertheless, this model has led to the generation of monoclonal stimulating Abs against TSHR (Sanders et al., 2002, Costagliola et al., 2004). Despite of the simplicity of this model, it continues to be difficult to reproduce (Pichurin et al., 2001, Pichurin et al., 2002, Rao et al., 2003).

Nevertheless, the model was improved by immunisation of transgenic HLA-DR3 mice, lacking endogenous MHC class II, in conjunction with cytokines (IL-4 or GM-CSF) resulting in an increase in disease incidence to 30%. The increased in disease incidence was accompanied by focal lymphocytic infiltrates in the thyroid glands of some immune mice (Flynn et al., 2004).

By changing in delivery method of TSHR gene from plasmid to recombinant adenovirus in inbred mice (BALB/c), a significant improvement was achieved in terms of disease incidence (55%) and presence of TSAbs (Nagayama et al., 2002). Modification of the immunogen to a cDNA representing the TSHR A-subunit instead of full length TSHR caused an increase in the hyperthyroidism to 70% to 80%, as well as high levels of TSAbs (Chen et al., 2003). This method was also reproduced by other groups (Gilbert et al., 2006, Land et al., 2006, Mizutori et al., 2006, Wu et al., 2011, Ye et al., 2012). The major drawback of viral immunisation is that the virus has immunogenic elements that cause the immune response to be directed to nonspecific viral proteins (Veron et

al., 2012). Furthermore, the TSHR antibody declines rapidly after the last immunisation, hence long-term immunity is difficult to maintain in this model (McLachlan et al., 2012).

The next step toward development of an animal model for Graves' disease is based on the immunisation with plasmid vector containing TSHR A-subunit cDNA in conjunction with delivery by electroporation (Kaneda et al., 2007). Using electroporation to transfer TSHR A-subunit gene into the leg muscles of BALB/c mice caused induction of hyperthyroidism in 70-80% of the immune mice. Most importantly, long-term immunity to the receptor was maintained for at least 8 months after the last injection (Kaneda et al., 2007). Therefore, this model is useful also to study pathology of Graves' disease and more importantly GO. This model has been recently reproduced in our laboratory and the persistence of long term immunity to the TSHR confirmed (Zhao et al., 2011).

More recently, a new model has been developed based upon mouse TSHR immunisations (rather than human TSHR immunisations in all the models described above) and hence represents a true, *bonafide* model for autoimmune Graves' disease. The model involves the transfer of TSHR autoimmunity from TSHR knockout (KO) mice to nude mice (Nakahara et al., 2012). Briefly, wild type mice are tolerant to mouse TSHR, which is impossible to 'break' by immunisation but, TSHR knockout mice do not develop tolerance to the receptor and hence amenable to induction of an immune response to the mouse receptor. However, no hyperthyroidism is expected because these mice lack the endogenous TSHR. By adoptive transfer of splenocytes from TSHR KO mice into nude mice, 50% of recipient mice were found to have TSHR Abs which persisted for 24 weeks. However, the majority of Abs were blocking antibodies and, by

week 24, those in whom stimulating antibodies had previously been detected had a dominant blocking antibody response. Nevertheless, two novel findings were reported in this model, long lasting immunity and a small degree of orbital inflammation was reported. The model is very recent and awaits confirmation by other groups, but the fact that orbital changes were reported makes it exciting model.

1.4.2 Graves' orbitopathy

In attempts to develop GO in experimental animal model, first successful study involved the transfer of TSHR-primed splenic T cells from mice immunised with TSHR fusion proteins to naive BALB/c mice (Many et al., 1999). The orbital tissue showed dissociation of orbital muscle bundles by oedema, accompanied by accumulation of glycosaminoglycans and adipose tissue together with an inflammatory infiltrate of T and B cells and macrophages, similar to GO in man (Many et al., 1999). In a separate study by the same group, but using genetic immunisation to induce hyperthyroidism in outbred mice, scattered mast cells were also reported in the orbital muscle tissues (Costagliola et al., 2000). Importantly, the reported findings have been difficult to substantiate (Baker et al., 2005). In another study, accumulation of mast cells in orbital tissue was also reported after genetic immunisation of outbred mice with TSHR cDNA and G2s cDNA (Yamada et al., 2002). More recently, improvements in the plasmid delivery with *in vivo* muscle electroporation (Kaneda et al., 2007) has resulted in increasing transfection efficiency and induction of a strong antibody response to TSHR. Importantly, this model generates long lasting immunity (Kaneda et al., 2007, Zhao et al., 2011), which may be critical for the development of tissue pathology. In the earlier study using plasmid immunisation with electroporation technique, fibrosis in orbital

tissue were reported by histology (Zhao et al., 2011). More recently, induction of mild

orbital inflammation was also reported in the new experimental model which was

based on the transferring TSHR autoimmunity from knockout (KO) mice to nude mice

(Nakahara et al., 2012). A common feature in two recent animal models of Graves'

disease was that both the models show long-term persistence of induced immunity to

the TSHR. Thus this may be a critical feature for development of complications of

Graves' disease, such as orbital pathology (Zhao et al, 2011; Nakahara et al, 2012).

1.5 Aims of Project

Scientific advancement for understanding the pathophysiology of GO has been hampered by the lack of an animal model. The objective of my project was to tackle this issue. Our laboratory has previously shown that genetic immunisation of female BALB/c mice with hTSHR A-subunit plasmid in combination with *in vivo* muscle electroporation leads to development of Graves' disease. However, this animal model has not led to extensive remodelling in orbital tissue. Thus, we hypothesised that the modification of the genetic delivery of hTSHR A-subunit plasmid immunisation scheme will lead to orbital manifestation. We aim to develop an animal model that recapitulate orbital pathology of orbital muscle inflammation and adipogenesis to that present in GO patients.

Thus, characterisation of orbital pathology in the preclinical GO model was the main aim. The development of preclinical animal model and the histopathological procedures to characterise the orbital tissue for better anatomical evaluation of orbital muscle, adipose tissue and inflammation are described in Chapter 3. Furthermore, small animal MRI of the orbital regions to demonstrate proptosis and the assessment of orbital tissue hypertrophy are described in Chapter 4. The final results Chapter deals with studies on the IGF-1R antibodies induced in the model following immunisation with hTSHR A-subunit plasmid *in vivo* electroporation.

Chapter Two

Material and Methods

2. Material and Methods

2.1   Materials

2.1.1   Medium and cell growth supplements

All medium and cell growth supplements were purchased from PAA, unless otherwise stated.

- Ham's F12

- RPMI1640 with L-Glutamine

- DMEM low glucose (1g/L) with L-Glutamine

- Sterile Dulbecco's phosphate buffered saline without calcium and magnesium

- Geneticin (G418) sulphate solution (50 mg/ml)

- Foetal calf serum (FCS) were purchased from Invitrogen, UK, and stored at -20°C freezer. FCS prior to use was treated at 56°C for 30 minutes to inactivate complement in all experiments.

- HEPES buffer solution (1M) (Invitrogen, UK)

- Sodium pyruvate (100mM) (Invitrogen, UK)

- Cell dissociation solution (non-enzymatic) (Sigma-Aldrich, UK).

- Doma Drive Hybridoma feeder supplements (Immune systems, UK).

2.1.2   Sterile tissue culture plastic ware

Cells were cultured in sterile tissue culture flasks (25, 75 and 175 ml) and 24, 48 and 96-well plates (CELLSTAR, Greiner Bio-One, Germany) as described below.

2.1.3 Cells

Transfected cell line expressing TSHR A-subunit (GPI9-5)

Chinese hamster ovary (CHO) cells expressing the TSHR A-subunit anchored by a glycosylphosphatidylinositol (GPI) moiety, and expressing the TSHR A-subunit at an approximate density of 500,000 receptors/cell (Metcalfe et al., 2002) were donated by Dr Phillip Watson, University of Sheffield, and called GPI9-5cells. Cells were cultured in Ham's F12 medium containing 10% FCS and 0.01% PSF. Geneticin G418 added to cell culture to a final concentration of 200 µg/ml.

Transfected cell line expressing TSHR (JP09)

CHO cells express the full-length TSHR at an approximate density of 90,000 TSHR/cell and called JP09 cells, were donated by Professor G Vassart, Brussels (Perret et al., 1990). The JP09 cells were used for cAMP stimulating bioassays and the GPI9-5 cells were used in flow cytometry assays. Cells were cultured in Ham's F12 medium containing 10% FCS and 0.01% PSF. The cells in culture were supplemented with Geneticin G418 added to cell culture to a final concentration of 200 µg/ml.

Non-secretor Myeloma (X63-Ag8653) cells

Non-secretor Myeloma X63-Ag86S3 (X63) cells (Kohler and Milstein, 1975) were available in the laboratory (Ewins et al., 1992) and used for fusion with murine splenocytes to generate hybridomas. The cells were cultured in suspension in RPMI medium, supplemented with 10% FCS and 0.0 1% PSF.

Transfected cell line expressing IGF-1R (NWTB3)

The NWTB3 cells, mouse fibroblast cell line stably transfected to express hIGF-1R were kindly provided by Professor LeRoith (Mount Sinai hospital, New York, NY). The transfected cells were reported to express 410,000 receptors per cell (Blakesley et al., 1995). Cells were cultured in DMEM medium containing 10% FCS and 0.01% PSF. Geneticin G418 added to cell culture to a final concentration of 750 µg/ml.

2.1.4 IGF-1 and IGF-1R

Recombinant hIGF-1R (rhIGF-1R) is commercially available from R&D Systems (catalogue number: 391-GR). It is a recombinant protein comprising the ectodomain (α subunit) of the receptor, which has been expressed in transfected mouse myeloma cell line and then purified from tissue culture supernatants by biochemical procedures. As specified, 50 µg of freeze-dried, purified rhIGF-1R was reconstituted in 500 µl of sterile phosphate buffer solution (PBS) to achieve a concentration of 100 µg/ml. rhIGF-1R was then made into aliquots and stored at -80°C.

Chemiluminescent labelled IGF-1 (Lumi-IGF-1)

Lumi-IGF-1 was a gift from Professor Lutz Schomburg and Dr Waldemar Minich (Minich et al., 2013), (Institute for Experimental Endocrinology, Charité Campus Virchow-Klinikum, Berlin, Germany). The Charité group labelled IGF-1 with acridinium ester, which was then purified by gel filtration. Lumi-IGF-1 at a concentration of 10^8 RLU/µl in PBS/1% bovine serum albumin (BSA) was made into aliquots and stored at -80°C.

IGF-1

The ligand, IGF-1, was a gift from Ipsen Pharma (Slough, UK) kindly arranged through Dr Charles Buchanan (Consultant paediatric endocrinologist). Increlex, also known as Mecasermin, is a therapeutic preparation of recombinant human IGF-1 which is used to treat primary IGF-1 deficiency in children or adolescents presenting with short stature and growth failure (BNF, 2010). It was supplied in a vial as a 4 ml (10 mg/ml) sterile solution. For experimentation, Increlex was diluted in sterile PBS to achieve a concentration of 1mg/ml, made into aliquots and stored at -80°C.

2.1.5 Sodium dodecyl sulphate polyacrylamide gel electrophoresis (SDS-PAGE)

Reagent	Separating gel (12%)	Stacking gel (6%)
Polyacrylamide (30%)	6.4 ml	1.7 ml
Tris	4.0 ml (pH 8.8)	1.25 ml (pH 6.8)
10% ammonium persulphate (APS)	160 µl	100 µl
10% sodium dodecyl sulphate (SDS)	300 µl	100 µl
Distilled water (dH$_2$0)	5.3 ml	6.8 ml
Tetramethylethylenediamine (TEMED)	16 µl	10 µl

Table 2.1: **Reagents for separating and stacking gels**

- Precision Plus Protein Dual Colour Standards, commercially available from Bio-Rad

- Bromophenol blue

- Coomassie Brilliant Blue

- 20% methanol/10% acetic acid

2.1.6 Enzyme-linked immunosorbent assay (ELISA)

- Nunc MaxiSorp 96-well plates which have high protein-binding capacity

- Anti-mouse IgG–alkaline phosphatase(Sigma-Aldrich)

- Alkaline phosphatase yellow (pNPP) from (Sigma-Aldrich)

- 3M NaOH

- BioTek EL808 microplate reader with Gen5 1.10 software

2.1.7 Abs

- CD3, rat anti-mouse monoclonal (CD3-12), AbD Serotec, UK

- CD4, rat anti-mouse monoclonal (GK1.5),TONBO biosciences, USA

- CD8α, rat anti-mouse monoclonal (53-6.7),TONBO biosciences, USA

- F4/80, rat anti-mouse monoclonal (CI:A3-1), AbD Serotec, UK

- B220, rat anti-mouse monoclonal,(RA3-3A1/6.1), Ancell Corp, USA

- CD221 (IGF-1R), anti-human monoclonal (1H7 mAb), BioLegend, UK

2.1.8 Other materials

Ammonium molybdate, ampicillin, bovine serum albumin (BSA), $CaCl_2.2H_2O$, chloramphenicol, $CaCl_2.6H_2O$, Coomassie blue R250, $CuSO_4$, dimethyl sulphoxide (DMSO), DNase I, ethidium bromide, $FeSO_4$, glucose, H_2O_2, imidazole, KCl, $MgCl_2$, molecular biology water, Trypsin, EDTA, Triton-X-100, Tween-20, $ZnSO_4$, HEPES, isopropanol, KH_2PO_4, $MgSO_4.7H_2O$, NaAc, NaCl, $NaHCO_3$, Na_2HPO_4, NaOH, NH_4Cl, $(NH_4)_2S_2O_8$, SDS, sucrose, Tris base.

2.2 Methods

2.2.1 Human (h) TSHR A-subunit and hIGF-1Rα plasmids

Human TSHR A-subunit cDNA and IGF-1Rα cDNA were cloned pTriEx1.1 Neo vector by my predecessor, Dr Susan Zhao as described in their published report (Zhao et al., 2011). The pTriEx™-1.1 Neo is a commercial vector supplied by Novagen (**Fig 2.1**). In addition, pTriEx1.1 Neo β-Gal (Novagen, Merk, Germany) was used as a control plasmid for immunisation.
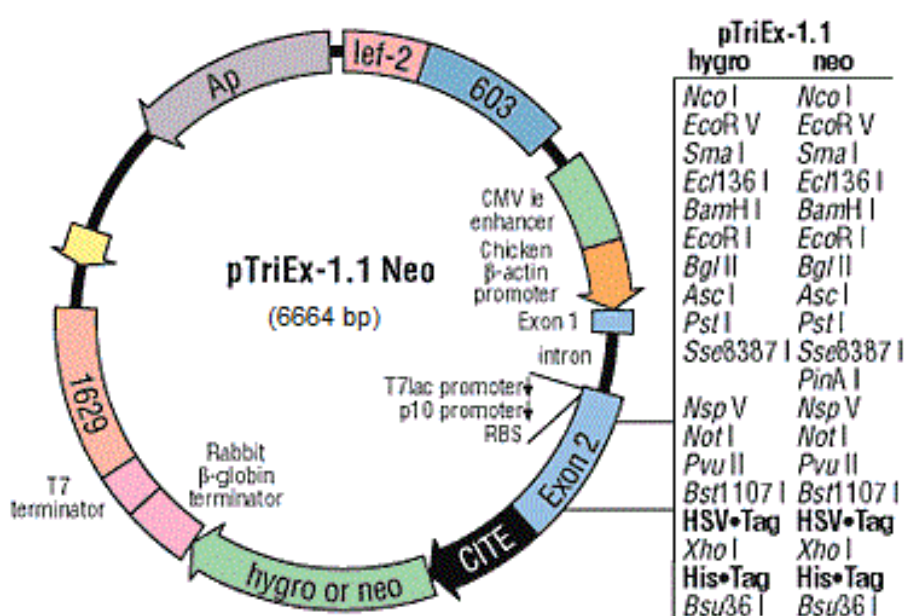
Fig 2.1 pTriEx™-1.1 Neo plasmid map.

The schematic map of the plasmid shows the size, expressing genes and restriction sites.

Procedure of cloning and primer details is briefly outlined below. Human TSHR A-subunit (amino acid residues 1–289) and human IGF1Rα subunit (741 amino acids) cDNA was cloned into BamH1 and Not1 restriction sites in pTriEx-1.1 Neo by amplification from pcDNA3.1-human TSHR plasmid using forward primer 5'-

CGCGGATCCATGAGGCGATTTCGGAGG-3' and reverse primer 5'-ATAAGAA TGCGGCCGCTTACTGATTCTTAAAAGCACAGC-3'. The cDNA was fully sequenced and then excised and subcloned into BamH1 and Not1- digested pTriEx-1.1 Neo vector.

IGF1Rα (741 amino acids) cloned into the pTriEx-1.1 Neo by using the region of 2223 bp (including the stop codon) forward primer with BamHI site: 5'- CGCGGATCCATGAAGTCTGGCTCCGG-3' and reverse primer with NotI site: 5'- ATAAGAATGCGGCCGCTTATCTCCGCTTCCTTT CAGG-3'. The cDNA was fully sequenced and then excised and subcloned into BamH1 and Not1- digested pTriEx-1.1 Neo vector.

All plasmids were grown in E. coli XL-1 Blue cells in LB medium in 2.5 litres cultures and were purified using the QIAfilter Plasmid Giga Kit (Qiagen, UK).

2.2.2 Plasmid purification

Plasmids were purified in milligram quantities for immunisation of mice. For purification, a single small colony from a freshly streaked selective plate was picked and incubated a starter culture in 10 ml LB medium containing the 10 µl ampicillin. After 8 hours incubation at 37°C in shaking incubator (for good aeration in the culture) at 250 revolutions per minute (rpm), each 2 ml of starter medium was diluted to 500 ml fresh medium. The 500 ml culture was incubated at the same condition overnight. Next day, the wet bacterial pellet was harvested and was weighed (the optimum weight range is approximately 3 g/l). The bacterial pellet was resuspended in provided reagents by Giga Kit to lyse the bacterial cells. To isolate plasmids from bacterial contents, two steps of filtration was applied with the prepared cartridges and tips. Purified plasmid concentrations were measured using a Nanodrop spectrophotometer, resuspended in sterile water, and stored at -80˚C. Purity of DNA was assessed by

agarose gel electrophoresis. Plasmids were treated either with one of the restriction enzymes, BamH1 and Not1, or both. In addition, in order to future confirmation of inserted DNA to plasmid, bands on the right size were purified from agarose gel and were treated with restriction enzymes. To examine TSHR A-subunit, the isolated cDNA from agarose gel treated with HindIII that provided two bands of 220bp and 732bp. In the same concept, IGF1Rα cDNA treated with Xho1 which cut the inserted cDNA at 277bp.

2.2.3 Assay for thyroid antibodies

2.2.3.1   Thyroid radiobinding assay (TRAK)

To study the presence of TSHR antibodies in immune mice sera, displacement radiolabelled ^{125}I-TSH from binding immobilised TSHR is assayed using commercial kits, Brahms TRAK Human RIA (Thermo Fisher Scientific, Germany). This kit is based upon capturing of recombinant human TSHR by immobilised mAb on tubes and ^{125}I-TSH (Costagliola et al., 1999). Results are presented as % inhibition of ^{125}I-TSH binding where values up to 15% (grey zone) scored as negative and greater value scored as positive. The brief technical protocol is described below.

 50 μL of mice sera were diluted 1:1 in normal human serum for saving valuable mice sera, as the kits are optimised for 100 μL of sera. All samples were diluted in normal human serum (that did not interfere with the assay) from the same donor (SM or JPB). For mAb screening, medium or purified mAbs was diluted 1:2 in normal human sera. The experiment was performed on a single basis with an appropriate number of positive and negative controls. 200 μL of Buffer 0 was added to TSHR-coated tubes,

except the first two tubes. 100 μL of each of standards was added to the appropriate tubes. Test samples were prepared by adding 50 μL mice sera to 50 μL normal human serum. 100 μL of this was added to the appropriate tube. The tubes were incubated for 2 h with shaking at room temperature. After washing twice with 2 mL wash buffer, 200 μL of ^{125}I-TSH was added to each tube and incubated for 1 h with shaking at room temperature. The tubes were washed three times with wash buffer and counted in a gamma counter for 1min (DSLaboratories). Generally, the maximum count of 200μL of tracer (^{125}I-TSH) was about 10000 cpm while the maximum binding by standard 0 (B_0) was about 10% which is around 1000 cpm. The inhibition of binding of mice sera was expressed as percentage inhibition of ^{125}I-TSH binding to TSHR. Percentage inhibition of ^{125}I-TSH binding to TSHR was calculated by dividing radioactivity of each sample by B_0 times 100. Dose response of KSAB1 has been performed for each new lot number of kits. The maximum coefficient variation (CV) of intra-assay and inter-assay precision of the kit were 9.3% and 14.1% respectively. Moreover, it was mentioned by company that the functional assay sensitivity is 1.0 ± 0.2 IU/L.

2.2.3.2   Assay for thyroid stimulating antibody

The JP09 cells, CHO (Chinese Hamster Ovary) cell line stably transfected to express full length human TSHR were kindly provided by Professor G Vassart (Belgium) (Perret et al., 1990). This cell line provides a powerful response by TSAbs. The concentration of TSHR stimulating antibodies is directly correlated to production of cAMP. Thus, TSAbs are specifically detectable by measuring of cAMP produced from JP09 cells. This assay

was well validated in our laboratory (Gilbert et al., 2006, Padoa et al., 2010, Rao et al., 2003)

JP09 cells (30,000 cells per well) were added to 96 flat well plates and left to grow for 18-20 hrs grown in F12 complete medium (37° 5% CO_2). The medium was removed and cells were gently washed with PBS, taking care not to disrupt the monolayer of cells, before adding samples and controls. Forskolin and different doses of bovine TSH and KSAB1 were used as a positive control. Mice sera samples and controls were diluted in complete Hank's buffer salt free solution (HBSS). The components of HBSS, which is a fairly complex solution, are listed in **Table 2.3**. Complete HBSS was made by adding 50 µl IBMX (50 ml IBMX + 450 µl DMSO) and 0.75g BSA to 50 ml HBSS. Mice sera samples and controls were diluted in complete HBSS as summarised in **Table 2.4**. 150 µl of prepared samples was added to each well and was incubated for 4 hours at 37^oC, 5% CO_2. After incubation time, supernatant was collected and stored in -80^oC to test the concentration of cAMP by cAMP ELISA kit (Enzo Life Sciences).

Component	Formula	M.W.	Molarity (mM)	Conc (g/L)
Calcium chloride	$CaCl_2.2H_2O$	147.0	1.26	0.185
Potassium chloride	KCl	75.0	5.33	0.400
Potassium dihydrogen orthophosphate	KH_2PO_4	136.0	0.44	0.060
Magnesium chloride	$MgCl_2$	95.2	0.50	0.048
Magnesium sulphate	$MgSO_4.7H_2O$	246.0	0.41	0.101
Sodium bicarbonate	$NaHCO_3$	84.0	4.00	0.336
Disodium hydrogen orthophosphate	Na_2HPO_4	142.0	0.30	0.043
Glucose		180.0	5.6	1.008
HEPES		238.3	20.00	4.766
Sucrose		342.3	222.0	75.991

Table 2.3 List of the chemical components in HBSS.

Briefly, 100 µL of Standards (#1 through #5) and samples were transferred to the bottom of the appropriate wells. 50 µL of the blue conjugate was added into each well except the TA and Blank wells. Afterwards, 50 µL of the provided antibody was added into each well except the Blank, TA, and NSB wells. Plate wasIncubated for 2 hours on a plate shaker (500 rpm) at room temperature before washing 3 times with 400 µL of wash buffer. 5µL of the blue conjugate was added to the TA wells. Subsequently, 200

μL of the substrate solution was added into each well and incubated for 1 hour at room temperature without shaking. In the last step, 50 μL stop solution was added into each well and read optical density (OD) at 405 nm.

	Samples	Sample volume	HBSS
1	Forskolin	15 μl	135 μl
2	bTSH (1.6, 0.8, 0.4, 0.2, 0.1, 0.01 mU/ml)	54 μl	96 μl
3	KSAb1 mAb (100ng/ml)	54 μl	96 μl
4	KSAb1 mAb (10ng/ml)	54 μl	96 μl
5	IgG2b (100ng/ml)	54 μl	96 μl
6	IgG2b (10ng/ml)	54 μl	96 μl
7	Mice sera	3 μl	147 μl

Table 2.4 Preparation of working sample for cAMP bioassay.

The volume of sera samples and controls need to be added in each well of 96 well plate of JP09 cell.

2.2.3.3   Assay for thyroid blocking antibody

The blocking assay designed to evaluate TSBAbs in the test serum sample by measuring inhibition of cAMP production induced by sub-saturating concentration of bovine TSH. This assay is similar to the above assay to measure thyroid stimulating antibody. The only difference between these two assays is that, JP09 cells were incubated by prepared mice sera samples (as explained in 2.2.4.2) for 2 hours to inhibit induction of cAMP (in case of TSBAbs present) from bovine TSH which has been added later and incubate for another 2 hours.

Briefly, JP09 cells were cultured in 96 flat well plates for 18-20hrs in F12 complete medium (37° 5% CO_2). The medium was removed and cells were gently washed with PBS. The suboptimal dose of bovine TSH was already examined from the prior assay. A patient serum (named as Patritia) kindly provided by Dr Philip Watson (University of Sheffield) that considered possessing blocking activity used as a positive control. Mice sera samples and controls were diluted in complete HBSS as summarised in **Table 2.4**. 150 µl of prepared samples was added to each well and was incubated for 2 hours at 37^oC, 5% CO_2. After 2 hours incubation, 150 µl of 0.2 mU/ml bTSH was added to all wells and incubated for 2 hours at 37^oC, 5% CO_2. After incubation time, supernatant was collected and stored in -80^oC to measure concentration of cAMP, as explained earlier in 2.2.4.2. The acquired raw data was then calculated by dividing level of cAMP from each well by the suboptimal value of 0.2 mU/ml bTSH. Results were express as percentage of blocking of induced cAMP.

2.2.4 Thyroid function tests

The hyperthyroid states of immunised mice were assessed by measuring total serum T4 concentrations using a commercial kit that uses the smallest volume of serum, Ratio Diagnostics, (Germany). In order to outset the assay, 25 µL of mice sera and standards (**Table 2.5**), was added to each well. It was followed by adding 200 µL of working conjugate solution to each well. The plate was incubated for 30 min at 37° C on a thermoshaker 500rpm followed by washing 5 times with 300 µL with provided washing solution. Subsequently, 100 µL of TMB was added to each well and incubated for 15 min at room temperature in the dark. In the last step 150 µL stopping reagent was added and gently mixed for 10 seconds. Optical density was measured on the micro-plate reader at 450 nm. Total T4 of mice sera was calculated based on the absolute OD of provided standards.

Standards number	Total T4 value (nmol/L)
C0	0
C1	10
C2	50
C3	100
C4	200
C5	400

Table 2.5: List of T4 standards.

2.2.5 Purification of IGF-1R mAbs by protein G chromatography

Professor Kenneth Siddle(University of Cambridge, UK) kindly provided four anti-IGF-1R mAbs with different specificity, called 24-31mAb, 24-60mAb, 17-69mAb and 24-57mAb as freeze-dried ascites (Soos et al., 1992). To purify freeze-dried ascites, initially each mAb vial was resuspended in 1 ml of sterile distilled water. Salt reconstitution was not necessary because mAbs had been freeze-dried from mouse ascitic fluid. Resuspended mAbs were passed through the column containing protein G Sepharose gel and the columns were washed with 10 x 1 ml of 100 mM Tris (pH 8.0) and then with 10 x 1ml of 10 mM Tris (pH 8.0). The mAbs were eluted from protein G with 5 x 1 ml fractions of eluting buffer (50 mM glycine, pH 3.0). The eluted fractions (0.5 ml) were collected in individual microcentrifuge tubes containing 50 µl of 1M Tris buffer to neutralise acidity. In addition, the starting sample (SS), flow through (FT), column wash (CW) samples were already collected in the separate tubes. The samples were individually dialysed overnight in sterile PBS at pH 7.4 at 4°C.

2.2.6 Protein detection assays

2.2.6.1 Protein assay

To analyse the mAbs concentration which were purified by column chromatography micro-scale protein assay using BCA Protein Assay Kit (Novagen). Initially, the BCA working reagent was prepared in a microcentrifuge tube; each well required 200 µl of BCA solution and 4 µl of 4% cupric sulfate. 25 µl of each standard and protein sample (elute 1–5) was added into single wells of a standard 96-well microtitre plate and then

200 µl of BCA working reagent was added to the wells. The plate was covered with adhesive plate sealing film and placed on a plate shaker for 30 seconds to enable mixing. There were 2 options for incubation; the standard assay and the enhanced assay. This experiment followed the standard assay with incubation at 37°C for 30 minutes. After incubation, plate was remained for few minutes to cool down to the room temperature. The absorbance was measured at 630 nm using a microplate reader.

2.2.6.2 SDS-PAGE

The separating and stacking gels were prepared with the reagents in **Table 2.1**. TEMED is required to polymerise the gels and should be added just before pouring the gels into the gel cassette. The separating gel was first poured into the gel cassette up to about 1 cm below the position of the comb and isopropanol was then added to remove air bubbles. The gel was left to set for 10–15minutes before washing the gel cassette with distilled water. The stacking gel was then poured to fill the gel cassette and the comb was inserted into stacking gel. Again, isopropanol was added before allowing the gel to set for 10–15 minutes. The gel cassette was removed from the gel caster and placed into the electrophoresis tank which was then filled with SDS running buffer. 5 µl of the protein ladder was first added to the gel, followed by samples prepared with bromophenol blue (refer to **Table 2.6**). The gels ran at 70V until the bands passed through the stacking gel and then the voltage was increased to 200V.

	Preparations	Volume used
1	5 µl of SS + 5 µl of bromophenol blue	5 µl
2	5 µl of FT + 5 µl of bromophenol blue	5 µl
3	5 µl of CW + 5 µl of bromophenol blue	5 µl
4	15 µl of E1 + 15 µl of bromophenol blue	20 µl
5	15 µl of E2 + 15 µl of bromophenol blue	20 µl
6	15 µl of E3 + 15 µl of bromophenol blue	20 µl
7	15 µl of E4 + 15 µl of bromophenol blue	20 µl
8	15 µl of E5 + 15 µl of bromophenol blue	20 µl

Table 2.6 Preparation of samples for SDS gel

SS – Starting sample; FT – Flow through; CW – Column wash; E1–5 – Elute 1–5

Following electrophoresis, in order to visualise the separate protein bands, the gel was stained with coomassie brilliant blue and destained in 20% methanol/10% acetic acid solution. The molecular mass of these protein bands can be approximated with reference to the protein ladder (molecular weight size marker).

2.2.6.3 Western blotting

Samples were run on SDS-PAGE gels (as described in 2.2.7.2) with coloured markers (Fisher Scientific, UK). The gel was placed on three sheets of wet 3 mm filter paper on the top leaf of the Western blotting cassette (Trans-Blot Electrophoretic Transfer Cell, BioRad). The gel was covered with a wet Protan Nitrocellulose membrane (Scheiler and Schuell, Dassel, Germany), ensuring no-air bubbles were present by rolling with a pastette. Three further sheets of filter paper were placed over the membrane and the cassette was closed. The cassette was placed in the tank such that the gel-side of the sandwich was facing the cathode, and the nitrocellulose membrane was facing the

anode. The tank was filled with 1X transfer buffer, connected to the power pack, placed in a polystyrene box containing ice and run for 1 h at 100 V, or until the prestained MW ladder had fully transferred to the blot. Following transfer, the nitrocellulose membrane was blocked for 1 h at room temperature with PBST/5% marvel milk protein/0.05% Tween-20. The blocked membrane was incubated with anti-penta His HRP Conjugate (Qiagen; 1:1000 dilution), for 1 h at room temperature. The membrane was then washed 3 times for 5 minutes each in PBST, incubated with AEC developer for 5 minutes, and rinsed with dH20 to stop the reaction.

2.2.7 Flow cytometry

Flow cytometry technique was used to evaluate expression of TSHR and IGF-1R in transfected cell lines. BD Canto II flow cytometer (BD Bioscience), equipped with two laser channels was used. Data analysis was done by FlowJo software.

2.2.7.1 Evaluation of IGF-1R expression in NWTB3 cells by flow cytometry

The NWTB3 cells, mouse fibroblast cell line stably transfected to express human IGF-1R were kindly provided by Professor LeRoith. The transfected cells were reported to express 410,000 receptors per cell (Blakesley et al., 1995). IGF-1R expression on NWTB3 cells was examined by flow cytometry. NWTB3 cells were grown in T25 tissue culture flasks in DMEM medium. Flasks with confluent cells (70-90%) were prepared for flow cytometry as follows:

Medium removed and cells washed with PBS twice before adding 2ml of cell dissociation medium (Sigma-Aldrich) to T25 flasks. Flasks incubated at 37°C for 5-7

minutes until cells have detached. Afterwards, 8ml of complete medium added to each flask and resuspend cells. Cells transferred into a 15 mL falcon tube and counted before centrifugation at 1000 rpm for 5 min. Cell pellet resuspended in PBS containing 1% BSA, 0.05% sodium azide to a concentration of 1×10^6 cells/ml and then 1ml of cells transferred to an FACS tube (BD Bioscience) through their cell strainer cap to avoid aggregation of cells and centrifuged at 1500 rpm for 5 min. The supernatant was removed and cells resuspended in 100 µl of primary antibody and incubated for 1 hour on ice. Primary antibodies were included 1H7 (Santa Cruz Biotechnology) as a positive control, IgG1 isotype or blank as a negative control, 17-69 and 24-57 IGF-1R monoclonal antibodies provided by Professor Kenneth Siddle (University of Cambridge, UK). After 1 hour cells were washed twice in 1ml cold PBS +BSA +azide and then centrifuged at 1500rpm for 5min before adding 100 µl of secondary antibody. Cells with secondary antibody incubated on ice for 30 min. FACS tubes are ready to read by flow cytometer BD Canto II after three times washing as before and resuspended in 300 µl of PBS, BSA, azide.

2.2.7.2   Evaluation of TSHR expression in GPI9-5 cells by flow cytometry

The GPI9-5 cells, CHO cell line stably transfected to express human TSHR A-subunit were kindly provided by Dr Phillip Watson (University of Sheffield, UK) (Metcalfe et al., 2002). TSHR A-subunit expression on GPI cells was examined by flow cytometry as describe above. Primary antibodies included 4C1 the gold standard mAb for evaluating TSHR expression by FACS for positive control and IgG2b for negative control.

2.2.8 Establishment of assays for IGF-1R Abs

To our knowledge, there is no commercial kit available for detection of IGF-1R Abs. Herein, establishment of two assays including ELISA assay and competitive binding assay are described.

2.2.8.1   ELISA

IGF-1R Ab ELISA established based on the protocol described by Yin and colleagues (Yin et al., 2011).   IGF1R extracellular domain (IGF1R ECD) was purchased from R&D Systems (UK). The source of receptor (102.9 kDa) is recombinant protein in murine myeloma cells. MaxiSorp (Nunc, Roskilde, Denmark) flat bottom ELISA plates were coated with 100 µl (30.6 ng/well) of IGF1R ECD suspended and diluted in PBS buffer at 4°C for 12–16 hours. After washing three times with 250 µl of washing buffer (PBS 0.05% Tween/ 2% BSA), coating step were blocked with incubation with 1% BSA in PBS-Tween for 2 hours. Mouse serum (diluted 1:30 and 1:90 in washing solution), was incubated in antigen coated wells at room temperature for 1 h. After washing, 100 µl of alkaline phosphatase conjugated goat anti-mouse IgG Fc antibody (Sigma-Aldrich) in 1:5000 dilution was added and incubated for 1 hour. After washing, substrate solution containing p-nitrophenylphosphate (pNPP) was added to each well for 40 min. Substrate conversion was measured at 405 nm using a Titertek Plus reader.

2.2.8.2   Competitive binding assay

Competitive binding assay were established based on the displacement of labelled-IGF-1 by cold IGF-1 in the receptors, similar to that reported by Weightman and colleagues (Weightman et al., 1993). However, there are some technical differences between

these two studies: (i) radioactive (^{125}I) labelled IGF-1 has been replaced by acridinium ester labelled IGF-1 (called Lumi-IGF-1) and (ii) transfected cells (NWTB3) were used instead of human orbital fibroblasts as source of IGF-1R in the assay. Lumi-IGF-1 is kindly provided by Professor Lutz Schomburg and his colleagues (University of Berlin, Germany) (Minich et al., 2013). Luminescence activity of the stock tracer (Lumi-IGF-1) was at 10^8 RLU/µl. For first instance, concentration of trace and number of cells were evaluated to optimise the assay. NWTB3 cells were grown as monolayer cell culture in 96 well, 48 well and 24 well plates overnight in complete medium (DMEM 10% FCS). Next day, cells were washed with sterile PBS and different concentration of tracer and competitor (unlabelled IGF-1) were added and incubated for 6 hours at 4°C. Unlabelled IGF-1 at different concentration (10 fold dilution) used as competitor. Highest concentration of unlabelled IGF-1 was 10^{-7}M which decreased to 10^{-10} M. Dilution worked out based on the 10^{-7}M equal to 1µg/ml of IGF-1. Is'nt this in Appendix, please refer to it! Sterile PBS used as dilution buffer. Equal volume of tracer and competitor added to each monolayer cultured wells. Concentration of Lumi-IGF-1 is based on luminescence signalling (RLU/µl). 100 µl of mixture was added for 96 well plate and 400 µl for 24 well plate.

96 well plate were washed with PBS two times and directly read with luminometer (Berthold TriStar LB 941). Since the 24 and 48well plates were not suitable for direct reading in the luminometer, after the washing step in the binding assay, the monolayer cells were dissociated with cell dissociation medium and transferred to a fresh 96 well plate for counting of the luminescence signal. Percentage Binding of trace was calculated by dividing of counting from each well by count from no competitor times 100.

2.2.9 Development of mAbs

Non-secretor X63-Ag8.653 (X63) myeloma cell line (the fusion partner cell line) began expansion one week before fusion in complete RPMI-10/HEPES/pyruvate. Myeloma cells were checked under the microscope every day and transferred to fresh medium every alternate day. By the day cell fusion was to be performed, total number of 1×10^8 cells in two or three flasks (175 cm^2) myeloma cells must be available. One day before fusion, myeloma cells were split into fresh complete RPMI-10/HEPES/pyruvate medium. Vigorous growth of myeloma cells is generally required for good fusion.

Three days before fusion, animal was primed by i.v. injection of 2×10^6 NWTB3 cell as booster. At the day of fusion, boosted animal was sacrificed and spleen was harvested under sterile condition. Spleen was Transferred to a sterile 100-mm-diameter petri dish filled with 10 ml sterile complete serum-free RPMI. Spleen was teased into a single-cell suspension by squeezing with angled forceps and fine-tipped dissecting scissors. Debris was removed and cells were dispersed further by passage through a fine-mesh metal screen. Spleen cell suspension was transferred to a sterile 50-ml conical centrifuge tube and filled with sterile complete serum-free RPMI before spinning them down for 5 min at 1500 rpm (500 × g), room temperature. Red   blood cells (RBC) were lysed by resuspending pellet in 5 ml ammonium chloride solution for 5 min at room temperature. 45 ml sterile complete serum-free RPMI was added and centrifuge as in earlier step condition. Cell pellet was resuspended in 50 ml sterile complete serum-free RPMI and centrifuged once again.

While spleen cells were being washed, separately myeloma cells were harvested by transferring the cells to 50-ml conical centrifuge tubes. Myeloma cells were centrifuged for 5 min at 1500 rpm (500 × g), room temperature. Myeloma cells were

resuspended in RPMI and all cells were pooled into one 50-ml conical centrifuge tube.

Myeloma cells were washed three times at the same condition explained earlier.

Separately, the spleen and myeloma cells were resuspended in 10 ml complete serum-free RPMI. On basis of cell counts by using a haemocytometer, the amount of pre-warm complete RPMI-20/HEPES/pyruvate needed to plate cells at about 4×10^6 total cells/ml was calculated. Myeloma and spleen cells were mixed at a 1:1 ratio in a 50 ml conical centrifuge tube. The tube was filled with complete serum-free RPMI and then cell mixture was centrifuged at 500 × g, room temperature for 5 min. The cell fusion was performed at 37°C by adding 1 ml pre-warmed 50% PEG to the mixed-cell pellet drop-by-drop over 1 min. Stirring the cells with the pipet tip after each drop was carefully done. By using a clean pipet, 1 ml prewarmed complete serum-free RPMI was added to the cell mixture drop-by-drop over 1 min, with stirring after each drop. An additional 1 ml of prewarmed complete serum-free RPMI was repeated once. Finally, with a 10-ml pipet, 7 ml prewarmed complete serum-free RPMI was added drop-by-drop over 2 to 3 min. Fused cells were centrifuged at 500 × g, room temperature for 5 min and the supernatant was discarded before adding 50 ml prewarmed complete RPMI-20/HEPES/pyruvate. Gently, 10 ml of cell suspension aspirated with a 10 ml pipet. 2 drops (100 to 125 µl) of suspension was added to each well of a 96-well flat-bottom plate and plates incubated overnight in a humidified 37°C, 5% CO2 incubator.

After one day of incubation, wells were checked under an inverted microscope. If seeded with the appropriate number of cells, there should be a nearly confluent monolayer of highly viable cells on the bottom and obvious clumps of cells. Subsequently hybridomas were selected in RPMI-20 supplemented with hypoxanthine (15 µg/ml), aminopterin (0.2 µg/m1) and thymidine (5 µg/ml) (HAT) or hypoxanthine

(15 µg/ml) and aminopterin (0.2 µg/ml) (HT). 2 drops complete RPMI-20/HEPES/pyruvate/HAT/10% Doma Drive was added to each well with a 10 ml pipet. Plates were placed in humidified 37°C, 5% CO2 incubator again. On days 4, 5, 7, 9, and 11, half the volume of each well was aspirated and fed the cells by adding 2 drops complete RPMI-20/HEPES/pyruvate/HAT/10% Doma Drive from a 10 ml pipet to each well. On day 14, feeding protocol repeated, except use complete RPMI-20/HEPES/pyruvate/HT to feed cells and to return to 37°C, 5% CO2 incubator. On day 15 and subsequently, wells were fed as noted using complete RPMI-20/HEPES/pyruvate without HAT or HT. The hybridomas then were ready for screening when most of the wells containing growing cells demonstrate 10% to 25% confluence and when those with denser populations turn yellow within 2 days after feeding.

2.2.10   Histology

Histology is the microscopic study of a normal structure of body tissues. Study in tissue structure is almost impossible as very small size of cells and lack of refractive contrast between them unless using a certain method to stain a very thin layer of tissue. Thus, histology is set of complex techniques from excised of tissue to study it under microscope including tissue preservation (fixation), embedding, cutting and staining. As soon as tissue is excised, it begins to degenerate due to cell necrosis.

To prevent this process tissue must be preserved either chemically (formaldehyde solution) or physically (snap frizzing). Tissue fixation also protects cells and tissue constituents from the subsequent processes. After fixation, tissue is ready to be embedded either in paraffin or OCT cryostat sectioning medium depend on the fixation method. Paraffin embedding is long process (from 12 hours to few days) that

facilitates penetration of melted paraffin into the fixed tissue to prepare it for cutting section. A very thin slice (normally between 4-6 µm) of tissue can be cut using microtome. Finally, to facilitate differentiation in the refractive indices of certain cell elements a particular staining is required. Haematoxylin-eosin is undoubtedly the most common staining method in histological laboratories to study tissues structure. However, there are more than hundreds staining method and techniques to study in more depths and specificity.

Structure always follows function and histology is therefore a tool for determining the normal function and pathology of different tissues and organs. Particular changes in the microscopic structure of the tissues may reveal a certain disease. The study of these changes is known as histopathology. Obviously, it is essential to know the normal structure for an understanding of pathology. Thus in this project, study of tissue from healthy animal has been first performed to gain a sound knowledge in principles of histology techniques and normal structure of tissues which are in our interest.

2.2.10.1 Mouse thyroid histology

Initially, histology of mouse tissue was examined on tissue from normal mouse donors and then moved to immunised mice tissues. Mouse thyroid tissues were fixed in 10% buffered formalin, embedded in paraffin, and sectioned for haematoxylin and eosin (H&E) staining. Haematoxylin and eosin stain is the standard stain for almost all tissue. It gives a visible look at the nucleus of the cells and their present state of activity in addition to abnormal growth, inflammation or fibrosis. The haematoxylin and eosin stain uses two separate dyes, one staining the nucleus and the other staining the cytoplasm and connective tissue. Haematoxylin is a dark purple dye that will stain the

chromatin (nuclear material) within the nucleus, leaving it a deep purplish-blue colour. Eosin is an orange-pink to red dye that stains the cytoplasmic material including connective tissue and collagen. The normal thyroid gland was sectioned serially at 4 µm, with discarding next ten serial step sections. Sections which have been flowed on the warm water, transferred on the normal glass slides. Slides have been left at room temperature for 5 to 10 minutes to dry out and putted in the automated staining machine for normal H&E.

2.2.10.2   Establishment of histology technique for orbital tissue

Initially, normal mouse extraocular muscles were accessed by transcranial dissection method provided by Dr Swaraj Bose (UC Irvine, USA). The entire orbital bony tissue comprising the orbital bones with the eyeball, extraocular muscles, and the optic nerve was carefully separated from the mouse and fixed in buffered 10% formalin. From this stage to remove bony structure of orbital tissue, two different methods have been set up, decalcification and dissection. In decalcification method which is routine method in histopathology lab, after 24 h, the orbital bony tissue was placed in 10% decalcification solution for 3-5 days with change the solution daily basis and checking the remain free calcium ion un the solution. In the dissection method by using fine forceps and scissors bones have been removed from the orbital tissues under the dissection microscope. The most important part of retrobulbar histopathology is tissue embedding. We were advised by Dr Anja Eckstein (Germany) to use optical nerve as a reference point (Johnson et al., 2013), so it was important that the orientation of the orbit for embedding was correctly positioned to have this reference point in the middle of the

section. Thereafter, the orbital tissue was embedded in the same orientation in paraffin block, serial and step sections as described above were performed starting from the lateral side (optic nerve side). Three serial sections were collected after every ten sections and subjected separately to H&E and masson's trichrome (MTC) staining. At least three to five sections (after ten-step sections discarded) were examined. All sections have been studied by consultant pathologist (Dr Diaz-Cano, King's College Hospital, London, UK) and also examined by independent colleague (Mrs. Gina-Eva Goertz, Essen, Germany with large experience on orbital histology) in double–blinded fashion to determine the differences between mice immunised with hTSHR A-subunit and control mice in terms of inflammation, adipogenesis, and fibrosis. For double-blinded examination each slide has been scored based on the histopathological parameter including lymphocytic infiltration into orbital tissue, expansion of adipose tissue and fibrosis. At the end of double-blinded evaluation, the mice codes were revealed and data was assembled. MRI acquisition protocol

In vivo MRI was performed under complete supervision of Dr. Po-Wa So on immune (n=8) and age-matched control mice (n=3) on a horizontal bore 7T MRI scanner (Agilent Technologies Inc, USA). Anaesthesia was induced and maintained in mice by inhalation of a 1-2% isoflurane-oxygen mix throughout imaging. The mouse head was located within a 25mm internal diameter quadrature MRI volume coil (PulseTeq Ltd, UK). T2-weighted MR images were acquired using a fast-spin-echo (FSE) sequence with repetition time (TR), 4s; effective echo time (TE), 60; echo train length of 8, RARE factor of 16; field of view (FOV) 26mm x 26 mm; matrix size 256 x 192 (100 μm in-

plane resolution) and 4 averages. Twenty-four contiguous coronal 0.61mm thick slices including the eyes and much of the brain were collected (**Fig 2.2**).
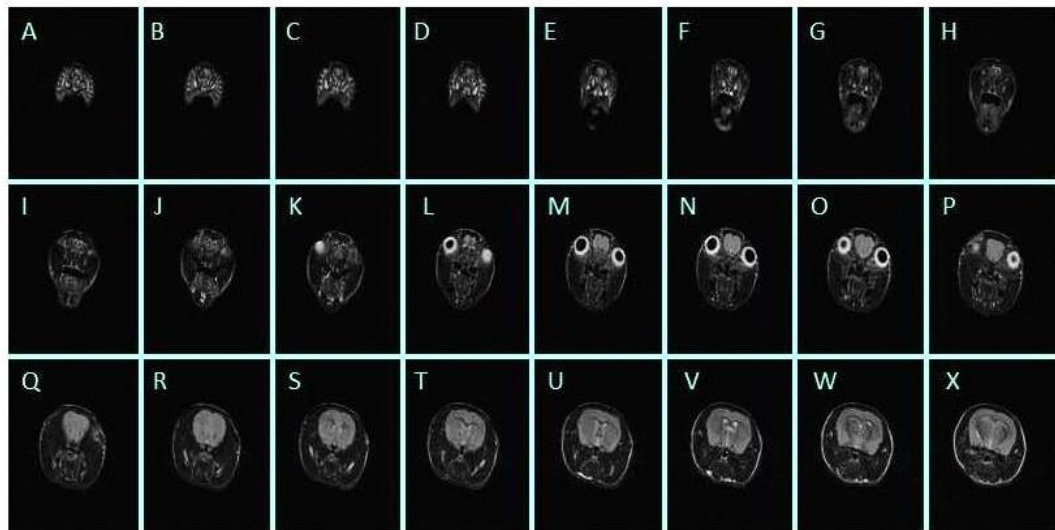
Fig 2.2 A series of contiguous coronal T2w MRI
A series of Twenty-four contiguous coronal T2-weighted MR images, from the front of the head towards the back of the head (A through to X).

The MRI data were then used as scout images for MRI of the right eye at an oblique angle, comparable to that for histology. The position of the imaging slices to image the eye specifically with respect to the head is shown in **Fig 2.3**.
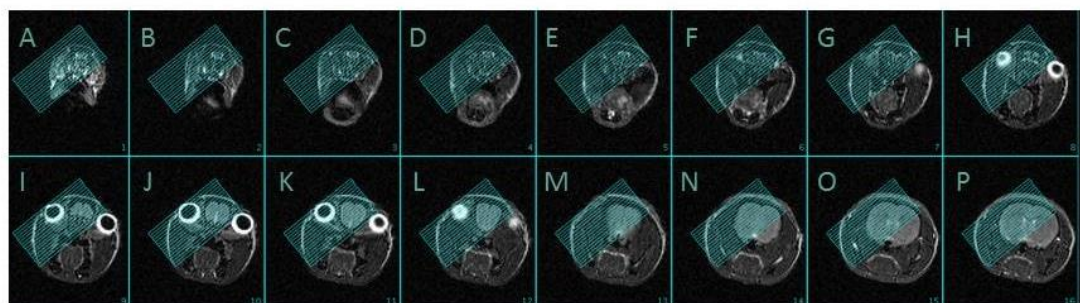
Fig 2.3 A series of contiguous T2w MRI with axial slices guide.
A series of contiguous T2-weighted MR images, from the front of the head towards the back of the head (A through to P), was used as scout images to

guide positioning of imaging slices (shown in blue) for the right eye to visualise the orbital muscles.

Twenty-four contiguous 0.4mm thick, 94 μm in-plane resolution, MR images were collected from the surface of the eye towards the back of the eye (perpendicular to the long axis of the eye, similar to the orientation for histological processing), using a FSE sequence with TR, 1400; effective TE, 7.84; FOV, 12mm x 12mm; matrix size, 128 x128 (94 μm in-plane resolution) and 24 averages (**Fig 2.4**). Respiration and temperature was monitored throughout MRI, with body temperature maintained at 37°C using warm air (SA Instruments, USA).
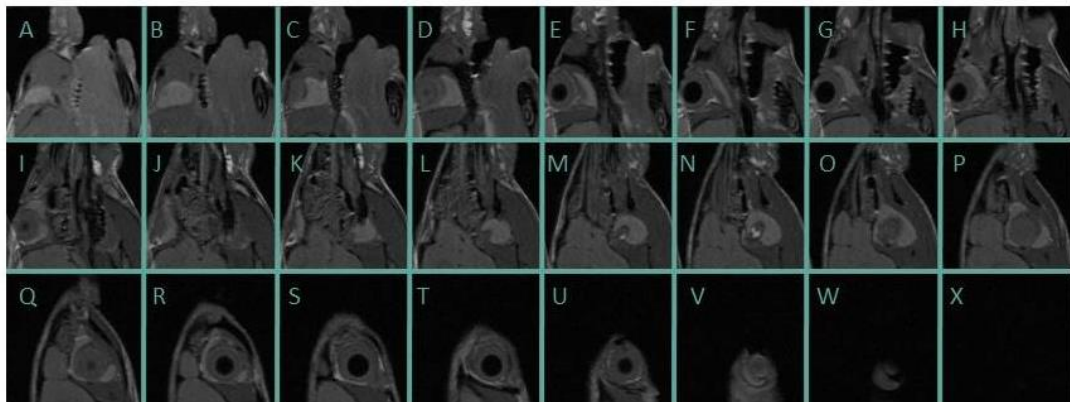
Fig 2.4 A series of contiguous axial T2w MRI.
A series of Twenty-four contiguous axial T2-weighted MR images, from the surface of the eye towards the back of the eye perpendicular to the long axis of the eye (A to X).

2.2.11   Quantification

In this thesis, in order to get a better comparison between different conditions, quantification analysis has been done in three parts; infiltration of CD3$^+$ T cell into orbital tissue, enlargement of orbital tissue by MRI, and size of eyeball by MRI. The method has been used for each of these quantification analysis is described below. Quantification analysis of infiltrated CD3$^+$ T cells into orbital tissue for each group of immunisation was performed by "cell counter" plug-in of ImageJ (NIH) software. The analysis simply performed by uploading 5 different fields (100x magnification) of each immunohistochemistry section to the software where the size and colour of CD3$^+$ T cells were already defined. For each mouse, mean of infiltrated cells per region of interest (ROI) were calculated and presented as CD3$^+$ T cell infiltration index.

In the axial MR images hypertrophy of extraorbital muscles were readily apparent. To confirm hypertrophy of extraorbital muscles we have used computer based software, ImageJ (NIH). ImageJ allowed us to draw a "free hand line" around the muscles and then it automatically measured the marked area. The calculated area was then multiplied by the thickness of the slice (0.4 mm) to measure the muscle volume at that particular area. The same process was repeated for all MR slices where extraorbital muscles present. Eventually, the calculated muscle volumes were summed up to calculate the extraorbital volume throughout the orbit.

Finally, the size of eyeball in MR images was quantified in order to assure observed proptosis in immune mice is not due to larger size of eyeball. In coronal view of MR images in five immune mice and three age-matched controls, diameter of eyeball was calculated by ImageJ software. The results are presented in Section 4.3.1.

Chapter Three

Development and Characterisation of a

Preclinical Mouse Model of GO

3. Development and characterisation of a preclinical mouse model of GO

3.1 Introduction

As already outlined in the section 1.8, a number of experimental models of Graves' disease in mice and hamster have been developed since the first model described by Shimojo and colleagues (Shimojo et al., 1996). This was followed by an outbred mouse model immunised with naked hTSHR plasmid (Costagliola et al., 2000). Collectively, earlier studies from our laboratory and other groups showed both the Shimojo model and naked plasmid model suffer from two main issues; low disease incidence and poor disease severity (low activity of TSAbs) (Rao et al., 2003, Seetharamaiah, 2003). The development of the experimental model using adenovirus for gene delivery coding for human TSHR (hTSHR) by Nagayama and colleagues (Nagayama et al., 2002) and in particular the idea of using hTSHR A-subunit instead of full length (Chen et al., 2003) has led to a model most widely used for Graves' disease that has been successfully replicated (Gilbert et al., 2006, Land et al., 2006, Mizutori et al., 2006, Wu et al., 2011, Ye et al., 2012, Wiesweg et al., 2013) . From hereon, the adenovirus hTSHR A-subunit will be referred to hTSHR A-subunit-Ad. Importantly, despite the advantages of this experimental model, the model has two major drawbacks; (i) the majority of immune response is directed toward the highly antigenic adenovirus capsid antigens, which therefore limits the immunisation to maximum two or three injections (ii) the induced TSAbs decline rapidly after the last immunisation (McLachlan et al., 2012, McLachlan and Rapoport, 2014). Whilst the adenovirus model has been the most popular model for Graves' diseases, careful analysis of the orbital tissue have shown that it does not

led to orbitopathy (Nagayama et al., 2002, Gilbert and Banga, 2006, Wiesweg et al., 2013, Johnson et al., 2013). Along similar lines, a few reported animal models of GO in last two decades (Many et al., 1999, Costagliola et al., 2000) have also proved difficult to reproduce (Baker et al., 2005).

In the course of experimental Graves' disease model in Professor Banga's laboratory, the group recently modified the animal model described by Kaneda and colleagues (Kaneda et al., 2007), by immunising hTSHR plasmid *in vivo* electroporation using calliper electrodes (Zhao et al., 2011). It was shown that this model maintains the longevity of induced antibody response to TSHR. Strikingly, orbital fibrosis was detected in some of animals undergoing experimental hyperthyroidism. This was the first sign that orbital manifestation could be induced in animals immunised by hTSHR *in-vivo* electroporation (Zhao et al., 2011).

Upon observing orbital fibrosis in animals immunised by hTSHR A-subunit plasmid *in vivo* electroporation (Zhao et al., 2011), my PhD project was based upon modifications to the Zhao et al procedure to develop an improved mouse model of GO with features of orbital inflammation and adipogenesis.

Earlier studies using hTSHR A-subunit-Ad as immunogen by McLachlan and colleagues showed that alteration of the antigenic dose resulted in change of the spectrum of anti-TSHR antibodies from TSAbs to TSBAbs (Chen et al., 2004). Therefore, we hypothesised that changing the antigenic dose of TSHR A-subunit plasmid prior to *in vivo* electroporation may result in altering the spectrum of induced anti-TSHR antibody and T cell responses to the hTSHR (Chen et al., 2004, Cemazar et al., 2006).

In their early attempts to alter the antigenic dose of plasmid electroporation, in preliminary studies, Dr Zhao and Professor Banga altered the injection protocol over a

larger area as part of the immunisation evaluation. They tried to achieve this by injecting the 50 μl plasmid as separate injections of 5x10 μl in different, but close by sites over the shaved quadriceps leg muscle spread over an area of approximate 7 mm diameter of leg muscle area (to ensure muscle was covered by the 7 mm calliper plate electrode during electroporation). However, this technique was deemed technically difficult for large number of animal immunisations in terms of accuracy and reproducibility of the injections and not taken further (Zhao and Banga, unpublished data). Therefore, the working hypothesis was based on injection of 50μl plasmid over the wider surface area instead of a small area limited by the single injection protocol described by Zhao and colleagues (Zhao et al., 2011). For my project, the method to alter the delivery of the plasmid in an attempt to change the antigenic dose was to either inject the plasmid slowly as the needle was penetrated into the muscle or alternatively, releasing the plasmid gently from the syringe as the needle was withdrawn from the muscle. Small trial experiment showed that the later technique was easier to manipulate on the leg muscle of the anaesthetised mouse and thus was selected as the method of choice for injections in all the studies reported for the GO model.

To summarise, my modified protocol for the delivery of hTSHR A-subunit plasmid involved a deeper injection of the plasmid over a larger muscle area, on the basis that this may lead to greater transfection efficiency after *in vivo* electroporation, resulting in alteration of antigenic stimulus. In contrast to the previous findings (Zhao et al., 2011), modification of plasmid delivery in this manner resulted in marked different outcome in the immune response and consequent thyroid function, as well as the resultant orbital pathology. These studies are described in this Chapter.

3.2   Aims

The objectives of this Chapter deal with induction of experimental Graves' disease with concomitant complications of experimental Graves' orbitopathy.

- Set up an experimental mouse model for Graves' orbitopathy following modified immunisation protocol.

- Evaluation of initiation and progression of any changes to the orbital tissue by histological analysis.

- Characterisation of immunological and biochemical (thyroid function) changes in the experimental GO model.

- Determination of long term consequences of modified immunisation protocol in experimental GO model e.g. longevity of anti-TSHR response, maintenance of hyperthyroidism.

3.3   Results

In the following subsection of this Chapter, the results of evaluation for onset of Graves' disease and concurrent orbital manifestations in a total number of 22 immune mice will be described. The animals were immunised in three separate cohorts:

(i) Group 1 immunisation; evaluation of experimental GO model following modification of immunisation (8 immune mice sacrificed 6 weeks after end of immunisation),

(ii) Group 2 immunisation; longitudinal studies on TSHR antibodies (8 immune mice sacrificed 9 weeks after end of immunisation)

(iii) Group 3 immunisation; characterisation of long-term immunity to hTSHR (6 immune mice sacrificed 15 weeks after end of immunisation).

Control animals immunised with β-gal and IGF-1Rα plasmids were also described in each cohort.

Finally, a separate cohort of mice, Group 4 immunisation, was immunised with hTSHR A-subunit plasmid *in vivo* electroporation to especially study IGF-1R antibodies which will be discussed later in Chapter 5.

3.3.1 Evaluation of experimental GO model after modification of immunisation

Eight mice were challenged with hTSHR A-subunit plasmid by the modified protocol. Animals were weighed weekly during the course of immunisation until six weeks after end of immunisation. Animals similarly immunised with pTRiEx1.1 neo-IGF-1Rα (n=3) and pTRiEx1.1 neo-β-Gal plasmids (n=3) were used as the control group (Appendix 1). None of the control mice led to any visible changes in their health or to any histological manifestations in thyroid and orbital tissue. Immune animals and controls were sacrificed six weeks after end of immunisation. The two exceptions were one immune mouse that was selected for hybridoma fusion at four weeks after end of immunisation as well as another immune animal that showed severe signs of sickness at five weeks after end of immunisation.

Thyroid glands were studied by histological analysis. Retrobulbar tissue of immune animals and controls was examined to evaluate sign of Graves' orbitopathy which was include H&E staining on extraorbital muscles in first instance and then immunohistochemistry for CD3$^+$ T cell and F4/80$^+$ macrophages. Two animals showed chemosis, which was confirmed by histological studies on tissue form eyelid. Thyroid hormone level was measured to confirm histological finding of thyroid gland. Therefore, to understand effect of TSHR antibodies in changes of thyroid histology and physiology, thyrotropin blocking inhibition immunoglobulin assay was performed. Presence of different TSHR antibodies subtypes was also determined. All findings are described in detail in the following subsections.

3.3.1.1 Changes in weight of immune animals during course of immunisation

The weight of the animals during the course of immunisation was monitored at weekly intervals. Usually, autoimmune hyperthyroidism results in significant weight loss, whereas weight gain is generally an indicator of hypothyroidism. As mentioned earlier, eight mice were challenged with hTSHR A-subunit plasmid and six mice were similarly immunised with control pTRiEx1.1 neo-IGF-1Rα (n=3) and pTRiEx1.1 neo-β-Gal plasmids (n=3) were weighed weekly during the course of immunisation until six weeks after end of immunisation (sacrifice point). Analysis of the animals' weight demonstrated significant weight gain in immune animals that were immunised with hTSHR A-subunit *in vivo* electroporation in comparison with controls. The mice weight presented at two time points, one week before last injection where there is no significant differences between immune mice and controls, and four weeks after end of immunisation that demonstrated a significant weight gain in immune mice (**Fig 3.5**). The result was unexpected since the weight gain suggested hypothyroid status in the immune animals. The ongoing weight gain by the animals during the course of the experimental study was the first exciting indication that the modified immunisation protocol may be resulting in a different manifestation of clinical presentation of the disease.
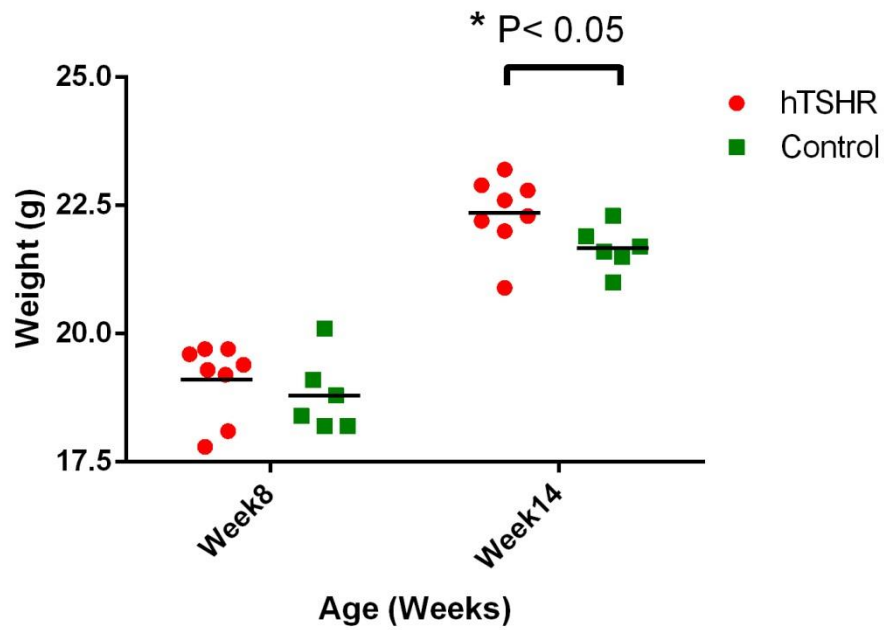
Fig 3.5 Immune mice weight monitoring
Significant weight gain in Group 1 mice during the course of immunisation with pTRiEx1.1 hTSHR A-subunit plasmid (🔴) (labeled hTSHR) compared to combined groups of IGF-1Rα and β-Gal that labelled as control (🟩

3.3.1.2   Histological study of thyroid gland

We next evaluated the thyroid glands of the immune mice in the group, which by weight analysis had been suspected for hypothyroid status. Examination of thyroid glands by hematoxylin-eosin (H&E) staining showed typical pattern of hypothyroidism in seven immune mice. Hypothyroid thyroid glands were characterised by thinning epithelial cells as well as disappearance of follicular membrane in some cases. The H&E staining (100x magnification) of each immune animal are presented to demonstrate hypothyroid gland features as described above (**Fig 3.6 A-G**). Interestingly, one thyroid gland presented with hyperthyroid features (**Fig 3.6 H**). Hyperthyroid gland

characterised by hypertrophy and hypercellularity of the follicular epithelial cells without any signs of thyroid inflammation.

Thyroid glands excised from control animals including both IGF-1Rα and β-Gal mice showed normal features of mice thyroid. The normal thyroid tissue appears as closely packed follicles consisting of a single layer of thyroid follicular cells surrounding a lumen (**Fig 3.7**).
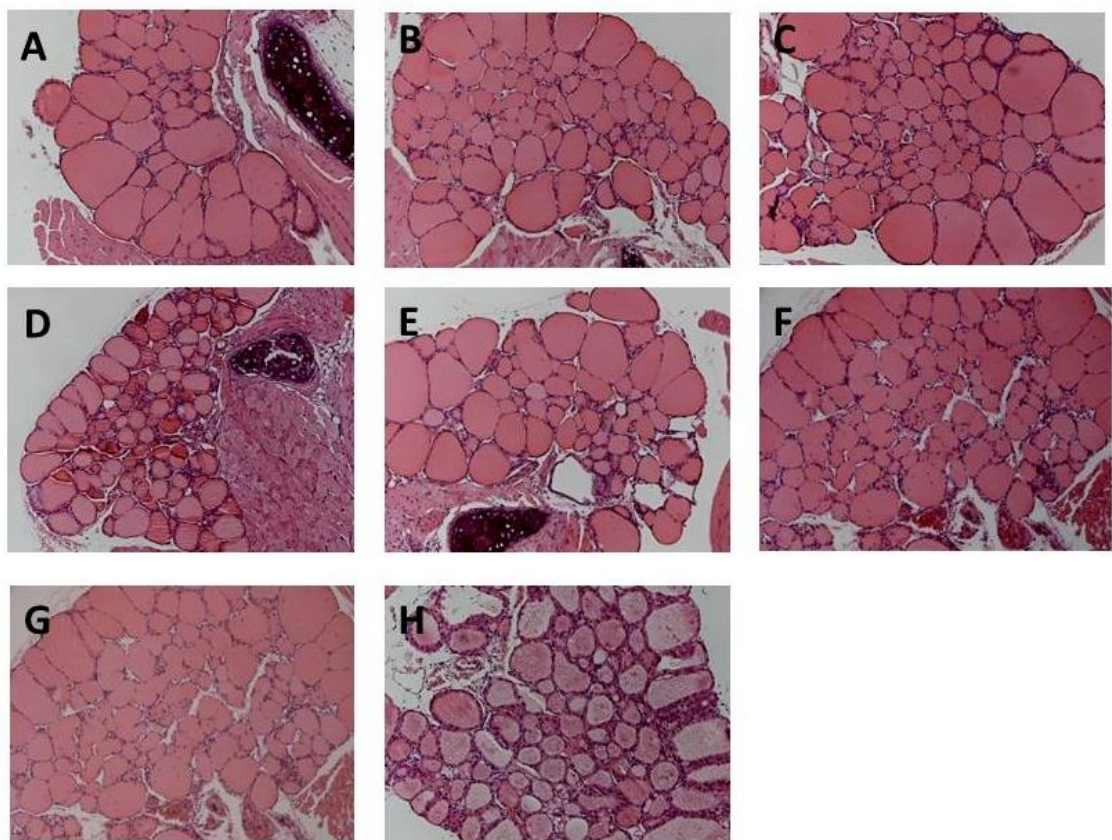
Fig 3.6 Thyroid histological studies in immune mice of Group 1
Thyroid histological studies on n=8 mice immunised with hTSHR A-subunit *in vivo* electroporation and sacrificed 6 weeks after end of immunisation. All sections are at 100x magnification (**A**-**G**) pathological feature of hypothyroidism, characterised by thinning epithelial cells and in some instances the follicular membrane was almost not visible (**H**) pathological feature of hyperthyroidism, characterised by hypertrophy and hypercellularity of the follicular epithelial cells without any signs of thyroid inflammation.
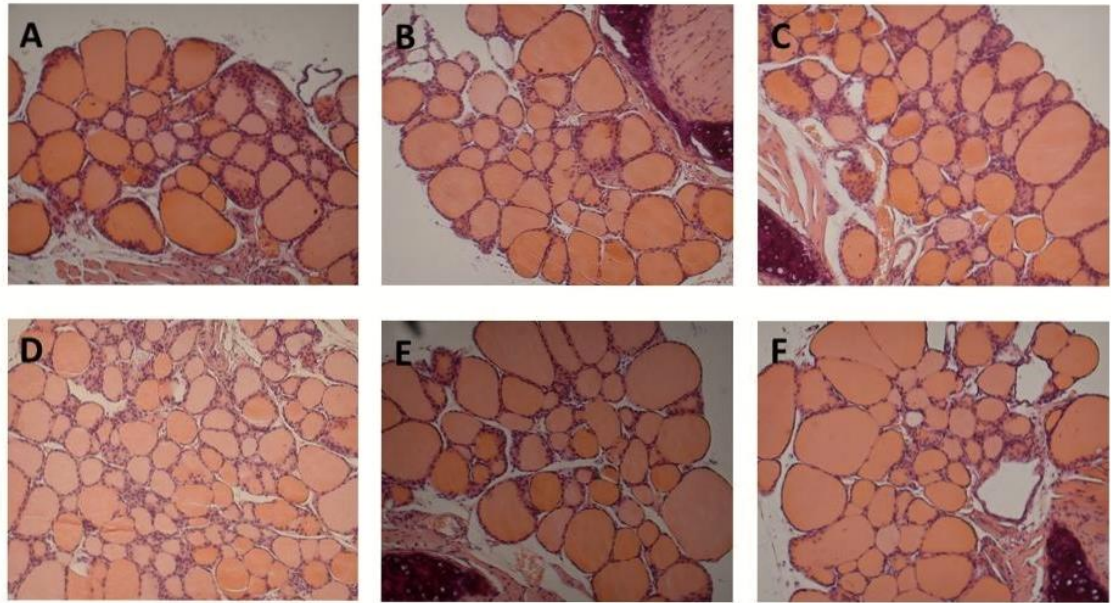
Fig 3.7 Thyroid histological studies in control mice of Group 1

Thyroid histological studies in control mice. All sections are at 100x magnification (**A**-**C**) n=3 thyroid glands from mice immunised with pTRiEx1.1 IGF-1Rα with normal features and (**D**-**F**) thyroid gland from mice immunised with pTRiEx1.1 neo-β-Gal plasmids (n=3) with normal features. The normal thyroid characterised with closely packed follicles consisting of a single layer of thyroid follicular cells surrounding a lumen.

3.3.1.3 Studies into retrobulbar histopathology

Establishing the technique of orbital histopathology was an essential component of the project. In contrast to the earlier project in Professor Banga's laboratory (Zhao et al., 2011), on this occasion we determined to set up a reference point , such as the optic nerve in the middle of the section, in the orbital histology as described in the recent study by Professor Eckstein (Wiesweg et al., 2013). Although histology processing and studying of mouse orbital tissue is difficult and not straightforward, as part of this project, all these procedure have been set up properly. Optic nerve has been selected as a land mark to study extra-orbital muscles and retrobulbar connective tissue (Johnson et al., 2013, Wiesweg et al., 2013) (**Fig 3.8**). Two different methods were tried to separate extraorbital muscles from bones and rigid structures. Tissue decalcification

was executed as the recommended method from previous project (Zhao et al., 2011). However, the results indicated that excision of the bone by dissection had higher quality and with less artefact. Fig 3.8 represents histology of orbital tissue from a normal mouse showing optic nerve, extraorbital muscles and harderian gland. Variability in normal histology of orbital tissue was mostly seen in size of adipose tissue around optic nerve. However, this was not comparable with what we reported as expansion of adipose tissue in our immune mice.
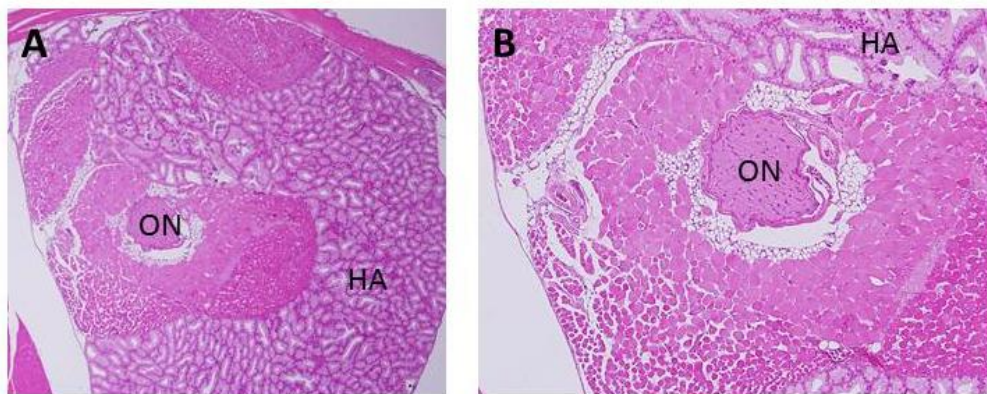
Fig 3.8 Histology of orbital tissue from a normal mouse

(A) Orbital tissue including optic nerve (ON), extraorbital muscles and harderian gland (HA), 40x. (B) Higher magnification of normal mouse orbital tissue focusing on optic nerve and extraorbital muscles (100x).

Subsequently, orbital samples of immunised mice were studied by using optic nerve as a reference point. Animals immunised with hTSHR A-subunit plasmid showed orbital pathology, with asymmetric bilateral disease. Two subtypes of orbital pathology were recognised: (i) interstitial inflammatory infiltrate into extra-ocular muscle, extending into the muscle tissue and isolating individual fibres. Importantly, one animal with severe sickness showed a large inflammatory infiltrate around the optic nerve, revealing dense perineural inflammatory infiltrate, along with intense intermuscular lymphocytic infiltrate dissecting the orbital muscle fibre bundles. (ii) the orbital

pathology developed by another animal with extensive adipogenesis, characterised by expansion of retrobulbar adipose tissue and widely separating the orbital muscle fibre bundles. By immunohistochemistry, the inflammatory cells were identified as $CD3^+$ T cells and $F4/80^+$ macrophages; the infiltrate was uniformly negative for B cells using anti-mouse B220 mAb.

The interstitial inflammatory infiltrate into extraocular muscle was clearly demonstrated by histological analysis in six immune animals. The H&E staining from each immune animal represented to show retrobulbar tissue inflammation, animals indicated by their codes (**Fig 3.9 A-D, G,H**). Importantly, one animal (sacrificed early due to severe sickness) showed a large inflammatory infiltrate around the optic nerve, revealing dense perineural inflammatory infiltrate, along with intense intermuscular lymphocytic infiltrate dissecting the orbital muscle fibre bundles (**Fig 3.9 E**). One animal showed extensive adipogenesis, characterised by expansion of retrobulbar adipose tissue and widely separating the orbital muscle fibre bundles (**Fig 3.9 F**). In all presented H&E sections, optic nerve (ON) has been marked to facilitate histological analysis. Examination of the orbital tissues by H&E demonstrated that control mice had normal appearance of retrobulbar tissue. All histological slides were also examined by independent colleague (method was explained in section 2.2.11.2) to provide an assurance of the authentic differences between mice immunised with hTSHR A-subunit and control mice in terms of inflammation, adipogenesis, and fibrosis (**Table 3.2**). The data from independent examination of histological slides showed less than 10% (3 out of 34) variability between double-blind reported histological manifestations and expected results based on the immunisation plasmid in all three groups of immunisation (**Appendix 1**).

Weeks after end of immunisation		Animal code	Immunisation Plasmid	Double-blind examination of histological slides
6 Weeks (Group 1)	1	59/0	pTriEx-TSHR A-subunit	Inflammation of EOM
	2	59/L	pTriEx-TSHR A-subunit	Inflammation of EOM
	3	59/R	pTriEx-TSHR A-subunit	Inflammation of EOM
	4	59/2	pTriEx-TSHR A-subunit	Inflammation of EOM
	5	60/0	pTriEx-TSHR A-subunit	Intense infiltration
	6	60/L	pTriEx-TSHR A-subunit	Adipose expansion
	7	60/R	pTriEx-TSHR A-subunit	Inflammation of EOM
	8	60/2	pTriEx-TSHR A-subunit	normal*
Controls	9	61/0	pTriEx-IGF-1Rα	normal
	10	61/L	pTriEx-IGF-1Rα	normal
	11	61/R	pTriEx-IGF-1Rα	normal
	12	62/0	pTriEx-β-Gal	normal
	13	62/L	pTriEx-β-Gal	normal
	14	62/R	pTriEx-β-Gal	normal
longitudinal study, 9 Weeks (Group 2)	15	63/0	pTriEx-TSHR A-subunit	Inflammation of EOM
	16	63/L	pTriEx-TSHR A-subunit	Inflammation of EOM
	17	63/R	pTriEx-TSHR A-subunit	Inflammation of EOM
	18	63/2	pTriEx-TSHR A-subunit	Inflammation of EOM
	19	64/0	pTriEx-TSHR A-subunit	Inflammation of EOM
	20	64/L	pTriEx-TSHR A-subunit	adipose expansion
	21	64/R	pTriEx-TSHR A-subunit	normal*
	22	64/2	pTriEx-TSHR A-subunit	Inflammation of EOM
long term study, 15 Weeks (Group 3)	23	57/0	pTriEx-TSHR A-subunit	Fibrosis/EOM inflammation
	24	57/L	pTriEx-TSHR A-subunit	EOM inflammation (no fibrosis*)
	25	57/R	pTriEx-TSHR A-subunit	adipose expansion
	26	58/0	pTriEx-TSHR A-subunit	Fibrosis/ EOM inflammation
	27	58/L	pTriEx-TSHR A-subunit	Fibrosis/ EOM inflammation
	28	58/R	pTriEx-TSHR A-subunit	intense infiltration
Controls	29	56/0	pTriEx-IGF-1Rα	normal
	30	56/L	pTriEx-IGF-1Rα	normal
	31	56/R	pTriEx-IGF-1Rα	normal
	32	55/0	pTriEx-β-Gal	normal
	33	55/L	pTriEx-β-Gal	normal
	34	55/R	pTriEx-β-Gal	normal

Table 3.2 Double-blinded examination of orbital histology

The histological manifestations presented in the last column of this table are based on the double-blinded examination of all immune mice from three groups of immunisations. The histological manifestation is highlighted in red with * if there was differences from what was expected.
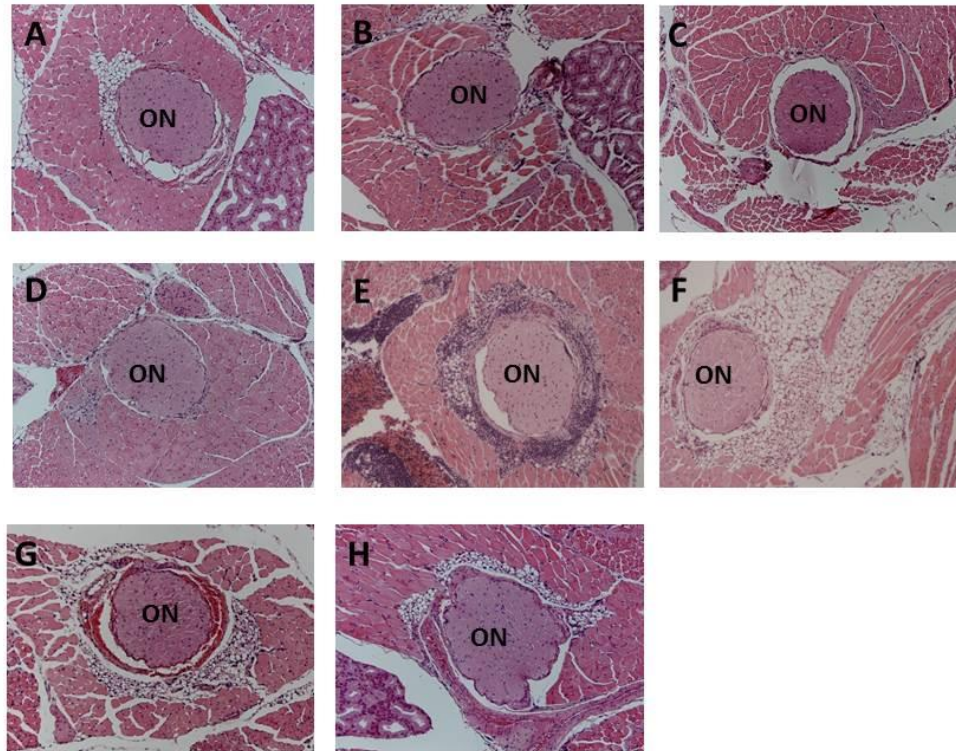
Fig 3.9 H&E stained section of retrobulbar tissue from immune mice of Group 1

H&E stained section of retrobulbar tissue from individual mice immunised with hTSHR A-subunit plasmid. All histological slides are at 100x magnification. (**A**) 59/0, (**B**) 59/L, (**C**) 59/R, (**D**) 59/2, (**G**) 60/R, (**H**) 60/2 are shown extraorbital muscles changes including infiltration of inflammatory cells clear from increasing cellularity in muscle tissue. (**E**) 60/0, intense infiltrations of inflammatory cells around the optic nerve along with intense intermuscular lymphocytic infiltrate are clear. (**F**) 60/L Expansion of adipose tissue in retrobulbar fat showing adipose tissue widely separating the orbital muscle fibre bundles.

3.3.1.4   Histopathological studies by immunohistochemistry into retrobulbar tissue

Subsequently, orbital tissue was used for specific histological studies by immunohistochemistry (IHC). Immunohistochemistry studies revealed that the majority of infiltrated inflammatory cells in extraorbital muscles were $CD3^+$ T cells. The number of infiltrated cells in the orbital tissue varied in different mice. Control mice immunised with β-Gal did not show any infiltrated $CD3^+$ T cells in orbital tissue. In addition, $F4/80^+$ macrophages were detectable in orbital tissue from animals immunised with hTSHR A-subunit plasmid *in vivo* electroporation significantly more than in orbital tissue from control mice. The infiltrate was uniformly negative for B cells using anti-mouse B220 mAb.

Herein below, a representative histopathological section of orbital tissue from each immune mice are illustrated to show more detail of two different subtypes of infiltrated inflammatory cells in mice undergoing experimental GO that were examined six weeks after end of immunisation. For clearer demonstration, different magnifications of H&E staining of retrobulbar tissues in immune mice were presented alongside with the next section of immunohistochemistry staining.

Intense interstitial inflammatory cells infiltration is clearly shown by H&E in mouse 60/0 (**Fig 3.9 A-C**), where immunohistochemistry staining confirmed the majority of them are $CD3^+$ T cells (**Fig 3.9 D-F**). Moreover, higher magnifications of H&E staining of mouse 60/L clearly demonstrates the adipose expansion that widely separating the orbital muscle fibre bundles (**Fig 3.0 G-I**). Furthermore, immunohistochemistry analysis in other immune animals that showed retrobulbar inflammation by H&E (**Fig 3.10 A, D**), revealed infiltration of $CD3^+$ T cells (**3.10 B** and **E**) and $F4/80^+$ macrophages (**Fig 3.10**

C and **F**) into extra-ocular muscle (marked by arrowhead). Quantification analysis in number of lymphocytic infiltrated cells in extraorbital mucsels was performed for all immune animals (**Fig 3.12**), the two mice with intense infiltration mostly around the optic nerve were delibrately excluded. The quantification data confirmed significant differences in number of infiltrated CD3^{+} T cells between hTSHR immunised mice and controls. The number of cells was analysed by ImageJ software on double-blinded fashion.
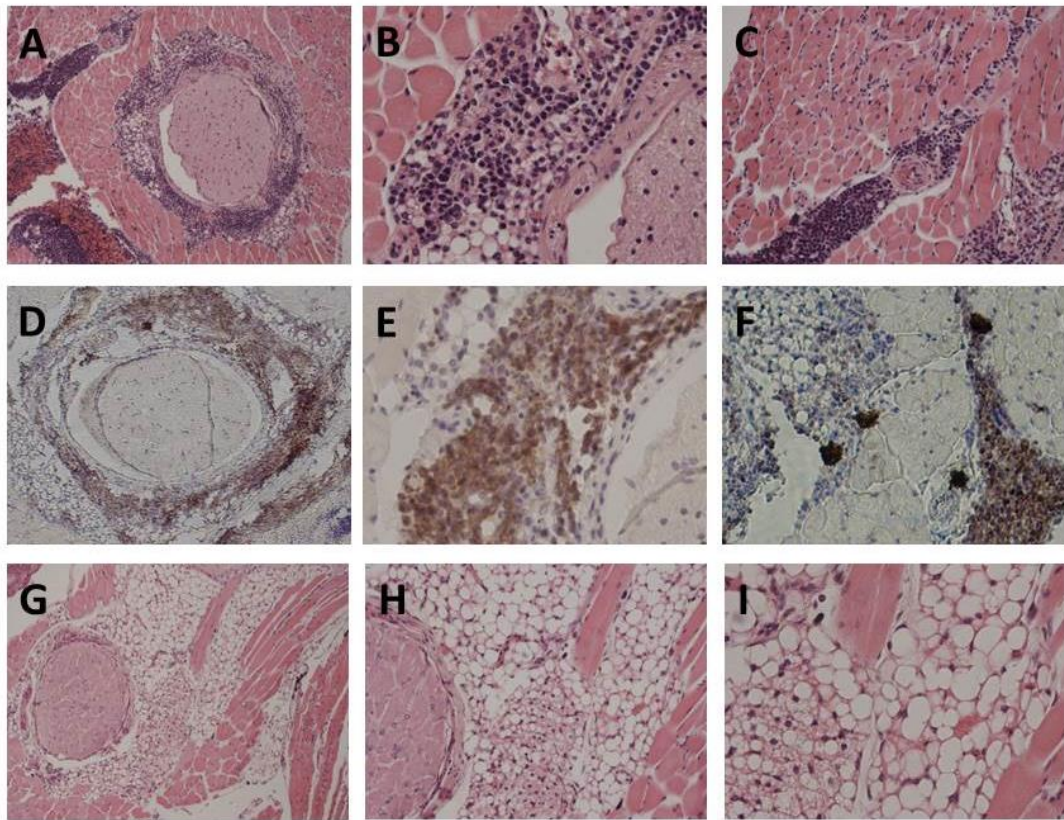
Fig 3.10 H&E and IHC studies in orbital tissue from mice 60/0 and 60/L

Histopathological study by H&E and IHC in orbital tissue from two mice immunised with hTSHR-A subunit plasmid [60/0 (panel A-F) and 60/L (panel G-I)]. (**A**) H&E staining of orbital tissue (100x) showing massive inflammatory infiltrate surrounding optic nerve and extraorbital muscles. (**B**) higher magnification of panel A (400x) to show intense infiltration around optic nerve. (**C**) higher magnification of panel A (200x) to show massive infiltration dissecting the orbital muscle fibre bundles. (**D**) IHC in serial section of panel A to identify CD3^{+} T cells showing massive CD3^{+} T cells (stained in brown using DAB as chromogen) infiltrating around the optic nerve and into the orbital muscle tissue (100x). (**E**) higher magnification of panel D (200). (**F**) higher magnification of panel D (200). (**G**) H&E staining of orbital tissue (100x) showing expansion of adipose tissue in retrobulbar fat. (**H**) higher magnification (200x) to show adipose tissue widely separating the orbital muscle fibre bundles. (**I**) higher magnification of panel H to demonstrate two different type of fat (white adipose tissue and brown adipose tissue are distinguishable by morphology).
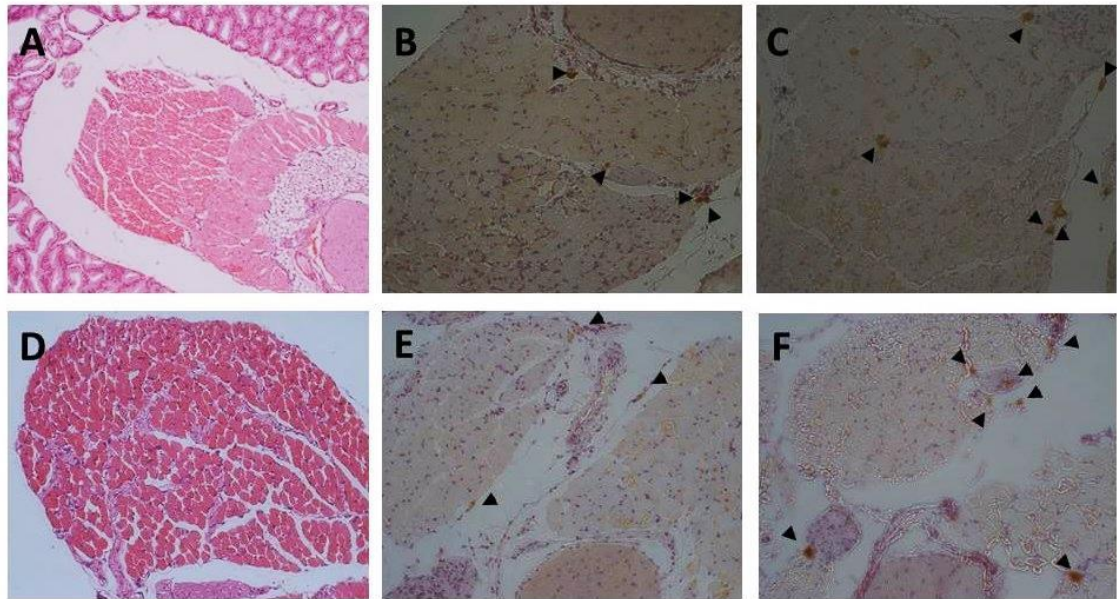
Fig 3.11 H&E and IHC studies in orbital tissue from mice 59/0 and 59/L

Histopathological study by H&E and IHC in orbital tissue from a mouse immunised with hTSHR-A subunit plasmid (59/0 and 59/L) sacrificed 6 weeks after end of immunisation. (**A**) H&E staining of orbital tissue (59/0) (100x) showing hypertrophy of extraorbital muscles and interstitial inflammatory infiltrate. (**B**) IHC to identify CD3^{+} T cells (arrowhead) showing CD3^{+} T cells (stained in brown using DAB as chromogen) infiltrating into the orbital muscle tissue (200x). (**C**) IHC to identify F4/80^{+} macrophages (arrowhead) showing macrophages infiltrating into the orbital muscle tissue (200x). (**D**) H&E staining of orbital tissue from a mouse immunised with hTSHR-A subunit plasmid (59/L) to show hypertrophy and dissecting the orbital muscle fibre bundles (200x). (**E**) IHC to identify CD3^{+} T cells (arrowhead) showing CD3^{+} T cells (stained in brown using DAB as chromogen) infiltrating into the orbital muscle tissue (200x). (**F**) IHC to identify F4/80^{+} macrophages (arrowhead) showing macrophages infiltrating into the orbital muscle tissue (200x).
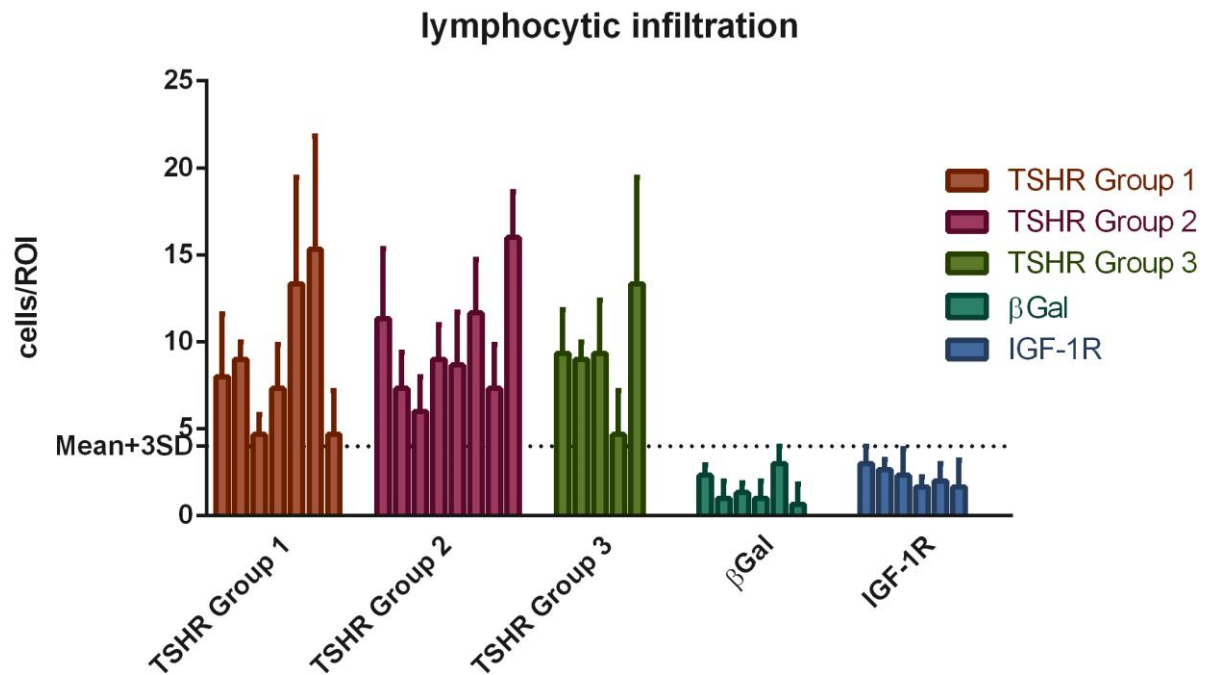
Fig 3.12 Quantification of number of infiltrated CD3⁺ T cells into retrobulbar tissue.

TSHR Groups 1,2, and 3 are outlined in Appendix 1. Note: two mice showing intensive infiltration of CD3+ T cells around the optic nerve (one from Group 1 and one from Group 3) were excluded.

The graph shows significant increase in number of lymphocytic infiltrated cells in all mice immunised with hTSHR A-subunit plasmid in three different groups comparing with control mice immunised with βGal and IGF-1R plasmid. The horizental dotted line represent meant+3SD of βGal mice.

3.3.1.5 Histopathological studies of chemosis

Graves' orbitopathy is characterised by orbital muscle inflammation and adipogenesis, resulting in expansion of the extraorbital tissue and proptosis. The extension of inflammation to eyelids and conjunctiva leads to swelling, redness and oedema which is called chemosis (Dickinson, 2010a).

From eight mice that were challenged with hTSHR A-subunit plasmid *in vivo* electroporation, two animals showed extraorbital changes with typical signs of acute orbital congestion, chemosis. Professor Miles Stanford (Consultant ophthalmologist) diagnosed the onset of chemosis in the immune mice. Interestingly, monitoring of chemosis over time in the animals showed one animal spontaneously to remit from the visual signs of chemosis after few days and the other animal remained congested over the period of two weeks of monitoring (**Fig 3.13**). Histological examination of the eyelid showed dilated and congested orbital blood vessels with typical features of vascular inflammatory reaction as well as infiltrating mast cells into the tissue (**Fig 3.14 A-C**).
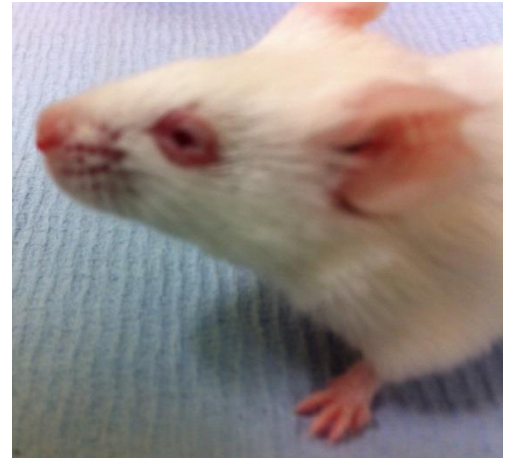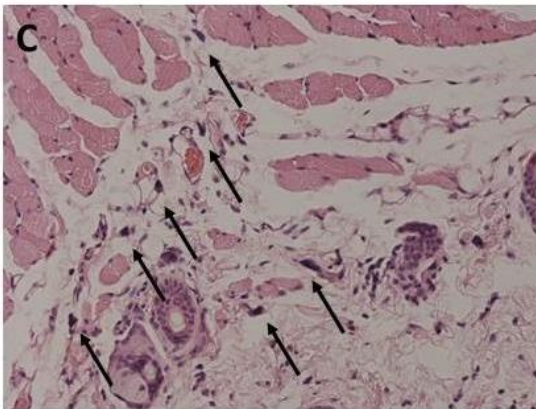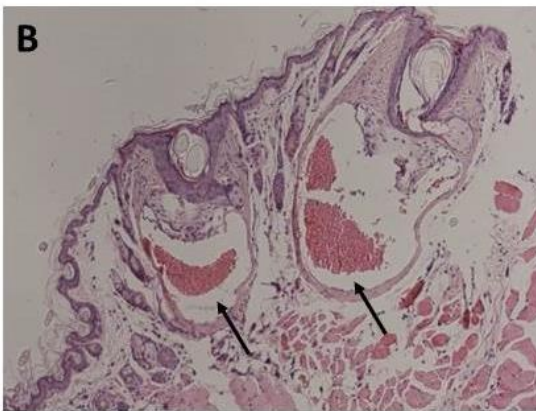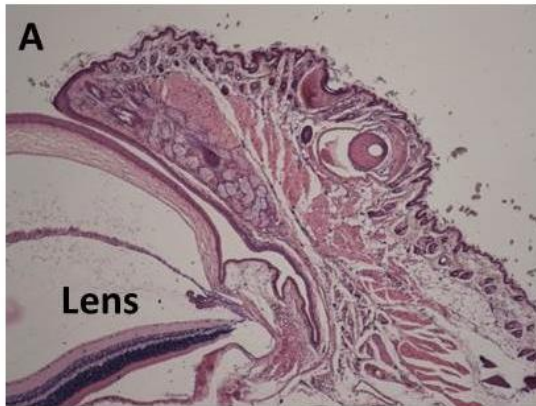
Fig 3.13 Appearance of head region of hTSHR-A subunit plasmid immunised mouse (59/2) undergoing chemosis

Fig 3.14 H&E stained section of eye lid tissue with chemosis
(**A**) Eyelid tissue to show dilated and congested orbital blood vessels, the lens is labelled (40x). (**B**) Higher magnification (100x) to show congested blood vessels (arrowed). (**C**) Higher magnification (200x) to show mast cell infiltration into congested eyelid tissue (arrowed).

3.3.1.6 Evaluation of thyroid function

Following the histopathological analysis of thyroid gland and retrobulbar tissue in experimental GO model, evaluation of thyroid function was proceeded to uncover the alteration thyroid status. Total T4 measurements in mice undergoing experimental thyroid autoimmunity are commonly used for first assessment of endocrine status during the course of disease. However, mouse total T4 concentrations are variable and also dependent on the strain (McLachlan et al., 2012), thus it is not the most reliable indicators of thyroid function, but are commonly measured in experimental models as an indicator of thyroid function (Nagayama et al., 2002, Chen et al., 2003, Gilbert et al., 2006). We first determined the range of serum total T4 in 13 normal female BALB/c mice. Absolute values of serum total T4 in normal mice ranged between 115.5 and 142.7 nmol/L. Based on these results, statistical analysis indicated mean of population and standard deviation (SD) respectively were 126.1 and 9.113. Thus, the range of mean- 3SD (95 nmol/L) set as lower range and mean+3SD (156 nmol/L) set as upper range for normal mice sera and any value out of this range would be recognised as abnormal.

Total serum T4 was measured in the serum samples from immune mice sacrificed 6 weeks after end of immunization (**Fig 3.15**). Two animals showed significant reduction in total T4, confirming hypothyroidism. The remaining five immune mice showing trend towards lower T4 values which is in close correlating with the findings of hypothyroid glands by histology (**Fig 3.6 A-G**). The one animal with hyperthyroid histology showed significantly elevated levels of T4. Coupling thyroid histology and total T4 test results confirmed that thyroid status of this set of immune animals have

been truly hypothyroid. T4 values in mice similarly immunised with pTRiEx1.1 neo-IGF-1Rα plasmid and pTRiEx1.1 neo-β-Gal plasmids *in vivo* electroporation showed not significant changes from normal mice sera.
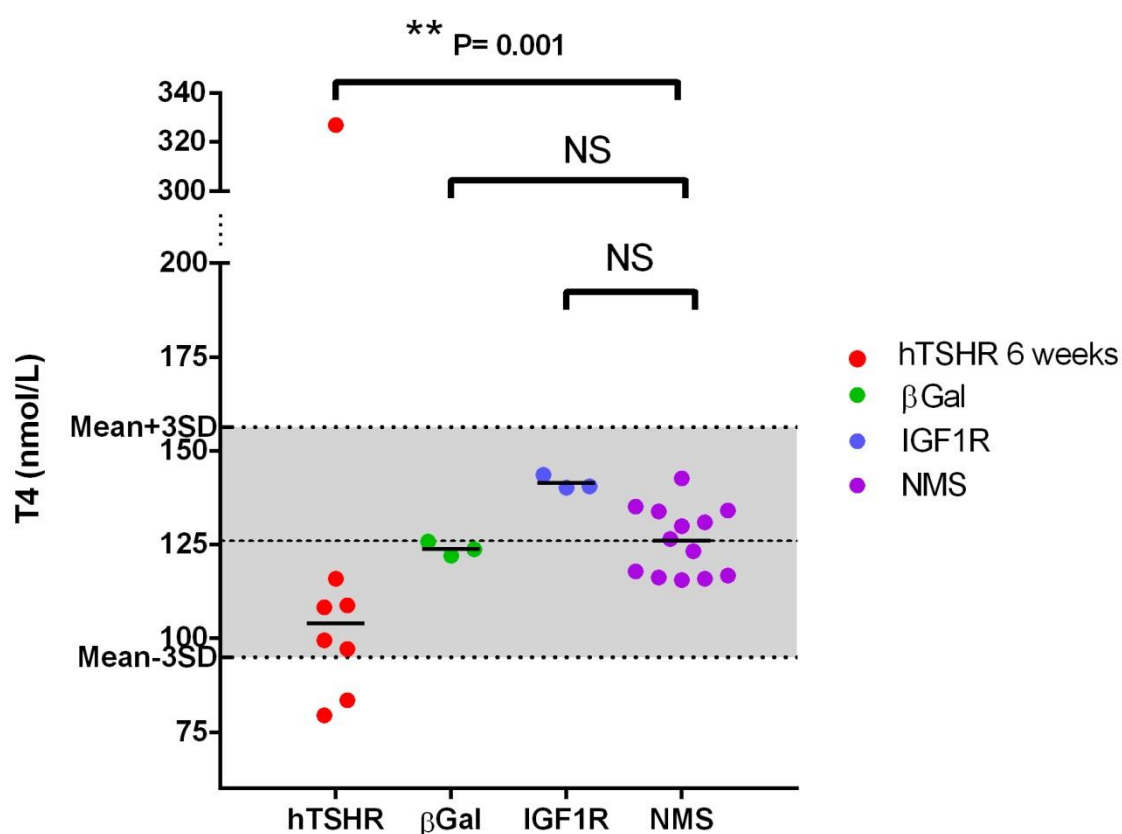
Fig 3.15 Evaluation of thyroid function by ELISA in mice sera of Group 1
Evaluation of thyroid function by ELISA in mice sera obtained 6 weeks after end of immunisation**.** Results indicate significant general downward trend in T4 level of mice immunised with hTSHR A-subunit plasmid (hTSHR) in comparison to non-immune control mice (NMS). There are two immune animals with statistically significant decrease T4 level and one with significant increase. The T4 value for animals immunised with IGF-1Rα plasmid and with β-Gal plasmid did not show alteration compared to NMS.

3.3.1.7   Evaluation of thyrotropin binding inhibition immunoglobulins activity (TBII)

The hTSHR A-subunit plasmid *in vivo* electroporation immunisation in female BALB/c mice is recognised for robust antibody responses to TSHR, which persist for months after end of immunisation (Kaneda et al., 2007, Zhao et al., 2011). To evaluate immune response, thyrotropin binding inhibition immunoglobulin (TBII) level in immune animals was measured (**Fig 3.16**). As the TRAK kits are highly optimised for using 100μl serum sample in the assay, due to limiting quantity of mouse serum, the assay was modified to use 50 μL mouse serum mixed with 50μl human serum known to be negative for TBII activity.

All immune serum samples showed more than 50% inhibition of ^{125}I-TSH binding activity, with the majority of sera showing more than 70% inhibition. Basically, sacrifice sera from majority (7 out of 8) of immune mice could inhibit more than 70% of radiolabeled bTSH which scored as highly positive. Only one animal from this group of immunisation showed 50% inhibition of ^{125}I-labeled bovine TSH which was still far more than suggested grey zone by the assay instruction (15%) and control samples (**Fig 3.16**). This result showed that hTSHR A-subunit plasmid *in vivo* electroporation immunisation in this group of mice successfully maintain humoral immunity for six weeks after end of immunisation which is similar to the finding by former study in our laboratory (Zhao et al., 2011).
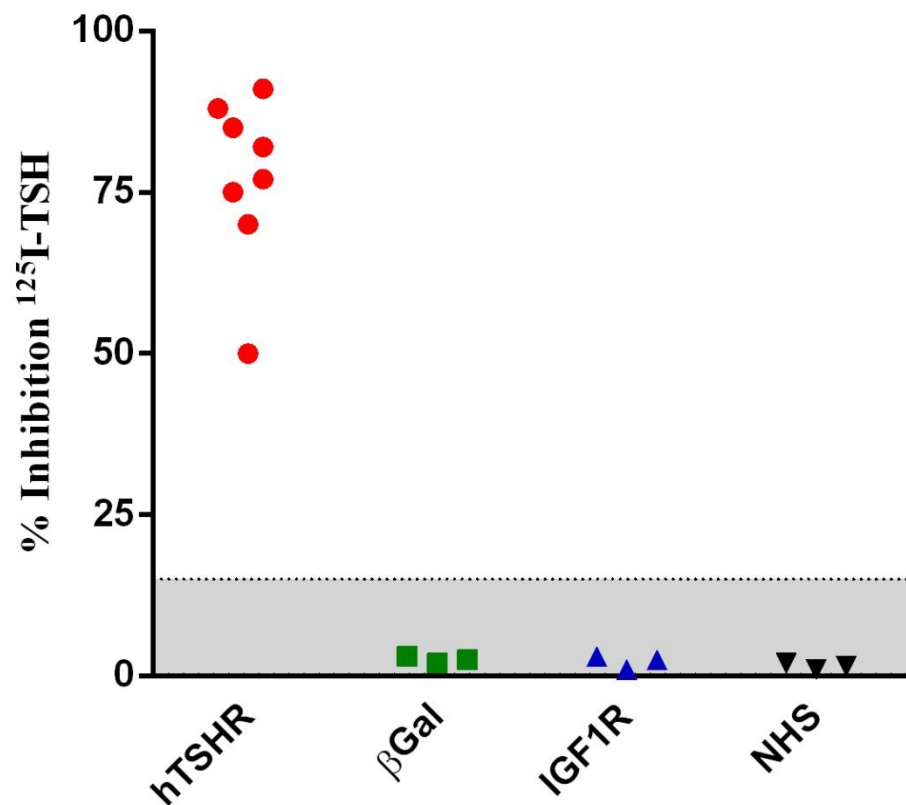
Fig 3.16. **TRAK assay in immune mice sera of Group 1**

Measurement of TSH binding inhibitory immunoglobulin activity in Group 1 mice by competition with ^{125}I-labelled bTSH (TRAK assay). The ordinate refers to % inhibition of ^{125}I-labelled bTSH binding. By the instruction of TRAK kit the area between 0-15% inhibition represents the 'grey' zone and values above this area generally scored positive. The control samples including mice sera that immunised with β-Gal plasmid (βGal) and IGF-1Rα plasmid (IGF1R) as well as normal human samples (NHS) were proved to be negative.

3.3.1.8 Determination of TSHR stimulating and blocking Abs

The antibodies to TSHR comprise three different types, thyroid stimulation antibodies (TSAbs), thyroid stimulation blocking antibodies (TSBAbs) and neutral antibodies (Rees Smith et al., 1988). TSAbs mimic the actions of TSH and initiate the TSHR signalling cascade leading to hyperthyroidism. In contrast, TSBAbs inhibit the stimulation of TSHR

by TSH leading to decrease thyroid hormone secretion (Rees Smith et al., 1988, Jaume et al., 1997). TSHR blocking antibodies binding site is not exactly similar to stimulating Abs (Sanders et al., 2007, Sanders et al., 2011, Morshed et al., 2012), however, TSBAbs inhibit the binding of TSH to receptor which then leads to hypothyroidism. On the other hand, neutral TSHR antibodies neither block TSH binding site nor induce cAMP generation. Thus, determination of anti-TSHR antibody subtypes was necessary.

To examine subtypes of antibodies to TSHR, there are few different bioassay methods (Lytton and Kahaly, 2010). In this study, cell based cAMP endpoint assay was performed to measure TSAbs and TSBAbs in mice sera. The JP09 cells, CHO (Chinese Hamster Ovary) cell line stably transfected to express full length human TSHR (Perret et al., 1990) provides a powerful response when stimulates with TSH or thyroid stimulating antibodies. The strength and concentration of TSHR stimulating antibodies is directly correlated to production of cAMP from JP09 cells. Examination of TSBAbs in mice sera requires an extra step, incubation of cells with sub saturation dose of bovine TSH (bTSH).

The first bioassay experiment was performed to evaluate suboptimal dose of bTSH. The bTSH dose response (concentration from 0.005 to 1.6 mU/ml) was demonstrated that 0.2 mU/ml bTSH can be used as sub-optimal dose for subsequent studies (**Fig 3.17**). In all experiments, Forskolin and KSAb1 mAb (100, 10, 1 and 0.1 µg/ml) were used as the positive controls and IgG$_2$b (100 and 10 µg/ml) as the negative control.
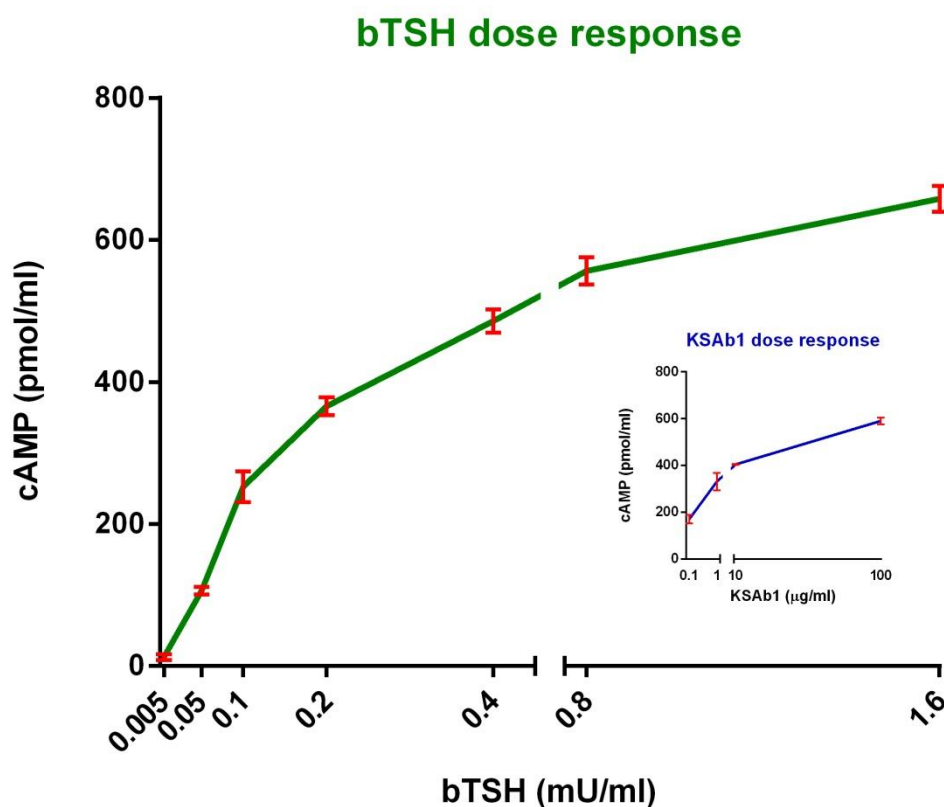
Fig 3.17 The bovine TSH dose response in cAMP bioassay
Different concentration from 0.005 to 1.6 mU/ml was tested. Based on the results of this experiment the concentration of bTSH at 0.2 mU/ml was used as sub-optimal dose for subsequent studies. The experiment has performed twice in different days to assess reproducibility of assay which shows very close outcome (less than 5% difference throughout). The inset shows the results of different concentration (0.1-100µg/ml) of TSHR mAb (KSAb1), which has been done twice. The bar represents standard deviation.

3.3.2 Longitudinal studies on TSHR antibodies during the course of disease

To evaluate TSHR antibodies, longitudinal study was performed in a new cohort of

eight female BALB/c mice. Animals were challenged with 50µl plasmid (1mg/ml) TSHR

A-subunit plasmid into each biceps femoris muscle with *in vivo* electroporation. This

new group served to evaluate the reproducibility of the model and also serum was

analysed from weekly serial bleeds for longitudinal studies. Extra attention was paid to retain consistency in each injection of plasmid using modified protocol. Animals were sacrificed nine weeks after end of immunisation. In addition, in week seven after end of immunisation, some immune animals underwent MRI (see Chapter 4). Serum T4 measurements showed significantly depressed hormone levels in this new cohort of animals. The reduction in serum total T4 and hence hypothyroid status in immune animals was replicated. High levels of anti-TSHR antibodies were present at point of sacrifice. TSHR antibodies comprised predominantly of TSBAbs, which evolved early during the immune response and persisted for several weeks. Histological analysis of thyroid glands showed majority of mice with hypothyroid glands. In addition, histological analysis of the orbital tissue in this group showed the same pattern of orbital pathology as described for the six weeks after end of immunisation group, comprising predominantly of interstitial inflammatory infiltrate into extraorbital muscle. Importantly, disease heterogeneity was apparent by histological analysis of the orbital tissue. Two animals showed visible chemosis, confirmed by dilated blood vessels with accompanying oedema.

3.3.2.1 Histological study of thyroid gland

Animals were sacrificed nine weeks after end of immunisation. Interestingly, similar to the former group of immune mice, Group 1 immunisation (sacrificed six weeks after end of immunisation), histological studies in this cohort of animals predominantly showed hypothyroid features in thyroid gland (**Fig 3.20 A-F**). Thyroid gland from two

mice in this group showed hyperthyroidism (**Fig 3.20 G, H**). Importantly, histological

analysis of thyroid gland in this cohort of immune animals compare to the former

group proved reproducibility of animal model with hypothyroidism in mice immunised

with hTSHR A-subunit.
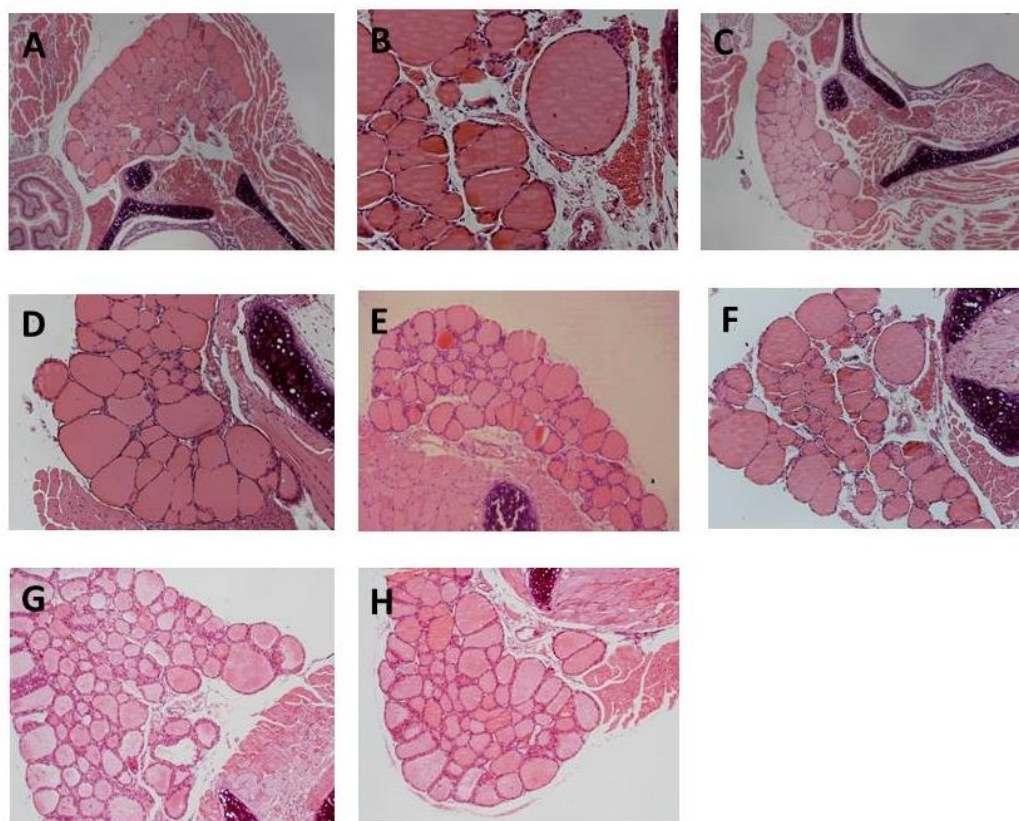
Fig 3.20 Thyroid histological studies in immune mice of Group 2
Thyroid histological studies on n=8 mice immunised with hTSHR A-subunit *in vivo* electroporation and sacrifice 9 weeks after end of immunisation. All sections are at 100x magnification (**A**-**F**) pathological feature of hypothyroidism (**G**, **H**) pathological feature of hyperthyroidism.

3.3.2.2   Studies into retrobulbar histopathology

Animals immunised with hTSHR A-subunit plasmid showed histological signs of orbital pathology. Histological analysis of the orbital tissue in this group showed the same pattern of orbital pathology as described for the former group of immune mice. Seven out of eight immune animals showed interstitial inflammatory infiltrate into extraocular muscle, extending into the muscle tissue (**Fig 3.21 A-D, F-H**). In addition, one animal showed extensive adipogenesis, characterised by expansion of retrobulbar adipose tissue and widely separating the orbital muscle fibre bundles (**Fig 3.21 E**).
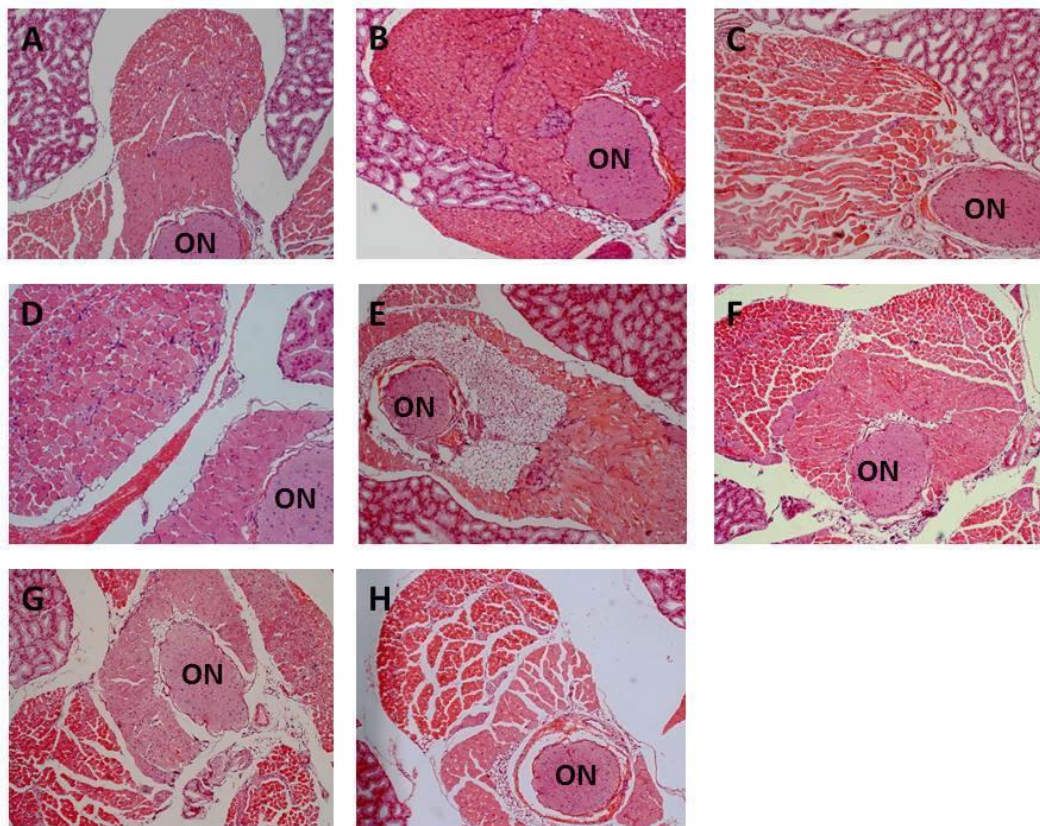
Fig 3.21 H&E stained section of retrobulbar tissue from immune mice of Group 2
H&E stained section of retrobulbar tissue from individual mice immunised with hTSHR A-subunit plasmid. All slides are at 100x magnification. (**A**) 63/0, (**B**) 63/L, (**C**) 63/R, (**D**) 63/2, (**E**) 64/0, (**F**) 64/L, (**G**) 64/R, (**H**) 64/2.

3.3.2.3 Histopathological studies of chemosis

From eight mice that were challenged with hTSHR A-subunit plasmid by the modified protocol two animals showed extraorbital changes with typical signs of acute orbital congestion, chemosis (**Fig 3.22 A, B**). Histological analysis of the animals confirmed dilated blood vessels with accompanying oedema (**Fig. 3.23 A, B**). Interestingly, mast cells were readily recognised by morphology. (**Fig. 3.23 C**).
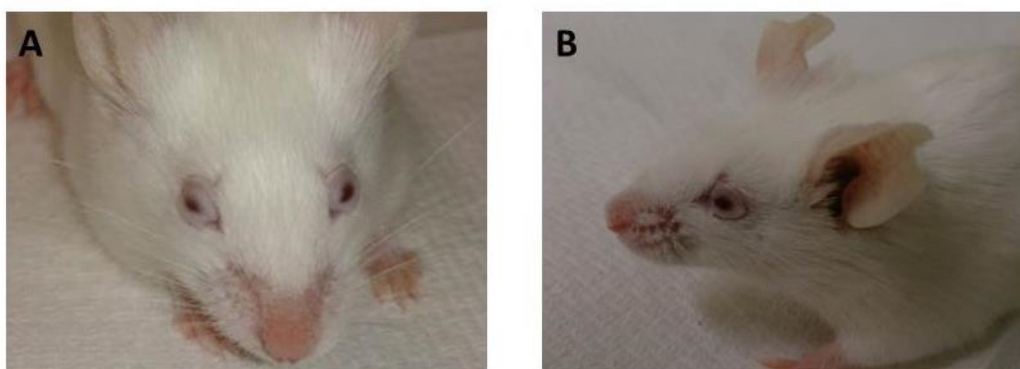
Fig 3.22 Appearance of head region of two immune mice with chemosis
Appearance of head region of two mice immunised with TSHR A-subunit plasmid *in vivo* electroporation sacrificed 9 weeks after end of immunisation showing chemosis.
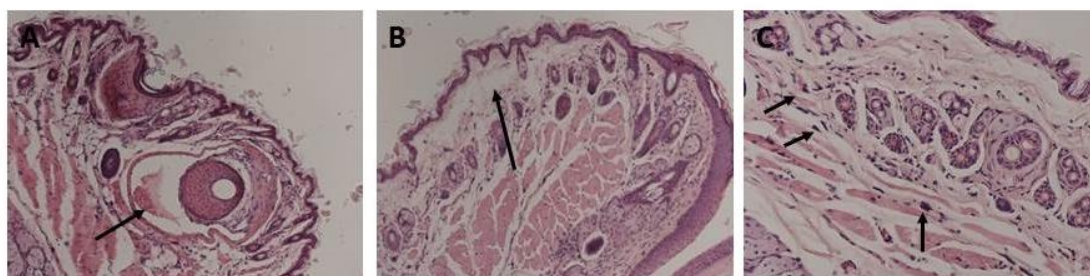
Fig 3.23 H&E stained section of eyelid with chemosis
H&E stained section of eyelid congested tissue from mouse head shown in (Fig 3.27 A) to show (**A**) dilated and congested orbital blood vessels (arrowed) (100x), and (**B**) highlighting oedema (arrowed) (100x) and (**C**) mast cells infiltration (arrowed) (400x).

3.3.2.4   Evaluation of thyroid function

To confirm histological analysis of thyroid gland from immune animals, thyroid function was evaluated in serum obtained 9 weeks after end of immunisation (**Fig 3.24**). Similarly to the former cohort of immune mice, results from total T4 test also showed a hypothyroid status;. Three animals showed significant depressed values of total T4, with one animal very close to the lower border of normal range for T4 values, correlating with the findings of hypothyroid glands by histology (**Fig 3.20 A-D**). Two animals with hyperthyroid histopathology (**Fig 3.18 G, H**) showed significantly elevated levels of T4.
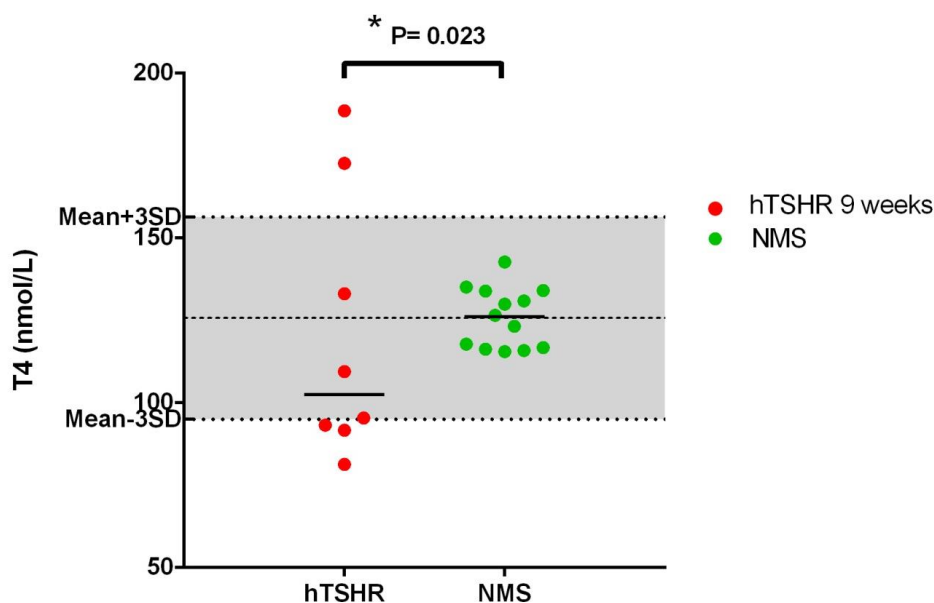
Fig 3.24 Evaluation of thyroid function by ELISA in immune mice sera of Group 2

Evaluation of thyroid function by ELISA in mice sera obtained 9 weeks after end of immunisation. Results indicate general downward trend in T4 level of mice immunised with TSHR A-subunit plasmid (TSHR) in comparison to non-immune control mice (NMS). It also shows that 2 immune animals with significant increase T4 level while 3 other immune mice are significantly depressed.

3.3.2.5 Longitudinal studies into TSHR Abs

We performed longitudinal studies to evaluate TSHR antibodies. Serum was analysed from weekly serial bleeds. All animals were sacrificed nine weeks after end of immunisation. At the sacrifice point high levels of anti-TSHR antibodies were present, and comprised predominantly of TSBAbs, which evolved early during the immune response and persisted for several weeks (**Fig 3.25**). Basically, six out of eight immune mice were highly positive for TSBAbs throughout all points of bleeding (one week before last injection to six weeks after end of immunisation). The TSBAbs level in other two animals did not show significant increase, although it was weak positive in some points.

The longitudinal study revealed that the TSAbs level in majority of immune mice did not increase during the course of immunisation (**Fig 3.26**). There was only one animal showed very high level of TSAbs which gradually decline by time. It is in contrary with results provided by adoptive transfer of TSHR autoantibody where the majority of TSHR antibody were TSAbs at the beginning point and turn to the TSBAbs after 22 weeks (Nakahara et al., 2012).
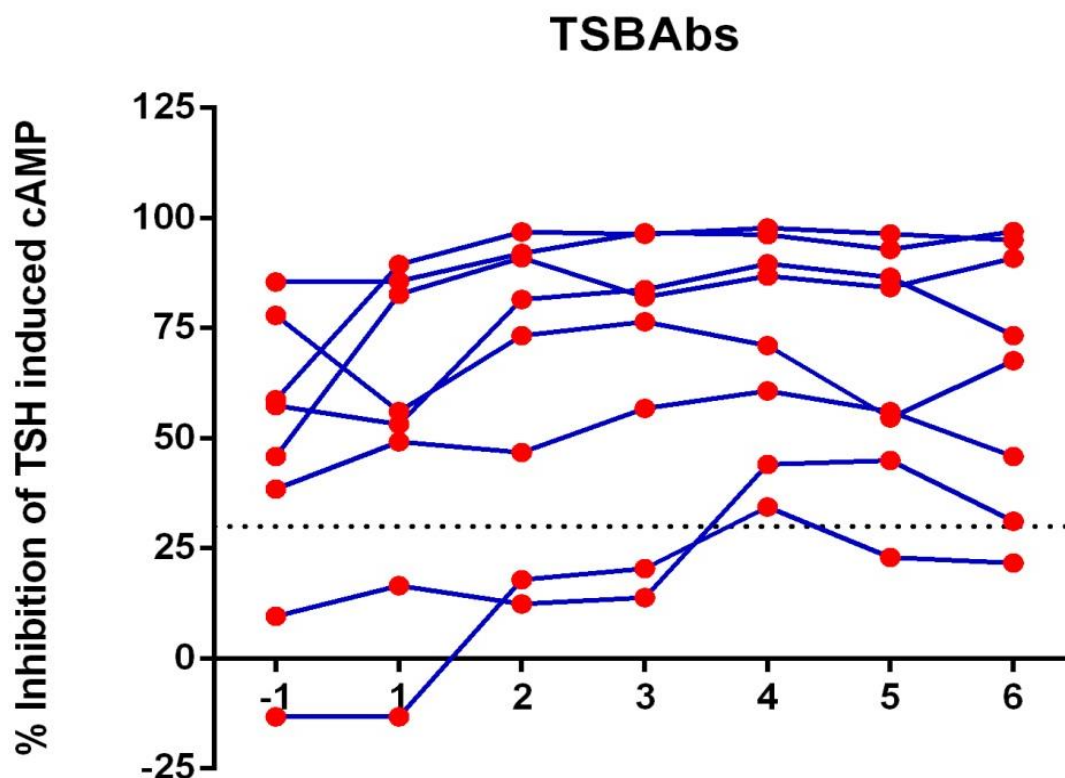
Fig 3.25 Longitudinal analysis of TSBAbs

Longitudinal analysis of TSHR antibodies induced after TSHR A-subunit plasmid-*in vivo* electroporation in individual eight immune mice in Group 2 immunisation. Serum samples were collected for TSHR antibody analysis on a weekly basis. The ordinate shows week when serum sample collected, with the first sample collected one week before the end of immunization (labelled -1), with all subsequent bleeds collected weekly until 6 weeks end of immunization. Measurement of blocking TSBAbs as % inhibition of TSH mediated stimulation (abscicca). Six animals were highly positive for TSBAbs, which evolved early during the immune response and persisted for several weeks.
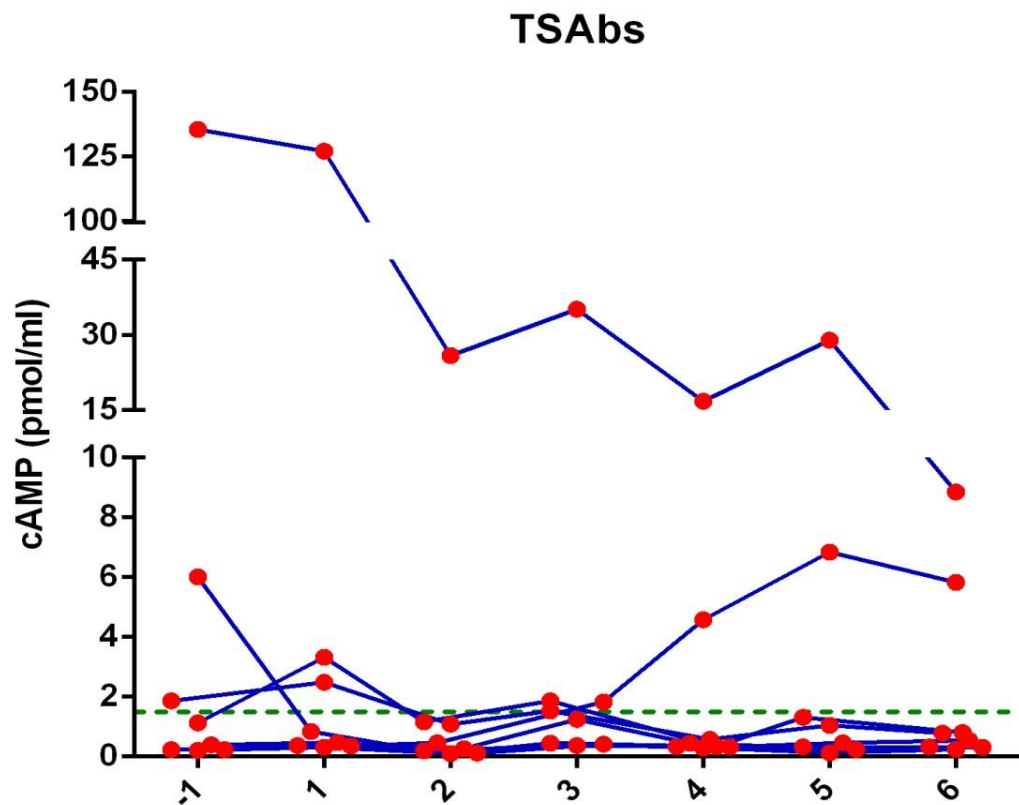
Fig 3.26 Longitudinal analysis of TSAbs

Longitudinal analysis of TSHR antibodies induced after TSHR A-subunit plasmid-*in vivo* electroporation in individual eight immune mice in Group 2 immunisation. Serum samples were collected for TSHR antibody analysis on a weekly basis. The ordinate shows week when serum sample collected, with the first sample collected one week before the end of immunization (labelled -1), with all subsequent bleeds collected weekly until 6 weeks end of immunization. Measurement of TSAbs shown as cAMP responses (pmols/ml) of serum sample bleeds (abscicca). Note the one animal positive for TSAbs, which gradually decline with time.

159

3.3.3 Characterisation of long-term immunity to hTSHR

The hTSHR A-subunit plasmid *in vivo* electroporation model in female BALB/c mice is recognised for robust antibody responses to TSHR, which persist for months after end of immunisation (Kaneda et al., 2007). To study long-term effect of modified immunisation in ongoing immune animals, a group of six animals were immunised, Group 3 immunisation. Histopathology of thyroid and retrobulbar tissues as well as hormone and antibody levels examined 15 weeks after end of immunisation. In addition to six animal immunised with pTRiEx1.1 neo-hTSHR A-subunit plasmid *in vivo* electroporation, control animals immunised with pTRiEx1.1 neo-IGF-1Rα (n=3) and pTRiEx1.1 neo-β-Gal plasmids (n=3) were also examined 15 weeks after end of immunisation (**Appendix 1**). Antibodies to TSHR that persisted for 15 weeks, demonstrated 4 out of the 6 animals with strong TSBAb antibodies with weak TSAbs. H&E examination of orbital tissue was characterised by orbital muscle fibrosis, which by Masson's Trichrome staining exhibited extensive deposition of glycosaminoglycans with pericellular fibrosis in retrobulbar tissue. Thyroid gland histology from five out of the six animals showed hypothyroid status.

3.3.3.1   Studies into retrobulbar histopathology

Orbital tissue of immune animals and controls were examined by histological analysis. H&E stained sections of immune animals demonstrated inflammation in retrobulbar tissue. Inflammed retrobulbar tissue in immune mice was characterised by inflammatory cells infiltration into the extraorbital muscles that were confirmed by immunohistochemistry. A representative figure of H&E stained section of orbital tissue from immunised mice with pTriEx-hTSHR A-subunit plasmid are shown in **Fig 3.30 A-I**.

Interestingly, one immune mouse demonstrated intense lymphocytic infiltration in retrobulbar tissue particularly around the optic nerve (**Fig 3.31 A-C**). Moreover, another immune mouse showed excessive adipogenesis (**Fig 3.31 D-F**). In addition, fibrosis in orbital muscles by Masson's Trichrome staining exhibited extensive deposition of glycosaminoglycans with pericellular fibrosis in retrobulbar tissue (**Fig 3.32** **A-F**).
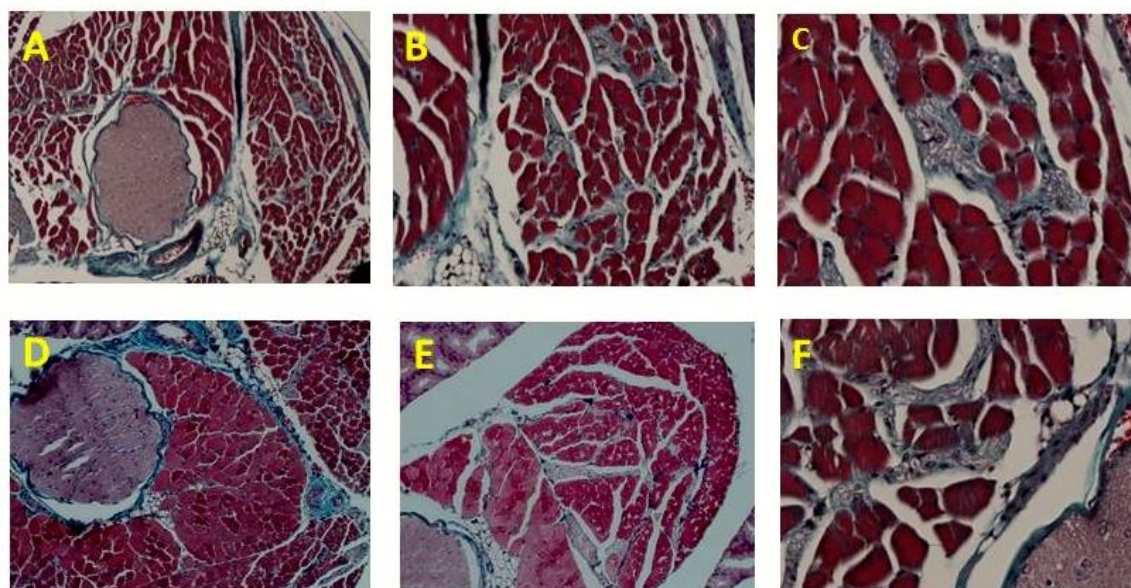
Fig 3.32 Masson's Trichrome staining in mice from Group 3

Masson's Trichrome staining to detect fibrosis in the retrobulbar tissue of mice were immunised with pTriEx-hTSHR.

3.3.3.2   Evaluation of thyroid function

Thyroid hormone level (total T4) was investigated in sera collected from immune mice sacrificed at 15 weeks after end of immunisation (**Fig 3.31**). Results from total T4 test proved thyroid histopathology. Interestingly, in this cohort of immunisation there was not any elevated T4 level as it expected from thyroid histology. Two mice showed significant depressed values of total T4, with remaining four mice showing a trend towards lower T4 values, correlating with the findings of hypothyroid glands by

161

histology (**Fig 3.26 A-G**). T4 values in mice similarly immunised with pTRiEx1.1 neo-IGF-1Rα plasmid and pTRiEx1.1 neo-β-Gal plasmids *in vivo* electroporation showed not significant changes from normal mice sera.
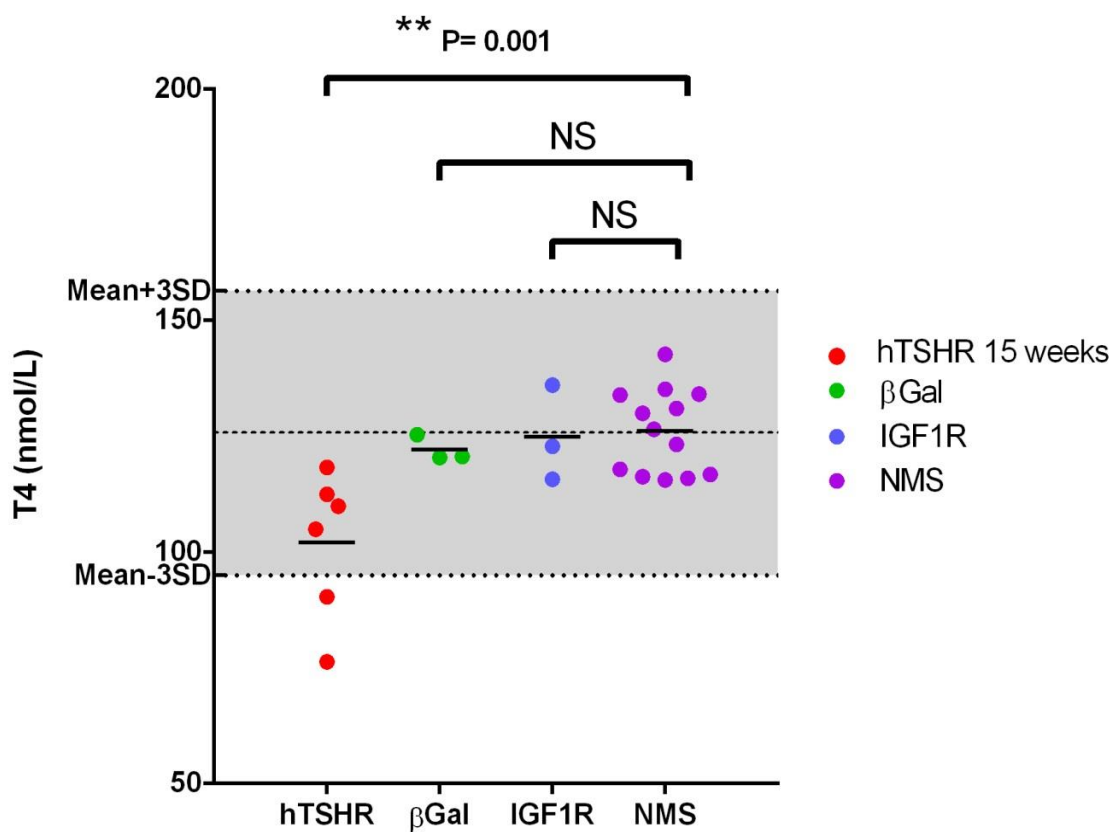
Fig 3.33 Evaluation of thyroid function by ELISA in mice sera from Group 3
Evaluation of thyroid function by ELISA in mice sera obtained 15 weeks after end of immunisation. Results indicate general downward trend in T4 level of mice immunised with TSHR A-subunit plasmid (TSHR) in comparison to non-immune control mice (NMS). It also shows that 2 immune mice with significantly depressed T4 value.

3.4 Discussion

In the studies described in this Chapter, a total number of 22 mice were evaluated in depth for onset of Graves' disease and concurrent orbital manifestations following the modified immunisation protocol with hTSHR A-subunit plasmid *in vivo* electroporation, together with 12 control mice immunised with pTRiEx1.1 neo-IGF-1Rα (n=6) and pTRiEx1.1 neo-β-Gal plasmids (n=6). In addition, following the publication of the latter data(Moshkelgosha et al., 2013), another cohort of mice (n=8) was immunised with hTSHR A-subunit plasmid *in vivo* electroporation to especially study IGF-1R antibodies which will be discussed later in Chapter 5 (**Appendix 1**).

This study was initiated based upon the earlier study from our laboratory which showed that hTSHR A-subunit plasmid *in vivo* electroporation led to the onset of Graves' hyperthyroid disease (disease incidence of 66%) accompanied in some animals with fibrosis in orbital tissue (Zhao et al., 2011). Having successfully obtained experimental Graves' disease with the new model accompanied by signs of orbital disease, the objective of my project was to modify the immunisation procedures in an attempt to induce experimental disease accompanied by *bona fide* GO. Earlier, preliminary studies from our laboratory to modify the immunisation procedure by reducing the concentration of hTSHR A-subunit plasmid from 50μg to 25μg led to a dramatic reduction in disease incidence to 12.5% (Zhao and Banga, Unpublished data). In other preliminary experiments to modify the delivery of the plasmid injection, we attempted giving the injection of 50μl plasmid in five closely, but separate areas of the leg muscle to increase the surface area of the injection site prior to the electroporation. However, we found that 5x10μl injections in a small localised area

was technically difficult to replicate and too demanding. In order to pursue with alteration of the antigenic dose of hTSHR A-subunit plasmid, we aimed to 'spread' 50 µg of plasmid over wider area of muscle. This was achieved during the injection procedure by slow withdrawal of the needle as the plasmid was injected, resulting in a 'wider spread' of the plasmid in the leg muscle. For reproducibility, this method was performed with great care and was remarkably successful in inducing the onset of orbital pathology in the model.

In comparison with study reported by Dr Zhao and colleges (Zhao et al., 2011), the modification of plasmid delivery resulted in marked different outcome in the immune response and consequent thyroid function, as well as the resultant of orbital pathology. The comparison between previous study in our laboratory (Zhao et al., 2011) and Group 1 of immunisation in this study, is reasonably legitimate as the immune animals in both the different studies were evaluated at six weeks after end of immunisation. Surprisingly, however the outcome of thyroid function following the two immunisations procedures was dramatically different. Hyperthyroidism was induced in 8 out of 12 immune animals (66%) in the Zhao et al study, compared to 1 out of 8 immune animals (12.5%) in Group 1 in this study. Moreover, the modified protocol induced dramatic remodelling of the orbital tissue. The different pathological, immunological and thyroid function outcomes in the Zhao et al study and the model described herein are not due to a change in the commercial supplier of the mice (Harlan Laboratories, UK) nor in the rodent chow diet with an iodine content of 1.2mg/Kg (Zhao et al., 2011). In addition, the animal unit housing conventional clean

rooms for the mice in the Zhao study and the unit housing the animals in this study was unchanged.

Thus, we conclude that the modification in the plasmid immunisation resulted in a dramatic different outcome in the immune response to TSHR (Chen et al., 2004) with resultant orbital pathology. Interestingly, a recent study in an experimental optic neuritis inflammation which is one of the first complications of multiple sclerosis (MS) clearly emphasised that alteration in antigenic dose led to different outcome of the disease conditions (Soares et al., 2013). Soares and colleagues showed that injection of either 100 µg or 300 µg of a peptide immunoge (MOG35–55) in complete Freund's adjuvant, resulted in a different immune response during the course of disease development and also different forms of evolution of optic neuritis. In our study, although we have not altered the immunogenic dose, the modification of immunisation has changed the immune response as well as orbital pathology (Moshkelgosha et al., 2013).

For the GO model developed in this thesis, the contribution of environmental pathogens to the onset of orbital disease is not known, since an independent group of animals has not been evaluated under specific pathogen free (SPF) conditions. Infection is an important environmental factor for development of Graves' disease, particularly with the bacterium *Yersinia enterocolitica* (Bech et al., 1974, Lidman et al., 1974, Shenkman and Bottone, 1976). Our animal unit is tested quarterly for a wide range of pathogens, with no new or opportunistic infections reported. It would be in particular interest to compare the histopathological results of immune mice maintained in SPF or conventional clean rooms to address this issue. Interestingly, the

adenovirus model demonstrates no major difference in the development of experimental Graves' disease when the animals were housed under SPF conditions (Nagayama et al., 2002, Chen et al., 2003, Ye et al., 2011, Wu et al., 2011, Ye et al., 2012) compared to animals housed in conventional clean conditions (Gilbert et al., 2006, Johnson et al., 2013).

The results of this Chapter clearly demonstrate the hypothyroid status in the immune animals. Hypothyroidism status has been confirmed by histological analysis of thyroid gland, total T4 level in the immune mice sera and significant weight gain. Examination of thyroid glands of GO experimental model by H&E staining shows typical pattern of hypothyroidism, with features including of thinning epithelial cells. In addition to histological analysis of thyroid gland, significant weight gain in immune mice during course of disease suggests the under activity of thyroid gland i.e. hypothyroidism. Furthermore, total T4 level in immune mice sera demonstrates significant downward trend in comparison to controls. The gold standard assay for determining thyroid status in the experimental model of Graves' disease is measurement of mouse TSH (mTSH). A number of highly sensitive assays have been described for assessing serum mTSH level (Carayanniotis et al., 1995, Pohlenz et al., 1999, Zhu et al., 1999, Shibusawa et al., 2000, Schneider et al., 2001, Li and Carayanniotis, 2007). However, as the hypothyroid status has been shown by a variety of different regimes including thyroid histology, reduction in weight and total T4 level, the majority of animals in this study are hypothyroid; although, mTSH has not been evaluated. We have considered using available commercial assays for measuring mTSH. All the available commercial kits are based on ELISA and have drawbacks such as requiring large serum volume (100µl) and

also suffer from a wide range of coefficient variation (CV). Moreover, the commercial assays use mTSH concentration measured as units of activity to quantify the concentration of mTSH in the assays. Although, we contacted company representatives to tackle these technical issues, we decided not to spend more time, effort, and valuable resources in measuring mTSH concentrations using these commercial kits.

3.5 Summary

To summarise the overall pathological findings in this study, 22 immune animals have been studied in depth following the modified immunisation protocol with hTSHR A-subunit plasmid *in vivo* electroporation. All animals show asymmetrical bilateral orbital pathology, comprising of inflammation of extraorbital muscle. Importantly, disease heterogeneity was apparent in some immune mice showing discreet orbital pathology, with two animals showing a large inflammatory infiltrate around the optic nerve and three animals with extensive adipogenesis accompanied by expansion of retrobulbar adipose tissue. Fibrosis in the retrobulbar tissue was apparent towards the end stage of disease when immune animals left for long time. Three animals showed signs of chemosis. None of the 12 animals immunized with control plasmids show any orbital pathology or disease. Orbital pathology of all 22 immune mice is summarised in **Appendix 1**.

Chapter Four

Neuroradiological analysis in experimental GO model

# 4.	Neuroradiological analysis in experimental GO model

## 4.1	Introduction

Graves' orbitopathy usually affects both the eyes symmetrically. However, in 15% of patients, it is asymmetric bilateral or unilateral (Muller-Forell and Kahaly, 2012). The clinical manifestation in most of GO patients are readily diagnosed by obvious lid retraction combined with proptosis and most likely with Graves' disease history (Dickinson, 2010b). But, for accurate diagnosis in patients with asymmetric bilateral or unilateral protrusion or suspected optic neuropathy, orbital imaging is necessary (**Fig 4.1**). Also, prior to decompression surgery, neuroradiological imaging is required to assess pathology (Pitz, 2010).
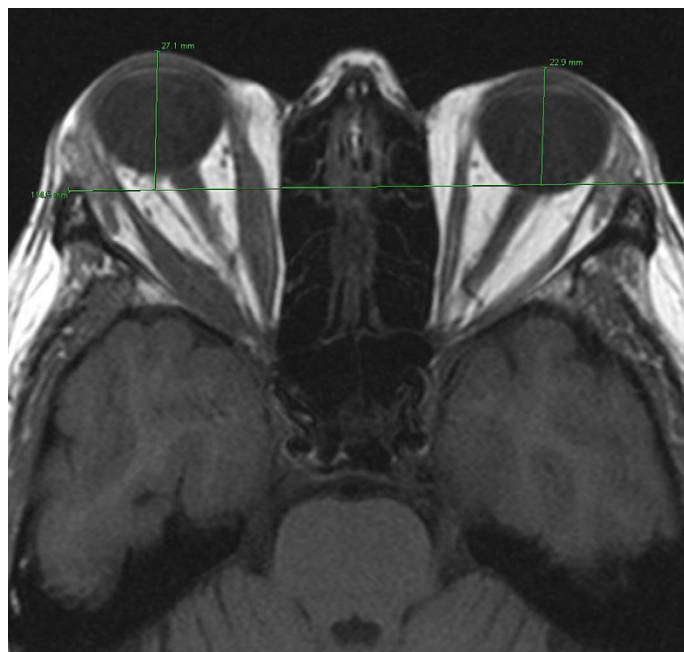
Fig 4.1 Axial T1w MRI of a GO patient
Axial T1w MRI showing unilateral orbital proptosis in the course of Graves' disease. The distance, taken perpendicular to the connecting line gives a quantitative value for protrusion. The picture is adapted from Muller-Forell and Kahaly, 2012 .

There are different imaging methods in neuroradiological clinics to study orbital manifestation of GO patients including orbital ultrasound and echography scanning, magnetic resonance (MR) imaging, computed tomography (CT) and positron emission tomography-computed tomography (PET/CT) (Kahaly, 1996, Muller-Forell et al., 1999, Kahaly, 2001, Aydin et al., 2003, Kahaly, 2004, Muller-Forell and Kahaly, 2012, Garcia-Rojas et al., 2013).

4.1.1 Clinical neuroradiological methods

4.1.1.1 Magnetic resonance imaging

Magnetic resonance imaging (MRI) has the unique ability to provide cross-sectional images of the interior of the body. Particularly, MR images give an excellent contrast to study soft-tissues. The principle of magnetic resonance phenomenon is the magnetic properties of atomic nuclei particularly those with an odd number of protons. Thus, each atom of the simplest and most abundant element in the body, hydrogen, behaves as a small magnetic dipole (**Fig 4.2 panel 1**). In the presence of static magnetic field, all hydrogen atoms align in and tumble around the direction of the magnetic field which is called precession (**Fig 4.2 panel 2-4**). By applying an external radio frequency current at the precession frequency, the hydrogen nuclei can be flipped (90°) in the magnetic field which is called excitation (**Fig 4.2 panel 5**). After termination electromagnetic field, the spin of the hydrogen nuclei returns to its prior state (relaxation) by emitting electromagnetic waves (**Fig 4.2 panel 6**) (Westbrook and Kaut Roth, 1998). The radio frequency of emission waves can be monitored to generate an image based on the brightness of signals (Wichmann, 2002).

As the emitting electromagnetic waves are measures during the time of relaxation, it is important to know how long it takes that most of the protons back to their thermodynamic equilibrium. The relaxation time that needs to be given to the "longitudinal" magnetic protons to mostly recover (63%) after being flipped is called the T1 relaxation. In addition to T1 relaxation, T2 relaxation time represents the given time to decay the measuring magnetic resonance signal.
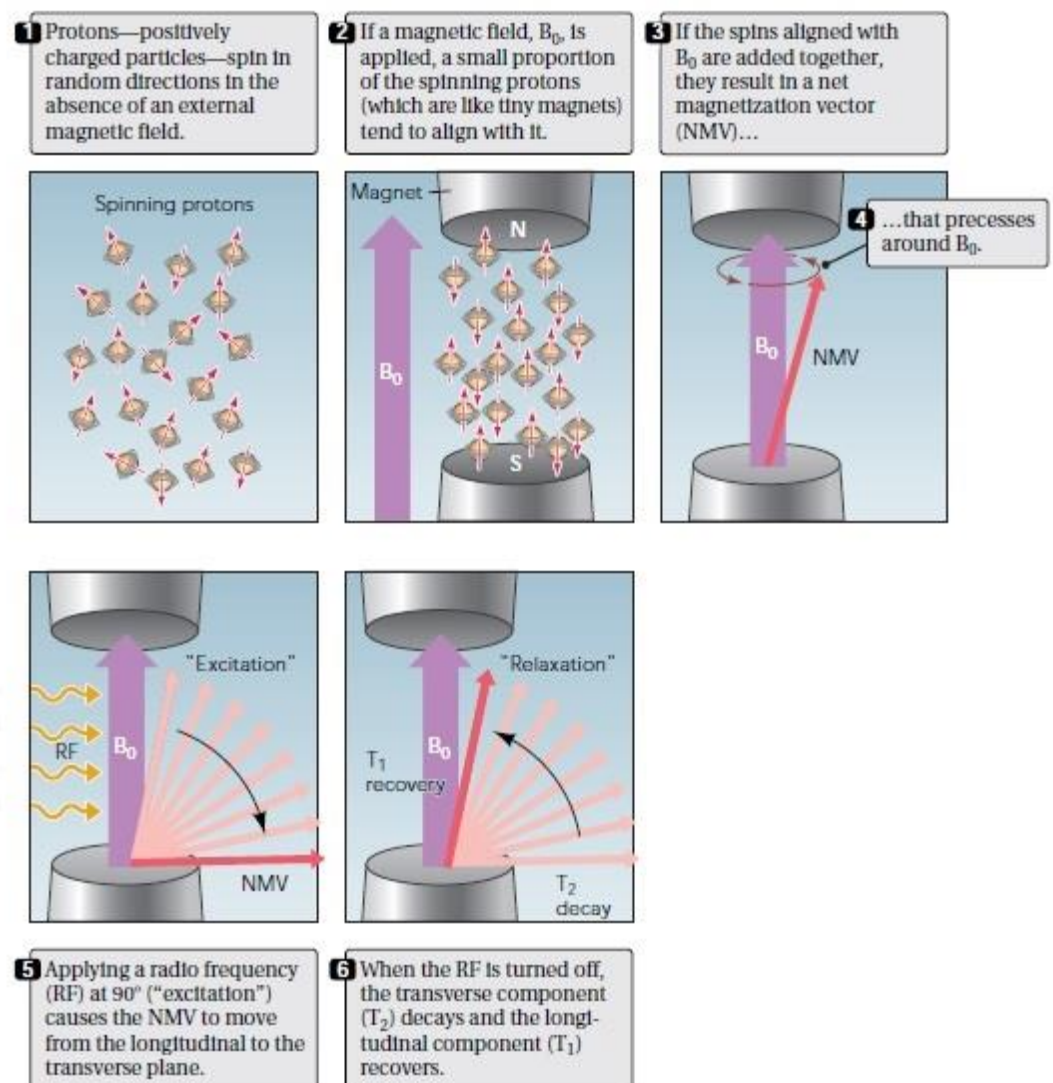
Fig 4.2 Basic concepts of MR imaging.
Adapted from Westbrook and Kaut Roth, 1998.

Generally, MR images are based on the type of relaxation and concentration of water in the biological tissues. So, if the MR images acquire with the setup of T1 relaxation it will be called T1-weighted (T1w) and it will be T2-weighted (T2w) when using T2 relaxation. High concentration of water (hydrogen) in the tissue cause to generate bright pixel (high signal) in the image with T2w characterisation, but low signal in T1w (Wichmann, 2002) as clearly shown in **Fig 4.3**.
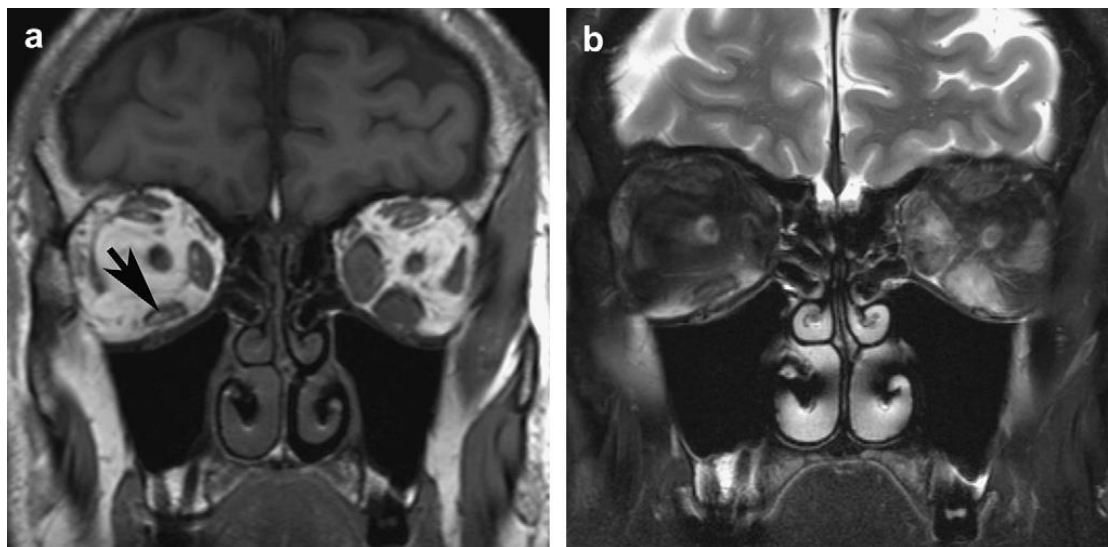
Fig 4.3 The differences between T1w and T2w in MRI of orbital tissue
(**a**) Coronal T1w MRI of patient with Graves' disease with asymmetry of the muscle involvement (**b**) Corresponding T2w fat suppressed, with bright signal of acute inflammation in the extraorbital muscles of left eye. The picture was adapted from Muller-Forell and Kahaly, 2012 .

The standard neuroradiological protocols for imaging of orbital tissue are; (i) T1w image of the transverse, coronal sections, (ii) T2w (fat suppression) image of the transverse, coronal and parasagittal section. The most informative MRI scan for GO patients is acquired with 3 mm thickness slice of coronal view (perpendicular to the axis of the optic nerve) in combination with axial view as shown in **Fig 4.4** (Muller-

Forell and Kahaly, 2012). This combination of MRI scans will reveal hypertrophy of extraorbital muscles, protrusion, and inflammation in retrobulbar tissues.
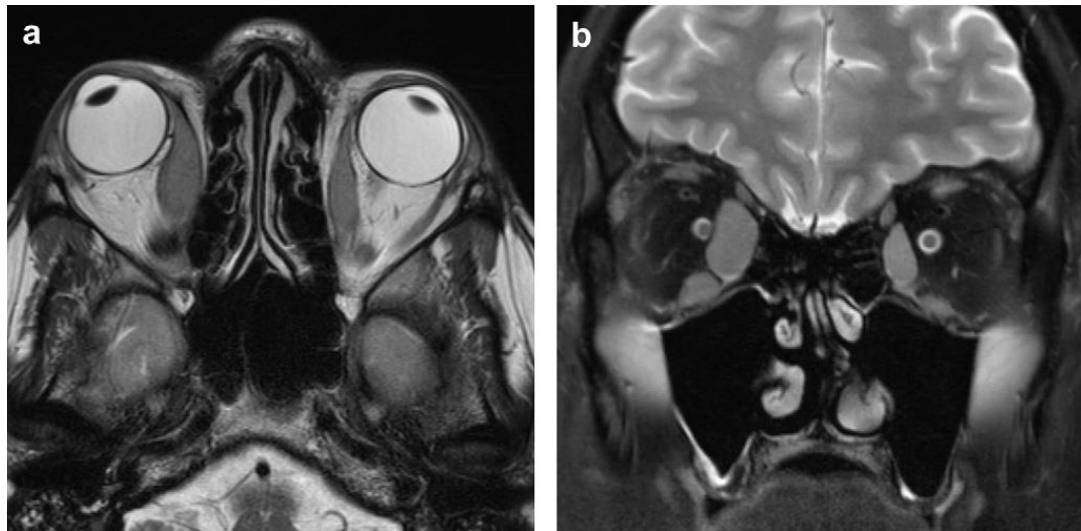
Fig 4.4 The standard protocol of neuroradiology for GO patients
(**a**) Axial T2w MR of a GO patient with hypertrophy of extraorbital muscles. (**b**) Corresponding coronal views. The picture was adapted from Muller-Forell and Kahaly, 2012.

4.1.1.2 Computed tomography

Computed tomography (CT) is the first and still most routinely used modern imaging technique that provides high accuracy in anatomical imaging. The distinctly different X-ray absorption allows distinguishes between various biological tissues by measuring their different densities. The rotating X-ray-tube and detector system in the helical technique provides continuous radiation that results in faster scan acquisition and higher resolution (Ohnesorge et al., 1999). Apparently, the main concern in CT is the radiation burden, particularly for orbital scan as the lens is the most sensitive organ for radiation exposure (Maclennan, 1995, Maclennan and Hadley, 1995). Generally, in comparison to MR imaging, the CT examination of the orbit is less expensive, less time

consuming and higher availability with relatively comparable image quality. For GO

patients, the standard protocol is quite similar to MRI acquisition protocol including

axial and coronal view. The axial intersection provides the image parallel to the optic

nerve and the coronal view acquire image of perpendicular to the axis of the optic

nerve (**Fig 4.5**).
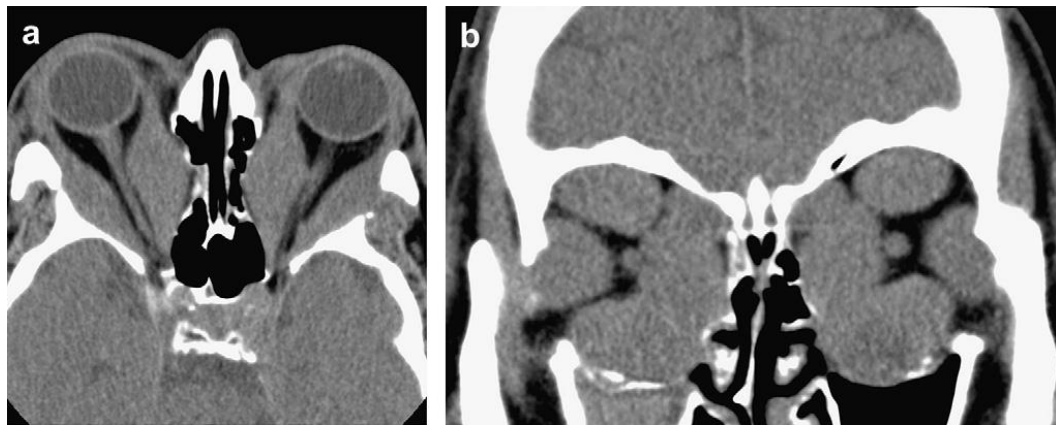
Fig 4.5 The CT scan of orbital region from a patient with GO
(a) Axial view of the orbital region showing bilateral enlargement of the
extraorbital muscles and orbital protrusion. **(b)** Corresponding coronal view.
The picture was adapted from Muller-Forell and Kahaly, 2012 .

4.1.1.3   Orbital ultrasound and octreotide scanning

The ultrasound examination of orbits in GO patients is far less informative in terms of

disease activity and precise anatomical structure in comparison to earlier mentioned

techniques. The beneficiary advantages are fast speed, low costs and lack of radiation

(Prummel et al., 1993, Benning et al., 1994). The other disadvantage of ultrasound

examination of extraorbital muscle volume in GO patients is that it is highly

investigator dependent (Kahaly, 2001, Kahaly, 2004). Thus, this technique is not a

recommended method for clinical investigation of GO in presence of CT or MRI.

The other semi objective and fairly sensitive technique that has been used for measurement of extraorbital muscle volume in GO patients is octreoscan (Kahaly et al., 1995a, Kahaly et al., 1995b, Kahaly et al., 1998, Krassas and Kahaly, 1999, Gerding et al., 1999). The positive results of octreoscan are reliable and patient should be treated while negative results will not reveal much information about the disease. The disadvantages of octreoscan are the high cost per image and its radiation burden; although, it is less than CT (Forster et al., 2000).

4.1.2 Preclinical imaging studies

A reliable method to study soft tissue in the experimental model is *in vivo* imaging. MRI is a non-invasive imaging modality which provides highly accurate qualitative and quantitative images of the anatomical structures. The recent technical advances in small animal MRI instruments made it a popular modality in preclinical research. The two main advantages that MR imaging provides to preclinical research are (i) *in vivo* studies on live animal repeated at different time points (non invasive longitudinal analysis) and (ii) high resolution images of soft tissue. As the imaging subject in the preclinical MRI is much smaller than the clinical MRI, factors affecting resolution are intensified to achieve a high quality MR image. Factors affecting resolution include receiver coil size, magnetic field strength and most importantly image acquisition time. In most of the preclinical MRI centres, the magnetic field is 7.0 T instead of 1.5 or 3.0 T in clinical scanner. Furthermore, animals for MRI scans are anesthetised which allows acquiring images with much longer acquisition time in comparison with clinical MRI protocol. In the small animal MRI, the term "magnetic resonance histology" (MRH)

(Johnson et al., 1993), describes the specific image resolution by MRI, which is comparable to the resolution achievable by histological methods, less than 100 μm. The technology and hardware design for MRH were described over two decades ago (Budinger and Lauterbur, 1984, Chance, 1989, Johnson et al., 1993). The typical preclinical MRI scans are acquired to determine the volume or surface area of a specific tissue in murine experimental model. The optimal tissue contrast can be provided by selecting the specific imaging sequence and other parameters. Acquired MRI data are then analysed to measure signal intensities to calculate surface areas or volumes.

4.1.3 Anatomy of mouse orbit and differences with human orbital structure

To analyse the anatomical changes by MRI and to be able to interpret the MR images results based on the MRI in GO patients, it is necessary to precisely know the anatomy of orbital structure in mice and the differences with human orbits. Thus as part of background, anatomy of mouse orbit is described here.

The orbital contents are protected in orbital cavity by eight bones in mice; maxilla, lacrimal, zygomatic, frontal, temporal, sphenoid, ethmoid and palatine (Smith, 2002). The depth of the mouse orbit, including the eye, is approximately 5 mm (Paterson and Kaiserman-Abramof, 1981). In rodents, in addition to six extraorbital muscles including four rectus muscles; superior, inferior, medial and lateral and two oblique muscles; superior oblique muscle and inferior oblique muscle that can be found in all mammals, there is a retractor bulbi muscle that surrounds the optic nerve (Pachter et al., 1976). The oblique muscles lie outside the ring formed by the rectus muscles. Another

important anatomical difference in orbital region between mice and human is the presence of the harderian gland in rodents. In mice, the extraorbital muscles are surrounded by the harderian gland which occupy much of the space in the orbital cavity (Paterson and Kaiserman-Abramof, 1981). The gland has a horseshoe shape with the concave surface closely in contact with the superior aspect of the globe. The Harderian gland has a pinkish-grey colour (Cohn, 1955). The anatomy of harderian gland has well-defined, but its function has remained obscure. It is found exclusively in animals with a nictitating membrane, to which its excretory duct is attached. Harderian secretions are thought to lubricate the nictitating membrane and may also be important in maintaining the tear film (Cohn, 1955).

4.1.4 Preclinical MRI in experimental GO model

In this chapter, we describe the development of MRI scanning method in orbital region of the experimental GO model. In addition, it will be discussed the importance of MRI data in future translational research. Immune animals undergoing orbitopathy have been examined by MRI which provided an undoubted evidence to study macroscopic view of orbital manifestations in live animals. For the imaging studies, animals were selected from the group of immunisation of longitudinal studies (sacrificed 9 weeks after end of immunisation). The histopathological studies of these animals were already described in Chapter 3.

Briefly, in 7 weeks after end of immunisation, immune animals (n = 5) examined by *in vivo* MRI to assess pathological changes in orbital region. Furthermore, age matched normal female BALB/c mice (n=3) were imaged as control. For each mouse, anaesthesia was induced and maintained by inhalation of a 1-2% isoflurane-oxygen

mix throughout imaging. Two distinct orientations have been chosen to acquire MR images, coronal and axial. For coronal view, T2w MR images were acquired with 100 µm in-plane resolution. The MRI data were then used as scout images for MRI of the right eye at an oblique angle, axial view. For axial view, 94 µm in-plane resolution MR images were collected from the surface of the eye towards the back of the eye (perpendicular to the long axis of the eye, similar to the orientation for histological processing). The data from MR imager then analysed to work out pathological differences between immune animals and age matched controls. All animals were then humanely destroyed at 9 weeks after end of immunisation (Moshkelgosha et al., 2013). Interestingly, Kuriyan and colleagues showed a similar analytical method for studying retrobulbar tissue changes in GO patients with MRI/CT (Kuriyan et al., 2013). By using this method they could distinguish two subtypes of GO in human patients (will be discussed later in this chapter).

4.2 Aims

The main purpose of this Chapter was to investigate the feasibility of using preclinical MRI as non invasive technique, alternative to histopathology. The objectives of this Chapter deal with quantitative and qualitative imaging of the orbital morphology in the GO experimental model developed in female BALB/c mice immunised with hTSHR A-subunit plasmid *in vivo* electroporation, including:

- Development of high resolution MRI scanning method in orbital tissue in the experimental GO model

- Quantitative analysis of MRI of orbital tissue from the experimental GO model.

- Correlation of orbital histology with MRI in the experimental GO model

- Correlation of MRI of the experimental GO model with clinical neuroradiological results of GO patients.

4.3 Results

To our knowledge, this is the first time that a neuroradiological analysis by small animal MRI method was conducted in extraorbital muscles. So, we had to characterise different parameters including imaging orientation. Based on the imaging orientation protocol for orbital MRI in clinical neuroradiology (Muller-Forell and Kahaly, 2012) and with consultations from Dr Neil Deasy (clinical neuroradiologist, King's College Hospital NHS Foundation Trust, London), we decided to perform coronal view and axial view.

4.3.1 Coronal view, to identify proptosis of the eye in the GO model

The coronal *in vivo* MRI was performed in mice immunised with hTSHR A subunit *in vivo* electroporation (n = 5) and age matched control mice (n = 3). T2w MRI images were acquired of the eyes and frontal region of the brain in anesthetised animals (**Fig 2.2**). Importantly, coronal MR images of the mouse head readily identified unilateral proptosis in two of five immune mice (**Fig 4.6, 4.7**), proptosis in the later immune animal was less pronounced, compared with the control mouse (**Fig 4.8**). Unilateral protrusion had been apparent on visual inspection of the immune animals but was readily confirmed by *in vivo* MRI. In addition, an extra quantification analysis has been performed to make sure what we reported here as proptosis is authentic and not due differences in the size of orbital globe (**Fig 4.9**).
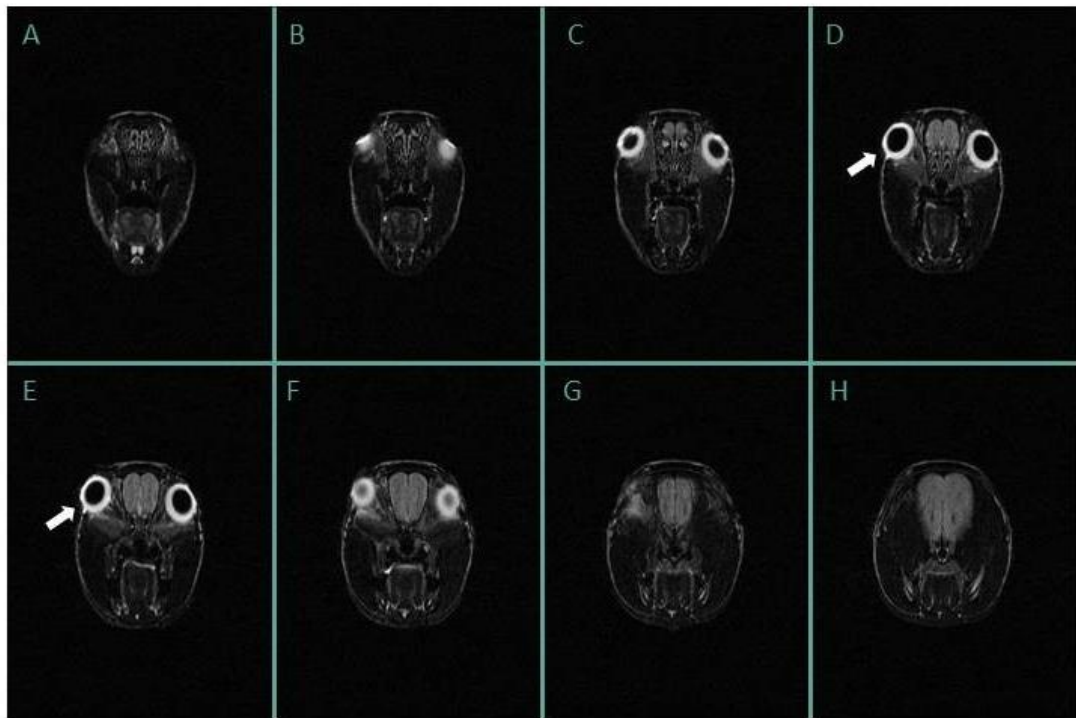
Fig 4.6 Contiguous coronal view T2w MRI of mouse 64/R with orbital protrusion

Contiguous coronal view T2-weighted MR images (imaging slice thickness of 0.61mm) of the head of an immune mouse 64/R are shown from A to H. Clear proptosis of the right eye compared to the left eye is observed even from the front of the eye through to the back of the eye (from image C through to E). The right eye clearly protrudes from the outline of the mouse head (highlighted by a white arrow) as defined by the high signal intensity of subcutaneous adipose tissue compared to the left eye which does not exhibit proptosis.
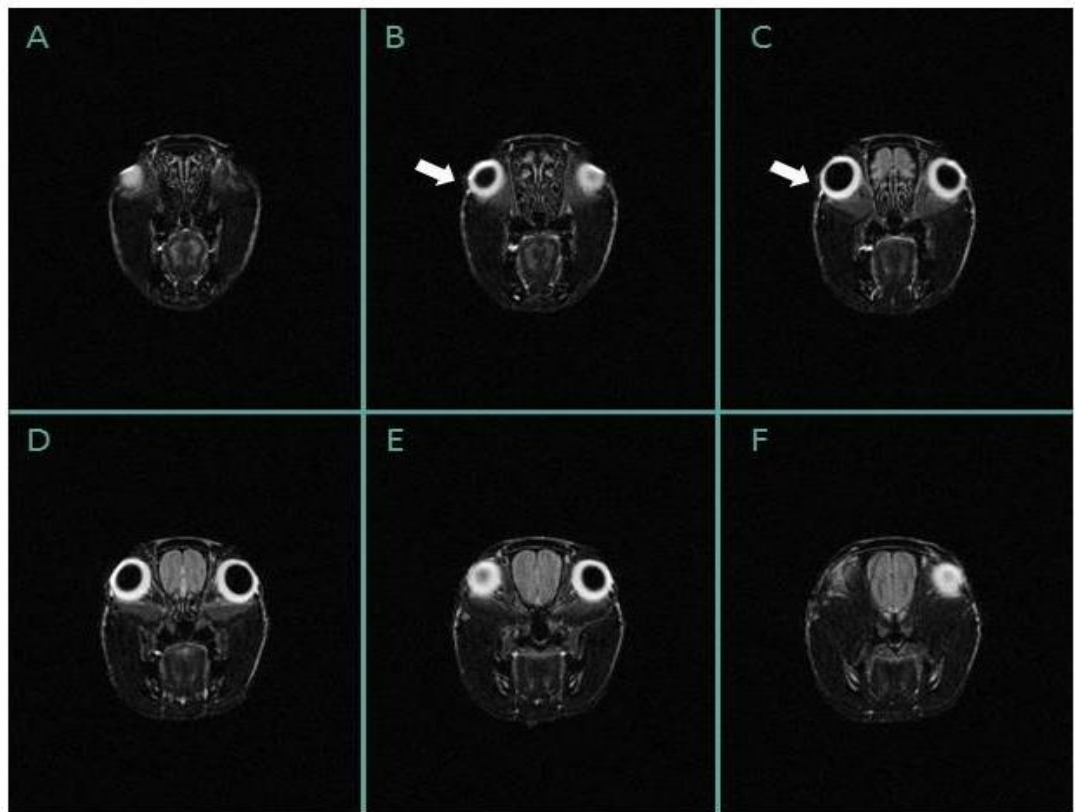
Fig 4.7 Contiguous coronal view T2w MRI of mouse 64/L with orbital protrusion

Contiguous coronal view T2-weighted MR images (imaging slice thickness of 0.61mm) of the head of an immune mouse 64/L are shown from A to F. Less pronounce proptosis than mouse 64/R (Fig 4.6) of the right eye compared to the left eye is observed through to the back of the eye (from image B through to D). The right eye clearly protrudes from the outline of the mouse head (highlighted by a white arrow).
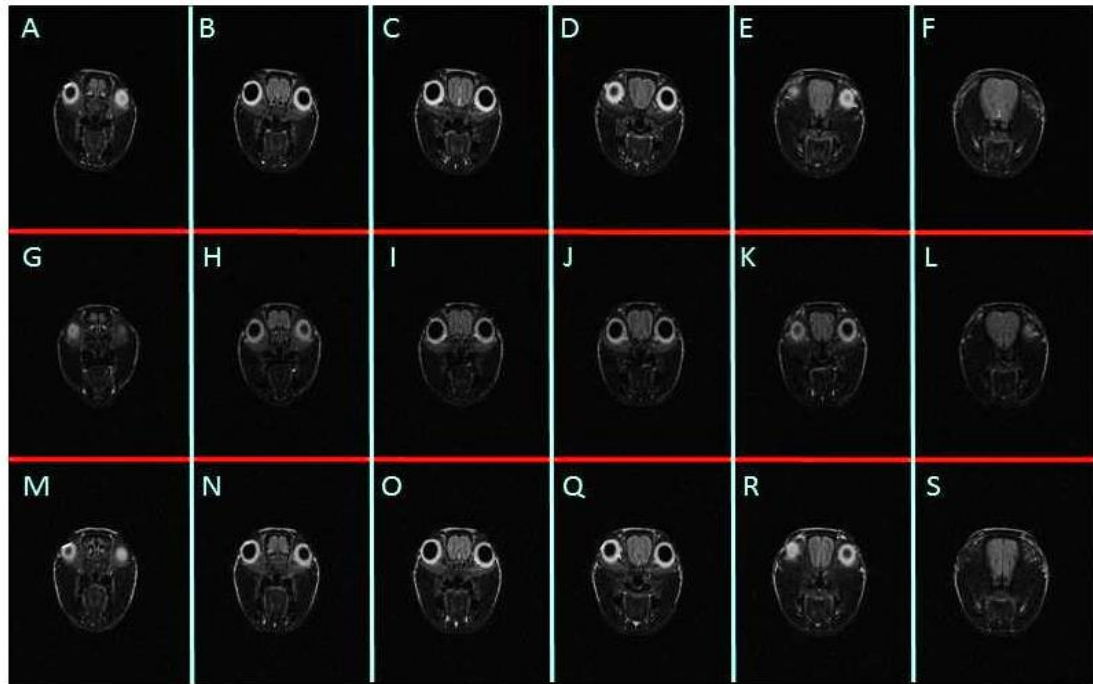
Fig 4.8 Contiguous coronal view T2w MRI of control mice

Contiguous coronal view T2-weighted MR images of the head region of three age-matched controls (AM1-AM3), AM1 is shown in **A** to **F**, AM2 in **G** to **L** and AM3 in **M** to **S**. It is clear that none of the age-matched controls show protrusion in either left or right eyes. The lack of eye protrusion in age-matched controls was defined by orbital location based on the surface of the head region. The head outline is defined by the high-signal intensity of subcutaneous fat.
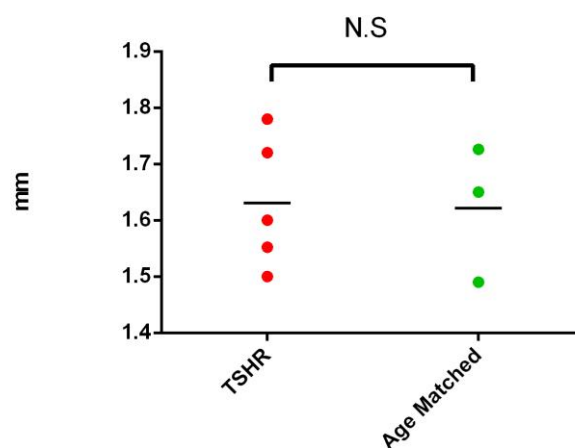
Fig 4.9 Diameter of eyeball in immune and age matched control mice

Quantitative analysis confirmed that proptosis that has been reported is not due to differences between the sizes of eyeball.

4.3.2 Quantification of extraorbital muscle hypertrophy

It was clear from MR images of axial view that there was a difference in the size of extraorbital muscles in immune animals compare to age matched controls. The optimal method to evaluate the differences in extraorbital muscles was to measure orbital muscle volumes from the MR images. Recently Dr Feldon and colleagues suggested a quantitative method to measure enlargement extraorbital muscles in GO patients (Kuriyan et al., 2013). Based on their method, a ratio of the total extraorbital muscles area to orbit area (EMA:OA) was calculated. Technically, the superior rectus and the levator palpebrae superioris were measured together due to the closeness of these muscles (Kuriyan et al., 2013). However, in our study, we were unable to use the exact method to show enlargement of specific muscles due to limitations of MRI resolution in preclinical setting. Thus, the quantification of -orbital region confirmed significant enlargement of retrobulbar tissue in immune animals (**Fig 4.11-4.15**) compared with the age-matched controls (**Fig 4.16-4.18**). For this purpose, ImageJ (NIH) was used to measurement of the volume of the orbital muscle of the right eye. The results of quantification of extraorbital volume are presented in **Fig 4.19.**
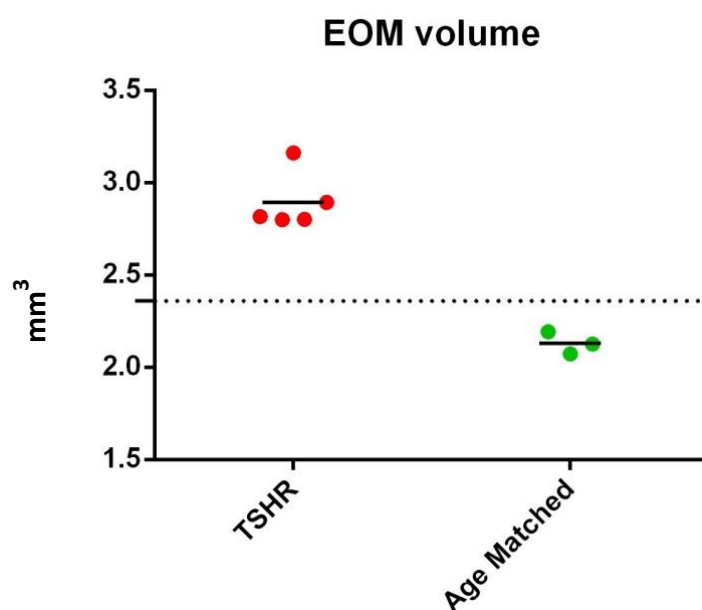
Fig 4.19 Quantification of MRI showing hypertrophy in the retrobulbar tissue
Enlargement of the retrobulbar tissue shown as EOM volume in mm^3 (abscissa) in the immune mice compared with age matched control mice. The hypertrophy was confirmed by segmentation analysis.

4.3.3 Alignment of MRI results with histological studies

The high resolution MR imaging of orbital region in preclinical model of Graves' orbitopathy clearly showed quantifiable enlargement of the retrobulbar tissue. As there was no literature reference for MR images analysis in extraorbital muscles in mice and due to the limitations of MRI resolution in preclinical setting, we aligned the MRI results with histological analysis of orbital region to get a better interpretation of the MRI data. For this reason, we purposely acquired axial MR images along the optic nerve exactly as the subsequent histological analysis of the same eye, following sacrifice of the animal a few days after MRI acquisition. The advantage of the

alignment of MRI with histology is to confirm hypertrophy of extraorbital muscles that has been readily apparent in MRI by another method.

As it was clear from MRI analysis of retrobulbar tissue, the enlargement mostly involved superior area of muscles (in the concave region of harderian gland). Interestingly, histological analysis of extraorbital muscles in mice undergoing experimental GO exhibited the hypertrophy of same muscles, rectus superior and oblique superior (**Fig 4.20**) compared to age-matched controls (**Fig 4.21**). For precise analysis, extraorbital muscles volume has been measured in the histological slides. To quantify extraorbital muscles volume, the same method, image analysis by ImagJ, was recruited which had been used for analyses of MR images. The quantification of extraorbital muscles volume in histological analysis from experimental GO mice demonstrated an increase trend compared to age-matched control mice (**Fig 4.22 A**). Strikingly, the quantification analysis has been revealed a significant hypertrophy in experimental GO mice when superior muscles were analysed specifically (**Fig 4.22 B**).

It is important to aware of the differences between the absolute value for muscle volume in MRI and histology. As it already described in the method of quantification, the measurement of volume is based on the mathematical algorithm of roundup measurement which apparently consist of quantisation error. The more slices that were measured the lower quantisation error. Thus, the extraorbital muscle volume is more realistic in the histological analysis in comparison with MRI. It would be suggested reducing thickness of slices (increasing number of slices) in MRI to obtain more precise quantification. However, the challenge for reducing thickness of slices is the time of acquiring image would be increased.
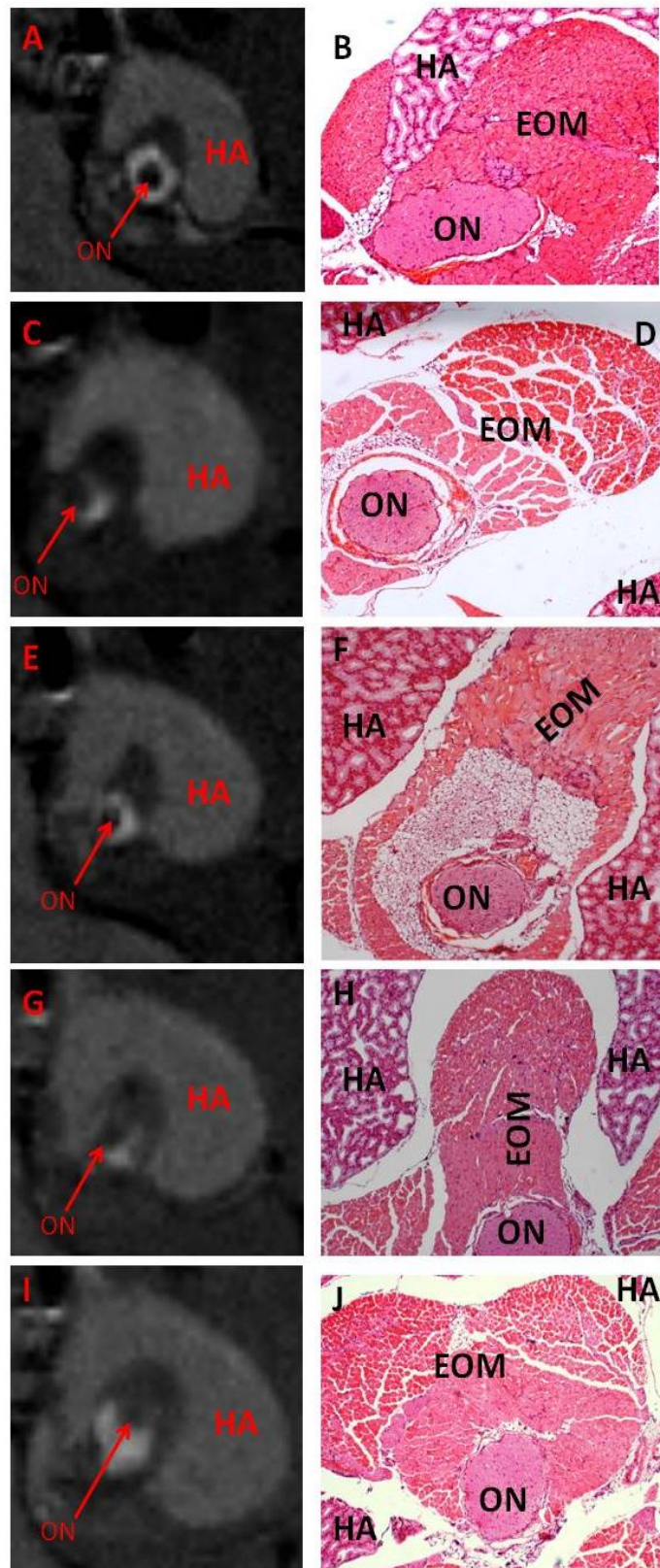
Fig 4.20 Alignment of MR images with histology of extraorbital muscles in mice undergoing GO

All MR images (left column) are contiguous axial view T2-weighted, perpendicular to the long axis of the eye. Harderian gland (HA) and optic nerve

(ON) marked in images. Extraorbital muscles (EOM), structures are clearly obvious from histological slide of the same area aligned with MRI (right column). **A, B** mouse code 63/2, **C, D** mouse code 64/0, **E, F** mouse code 64/L, **G, H** mouse code 64/R, **A, B** mouse code 64/2, **I, J** mouse code 63/2.
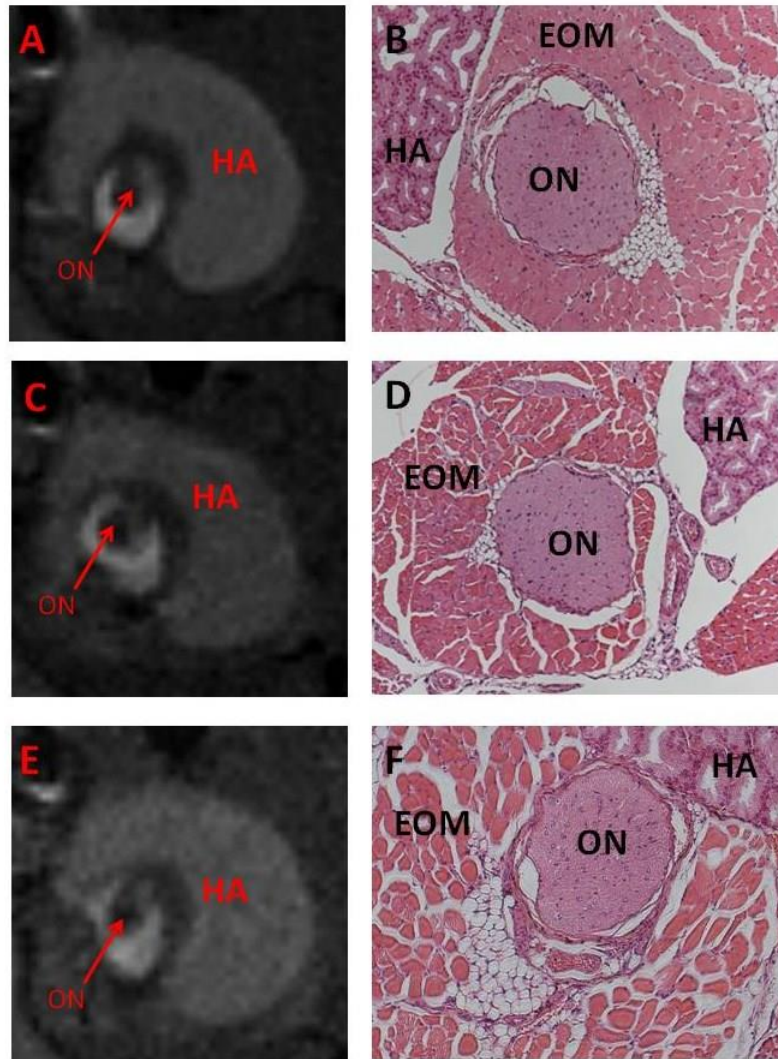
Fig 4.21 Alignment of MRI with histology of extraorbital muscles in control mice

All MR images (left column) are contiguous axial view T2-weighted, perpendicular to the long axis of the eye. Harderian gland (HA) and optic nerve (ON) marked in images. Extraorbital muscles (EOM), structures are clearly obvious from histological slide of the same area aligned with MRI (right column). **A, B** mouse code AM1, **C, D** mouse code AM2, **E, F** mouse code AM3.
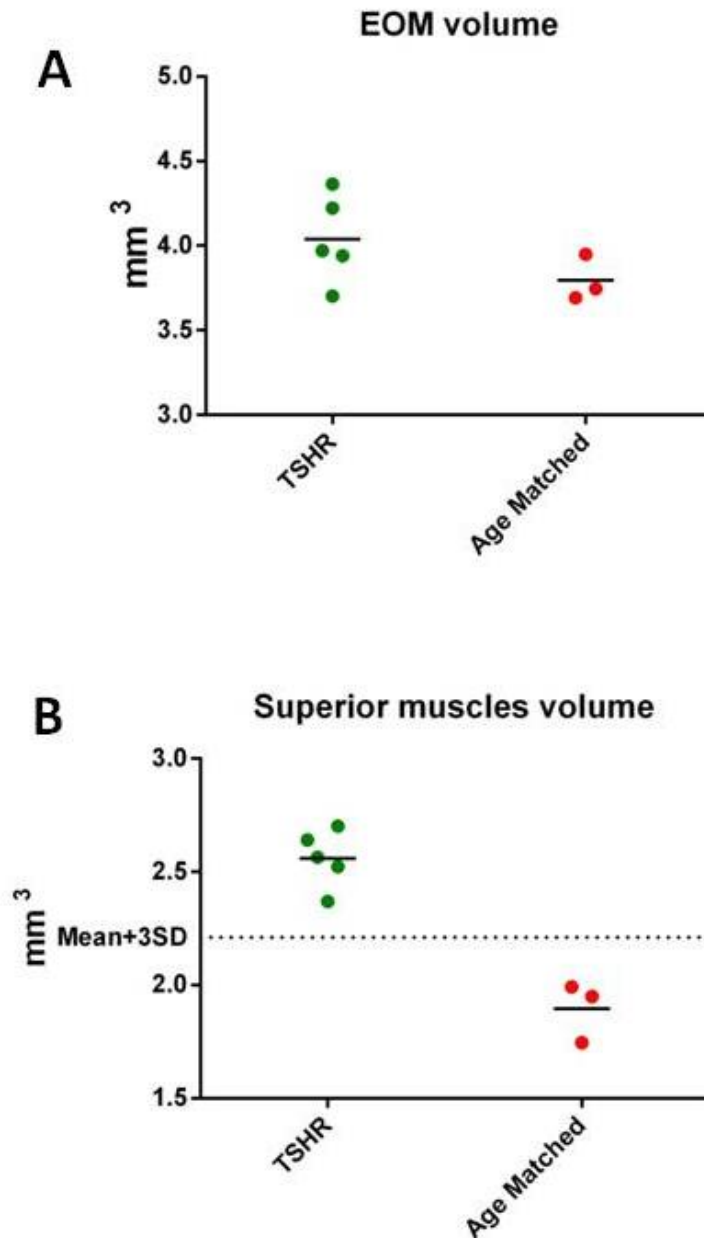
Fig 4.22 Quantification of hypertrophy in the extraorbital muscles by histology

(A) Shows the upward trend in the EOM volume in mm^3 (abscissa) in the immune mice compared with age-matched control mice. (B) Shows the significant hypertrophy in superior muscles in the immune mice compared with age-matched control mice (presented as volume in mm^3). Dotted line presents the mean value of superior muscle volume in control mice added with three times of standard deviation.

4.4 Discussion

In this Chapter, we have described the neuroradiological analysis by high resolution MRI in orbital region of preclinical GO model. A total number of 5 immune mice following the modified immunisation protocol with hTSHR A-subunit plasmid *in vivo* electroporation were evaluated by *in vivo* MRI for orbital morphology. The *in vivo* small animal MRI provided an undoubted evidence to study macroscopic view of orbital changes in live animals. In addition to 5 immune animals from the cohort of immunisation for longitudinal studies (sacrificed 9 weeks after end of immunisation), 3 age-matched female BALB/c mice were selected as controls. The analysis of MRI data described in this chapter and advantages of the established imaging method will be discussed below.

The studies on orbital pathology were initiated by careful literature review to find a standard protocol for acquiring MR images in orbital region. Although, number of studies recently reported using MRI technique in the experimental murine model of retinal development (Lindsey et al., 2007, Chen et al., 2008a, Muir and Duong, 2011, Chen et al., 2011, Wang et al., 2012) and optic nerve crash (Xu et al., 2008, Sun et al., 2011, Zhang et al., 2011, Talla et al., 2013) with particular interest in contrast agents (Lin et al., 2014), there were no reports dealing with preclinical extraorbital muscles of orbital region. We therefore had to set up the MRI technique based on the imaging orientation protocol for orbital MRI in clinical neuroradiology (Muller-Forell and Kahaly, 2012). For this reason we developed collaboration with Dr Neil Deasy (clinical neuroradiologist, King's College Hospital NHS Trust, London). From his consultations, we set up the MRI protocol described by two different image acquisition of head region with distinct orientations exactly as the clinical MRI protocol for GO patients.

Based on the clinical MRI method, two distinct orientations of coronal and axial view have been acquired. For coronal view, T2w MR images were acquired with 100 μm in-plane resolution. The MRI data were then used as scout images for MRI of the right eye at an oblique angle, axial view. For axial view, 94 μm in-plane resolution MR images were collected from the surface of the eye towards the back of the eye (perpendicular to the long axis of the eye, similar to the orientation for histological processing).

Although in clinical neuroradiology, orbital imaging is often applied for diagnosis in patients with GO (Muller-Forell and Kahaly, 2012), It has been postulated that differences in the orbital bone structure between humans and rodents (Smith, 2002) may not allow manifestation of eyeball protrusion in the orbital region of mice (Wiersinga, 2011). Despite this difference in orbital anatomy, we showed by high-resolution *in vivo* MRI, clear enlargement retrobulbar tissues and unilateral proptosis in some animals (Moshkelgosha et al., 2013). The coronal view of MR images clearly confirmed bilateral proptosis in 2 immune animals. Moreover, the quantitative analysis showed significant increase of extraorbital muscle volume in immune animals compare with age-matched controls. Interestingly, alignment of histological slides of extraorbital muscles with MR images confirmed the hypertrophy in orbital muscles.

Furthermore, neuroradiological studies in GO patients reported a common feature of considerable differences in the involvement of orbital muscles (Majos et al., 2007, Chen et al., 2012, Politi et al., 2014). To specifically classify the subtype of orbital tissue involvement in GO patients, a ratio of the total extraorbital muscles area to orbit area (EMA:OA) is calculated (Kuriyan et al., 2013). When this index for GO patients is within the controls mean ± two SD, they are classified as type I patients (Kuriyan et al., 2013)

which is associated predominantly with fat compartment enlargement (El-Kaissi et al., 2004). Patients with an EMA:OA ratio greater than the control mean ± 2 SD are classified as type II patients who are predominantly associated with extraorbital muscles enlargement. In this preclinical model we were unable to use the same index to classified immune mice due to the limitations in resolution of preclinical MRI setting. However, we could use the histological sections to integrate with MR images in order to specify involvement of orbital tissue. Interestingly, the alignment of histological sections with MRI revealed that the enlargement of orbital tissue is mostly associated with extraorbital muscles rather than fat expansion, i.e. type II. Of particular interest, the alignment of histology with MRI in preclinical model of GO demonstrated the higher rate of involvement in superior muscles. Thus, this is another advantage of the experimental GO model to recapitulate the clinical features in GO patients. The quantification of histological slides was demonstrated a most significant muscles hypertrophy in superior muscles rather that other extraorbital muscles. Higher magnification of histology analysis showed that the hypertrophy in muscles is due to inflammation and accumulation of fibrotic myofibroblast. However, to address the question why superior muscles are involved the hypertrophy more than other muscles, further molecular investigations are needed.

The significance of results presented in this Chapter will suggest setting up the preclinical MRI acquisition protocol for orbital region with larger number of animals. In addition, despite a high resolution image provided in this Chapter, it would be advised to acquire MRI with higher resolution by increasing acquisition time. Higher resolution MRI of orbital region will allow a better segregation of extraorbital muscles from surrounding tissue. The higher resolution imaging seems to be necessary in case of

using MRI as a method for longitudinal and therapeutic studies. As clearly shown by alignment of histology and MRI, the resolution of MRI in this chapter was not enough to distinguish adipose expansion in an individual mouse (64/L). The other way of improving the resolution in MRI is to add the contrast agents in order to increase brightness in tissue of interest. The role of contrast agents in increasing the resolution of different tissue has been very well studied (Hao et al., 2012, Talla et al., 2013, Cheng et al., 2013, Telgmann et al., 2013, Politi et al., 2014). Furthermore, the clinical evaluation of inflammatory activity is routinely studied by MRI (Politi et al., 2014). The clinical MRI acquisition method by T2w is able to show oedema in extraorbital muscles in order to investigate inflammation activity. In addition, a contrast agent, gadolinium, with T1w image acquisition is also suggested to distinguish between "active" and "inactive" inflammation in orbital muscles by quantifying signal intensity ratios (Politi et al., 2014). The different methods of MRI acquisition need to be validated by comparing the MRI results with the clinical activity score of experimental GO model.

4.5   Summary

In summary, in vivo MRI data of 5 immune animals undergoing orbitopathy following the immunisation with hTSHR A-subunit plasmid and 3 age-matched female BALB/c mice have been studied by the established method of small animal MRI. The coronal view of MR images clearly confirmed bilateral proptosis in 2 immune animals. The quantitative analysis showed significant increase of extraorbital muscle volume in immune animals compared with age-matched controls. The MRI results are concluded in **Table 4.1**.

Weeks after end of immunisation	Mouse code	Orbital histology	Chemosis	MRI	
				Coronal	Axial
Longitudinal studies 9 Weeks (Group 2)	AM1	Normal	-	Normal	Normal
	AM2	Normal	-	Normal	Normal
	AM3	Normal	-	Normal	Normal
	63/2	EOM	-	EOM hypertrophy	Normal
	64/0	EOM	-	EOM hypertrophy	Normal
	64/L	adipose expansion	-	EOM hypertrophy	+
	64/R	EOM	-	EOM hypertrophy	++
	64/2	EOM	§	EOM hypertrophy	Normal

Table 4.1 summary of *in vivo* MRI analysis of all 5 mice immunised with hTSHR A-subunit plasmid undergoing experimental Graves' orbitopathy and 3 age matched (AM) controls.

EOM: inflammation in extraorbital muscles based on the histological studies

§= positive by assessment for chemosis.

* + = unilateral proptosis; ++ = pronounced unilateral proptosis; Normal = no detectable protrusion,

Chapter Five

The enigma of antibodies induced to IGF-1R following immunisation with TSHR A-subunit plasmid

5. The enigma of antibodies induced to IGF-1R following immunisation with TSHR A-subunit plasmid

5.1 Introduction

The investigation of a 'long acting thyroid stimulator' (LATS) in the serum of patients with Graves' disease (Adams, 1958, McKenzie, 1958) following an observation of abnormal responses (Adams and Purves, 1956a) to an assay established to detect TSH stimulating activity (Adams and Purves, 1956b), represented a milestone for studies into the aetiology of the disease. Subsequent studies demonstrated that biologically active LATS resides in the gamma-globulin fraction of plasma (McKenzie, 1962). This finding was further developed by Kriss and colleagues who showed that LATS was an immunoglobulin G and therefore suggested the autoimmune basis for Graves' disease [(Kriss et al., 1964), reviewed in (Weetman, 2003)]. Further studies on autoimmunity in Graves' disease led to the identification of TSHR as the target autoantigen (Manley et al., 1974, Smith and Hall, 1974, Mehdi and Nussey, 1975). With the close association of Graves' orbitopathy and Graves' disease, the notion has been held that TSHR was also the target autoantigen in GO (Kriss et al., 1967, Rotella et al., 1986).

In the last two decades, however, different eye muscle and orbital connective tissue antigens have been implicated in GO pathogenesis. In particular, the flavoprotein subunit of succinate dehydrogenase, also known as 64 kDa antigen, a fragment of the FOX-P1 transcription factor G2s, orbital fibroblast membrane antigen collagen XIII, and calcium binding protein calsequestrin have all been implicated as autoantigens (Bernard et al., 1991, Wall et al., 1993, Mizokami et al., 2004, Gopinath et al., 2006, de

Haan et al., 2010, Wescombe et al., 2010, Lahooti et al., 2010, Wall and Lahooti, 2011, McCorquodale et al., 2012). Furthermore, extensive proliferation in the orbital tissue of patients undergoing orbitopathy has suggested that an excess of growth factors is responsible for the inordinate orbital tissue expansion. Among other growth factors, there is much evidence for insulin-like growth factor-1 (known as somatomedin C in the 1980s), to be implicated in the pathogenesis of Graves' orbitopathy. IGF-1 influences several aspects of immunity, including B and T cell development (Smith, 2010a).

More recently, platelet-derived growth factor (PDGF) has also been implicated as another putative growth factor in GO pathogenesis (van Steensel et al., 2009, van Steensel et al., 2010). PDGF is important in normal wound healing, and increased levels or activity of PDGF have been shown to be involved in pulmonary, liver, dermal, and cardiac fibrosis, in which it primarily acts as a mitogen for fibroblasts with a myofibroblast phenotype (Andrae et al., 2008). The laboratory of Professor Dik showed that both isoforms of PDGF, PDGF-AB and especially PDGF-BB, are produced by monocytes, macrophages and mast cells within the orbital tissue of GO patients (van Steensel et al., 2012). They also provided evidence for a potential role of PDGF-BB in increasing production of inflammatory mediators (e.g. CCL2, IL-6, and IL-8) and hyaluronan secretion, as well as proliferation of orbital fibroblasts (van Steensel et al., 2010). PDGF thus stimulates several key pathogenic pathways in GO and represents an attractive therapeutic target for the treatment of GO (van Steensel et al., 2009, van Steensel et al., 2011, Virakul et al., 2014).

5.1.1 IGF-1R and Abs to IGF-1R

The role of IGF-1 in GO was first reported from a case study in 1986 (Hansson et al.,

1986). Hansson and colleagues demonstrated that the concentration of somatomedin

C (IGF-1) in the retrobulbar biopsy specimens of GO patients were significantly

increased in comparison to controls, and in comparison with other tissues from the

same GO patients (Hansson et al., 1986). Subsequently, the same group reported a

specific role for IGF-1 in orbital tissue pathology by showing that other closely related

growth factors such as insulin and IGF-II were minimally involved in the disease

process (Hansson, 1989). However, examination of thyroid glands from patients with

Graves' disease showed no apparent changes in IGF-1 concentration compared with

normal thyroid tissue (Minuto et al., 1989). Other *in vitro* findings from Professor

Ingbar's laboratory revealed a close functional association between IGF-1 and TSH in

cell proliferation of the rat clonal thyroid epithelial cell line, FRTL-5 (Tramontano et al.,

1986, Tramontano et al., 1987, Tramontano et al., 1988a, Tramontano et al., 1988b).

They demonstrated that IGF-1 promoted FRTL-5 cell proliferation and enhanced the

effect of TSH on DNA synthesis (Tramontano et al., 1986) (see section 1.4.3 for more

details). Subsequently, substantial overlap between TSHR and IGF-1R downstream

signalling was reported. Both receptors extensively utilise the Akt/FRAP/mTOR/P70s6k

pathway (Cass and Meinkoth, 1998).

Meanwhile, a potential role of anti-IGF-1R Abs in the pathogenesis of Graves' disease

was proposed by Kohn and colleagues (Kohn et al., 1986). Their studies indicated that

immunoglobulins from patients with Graves' disease not only increased collagen

synthesis in human fibroblasts (Rotella et al., 1986), but also immunoprecipitated the

tyrosine kinase domain of IGF-1R (Kohn et al., 1986). Following these findings, Professor Kendall-Taylor's laboratory demonstrated the presence of IGF-1R Abs in sera of Graves' patients with and without overt orbital manifestation (Weightman et al., 1993). Initially, Weightman and colleagues confirmed the expression of high affinity IGF-1 binding sites in orbital fibroblast (**Fig 5.1 A**). Although this binding site has not been confirmed to be a part of the IGF-1R, its dissociation constant is similar to that previously reported for IGF-1R (Rosenfeld and Dollar, 1982, Jonas and Harrison, 1985, Tollefsen et al., 1987). Subsequently, they showed that immunoglobulins from Graves' patients but not control individuals can displace radiolabeled IGF-1 in human orbital fibroblasts obtained during surgery for squint, from two normal donors (Weightman et al., 1993). Purified IgGs from 12 out of 23 patients with Graves' disease significantly inhibited binding of labelled-IGF-1 to orbital fibroblasts, regardless of the clinical activity of the disease (**Fig 5.1 B**). Notably, one serum sample exhibited >50% inhibition in binding of the tracer (circled in red in **Fig 5.1 B**). Their data is shown below to illustrate the displacement plots and the single serum sample exhibiting >50% inhibition.
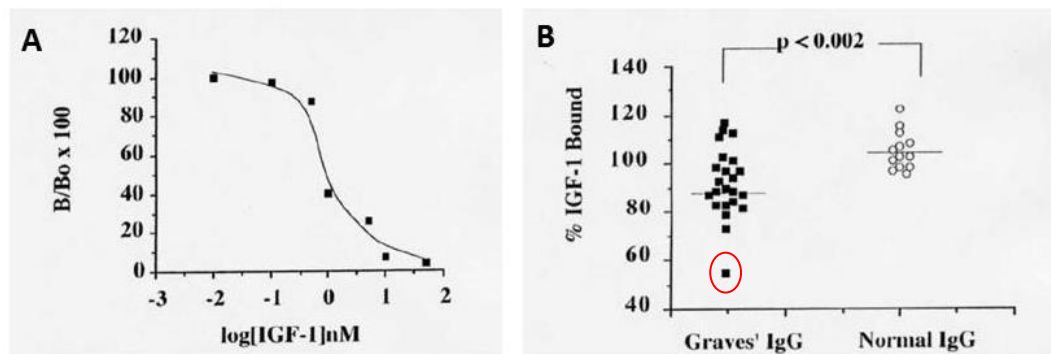
Fig 5.1 Displacement of labelled IGF-1 by purified IgG from GO patients. Adapted from Weightman et al. 1993.

The data from this study showed displacement of labelled-IGF-1 with purified IgG from individual patients with Graves' disease. **(A)** Competitive displacement of ^{125}I-IGF-1 binding to the monolayer culture of orbital fibroblasts by unlabelled IGF-1. **(B)** Distribution and comparison of ^{125}I-IGF-1 binding to orbital fibroblast monolayer after incubation with IgG prepared from normal (n = 13) or Graves' disease (n = 23) sera. The point circled in red in the Graves' IgG column has been highlighted by me in the figure to show the one serum sample with >50% inhibition of IGF-1 binding.

A decade after Weightman and colleagues had shown displacement of labelled-IGF-1 by purified IgG from Graves' patients, Professor Smith's laboratory reported that Graves' IgGs were able to stimulate the secretion of IL-16 and RANTES in human orbital fibroblasts (Pritchard et al., 2002). Interestingly, a blocking mAb to IGF-1R (1H7 mAb) inhibited the IL-16 and RANTES response, suggesting that IGF-1R may be implicated in the inflammatory response of the orbital fibroblasts (Pritchard et al., 2002, Pritchard et al., 2003). Therefore, the data provides experimental evidence that Graves' IgGs exert their effects on the orbital fibroblast at least in part through the IGF-1R pathway. Pritchard and colleagues also demonstrated that immunoglobulins isolated from patients with Graves' disease displaced labelled IGF-1 (Pritchard et al., 2003).

However, it is important to emphasise that Pritchard and colleagues did not evaluate inhibition of binding of labelled IGF-1 by serum from individual patients, but instead used pooled serum samples. They postulated that a subset of Graves' IgG contains Abs that stimulate the IGF-1R [(Pritchard et al., 2002, Pritchard et al., 2003) reviewed in (Smith et al., 2012)]. Their data is shown below in **Fig 5.2 A** and **5.2 B**.

Apart from the studies that illustrate the significant increase in concentration and immunoreactivity of IGF-1R Abs in GO patients, there is increasing *in vitro* evidence suggesting that the IGF-1R signalling pathway may operate in conjunction with the TSHR pathway in the pathophysiology of orbitopathy. A recent immunoprecipitation study, in combination with confocal microscopy, confirmed a close physical association between TSHR and IGF-1R (Tsui et al., 2008). It was suggested that the two receptors co-localise on orbital fibroblast plasma membranes, possibly forming a functional complex receptor (Tsui et al., 2008). In related receptor systems, crosstalk between IGF-1R and other receptors such as epidermal growth factor receptor (van der Veeken et al., 2009) and lysophosphatidic acid (LPA) receptor (Luttrell et al., 1995) has been demonstrated, potentially supporting a similar cross talk between IGF-1R and TSHR. In addition, evidence revealed a substantial overlap between TSHR and IGF-1R signalling pathway including the Akt/FRAP/mTOR/p70s6k pathway (Cass and Meinkoth, 1998, Park et al., 2000a, Park et al., 2000b, Park et al., 2005). IGF-1R-mediated signalling has a wide spectrum of functions in tissue growth and development, and may participate in the pathogenesis of several metabolic, neoplastic, and immunologic diseases (Bateman and McNeill, 2006, Kurmasheva and Houghton, 2006, Walenkamp and Wit, 2006). This mechanism can most likely be explained by the indirect association of two

receptors via downstream signalling molecules in orbital fibroblasts (Smith et al., 2008,

Morshed et al., 2009, Smith et al., 2012, Shan and Douglas, 2014).
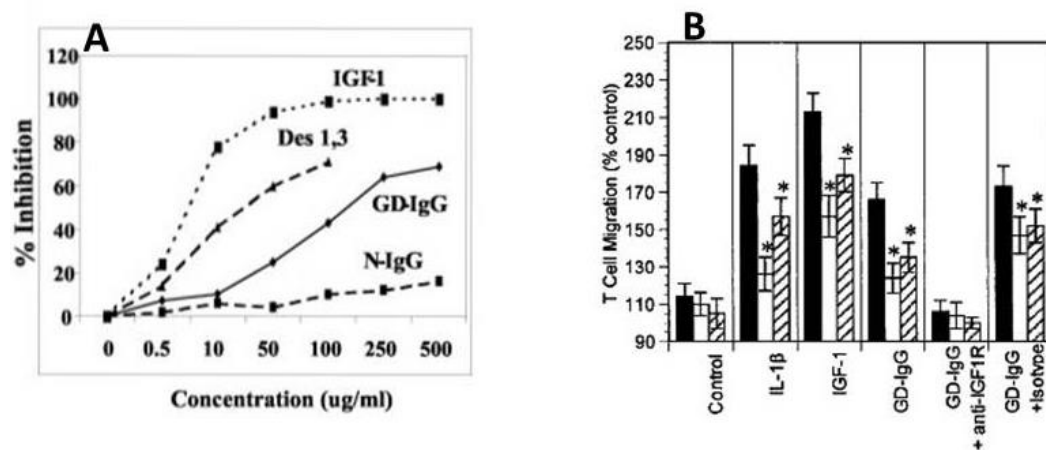
Fig 5.2 Displacement of labelled IGF-1. Adapted from Pritchard et al., 2003 with permission from Prof T. J. Smith
(**A**) ^{125}I-IGF-1 binding displacement with increasing concentrations of unlabelled IGF-1, Des(1–3), GD-IgG, and control IgG (named N-IgG). (**B**) The effects of IL-1β, IGF-1, and GD-IgG, without or with 1H7 mAb on T cell chemotactic activity showing that IGF-1 as well as GD-IgG can enhance T cell chemotactic activity which can be inhibited by 1H7 mAb.

Furthermore, studies on hyaluronan secretion from orbital fibroblasts has shed light on the functional interaction between TSHR and IGF-1R pathways. Notably, there is evidence that pathological activation of TSHR signalling, stimulation with TSHR mAbs or constitutive activation of TSHR by mutation can lead to increased production of the hyaluronan from preadipocyte fibroblasts (Zhang et al., 2009). Professor Smith's laboratory determined that IgG isolated from patients with Graves' disease (GD-IgG), but not recombinant human TSH, enhanced hyaluronan synthesis in undifferentiated orbital fibroblast (Smith and Hoa, 2004). Consequently, they confirmed that this response was mediated through IGF-1R, as the blocking IGF-1R mAb, 1H7 mAb, inhibited hyaluronan synthesis (Smith and Hoa, 2004). In contrast, Professor Wiersinga's group reported that neither GD-IgG nor recombinant human TSH could enhance hyaluronan synthesis in undifferentiated orbital fibroblast (van Zeijl et al., 2010). However, they subsequently confirmed the increase of hyaluronan production in response to GD-IgG, but not recombinant human TSHR, by using differentiated orbital fibroblasts (van Zeijl et al., 2011). More recently, Kumar and colleagues reported an increase in production of hyaluronan in response to bovine TSH as well as human stimulatory TSHR mAb (M22) in undifferentiated orbital fibroblasts from GO patients (Kumar et al., 2012). Regardless of differences between these studies (discussed in more detail in Chapter 1), the latter study also showed that blocking mAb to IGF-1R (1H7 mAb) inhibited hyaluronan synthesis (Kumar et al., 2012). Thus, functional studies in orbital fibroblasts suggest a close relationship at a functional level between TSHR and IGF-1R.

Supportive evidence for the role of IGF-1R pathway in the pathogenesis of Graves' orbitopathy has been recently revealed by an important molecular study from Dr Ezra

and colleagues (Ezra et al., 2012). In essence, they have applied gene expression profiling on archived histological samples of orbital fat from active, but untreated GO patients. The results of this study showed that in addition to Wnt signalling components, IGF-1R and its ligand, as well as downstream transcriptional regulators such as SGK (PDK/Akt signalling), score highly in a hit map of differentially expressed genes detected by microarray. These results were then confirmed by qRT-PCR (Ezra et al., 2012). Despite the limitation of rare availability of active GO orbital fat specimens, this study identified significant changes in IGF-1R molecular signalling systems in the orbital tissue. However, other groups using similar approach for studying orbital tissue of GO patients did not show significant changes in the components of IGF-1R pathway (Kumar et al., 2005, Lantz et al., 2005, Chen et al., 2008b, Planck et al., 2011). Differences in disease severity between patients, as well as a history of treatment with steroids and radiotherapy, may explain the differences between the results of the latest study of Ezra and colleagues (Ezra et al., 2012) compared with earlier studies (Kumar et al., 2005, Lantz et al., 2005, Chen et al., 2008b, Planck et al., 2011). The careful selection of specimens by Dr Ezra and colleagues may have been crucial for the demonstration of a role for the IGF-1R pathway in their study (Ezra et al., 2012).

Whilst all the above studies indicate a pathophysiological role for IGF-1R Ab in differentiation of orbital fibroblast, it has been extremely difficult to measure IGF-1R Ab in GO patients. Attempts to measure anti-IGF-1R Abs in patients' sera have been reported recently by two independent groups. In Professor Schomburg's laboratory, although they could specifically measure IGF-1R Ab in isolated IgG from human sera, there were no obvious differences between GO patients and controls (Minich et al., 2013). They have shown that there was no clear association between IGF-1R Ab levels

and the activity of GO when using a luminescent immunoprecipitation assay with human embryonic kidney cells stably transfected with IGF-1R (Minich et al., 2013). Professor Wiersinga's laboratory determined IGF-1R stimulating activity by using IGF-1R kinase receptor activation assay. The results indicated that in a subset of patients with GO, IgGs may have IGF-1R stimulating activities after taking TBII activity and age into account (Varewijck et al., 2013). They divided GO patients into two groups based on the TBII activity and demonstrated where TBII was above mean +1 SD, IGF-1R stimulating activity was positively correlated with age. In a subgroup of patients who had IGF-1R stimulating activity above mean -1 SD, depletion of IgGs significantly decreased IGF-1R stimulating activity (Varewijck et al., 2013).

An Editorial by Professor Smith accompanying the two articles (Smith, 2013) addressed the potential issues that may be responsible for the contradictory results between these two reports, as well as the earlier studies of Weightman et al and Pritchard et al (Weightman et al., 1993, Pritchard et al., 2003). The Editorial commented that both of these studies underestimated the complexities of IGF-1 binding proteins (IGFBPs) to influence binding of IGF-1 to IGF-1R. Six family members of IGFBPs have been identified with different cellular functions (Firth and Baxter, 2002). IGFBP2, for example, is able to modulate the actions of IGF-1 on IGF-1R and can influence post-IGF-1R signalling (Shen et al., 2012). The unavailability of IGFBPS in transfected cell lines may be responsible for inhibition in binding IGF-1 to its receptor. Therefore, it was suggested that the use of a transfected cell line (Minich et al., 2013, Varewijck et al., 2013) instead of human fibroblasts as used in earlier studies (Weightman et al., 1993, Pritchard et al., 2003) may be responsible for the disparate results (Smith, 2013).

Recently, our laboratory developed an experimental model of Graves' disease which also showed histological signs of fibrosis in the orbital tissue, based on hTSHR A-subunit plasmid *in vivo* electroporation (Zhao et al., 2011). It was shown that this model maintains longevity of induced antibody response to TSHR with accompanying hyperthyroidism in 8 out of 12 mice. A proportion of the animals immunised with hTSHR A-subunit plasmid were positive for IGF-1R Abs. To get an insight into potential mechanisms responsible for induction of IGF-1R Abs in mice immunised with hTSHR A-subunit plasmid, three models were proposed that may explain this activity. The proposed models could help us to investigate the role of induced IGF-1R Abs in the pathogenesis of GO.

5.2   Aims

The main purpose of this Chapter was to investigate the mechanisms of induction of anti-IGF-1R Abs in animals immunised with hTSHR A-subunit plasmid *in vivo* electroporation. I proposed to address this by the following aims:

- Development and validation of different assays for measuring anti-IGF-1R Abs.

- Evaluate the induction of anti-IGF-1R Abs in mice immunised with hTSHR A-subunit plasmid *in vivo* electroporation.

- Development of anti-IGF-1R Abs as mAbs from mice immunised with hTSHR A-subunit plasmid *in vivo* electroporation.

- Characterisation of the anti-IGF-1R mAbs to investigate their role in pathophysiology of GO.

5.3   Results

5.3.1 Development and validation of assays for IGF-1R Abs

There are no commercial kits available to measure mouse or human IGF-1R Abs. In this project, detection of IGF-1R Abs by a reproducible and rapid assay was crucially important. As mentioned earlier, in my supervisor's laboratory, a radioligand binding assay to measure anti-IGF-1R Abs had been developed (Zhao et al., 2011). To measure anti-IGF-1R Abs in mice, Zhao and colleagues used a radioligand-binding assay with antigen generated using an *in vitro* transcription and translation system (TnT, Promega) (Tree et al., 2000, Zhao et al., 2011) to produce radioactive ^{35}S-methionine-IGF-1Rα subunit. Mouse serum samples were incubated with radiolabeled IGF-1R in the immunoprecipitation buffer and immune complexes captured on protein G-Sepharose. The presence of IGF-1R Abs in serum leads to increase in the radioactive count. Although the coupled TnT assay has been widely used for generating radiolabelled antigens for measuring autoantibody binding to islet cell antigens such as glutamic acid decarboxylase (GAD) and IA-2 in type 1 diabetes (Bonifacio et al., 2010), it has not been used for measuring IGF-1R Abs.

Although Zhao and colleagues had used coupled TnT assay for measurement IGF-1R Abs in mice sera and published their results, I wanted to expand on evaluating different assay designs to select an assay that was reproducible and rapid and hence suitable for hybridoma screening. So, for my studies dealing with anti-IGF1R Abs in the mouse model, my first objective was to develop and validate other assays for anti-IGF-1R Abs.

5.3.1.1 Flow cytometry

NWTB3 cells, being a mouse fibroblast cell line (NIH/3T3) stably transfected to express human IGF-1R was provided by Professor LeRoith (Blakesley et al., 1995). The transfected cells were reported to express 410,000 receptors per cell (Blakesley et al., 1995). Initially, NWTB3 cells were evaluated on IGF-1R expression with IGF-1R mAb, 1H7 mAb (1µg/ml) (BioLegend, UK). Gating strategy was evaluated based on 75-80% of 50,000 counted cells (called P1) as shown in **Fig 5.3 A**. NWTB3 cells were positive for IGF-1R expression with >77% highly positive cells in the population, compared to less than 1% in isotype matched, IgG1 control mAb (**Fig 5.3 B, C**). Different concentrations of 1H7 mAb were tested and data analysed by determination of the mean fluorescence intensity (MFI), (**Fig 5.3 C-F**). Using anti-IGF-1R mAbs, the intra-assay coefficient of variation (CV), (precision within the assay) was determined to be 10%. Inter-assay CV (precision between assays) was calculated using the same anti-IGF-1R mAb, measured in three consecutive runs and determined to be <25%. The calculations of inter-assay and intra-assay CV for the flow cytometry assay are described in **Appendix 2**.
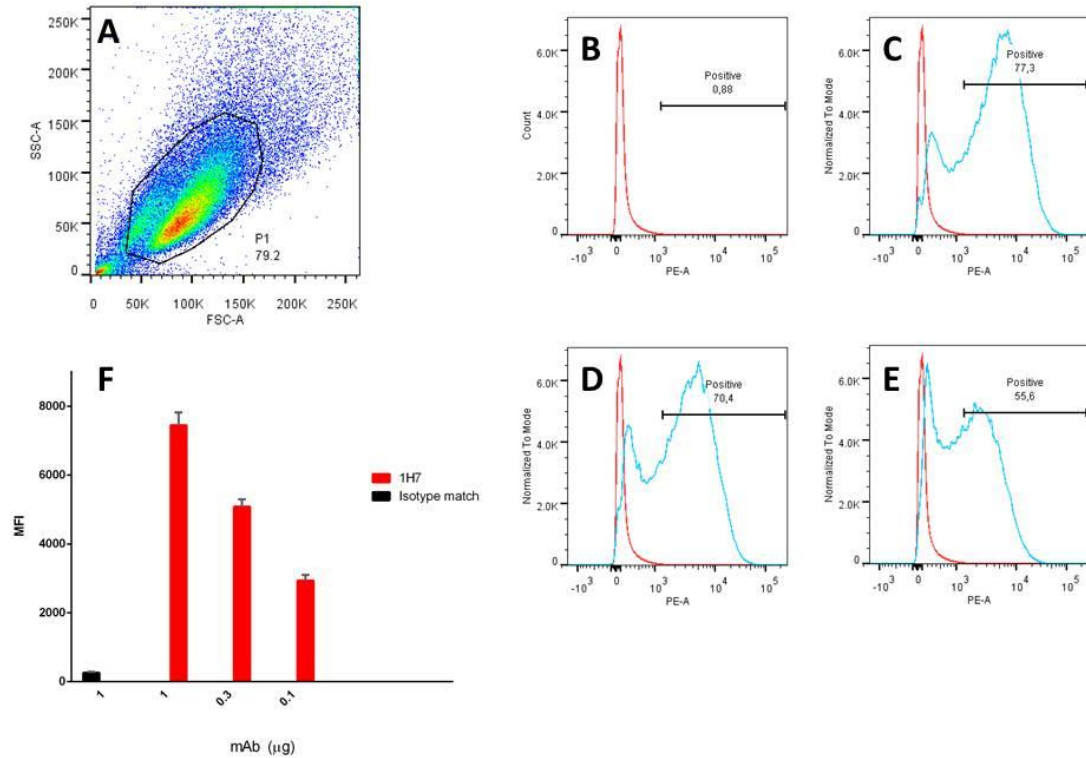
Fig 5.3 Flow cytometry in NWTB3 cells with 1H7 mAb

(A) Gating strategy. SSC-A: side scatter, FSC-A: forward scatter. (B) Fluorescence intensity histogram of negative control, isotype matched, IgG1 (1 µg). Fluorescence intensity histogram (blue histogram vs red as negative control) of (C) 1µg 1H7 mAb which showed 77% cell positive. (D) 0.3µg 1H7 mAb showed 70% cell positive. (E) 0.1µg 1H7 mAb showed 55% cell positive. (F) Mean florescent intensity of binding to different concentration of 1H7 mAb to NWTB3 cells. The experiment has been performed three times with comparable results. The bar represents standard deviation. 1µg of 1H7 mAb demonstrated 8000 MFI while the same concentration of isotype matched mAb resulted in <500 MFI.

In addition to the aforementioned flow cytometry study by indirect (sandwich) staining, another experiment evaluated IGF-1R expression in NWTB3 cells by direct staining using PE labelled 1H7 mAb (BD Biosciences) by flow cytometry. The percentage of positivity in stained cells (75% vs 83%) and fluorescent intensity (13100 vs 15900) for indirect and direct staining respectively, clearly showed that direct staining presents comparable results to the indirect 1H7 mAb **(Fig 5.4 A-C)**. Indirect staining methods are generally considered to be more sensitive and superior to direct staining methods due to 'amplification' of the signal in the former (Hay et al., 2001). Thus, the fact that direct and indirect staining for IGF-1R expression in NWTB3 cells was comparable, further support the high levels of expression of IGF-1R in the transfected cells.

To further investigate the flow cytometry analysis in NWTB3 cells, we tested a new set of IGF-1R mAbs. Professor Kenneth Siddle (University of Cambridge, UK) kindly provided four anti-IGF-1R mAbs directed to different determinants of IGF-1R (Soos et al., 1992). The mAbs termed 24-31 mAb, 24-60 mAb, 17-69 mAb and 24-57 mAb were supplied as freeze dried ascites (**Table 5.1**). The freeze dried ascites was gently resuspended in sterile water and purified by protein G column chromatography and tested by flow cytometry on NWTB3 cells. Data are shown in **Fig 5.4 D-H**. Determination of signal intensity by flow cytometry of IGF-1R mAb to different determinants resulted in wide range of MFI and positive staining for NWTB3 cells. At a concentration of 1 μg of 24-31 mAb showed 7% positive cells (**Fig 5.4 D**), 24-60 mAb showed 25% positive cells (**Fig 5.4 E**), 24-57 mAb showed 60% positive cells (**Fig 5.4 F**), and 17-69 mAb showed 30% positive cells (**Fig 5.4 G**). The mean fluorescence intensity of each experimental condition is concluded in **Fig 5.4 panel H**. Among the IGF-1R

mAbs, the highest MFI value belonged to 24-57 mAb. On the other hand, 24-31 mAb did not show significant difference from isotype match control. The variation in the results of the other mAbs is likely due to the differences in the specific epitope determinants exposed on native IGF-1R on the plasma cell membrane of NWTB3 cells. These anti-IGF-1R mAbs were not evaluated for binding by flow cytometry by Soos and colleagues, thus it is not possible to correlate the flow cytometry binding data described herein to the epitope binding patterns (**Table 5.1**) reported in their publication (Soos et al., 1992). However, it is well known from TSHR mAb analysis that the variation in mAbs determinants leads to differences in positivity of flow cytometry (Patibandla et al., 1997, Shepherd et al., 1999, Mizutori et al., 2009). For example, compared to other mAbs, 2C11 mAb and 4C1 mAb to TSHR are considered gold standard Abs for flow cytometry since their determinants appear to be most easily accessible on the native receptor.

anti-IGF-1R mAb	isotype	epitope	blocking activity
24-31	IgG1	283-440 or 586-908	0
24-60	IgG2a	184-283	++
24-57	IgG1	440-586	++
17-69	IgG1	440-586	+

Table 5.1 Specification of anti-IGF-1R mAbs received from Professor Siddle's laboratory

Anti-IGF-1R mAb codes are derived from the nomenclature used by Soos et al, 1992. Blocking activity classified based on the inhibition of ^{125}I-IGF-1binding to receptor; '0' = 20% inhibition, '+' = 35-60% inhibition and '++' > 80% inhibition.
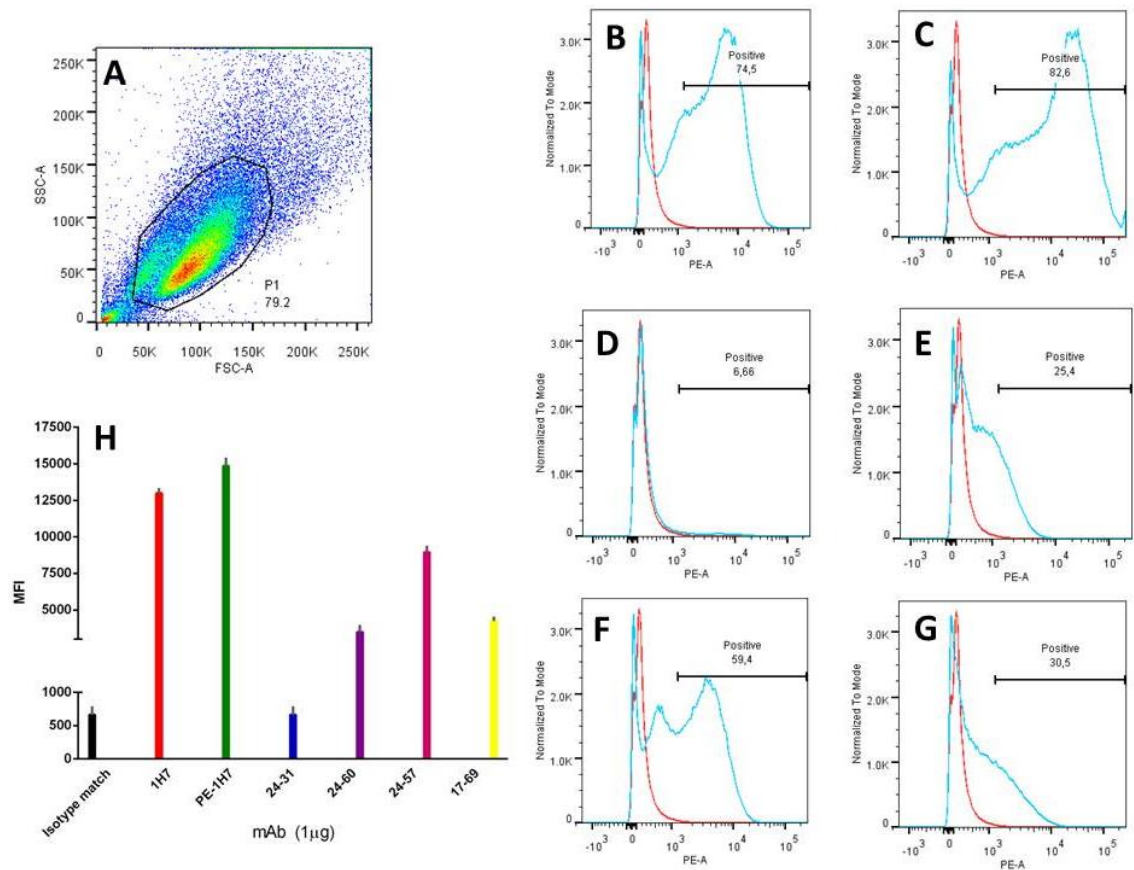
Fig 5.4 Flow cytometry in NWTB3 cells with different anti-IGF-1R mAbs

IGF-1R mAbs include PE-1H7 for direct staining and four other mAbs directed to different determinants of the receptor **(A)** Gating strategy. SSC-A: side scatter, FSC-A: forward scatter. For panels B to G**;** Fluorescence intensity histogram (blue histogram vs red as negative control) of **(B)** 1H7 mAb (1 µg, indirect staining) showed 75% positive cells (it is comparable with 77% positive cells in the different experiment presented in Fig 5.3) , **(C)** PE-1H7 mAb (direct staining) indicated 82% positive cells **(D)** 24-31 mAb (1 µg) showed 7% positive cells, **(E)** 24-60 mAb (1 µg) showed 25% positive cells, **(F)** 24-57 mAb (1 µg) showed 60% positive cells, **(G)** 17-69 mAb (1 µg) showed 30% positive cells. **(H)** Mean fluorescent intensity of binding different anti-IGF-1R mAbs to NWTB3 cells. The experiment has been performed two times with comparable results. The bar represents standard deviation.

5.3.1.2 Evaluation for constitutive expression of TSHR in NWTB3 cells

Since I planned to use the stably transfected NWTB3 cells expressing hIGF-1R in flow cytometry to evaluate anti-IGF-1R Abs in mice immunised with hTSHR A-subunit plasmid, it was important to first determine that the NWTB3 cells did not express TSHR. The gold standard anti-TSHR mAb for evaluating TSHR expression by flow cytometry, 4C1 was used for these experiments. In addition, another mAb with agonist activity to the TSHR developed in our laboratory (KSAb1) was utilised (Gilbert et al., 2006). Gating strategy for flow cytometry is shown in **Fig 5.5 A**. The flow cytometry results of NWTB3 cells clearly indicated that there is no binding site for the examined TSHR mAbs. The mean fluorescence intensity of 1H7 mAb at highest concentration was above 7000. However, the MFI value for TSHR mAbs at same concentration were not more than 600, equal to the value for control mAb (**Fig 5.5 B, C**).

In addition, expression of TSHR was examined in the GPI9-5 cells, which served as positive control, with 4C1 mAb used at the same concentrations (**Fig5.6**). GPI9-5 cells, CHO cell line stably transfected to express human TSHR A-subunit, were kindly provided by Dr Phillip Watson (Sheffield) (Metcalfe et al., 2002). Gating strategy for flow cytometry of GPI9-5 cells with isotype control (IgG2a) is shown in **Fig 5.6 A**. The flow cytometry results showed high level of TSHR expression by GPI9-5 cell. The highest concentration of 4C1 mAb exhibited 12,500 MFI with more than 77 percent of positive cells (**Fig 5.6 B, C**). The flow cytometry results of NWTB3 cells clearly indicated that there is no binding site for the examined TSHR mAbs. The mean fluorescence intensity of 1H7 mAb at highest concentration was above 7000. However, the MFI

value for TSHR mAbs at same concentration were not more than 600, equal to the

value for control mAb (**Fig 5.5 B, C**).
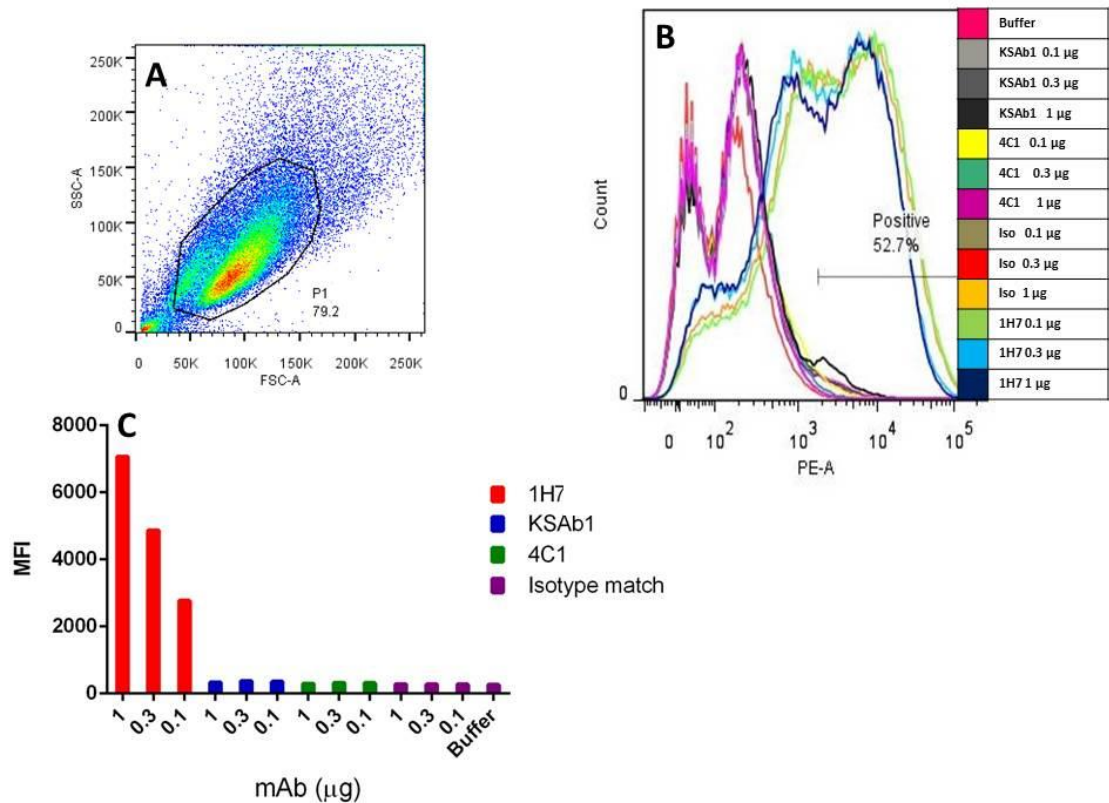
Fig 5.5 Evaluation of TSHR expression in NWTB3 cells by flow cytometry
Different concentrations of anti-TSHR mAbs (4C1 mAb and KSAb1) as well as
anti-IGF-1R mAb, 1H7 mAb, on NWTB3 cells were tested. **(A)** Gating strategy.
SSC-A: side scatter, FSC-A: forward scatter. **(B)** Fluorescence intensity histogram
of different concentrations (1µg, 0.3µg, 0.1µg) of four different mAbs, 1H7
mAb, KSAb1, 4C1 mAb and negative control IgG1. **(C)** Mean fluorescence
intensity shows that NWTB3 cells do not express TSHR. Negative controls are
buffer and IgG1.
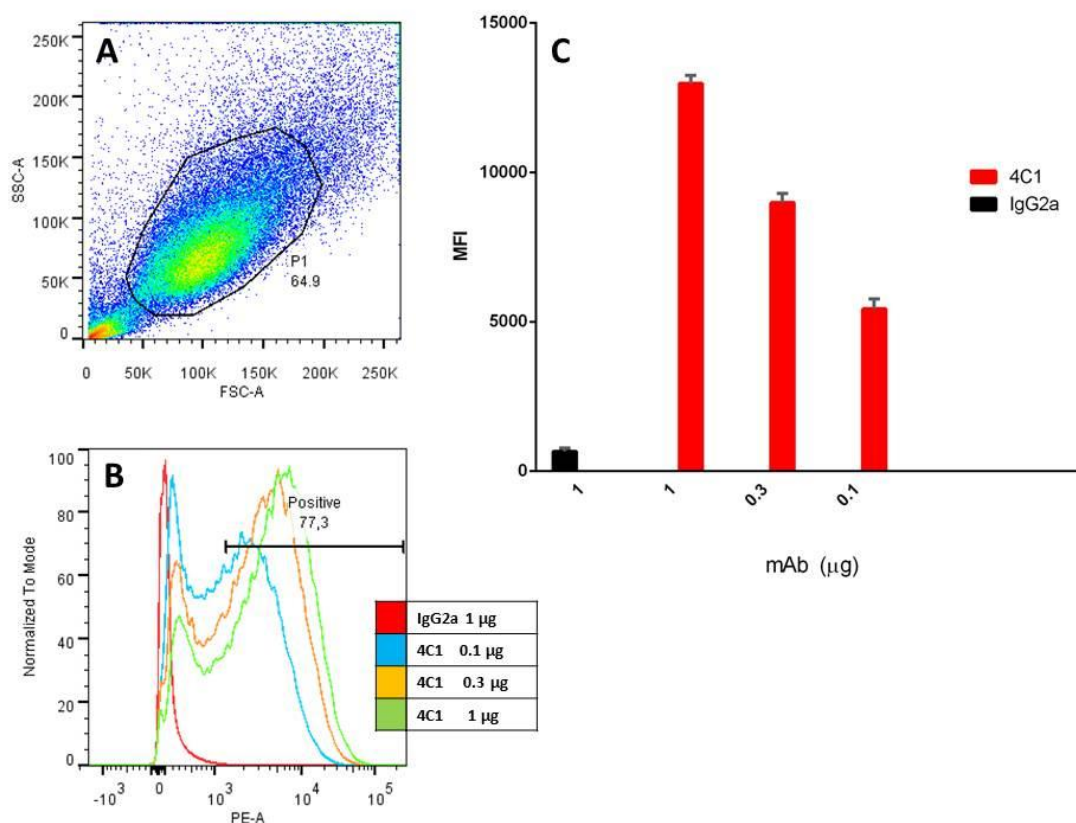
Fig 5.6 Flow cytometry in GPI5-9 cells by anti-TSHR mAb
(A) Gating strategy. SSC-A: side scatter, FSC-A: forward scatter. **(B)** Fluorescence intensity histogram of different concentrations (1µg, 0.3µg, 0.1µg) of 4C1 mAb and negative control, IgG2a. **(C)** The data of mean fluorescence intensity showed expression of TSHR by GPI5-9 cells.

5.3.1.3   Cell based competitive binding assay

After successful establishment of the flow cytometry assay to measure IGF-1R Abs and verifying the expression of IGF-1R by NWTB3 cells, the competitive binding assay was designed. The competitive binding assay was set up based on the displacement of labelled-IGF-1 by cold IGF-1, similar to that reported by Weightman and colleagues (Weightman et al., 1993). However, there are some technical differences between these two assays: (i) radioactive (^{125}I) tracer has been replaced by chemiluminescence

ligand and (ii) transfected (NWTB3) cells expressing hIGF1R were used instead of human fibroblasts in the assay. Lumi-IGF-1 was provided by Professor Lutz Schomburg (University of Berlin, Germany) (Minich et al., 2013). Luminescence activity of Lumi-IGF-1 was at 10^8 RLU/µL.   Initially, concentration of tracer and number of cells were evaluated to optimise the assay. Briefly, monolayer cells were cultured in 96 well and 24 well plates overnight, cells were washed and incubated for 6 hours at 4^oC with different concentration of Lumi-IGF-1. The concentration of Lumi-IGF-1 was between $5x10^5$ RLU/µl and $1x10^3$ RLU/µl with five fold dilution. **Fig 5.7** shows that Lumi-IGF-1 was able to bind to IGF-1R expressed in NWTB3 cells. Binding to receptors by Lumi-IGF-1 in 24 well plate were four fold higher in comparison to the binding observed in 96 well plate. It is most likely due to the larger number of the cells in the former plates. Thus, 24 well plate was selected for subsequent studies.
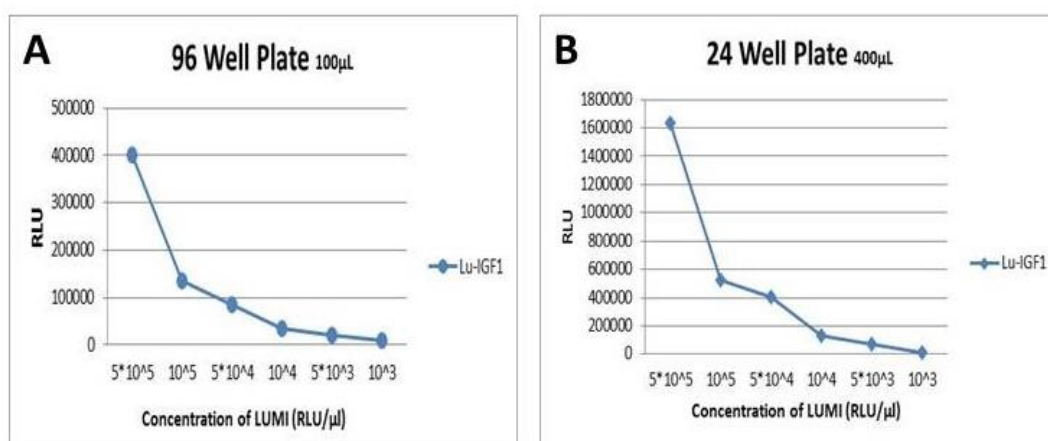
Fig 5.7 Binding of Lumi-IGF-1 NWTB3 cells in dose dependent manner
(A) 96 well plates with 20,000 NWTB3 monolayer cell cultures. **(B)** 24 well plates with 80,000 NWTB3 monolayer cell cultures. The results showed that binding of Lumi-IGF-1 to the receptor is 4 fold higher in 24 well plate compared to 96 well plate.

The next experiments examined the binding of Lumi-IGF-1 to NWTB3 cells in 24 well plates in competition with different concentrations of unlabelled IGF-1 to evaluate the sensitivity of assay. Monolayer of NWTB3 cells were cultured in 24 well plates overnight, cells were washed and incubated for 6 hours at 4^oC with different concentrations of tracer (Lumi-IGF-1) and competitor (unlabelled IGF-1). Highest concentration of unlabelled IGF-1 was 10^{-7} M which decreased to 10^{-10} M with 10 fold dilution. Dilution worked out based on the 10^{-7} M equal to 1μg/ml of IGF-1 in sterile PBS (details of calculation are presented in **Appendix 3**).

The competition binding results indicated that the concentration of $5x10^4$ RLU/μl of Lumi-IGF-1 is the optimum condition for binding assay. From the results in **Fig 5.8**, it is obvious that the sensitivity of assay increased as the tracer concentration declined from $5x10^5$ RLU/μl to $5x10^4$ RLU/μl. However, decrease in tracer concentration from $5x10^4$ RLU/μl to 10^4 RLU/μl caused to reduction in the binding sensitivity. The optimum condition (24 well monolayer NWTB3 cells with $5x10^4$ RLU/μl) provided the sensitivity of approximately 1.7 nM of IGF-1 (IC_{50} = 1.7nM) which was very close to the sensitivity demonstrated by competition assay in the study by Weightman et al (IC_{50} = 1nM) (Weightman et al., 1993) (**Fig 5.9 A,B**). The details of calculation to compare between two studies are presented in **Appendix 4**.
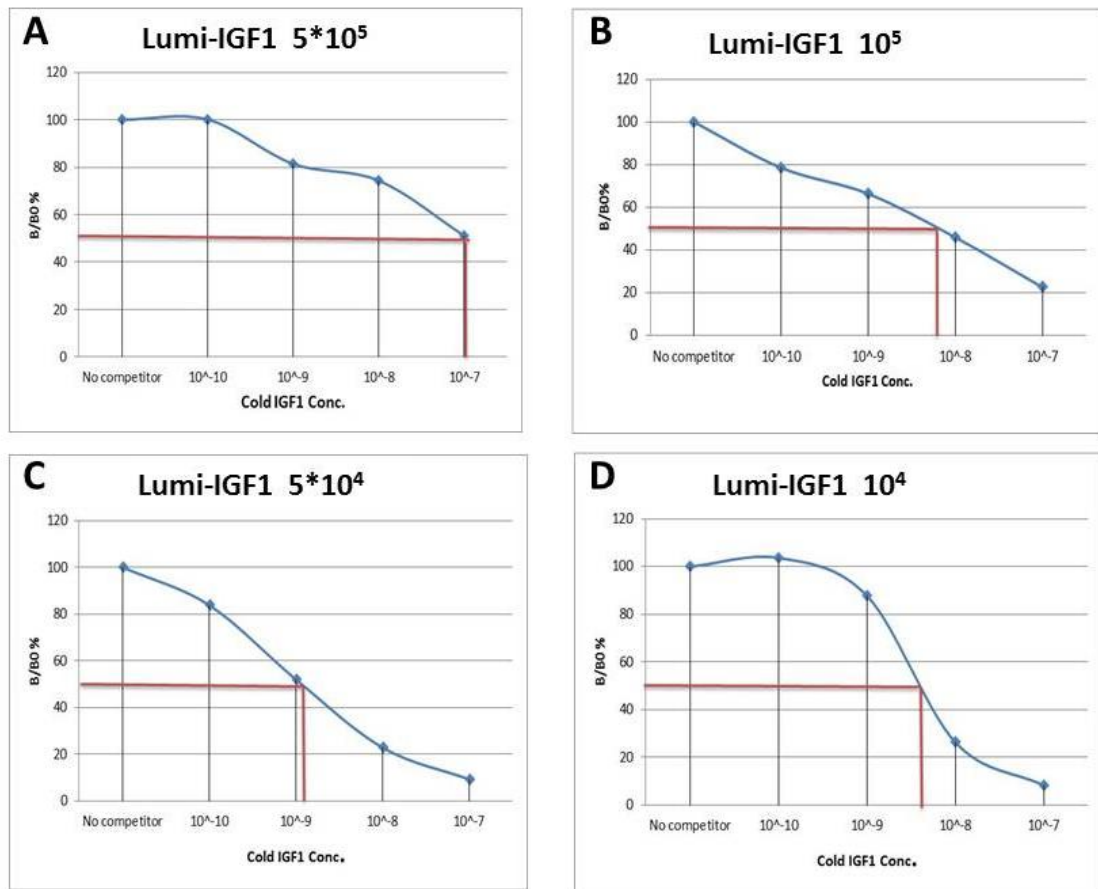
Fig 5.8 Competition curve of different concentrations of Lumi-IGF-1
The competition curve with unlabelled (cold) IGF-1 (24 well plates). is shown in
(**A**) Lumi-IGF-1 concentration is 5×10^5 RLU/µl, (**B**) Lumi-IGF-1 concentration is
10^5 RLU/µl, (**C**) Lumi-IGF-1 concentration is 5×10^4 RLU/µl, (**D**) Lumi-IGF-1
concentration is 10^4 RLU/µl. The red lines in each panel is represents the IC_{50}.

The next step was to verify the competition assay optimised for displacement with

cold IGF-1, for its ability to function with anti-IGF1-R Abs in a dose dependent manner.

In the studies reported by Weightman and colleagues, purified IgG from pooled sera of

Graves' patients were used for displacement ^{125}I-IGF-1 (Weightman et al., 1993). As

the sera of Graves' patients were not available for our study, I decided to evaluate two

IGF-1R mAbs directed to different determinants on the receptor. Purified 24-57 mAb

and 1H7 mAb, both characterised with strong blocking activity of binding IGF-1 to its receptor (Soos et al., 1992, Kusada et al., 2008), were examined for displacement of Lumi-IGF-1. Surprisingly, although, it was shown that Lumi-IGF-1 can be displaced by cold IGF-1 in a dose dependent manner with appropriate sensitivity, neither 1H7 mAb nor 24-57 mAb could displace Lumi-IGF-1 as effectively as cold IGF-1 (**Fig 5.9 C, D**). Hence, despite the fact that the competition assay were designed very carefully following the analysis of flow cytometry results, during the validation of assay, it was clear that measurement of anti-IGF-1R Abs in serum samples would be far beyond the capability of this assay. Therefore, further evaluations on this assay have not been continued.

5.3.1.4 ELISA

ELISA for detection IGF-1R Ab was established based on the protocol described by Yin and colleagues (Yin et al., 2011). They were able to detect IGF-1R Abs in sera from patients treated with Dalotuzumab, an anti-IGF1R Abs, intended for cancer therapy. For this reason, recombinant human IGF-1R extracellular domain (rhIGF-1R ECD) was obtained from a commercial sourse (R&D Systems). The source of receptor (102.9 kDa) was recombinant protein produced in murine myeloma cells. The purified receptor showed a single polypeptide band in SDS PAGE gels but details of the purification procedure for recombinant IGF-1R was not provided by supplier (R&D Systems, UK).

Initially, ELISA was examined by testing of 1H7 mAb at different doses (from 15 ng to 500 ng) to verify the capability of ELISA in measuring the Ab in a dose dependent manner (**Fig 5.10**). The analysis of 1H7 mAb at different doses by ELISA clearly indicated the ability of this assay for measuring anti-IGF-1R Ab from 30 ng per well (**Fig

5.10). 15 ng of 1H7 mAb did not show significant difference with blank. The significant difference started from 30 ng of 1H7 per well. For further evaluation the assay, serum samples of mice immunised with pTriEx-IGF-1Rα from the study by Dr. Zhao and colleagues (Zhao et al., 2011) were used to determine the inter-assay and intra-assay CV. The result of this experiment was used to analyse assay precision. Assay precision was determined using antiserum containing high and moderate levels of Abs to IGF-1R. The intra-assay CV calculated by analysing of 8 antisera in duplicate which determined to be less than 3.2%. Inter-assay CV was calculated by using the same set of antisera, measured in five consecutive runs and determined to be less than 6.6% (**Appendix 5**).
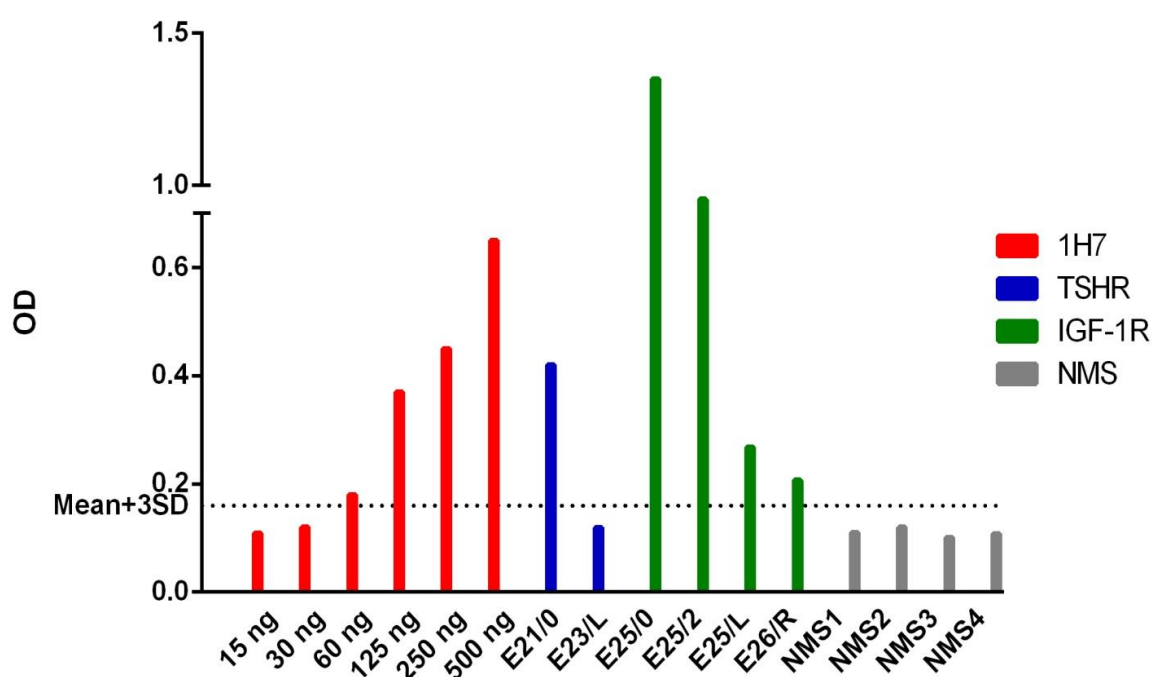
Fig 5.11 Re-examination of IGF-1R Abs by ELISA assay in serum samples in immune mice from study by Zhao and colleagues

The data of mice immunised with hTSHR A-subunit plasmid (blue), pTriEx-IGF-1Rα plasmid (green), and non-immunised mice sera (grey) presented by OD. E21/0, the mouse scored positive in the TnT assay, was significantly positive by ELISA too. Sera diluted 1:20. Numbering system is same as used in Zhao and colleagues. Different concentrations of 1H7 mAb (red) served as positive

control. NMS: normal mice sera. The dotted line shows mean of normal mice sera value plus 3 times of standard deviation (Mean+3 SD).

Once the assay evaluation had been successfully conducted, as well as re-examination of serum samples from Zhao and colleagues study (Zhao et al., 2011) confirmed the positivity of their serum samples for IGF-1R Abs by ELISA, I then initiated the examination of serum samples from my study for IGF-1R Abs.
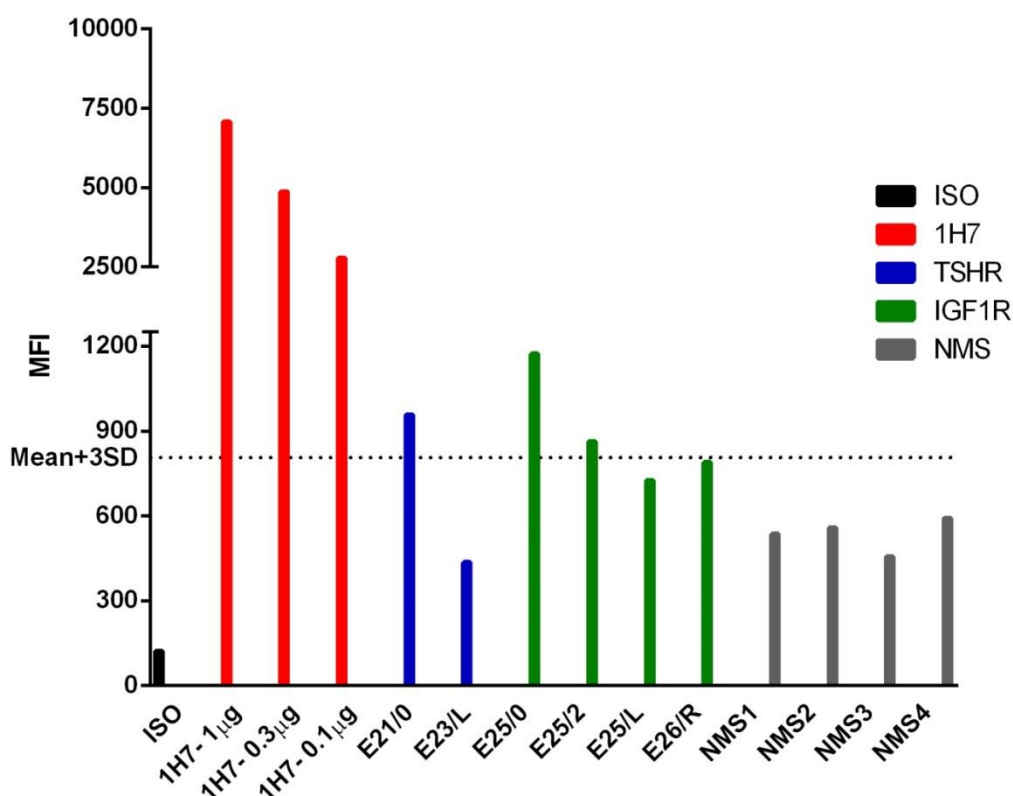
Fig 5.12 Re-examination of IGF-1R Abs by flow cytometrey in serum samples in immune mice from study by Zhao and colleagues
Different concentrations of 1H7 mAb (red) were tested as positive control. The data of mice immunised with hTSHR A-subunit plasmid (blue), pTriEx-IGF-1Rα (green) and non-immunised mice sera (grey) presented by mean fluorescent intensity. Numbering system is same as used in Zhao and colleagues. Control IgG1 served as isotype matched (ISO, black).

5.3.2 Evaluation of IGF-1R Abs in mice immunised with TSHR A-subunit using modified protocol

Having successfully developed and validated ELISA for measuring IGF-1R Abs in the sera of immune animals allowed us to examine IGF-1R Abs in mice immunised with hTSHR A-subunit plasmid from my studies. For better understanding, in this Chapter, the nomenclature of each group of immunised mice is changed to group number as outlined in **Appendix 1**. Therefore, from hereon, the results of anti-IGF-1R Abs in mice sera immunised with hTSHR A-subunit plasmid will be referred to the Group starting from the Group 1 (cohort of mice sacrificed 6 week after end of immunisation), following by the Group 2 (cohort of longitudinal study, sacrificed 9 weeks after end of immunisation) and Group 3 (long term effect study, sacrificed 15 week after end of immunisation). In addition, a new group of mice were immunised especially for IGF-1R mAb development and sacrificed 6 week after end of immunisation, this group is referred to as Group 4 (**Appendix 1**).

5.3.2.1 Studies into induction of IGF-1R Abs in Group 1 immunisation

As described earlier, in the Group 1 immunisation, eight mice were challenged with hTSHR A-subunit plasmid. Animals similarly immunised with pTRiEx1.1 neo-IGF-1Rα (n=3) and pTRiEx1.1 neo-β-Gal plasmids (n=3) were used as the control group. During the course of immunisation, one animal was sacrificed due to severe sickness. Rest of immune animals and controls were sacrificed six weeks after end of immunisation. Abs to IGF-1R in this group of animals was tested four weeks after end of immunisation by ELISA (**Fig 5.13**). Assessment of Abs to IGF-1R by ELISA demonstrated that 7 out of 8

animals immunised with hTSHR A-subunit plasmid were positive for anti-IGF-1R Abs when tested at 1:20 dilution. However, the Abs levels to IGF-1R were lower in comparison with the serum samples from mice immunised with IGF-1Rα plasmid. Control animals (mice immunised with pTRiEx1.1 neo-β-Gal plasmids) scored negative for IGF-1R Abs (**Fig 5.13**).
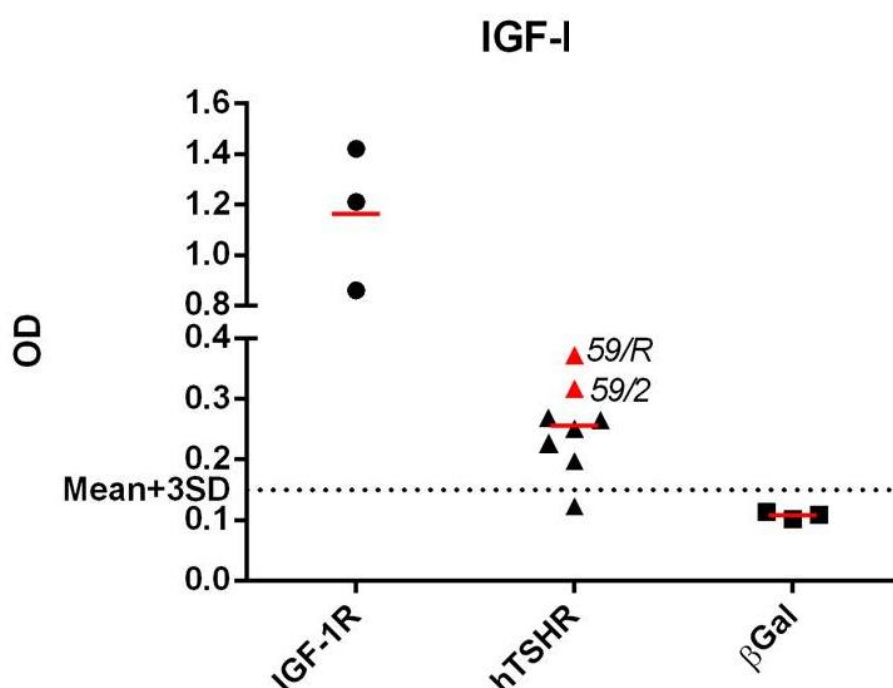
Fig 5.13 Evaluation of IGF-1R Abs by ELISA in mice immunised with hTSHR A-subunit plasmid of Group 1

Group 1 immunisation with hTSHR A-subunit plasmid (labelled hTSHR), IGF-1R plasmid (labelled IGF-1R) and control β-Gal plasmid (labelled βGal). The dotted line indicates mean+3 SD based on control β-Gal plasmid-immunised mice. Two mice immunised with TSHR A-subunit plasmid, 59/R and 59/2 were used to develop mAbs are indicated (see section 5.1.3)

To confirm the results of Abs to IGF-1R by ELISA, mice sera were also tested by flow cytometry assay (**Fig 5.14**). As already mentioned, flow cytometry was not able to detect anti-IGF-1R Abs in every individual mice immunised with TSHR A-subunit, but the serum samples with the strongest positivity in ELISA, also scored positive by flow cytometry (**Fig 5.14**). In addition, all three positive control sera from mice immunised with IGF-1Rα plasmid showed significant increase in MFI value.
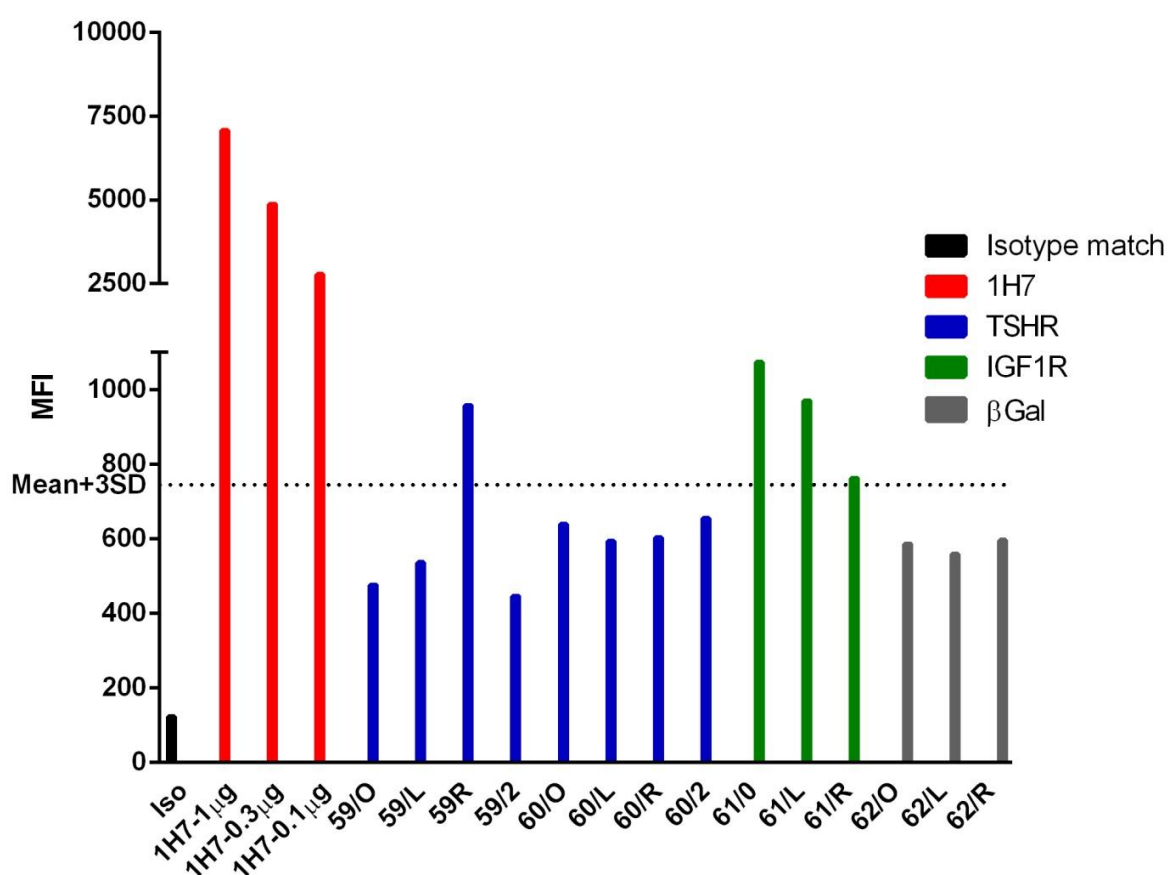
Fig 5.14 Determination of IGF-1R Abs by flow cytometry in mice immunised with hTSHR A-subunit plasmid of Group 1

Group 1 immunisation (labelled hTSHR, blue), IGF-1R plasmid (labelled IGF-1R, green) and control β-Gal plasmid (labelled βGal, gray). The dotted line indicates mean + 3 SD based on control β-Gal plasmid-immunised mice. 1H7 mAb (red) served as positive control.

5.3.2.2 Longitudinal studies into induction of IGF-1R Abs in the Group 2 immunisation

To evaluate alteration of antibodies in the GO experimental model, longitudinal study was performed in the Group 2 immunisation with eight female BALB/c mice. Animals were bled every week from one week before the last injection until week 6 and serum samples were analysed from the serial bleeds for longitudinal studies. All animals were sacrificed nine weeks after end of immunisation. Histological studies and TSHR Ab levels were presented in Chapter 3 and proved that this cohort of animals recapitulated orbital manifestation of earlier group of immunisation. However, in contrast to the earlier cohort of immunisation, all of the eight mice immunised with hTSHR A-subunit plasmid scored negative at all the time points (expect one weakly positive) for anti-IGF-1R Abs by ELISA (**Fig 5.15**). A weekly analysis of IGF-1R Abs for individual animals presented from one week before end of immunisation (-1) to six weeks after end of immunisation.
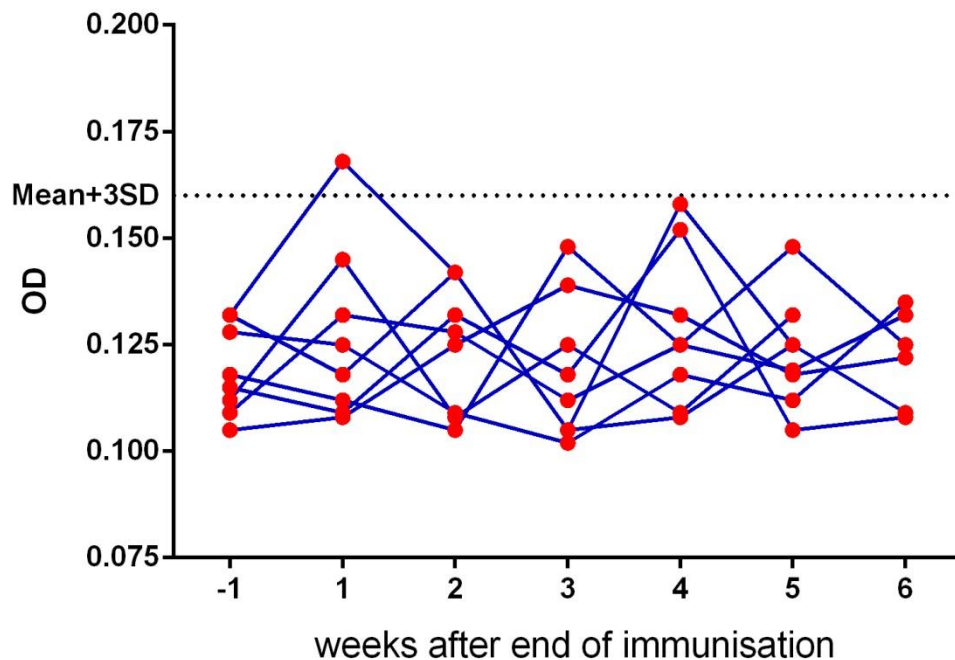
Fig 5.15 Longitudinal analysis of anti-IGF-1R antibodies by ELISA in immune mice of Group 2

Serum samples were collected every week in individual mice for IGF-1R Ab analysis in Group 2 animals. The ordinate shows week when serum sample collected, with the first sample collected one week before the end of immunisation (labelled -1), with all subsequent bleeds collected weekly until 6 weeks after end of immunisation. Measurement of IGF-1R Ab by ELISA, presented as OD. None of the immune animals were scored positive for IGF-1R Ab (except one weakly positive in week 1).

5.3.3 Development of mAbs to IGF-1R

Development of mAbs in an experimental model can be challenging if the goal is to generate mAbs to an antigen (IGF-1R) that is a different protein from the immunogen (TSHR). Initially, I planned to conduct mock fusions to practice the hybridoma technique, while the animals dedicated for the mAb project were undergoing the long immunisation scheme. The mock fusions would allow me to gain expertise in the technique to maximise number of wells with hybridoma cell growth, before moving to develop hybridomas from hTSHR A-subunit immune mice also positive for anti-IGF-1R Abs. However, before beginning on the mock fusions, I was overtaken by the events since at the same time immune mice from Group 1 immunisation unexpectedly appeared to be ready for fusion, with strong positive signal for IGF-1R Abs (**Fig 5.13, red**). Therefore, despite my lack of hybridoma technique, we decided to shelf the mock fusion plan and proceed ahead with hybridoma development from immune animals positive for IGF-1R Abs. Two fusions have been completed on mice immunised with pTriEx-TSHR A-subunit which were positive for IGF-1R Abs level in sera. The results of generation of hybridomas for IGF-1R mAbs in mice immunised with hTSHR A-subunit are described below.

5.3.3.1   First attempt on generation of hybridoma for mAbs to IGF-1R

In Group 1 immunisation, serum bleed samples were evaluated for IGF-1R Abs by ELISA, four weeks after the end of immunisation. Based on the ELISA results, animal *59/R* was selected for the first fusion, results are shown in **Fig 5.13** (two highest OD value including 59/R, highlighted with red triangle). All steps of fusion procedure were

followed by hybridoma protocol mentioned in Chapter 2. Briefly, three days before

fusion, mouse was given 0.5 ml of NWTB3 cell ($2x10^6$ cells/mL) in saline by i.v.

injection. On day of fusion, the animal sacrificed by CO_2 inhalation and the spleen

excised under aseptic conditions. Following hybridoma generation, the cells were

plated into five 96 flat well plates in complete DMEM-20/HEPES/pyruvate/HAT/10%

Doma Drive. Doma Drive (Immune systems, UK) is a concentrated feeder supplement

containing a complex mixture of growth factors to enhance hybridoma growth and

survival rates. Plates incubated overnight in a humidified 37°C, 5% CO2 subscript

incubator. On days 4, 5, 7, 9, and 11, half the volume of each well replaced with fresh

complete DMEM-20/HEPES/pyruvate/HAT/10% Doma Drive. On day 14, feeding

protocol changed to replace HAT with HT medium (complete DMEM-
20/HEPES/pyruvate/HT).

Total number of wells that showed growth of hybridoma was approximately 18%. All

the wells tested for IGF-1R Ab by ELISA 3 times (3-5 days apart) and for TSHR Abs with

TRAK kit. There was not any well showing positive signal either with ELISA (**Table5.2)** or

TRAK (data not shown).

	1	2	3	4	5	6	7	8	9	10	11	12
A	0.801	0.063	0.065	0.077	0.078	0.066	0.063	0.062	0.063	0.068	0.069	0.089
B	0.69	0.068	0.064	0.065	0.072	0.07	0.072	0.064	0.105	0.06	0.073	0.066
C	0.551	0.067	0.065	0.073	0.069	0.09	0.075	0.117	0.065	0.062	0.073	0.061
D	0.419	0.067	0.077	0.076	0.08	0.086	0.069	0.069	0.067	0.068	0.075	0.079
E	0.311	0.076	0.069	0.084	0.096	0.103	0.162	0.069	0.067	0.063	0.072	0.068
F	0.138	0.084	0.069	0.073	0.1	0.104	0.067	0.072	0.076	0.065	0.065	0.066
G	0.127	0.069	0.071	0.11	0.067	0.101	0.1	0.07	0.068	0.064	0.064	0.063
H	0.136	0.061	0.093	0.092	0.079	0.116	0.081	0.108	0.066	0.077	0.122	0.066

Table 5.2 Results of first attempt to generate IGF-1R
The anti-IGF-1R Abs in hybridoma supernatants were measured by ELISA (4 weeks
after fusion). As positive control, 1H7 mAb was used a serial dilutions, starting from
500ng (A1) to 100ng (E1) [shadowed in green]. Well numbers F1-E12 represent the

hybridoma culture supernatants. Well numbers F12-H12 represents the IgG1 negative control [shadowed in yellow]. The 'raw' data of OD is shown.

5.3.3.2 Second attempt on generation of hybridoma for mAbs to IGF-1R

Five weeks after the last injection, in the Group 1 immunisation, one animal, *59/2* which was positive for IGF-1R Abs suddenly showed signs of severe sickness. Thus, it was decided to sacrifice the animal immediately and use the spleen cells for hybridoma production, despite the fact that there was no opportunity to give the i.v. injection with NWTB3 cells. Moreover, the myeloma cells had not been split to achieve a 'perfect' log phase for fusions. The log phase growth condition of myeloma cells is critically important for the hybridoma technique. This immune mouse was thus sacrificed 5 weeks after last immunisation. All the fusion steps and feeding hybridoma was same as the protocol that already described for the first fusion.

Total number of wells showed hybridoma growth increased to 26%. All the wells tested for IGF-1R Ab by ELISA 3 times (3-5 days apart) and for TSHR Abs with TRAK kit. There was not any well showing positive signal neither with ELISA nor TRAK assay. **Table5.3** is shown the results of the final IGF-1R Ab measurement by ELISA in supernatant. Despite the fact that the hybridomas generated from this sick animal were all negative for anti-IGF1R (or TSHR) Abs, the growth of hybridoma fusion was 26% (compared to 18% in the first attempt), showing that my technique was improving.

P1	1	2	3	4	5	6	7	8	9	10	11	12
A	0.917	0.128	0.128	0.133	0.12	0.136	0.128	0.125	0.13	0.114	0.108	0.114
B	0.713	0.112	0.123	0.127	0.14	0.111	0.121	0.122	0.111	0.119	0.105	0.101
C	0.528	0.117	0.112	0.123	0.129	0.137	0.132	0.144	0.117	0.139	0.111	0.107
D	0.404	0.126	0.113	0.127	0.132	0.135	0.142	0.111	0.105	0.104	0.111	0.095
E	0.315	0.093	0.113	0.124	0.124	0.122	0.129	0.191	0.1	0.098	0.146	0.1
F	0.095	0.108	0.121	0.131	0.126	0.109	0.153	0.112	0.137	0.113	0.134	0.119
G	0.097	0.11	0.108	0.12	0.141	0.099	0.122	0.146	0.126	0.114	0.13	0.138
H	0.082	0.082	0.111	0.107	0.114	0.12	0.122	0.091	0.149	0.096	0.159	0.098

P2	1	2	3	4	5	6
A	0.918	0.07	0.068	0.067	0.1	0.052
B	0.721	0.066	0.067	0.068	0.166	0.056
C	0.594	0.065	0.07	0.073	0.203	0.071
D	0.415	0.065	0.068	0.076	0.214	0.079
E	0.286	0.069	0.072	0.074	0.117	0.06
F	0.127	0.069	0.069	0.142	0.058	0.059
G	0.122	0.063	0.065	0.096	0.056	0.06
H	0.137	0.061	0.061	0.089	0.059	0.059

Table 5.3 Results of second attempt to generate IGF-1R mAb

The anti-IGF-1R Abs in hybridoma supernatants measured by ELISA 24 days after hybridoma fusion. The experiment has been conducted in two ELISA plates, P1 and P2. As positive control, 1H7 mAb was used a serial dilutions, starting from 500ng (A1) to 100ng (E1) in both plates [shadowed in green]. Well numbers F1-E12 in P1 and F1-D6 in P2 are hybridoma supernatants from 2nd hybridoma fusion. Well numbers F12-H12 of P1 and F6-H6 of P2 are negative control [shadowed in yellow]. The 'raw' data of OD is shown.

5.4 Discussion

An earlier study from our laboratory showed that a proportion of hTSHR A-subunit plasmid immunised mice (3 out of 12) develop anti-IGF-1R Abs (Zhao et al., 2011). In the studies described in this Chapter, a total of 22 mice from three groups of animals immunised with hTSHR A-subunit plasmid were evaluated for induction of anti-IGF-1R Abs (Moshkelgosha et al., 2013). Another group of 8 animals were specially immunised as a separate group with hTSHR A-subunit plasmid for studies on generation of IGF-1R mAbs. Thus a total of 30 immune mice in four groups (**Appendix 1**) were evaluated for anti-IGF-1R Abs in this thesis. In addition, animals were also immunised with pTRiEx1.1 neo-IGF-1Rα (n=6) for induction of polyclonal Abs to IGF-1R. These immune animals as reported in the study by Dr Zhao et al did not show any manifestations of orbital alteration and remained healthy throughout the course of the study. Control animals were injected with pTRiEx1.1 neo-β-Gal plasmids (n=6). In comparison with the study reported by Zhao and colleges (Zhao et al., 2011), we developed the ELISA and flow cytometry assays to measure anti-IGF-1R Abs. Although, herein we have made a small modification of plasmid delivery as well as using different assay to measure IGF-1R Abs, the serum samples of mice from the Group 1 immunisation were positive for IGF-1R Abs, 7 out of 8. The other groups of immune mice, Group 2 and Group 3 were all negative for anti-IGF-1R Abs. Importantly, in the longitudinal study, Group 2, where animals were bled weekly to study the development of the immune response to hTSHR, anti-IGF-1R Abs were also measured. All the weekly bleed samples from this group notably were negative for IGF-1R Abs. This indicates that the appearance of IGF-1R Abs were neither restricted to 6 weeks after the end of immunisation, nor

disappeared following their appearance, when the immune animals were left for long term e.g. 9 weeks or 15 weeks after the end of immunisation. The possible reasons for the enigmatic results of this chapter in the development of IGF-1R Abs on GO pathogenesis will be discussed below.

The important role of IGF-1R Abs in the pathogenesis of GO was indicated by their ability to promote release of inflammatory cytokine and chemokine (Pritchard et al., 2003) and secretion of hyaluronan (Smith and Hoa, 2004, Kumar et al., 2011) in primary cultures of human orbital fibroblasts. However, measurement of IGF-1R Abs in sera of GO patients was difficult and results were contradictory due to lack of gold standard assay (Weightman et al., 1993, Pritchard et al., 2003, Minich et al., 2013, Varewijck et al., 2013, Smith, 2013). Thus, for this project development of reproducible and rapid assay for measuring anti-IGF-1R Abs was important.

The foremost method could be competitive displacement assay similar to that described independently by Weightman et al and Pritchard et al (Weightman et al., 1993, Pritchard et al., 2003), where orbital fibroblasts were used as source of the receptor. However, human orbital fibroblasts were not available to us, as we were unable to source human tissue in our laboratory due to ethical issues. We therefore obtained an IGF-1R transfected cell line (NWTB3) from Professor LeRoith's laboratory (New York, USA). Examination of NWTB3 cells by flow cytometry revealed high level of expression of IGF-1R, whilst TSHR was not expressed. The examination of TSHR expression by NWTB3 was important as we wish to measure IGF-1R Abs in the sera containing a mixture of TSHR Abs. Following the evaluation of IGF-1R expression in

NWTB3 cells, this cell line can be used for two assays, flow cytometry and competitive displacement assay.

To set up competitive displacement assay, the ligand labelled with ^{125}I or another tracer was required. We acquired IGF-1 labelled with the luminescent tracer (called Lumi-IGF1) from Professor Schomburg (Minich et al., 2013). Using Lumi-IGF1 in competition assay on confluent cultures of NWTB3 cells in 24 well plates showed that 1nM of unlabelled IGF-1 was able to inhibit 50% binding of Lumi-IGF-1. However, when anti-IGF-1R mAbs were evaluated for displacement of Lumi-IGF1 in the cellular binding assay, neither 1H7 nor 24-57 mAbs were able to compete with the tracer. Hence, the competitive binding assay was not further evaluated. Furthermore, flow cytometry were able to measure anti-IGF-1R mAbs. However, the assay was not sufficiently sensitive to distinguish IGF-1R Ab in sera of every individual immune mice and controls. The same issue of measuring polyclonal anti-sera by flow cytometry method was reported in detection of anti-TSHR Abs when using a TSHR transfected cell line (Harfst et al., 1992, Costagliola et al., 1994, Harfst et al., 1994, Patibandla et al., 1997, Jaume et al., 1997). This may be attributable to lower avidity or titre of Abs, or to the presence of Abs against many more epitopes (Harfst et al., 1994).

At the same time, a non-cellular based assay for measuring IGF-1R Abs was published using rhIGF-1 as source of receptor (Yin et al., 2011). This assay was set up using a commercial source of rhIGF1R for ELISA. Once the ELISA was developed and validated with different concentrations of 1h7 mAb and IGF-1R immunised mice sera, the serum samples of mice immunised with hTSHR A-subunit plasmid in the Group 1 immunisation was examined. The data showed the presence of anti-IGF-1 Abs in the sera of 7 out of 8 animals. Notably, the source of receptor in ELISA is hIGF-1R, which

may not be suitable for detection of Abs with specificity for mouse IGF-1R (mIGF-1R) which do not cross react with the human receptor. However, based on our knowledge, neither a transfected mouse IGF-1R (mIGF-1R) cell line nor purified recombinant mIGF-1R protein was available. Thus, to faithfully evaluate IGF-1R Abs in mice immunised with hTSHR A-subunit plasmid, the next step should be the development of mIGF-1R stably transfected cell line.

To confirm the presence of IGF-1R Abs in mice immunised with hTSHR A-subunit plasmid, development of mAbs was attempted in two separate experiments. However, these attempts were unsuccessful. My first attempt was unsuccessful most likely due to the lack of experience in the technique, as the percentage of the culture wells showing growth of hybridoma cells was relatively low (regardless of the enhancement in the second hybridoma fusion). The last attempt was made to generate anti-IGF-1R mAbs in Group 4 immunisation that was purposely immunised for this reason. Despite the improvement in the technical skills (90% of hybridoma wells showing growth, with three TSHR positive wells), I was not successful in developing IGF-1R mAbs due to poor IGF-1R Abs level in the sera.

It is unclear why induction of IGF-1R Abs in 7 out of 8 mice that were immunised with hTSHR A-subunit in Group 1 was not subsequently repeated in any other groups of immunisation reported in this thesis (**Appendix 1**). This is unlikely to be due to differences in plasmid preparation or the immunisation procedure, since all immune mice of Group 2, Group 3, and Group 4 immunisations responded to successful induction of experimental GO when the orbital tissue was examined by histopathology. The BALB/c animals in the different experimental groups were all derived from the same commercial source (Harlan, UK) and housed in the same animal unit, with no

reported opportunistic infections, which may influence the development of the model. Until we understand how the anti-IGF-1R Abs arise in animals immunised with hTSHR A-subunit plasmid in vivo electroporation, it is difficult to explain the discrepant results in the different groups. It may simply be due to 'stochastic event' that the anti-IGF-1R Abs have not been induced and if so, then examination of additional groups of animals immunised with hTSHR A-subunit plasmid *in vivo* electroporation should clarify this possibility. These experiments are presently underway, where new groups of BALB/c mice have been set up for immunisation with hTSHR A-subunit plasmid *in vivo* electroporation in our laboratory in KCL and in another laboratory in Essen, Germany (See Chapter 6) in studies to replicate the model, where all immune animals will also be examined for anti-IGF-1R antibodies by ELISA and flow cytometry. However, from the results that has been presented in this Chapter, it seems that IGF-1R is not an essential autoantibody in pathogenesis of GO.

In spite of the fact that I was not able to measure IGF-1R Abs in all immune animals undergoing GO, it is very important to understand how such an Abs may induce in positive cases. The experimental model of Graves' orbitopathy described in this thesis has revealed the critical role of TSHR as a primary target antigen in GO. However, evidence for substantial overlap between TSHR and IGF-1R signalling pathway including of the Akt/FRAP/mTOR/p70s6k pathway (Cass and Meinkoth, 1998, Park et al., 2000a, Park et al., 2000b, Park et al., 2005) suggested that IGF-1R and TSHR might participate together in the pathogenesis of GO. In addition to the in common signalling pathway of these two receptors, physical and functional interactions between IGF-1R and TSHR have been indicated (Tsui et al., 2008) that can explain induction of IGF-1R Abs in mice immunised with hTSHR A-subunit plasmid.

In summary, experimental model of GO described in this thesis has revealed the critical role of TSHR as a primary target antigen in the disease. Abs to TSHR were induced in all experimental animals, and some animals were also positive for anti-IGF-1R Abs in different assays developed in this thesis. However, the induction of anti-IGF-1R Abs was not reproducible in the groups of immune animals examined in this thesis, which made it difficult to generate mAbs. Additional studies are warranted to study the development of anti-IGF-1R Abs in animals immunised with TSHR A-subunit plasmid *in vivo* electroporation and these studies are presently underway, which will lead to a better understanding of how the anti-IGF-1R Abs develop and their role in the pathophysiology of GO.

Chapter Six

General discussion and future experiments

6. General discussion and future experiments

6.1   General discussion

The thyroid autoimmune diseases, Graves' disease and Hashimoto's thyroiditis, are the most common autoimmune disease affecting humans with a prevalence of approximately 2% in Caucasians (Hollowell et al., 2002). It is well known that these diseases arise in genetically susceptible individuals in association with environmental factors (Tomer and Huber, 2009). Considerable progress has been made in determining the genes responsible for thyroid autoimmune disease. Moreover, the processes involved in the breakdown in tolerance to "self" thyroid antigens are gradually being revealed (McLachlan et al., 2012, McLachlan and Rapoport, 2014) . A fundamental understanding of many biological and immunological processes of thyroid autoimmunity has stemmed from experimental studies in animal models, particularly in rodents. These models have been elucidated at the cellular and molecular levels. There is presently no evidence that spontaneously arising Graves' disease occurs in species other than humans, whereas autoimmune thyroiditis does occur spontaneously in a number of mammals and birds. Hashimoto's thyroiditis, without immunisation, develops spontaneously in Biobreeding rats (Allen et al., 1986), NOD mice (Bernard et al., 1992) and NOD.H2h4 mice (only if given iodine in their drinking water), (Rasooly et al., 1996), obese strain (OS) chickens (Aichinger et al., 1984) and laboratory breeds of dogs (Tucker, 1962). It is striking that unlike the occurrence of thyroiditis in many nonhuman species, neither TSHR antibodies nor Graves' hyperthyroidism develop spontaneously in animals. Recent investigations into the whether the species closely related to human evolution, the great apes develop

Graves' like syndromes have also proved negative (McLachlan et al., 2011). However, in last two decades, a number of induced experimental models have been developed for Graves' disease (Section 1.5). Despite the successful achievements in the development of experimental model of Graves' disease, several other attempts for development of experimental GO model were either unsuccessful (Johnson et al., 2013) or difficult to substantiate (Baker et al., 2005).

The TSHR A-subunit plasmid immunisation *in vivo* electroporation method (Kaneda et al., 2007) was initially evaluated in our laboratory for induction of Graves' disease and persistence of long term immunity to the TSHR (Zhao et al., 2011). At the same time, the model was studied further for development of signs of orbital manifestations (Zhao et al., 2011). This study showed that immunisation with hTSHR A-subunit plasmid *in vivo* electroporation led to the onset of Graves' disease (disease incidence of 66%) which was accompanied with orbital tissue fibrosis in some animals (Zhao et al., 2011). Therefore, the objective of my project was to modify the immunisation procedures in order to induce the orbital pathology of GO such as inflammation and adipogenesis. There were few variables that could be modified, including examining different inbred mice strains, changing the dose of the immunogenic plasmid, and altering the immunisation/electroporation procedure. In this study, we decided to modify the immunisation protocol in order to enhance the plasmid delivery. The rationale for this was based upon the earlier studies from Dr McLachlan's laboratory showing that changing the dose of adenovirus TSHR A-subunit delivery leads to alteration of disease outcome (Chen et al., 2004).

The plasmid was injected deeper into the leg muscle and was released while needle was gradually withdrawn. This resulted in spreading the plasmid over a larger muscle

area. We speculated that the modification in immunisation may lead to greater transfection efficiency which may lead to alteration of antigenic stimulus and outcome of the anti-TSHR response. In comparison with an earlier study (Zhao et al., 2011), the differences in orbital pathology, immunological responses and thyroid function are not due to a change in the commercial supplier of the mice (Harlan Laboratories, UK) nor in the iodine content (1.2mg/Kg) of rodent chow diet. In addition, the animal unit housing, conventional clean room, for the mice was unchanged in two studies. Thus, it is concluded that the modification in the plasmid immunisation resulted in a dramatic different outcome. The significant differences consist of the orbital pathology, the immune response to TSHR (Chen et al., 2004, Soares et al., 2013), and thyroid function which will be discussed in more detail below.

In this thesis, a total of 30 BALB/c female mice in four different groups were evaluated for the onset of Graves' disease and concurrent orbital manifestations. The study into the GO experimental model revealed that all immune animals show orbital remodelling, manifest with orbital heterogeneity as found in patients with GO. The heterogeneity of orbital pathology in GO experimental model that recapitulate orbitopathy in patients was divided into two main subtypes. The orbital pathology in majority of immune animals was characterised by infiltration of interstitial inflammatory cells into extraocular muscle. Concordantly, about 10% of immune mice showed expansion of retrobulbar adipose tissue and widely separating the orbital muscle fibre bundles. Importantly, two animals from different cohorts showed acute inflammation characterised by optic neuropathy with a large inflammatory infiltrate around the optic nerve as well as intense intermuscular lymphocytic infiltrate.

Strikingly, a rare orbital manifestation in GO patients, chemosis, was readily detectable in some animals. There was no correlation with subtype of GO pathology or onset of chemosis with thyroid status or presence and subtype of anti-TSHR (or IGF-1R) antibody in the model. In addition, 12 animals that served as controls, immunised with pTRiEx1.1 neo-IGF-1Rα (n=6) and pTRiEx1.1 neo-β-Gal plasmids (n=6). None of the 12 animals immunised with control plasmids showed any orbital pathology or disease.

Surprisingly, in the majority of immune animals, the thyroid function scored as hypothyroid status. Hypothyroidism status has been confirmed by histological analysis of the thyroid gland, total T4 level in the immune mice sera and significant weight gain. Examination of thyroid glands of GO experimental model by H&E staining showed a typical pattern of hypothyroidism, including thinning of the thyroid epithelial cells, a characteristic sign of underactivity of the gland. In addition to histological analysis of the thyroid gland, significant weight gain in immune mice during course of disease suggested the underactivity of thyroid gland i.e. hypothyroidism. Of particular interest, the thyroid gland did not show any sign of inflammation which is similar to the findings with the adenovirus model of Graves' disease (Nagayama et al., 2002, Chen et al., 2003, Gilbert et al., 2006, McLachlan and Rapoport, 2014). Furthermore, serum total T4 levels in most of immune mice sera demonstrated significant downward trend in comparison to controls. To address the question why the immune animals develop hypothyroidism following the modified immunisation protocol, the TSHR Abs and their subtypes were evaluated. Measurement of anti-TSHR antibodies by radiobinding (TRAK) assay in immune mice sera clearly indicated that all 30 mice were highly positive for TSHR Abs with greater than 50% inhibition of radiolabelled TSH binding (in

TRAK assay). The subtypes of TSHR Abs were assessed by bioassay using JP09 cells and measurement of induced cAMP (Rao et al., 2003, Gilbert et al., 2006). The data showed that the subtype of induced anti-TSHR antibodies was dominated by blocking antibodies. However, few immune animals showed positivity for stimulating Abs. Importantly, irrespective of whether the anti-TSHR response was blocking or stimulating antibodies, the animals developed orbital complications, indicating that disease development was not solely dependent on the subtype of antibody.

Further studies into the induction of anti-TSHR antibody subtypes by serial bleeding in longitudinal studies showed that the TSBAbs evolved early during immunisation and persisted for months. The longitudinal studies also indicate that the subtype of antibody spectrum to TSHR in the model is not prone to changing from stimulating to blocking antibodies or vice versa during the course of disease, as occasionally reported in patients (Takeda et al., 1988, Cho et al., 1989, Takasu et al., 1990, Kraiem et al., 1992, Takasu and Matsushita, 2012, McLachlan and Rapoport, 2013). The remarkable difference between subtypes of TSHR Abs in this study (TSBAbs) and in the adenovirus model (TSAbs) (Nagayama et al., 2002, Dağdelen et al., 2009, Wiesweg et al., 2013) may contribute to the orbital pathological outcome in the two models. Concordantly, more recent findings from Nagayama's laboratory in Graves' disease animal model provided some supportive evidence. In the long-term studies of their adaptive transfer animal model, the recipient animals developed TSBAbs as well as some weak signs of orbital inflammation (Nakahara et al., 2012). Therefore, it was emphasised the critical role of TSBAbs in the onset of Graves' orbitopathy. However, our results described some animals with predominant stimulating TSHR Abs that developed orbital

pathology too. In addition, the clinical studies suggested that the concentrations of different subtypes of TSHR antibodies are dynamic values that may alter during therapeutic intervention such as radioiodine therapy (Takeda et al., 1988, Cho et al., 1989, Takasu et al., 1990, Kraiem et al., 1992, Takasu and Matsushita, 2012) or normal physiological changes such as pregnancy (Hara et al., 1990, Zakarija et al., 1990, Kung and Jones, 1998, Lu et al., 2005). By dramatic changing in the mixed pool of TSAbs and TSBAbs, predominated subtype may alter the clinical presentation. Thus, switching of the anti-TSHR Abs from TSAbs to TSBAbs (Nakahara et al., 2012, McLachlan and Rapoport, 2013), or the dominant presence of TSBAbs during the course of autoimmunity as reported in this study, may be important contributory factors for the onset of GO. Apparently, the mechanism is not clear (McLachlan and Rapoport, 2013) and needs to be studied in more depth on GO experimental model. Regardless of the subtypes of TSHR Abs, the results of this study confirmed the pathological role of TSHR as primary autoantigen in Graves' orbitopathy.

Evidence supporting the TSHR as primary autoimmune target in Graves' hyperthyroidism has been derived from early studies in Graves' disease (Adams and Purves, 1956a, Kriss et al., 1964, Rapoport et al., 1998), however the role of TSHR in the pathogenesis of GO remained less clear and uncertain to this day (Diana et al., 2014, Wall, 2014). The demonstration by several clinical report and laboratory studies in the GO patients further connected the orbital and thyroidal manifestations. However, confirmatory *in vivo* data has not been provided until our report was published (Moshkelgosha et al., 2013). The results of this study have confirmed the substantial role of TSHR as primary target antigen in the *in vivo* model (Bahn, 2013).

The GO experimental model will allow further studies to investigate more detail of the role of TSHR and TSHR antibodies in GO diseases. It also provides an opportunity to study the role of other potential pathogenic antigens in the development of Graves' orbitopathy such as IGF-1R.

The enigmatic role of IGF-1R Abs in the pathogenesis of Graves' orbitopathy was studied in the experimental GO model. In the earlier study from our laboratory, Dr. Zhao and colleagues showed that a small number of hTSHR A-subunit plasmid immunised mice (3 out of 12) developed anti-IGF-1R Abs (Zhao et al., 2011).. Using other assays to measure anti-IGF-1R Abs, confirmed positivity of anti-IGF-1R Abs in the sera from mice that immunised with hTSHR A-subunit. In the Group 1 immunisation, n=7 immunised mice were evaluated by ELISA for anti-IGF-1R antibody and 6 out of 7 were significantly positive. However, the other three groups of immunisation, none of the immune mice were significantly positive for anti-IGF-1R antibody. In the longitudinal study, where animals were bled weekly to study the development of the immune response to hTSHR, anti- IGF-1R antibodies were also measured. All the weekly bleed samples from this group notably were negative for IGF-1R antibodies. This indicates that the appearance of IGF-1R antibodies is not restricted to 6 weeks after the end of immunisation.

Although, IGF-1R Abs did not appear in all immune animals, it is critical to investigate how such an antibody may induce and more importantly, what pathogenic role it may play in the onset of GO. Evidence for substantial overlap between TSHR and IGF-1R signalling pathway including of the Akt/FRAP/mTOR/p70s6k pathway (Cass and Meinkoth, 1998, Park et al., 2000a, Park et al., 2000b, Park et al., 2005) suggested that IGF-1R and TSHR might participate together in the pathogenesis of GO. To address the

potential role of IGF-1R as an autoantigen in GO, we immunised by electroporation a small number of animals with IGF-1Rα plasmid. Although these mice generated high levels of IGF-1R antibody, they developed no apparent pathology. Therefore, a conclusive method to study the nature of induction and potential pathogenesis of anti-IGF-1R Abs in the mice that immunised with hTSHR A-subunit plasmid is to generate mAbs. In this study, several attempts to generate anti-IGF-1R mAbs from the mice immunised with hTSHR A-subunit were not successful. The unsuccessful attempt to generate such mAbs was not due to lack of experience or technical issues as the primary hybridoma cells with a positive signal for anti-TSHR mAbs were obtained. Since high affinity TSAbs generated from murine models of Graves' disease have now been available for a number of years and been well characterised (Ando et al., 2002, Sanders et al., 2002, Costagliola et al., 2002, Gilbert et al., 2006), we decided not to take the primary hybridomas positive for TSHR antibodies further for cloning and long stability of antibody secretion to generate new TSAb mAbs to save on resources and my time. Thus, much more determined effort is clearly required to address the questions on the role of IGF-1R Abs in the pathogenesis of GO.

Apart from biochemical, immunological and histological studies on the GO model, in a number of immune animals, the orbital manifestation was examined by MRI. Initially, it was not clear that using MRI would improve our understanding of orbital manifestation in the GO model particularly in proptosis. Because, it had been postulated that differences in the orbital bone structure between humans and rodents (Smith, 2002) may not allow the eyeball protrusion happening in the mice (Wiersinga, 2011). Despite the differences in the orbital anatomy, we showed by high-resolution *in vivo* MRI the unilateral proptosis as well as clear hypertrophy of the orbital muscles in

some animals (Moshkelgosha et al., 2013). The coronal view of MR images clearly confirmed bilateral proptosis in two immune animals. Moreover, the quantitative analysis showed a significant increase of extraorbital muscle volume in immune animals compare with age-matched controls. The MRI method for examination of orbital manifestation in the GO model was set up based on the clinical neuroradiological methods. As there was not any scientific report in the literature dealing with MRI analysis of extraorbital muscles in the rodents, the MRI results needed confirmatory supports from different assay. Thus, to evaluate the MRI results on hypertrophy in extraorbital muscles, the quantitative analysis was performed in the corresponding area of histological slides. Interestingly, alignment of histological slides of extraorbital muscles with MR images confirmed the hypertrophy in orbital muscles. Therefore, the high resolution *in vivo* MRI method can be used for non invasive longitudinal studies into the GO model.

In conclusion, the robust mouse model developed for Graves' orbitopathy. The animal model described in this thesis recapitulates the orbital manifestation of GO patients including; orbital inflammation, infiltration of inflammatory cells, adipogenesis, chemosis, and proptosis. It is also a strong evidence for the primary pathogenesis factor of TSHR in GO. In addition, it is postulated the potential role of TSBAbs in pathogenesis of the disease. Furthermore, the experimental GO model will allow investigators to invent new approaches to the study of GO. The most important advantage of the GO model is to facilitate the studies in the delineation of immunologic processes and molecular events early in GO development. Moreover, novel approaches to disease prevention and new therapies for established disease can now be studied *in vivo*.

6.2 Limitations

No single animal model recreates exactly the diverse elements of human disease, and each different model carries advantages and limitations and highlights particular aspects of the disease. So, it is important to emphasise limitations of this animal model and differences with human GO patients' signs and symptoms. Some of the unique attributes of the mouse GO model that are different from the human disease are listed below.Spontaneous disease in human versus inducible in the mouse model

The major difference between GO in human patients and the mouse model is related to the fact that disease occurs spontaneously in human patients and autoimmune response is toward the self antigen (hTSHR), while in the mouse model the disease is induced with the xenogeneic antigen (hTSHR as the antigen). It is presently unknown whether immunisation of mice with mTSHR plasmid in combination with electroporation is sufficient to break the immune tolerance in the mice, although it was already shown that the mTSHR adenovirus injection in mice was not successful (Nakahara et al., 2010). Studies for developing experimental GO model using mTSHR plasmid with electroporation are ongoing in our laboratory.

- Absence of thyroid inflammation:

Studied in thyroid tissue from GO patients demonstrated inflammation comprising of a lymphocytic infiltrate into the thyroid tissue. There is also evidence on forming focal germinal centre in thyroid tissue of Graves' disease and GO patients. However, precise assessment of thyroid tissue from immune mice in this thesis did not show sign of inflammation of lymphocytic inflammation in thyroid tissue. Despite this dissimilarity between human GO patients and GO animal model in terms of thyroid inflammation, it

is already shown that thyroid inflammation is lacking in other animal models for Graves' disease such as the adenovirus model (Nagayama et al., 2002, Chen et al., 2003, Gilbert et al., 2006). The simple explanation for this could be the difference between immunogenicity of the antigen in human and animal models. In human GO and Graves' patients, the self-antigen immunogenic factor that causing the disease while in animal models it is immunisation against TSHR from different spices (hTSHR).

- Hypothyroid status in most of experimental GO mice:

Graves' disease is defined mainly by autoimmune hyperthyroidism which accompanies most cases with orbital complications (Weetman, 2000, Bahn, 2010). However, there is also evidence on individual cases with autoimmune hypothyroidism due to dominance of blocking TSHR Ab (not HT hypothyroidism) with GO symptoms (McLachlan and Rapoport, 2013). In the GO model described in this thesis, the thyroid status of most immune animals was hypothyroid. Studies on subtypes of TSHR Abs confirmed hypothyroidism in the immune mice are due to the presence of anti-TSHR antibodies with strong TSBAb activity. However, the incidence of hypothyroidism in patients undergoing autoimmune hypothyroidism mediated by TSH blocking antibodies is less frequent.

- Anatomical difference between orbital structure:

One of the main factors causing GO symptoms includes proptosis, which is the result of limited space in the bony structure surrounding the orbital tissue. In mouse orbital region, the orbital contents are protected in orbital cavity by eight bones called maxilla, lacrimal, zygomatic, frontal, temporal, sphenoid, ethmoid and palaextraorbital

In addition, the orbital region in the mouse is surrounded by a unique gland called Harderian gland (Paterson and Kaiserman-Abramof, 1981). However, as the Harderian gland is 'soft tissue', it provides space for expansion of the orbital tissue during any inflammatory event .This anatomical difference between the mouse and the human orbital region has led Prof Wiersinga to postulate the impossibility of developing proptosis in mice (Wiersinga, 2011). However, my data in the mouse model in combination with high resolution, small animal MR imaging clearly show that proptosis does indeed occur in immune mice undergoing experimental GO, which was clearly visualised by MRI (Moshkelgosha et al., 2013).

6.3   Proposed future studies

The availability of a preclinical model for Graves' orbitopathy that recapitulate orbital condition of GO patients will allow studies on a disorder that has proved immensely difficult to study in human patients. Progress in understanding the molecular basis of GO has been hindered in the past by the fact that the retrobulbar tissue that is available from decompression surgery is exceedingly small derived at the end stage of disease. Moreover, any clinical trial needs to be performed in multicentre trials to ensure the availability of adequate numbers of GO patients (for example, a trial utilizing Teprotumumab as an IGF-1R blocking strategy currently is underway, http://clinicaltrials.gov/show/NCT01868997). Thus, preclinical GO model is an ideal opportunity to study 1) natural history of the disease 2) molecular pathogenesis of GO and 3) therapeutic intervention by novel targeted biological therapies.

The priority has been to evaluate the reproducibility of the model in different laboratories. Professor Banga and I have made a start to reproduce the model by establishing the model in Professor Anja Eckstein's group in the Department of Ophthalmology, University of Duisburg-Essen, Germany. The animal licence has recently been approved by the German authorities for establishing the new GO model in University of Duisburg-Essen. We have provided the hTSHR A-subunit pTriEx1.1 plasmid and the control β-Gal plasmid to Professor Eckstein's laboratory for the replication studies. Milligram quantities of the plasmids have been prepared in Essen laboratory, using exactly the same procedure. Female BALB/c mice will be obtained from the same commercial supplier in Germany (Harlan GmbH) as the supplier in KCL (Harlan, UK). We have made in depth investigations with the commercial suppliers to ensure that the BALB/c strains in KCL and Essen laboratories will be the same strain derived from the same original breeding pairs. Both the commercial sources supply the same strain, termed BALB/cOlaHsd.

In addition, the immunisations in Essen laboratory will be synchronised with simultaneous immunisation run as positive controls in our laboratory in KCL. Moreover, for the London laboratory experiments, we aim to use both the plasmid preparations from the Essen laboratories, as well as the plasmid preparations of the London laboratories to run as positive controls, to ensure that differences in standard reagents (e.g. quality of distilled water) during the preparation of the plasmid does not influence the development of the model. The replication experiments in Duisburg-Essen are planned to start with the first immunisations in October 2014. All the animals will be housed in clean room facilities in Duisburg-Essen, like the animals housed in the unit in KCL. Animal health screening reports for the animal units in KCL

and University of Duisburg-Essen for the past 12 months have been carefully studied and compared with microbiologists to ensure that the pathogens reported in the 'clean' SPF facilities in the two units are not substantially different, which may potentially contribute to differences in the development of the GO model in different laboratories. The injection procedure combined with placing of the calliper electrodes requires considerable dexterity and skill. Hence, all the four immunisation *in vivo* electroporation steps every 3 weeks apart will be performed in the Essen laboratories by Professor Banga and myself to ensure that subtle differences in the precise injection and electroporation technique do not contribute influence the development of the GO model. With all the precautions we have taken, we are confident that we will successfully reproduce the GO model in the Essen laboratories. Overall, we aim to publish the results of the replication study to inform the scientific community of the transferability of the new GO model.

The new preclinical model described in this thesis can be used to study natural history of the disease. Recently, studies into the progression of GO (Piantanida et al., 2013, Menconi et al., 2014) recapitulated our understanding of the natural history of Graves' orbitopathy, known as Rundle's curve (Rundle and Wilson, 1945, Rundle, 1957, Wiersinga, 1992, Perros and Kendall-Taylor, 1998). It is well known that GO signs and symptoms become worse rapidly during the initial phase, up to its peak of maximum severity and then be improved and finally reached a static plateau. However, the mechanism of resolving the orbital conditions in the majority of GO patients has not been revealed. Hence, further studies in preclinical GO model can demonstrate (i) whether experimental GO model follow the Rundle's curve and importantly (ii) the mechanism of improvement in the orbital condition. The study into natural history of

the disease in the experimental GO model needs a large number of animals to investigate the disease condition longitudinally by histopathological method. Otherwise, the striking results of MRI imaging in this study can provide a non-invasive platform for the longitudinal study. However, as clearly shown by the alignment the results of histology and MRI, the resolution of MRI was not sufficient to distinguish adipose tissue expansion in the orbital tissue of an individual mouse. Thus, the preliminary study in order to improve the MRI resolution by adding contrast agents to increase brightness in tissue of interest is recommended.

Furthermore, the *in vivo* molecular mechanism of GO pathogenesis is the novel area that can be driven by GO model. Apart from studies into targeted genes from GO patients (Yin et al., 2012), a recent technological advance, array technology, developed a high throughput screening of gene profiling. This technology has been recruited to investigate alterations of transcriptome in orbitopathy from patients' sample (Planck et al., 2011, Ezra et al., 2012). The limitation in availability of patients' tissue is a great preventive problem for further studies. Thus, experimental GO model can be an advantage to overcome the limitations in molecular investigation of pathogenesis of disease. A better understanding of the inflammatory cytokines and the molecular pathways regulating endothelial migration of inflammatory cells into the orbital tissue will lead to new knowledge on orbital inflammation and potentially identify novel targets for therapeutic intervention.

In addition, the experimental GO model is a promising vehicle for translational studies of potential novel therapeutic agents and drug development. As mentioned earlier, apart from classical therapeutic strategies, there are two novel approaches for targeted biological therapy in GO (i) systemic dampening the immune response

dysregulation and (ii) antagonising excessive TSHR signalling. Rituximab (RTX), anti-CD20 mAb, is a well studied example for the targeted therapy with modulation in immune response. Although, the significant effect of RTX in activity and severity of GO patients has been recently documented (Salvi et al., 2013), the first randomised clinical trial (RCT) of RTX in moderate-to-severe GO patients has failed to support the role of RTX as a therapeutic agent for treatment of GO (Stan et al., 2013). Furthermore, recent *in vitro* studies using either SMLs antagonists for TSHR signalling (van Zeijl et al., 2012, Turcu et al., 2013) or PI3K inhibitor (Zhang et al., 2014) resulted in some reduction of hyaluronan synthesis and adipogenesis. Recently, SMLs have also been evaluated *in vivo* (Neumann et al., 2014, Davies et al., 2014) in a non-autoimmune, but endocrine induced mouse model of hyperthyroidism (Hamidi et al., 2010). The experimental GO model described in this thesis will open a new avenue for translational studies of these novel therapeutic agents. These studies will no doubt facilitate the initiation of randomised clinical trials of novel agents in patients with GO.

Finally, further studies in the putative role of IGF-1R in pathogenesis of GO by this animal model will improve our understanding of the molecular mechanisms of disease. As a future direction, a specific project dealing with the development an anti-IGF-1R mAbs induced in an individual mouse immunised with hTSHR A-subunit plasmid, would help to shed light on currently mysterious mechanism of action of this antigen in the pathophysiology of GO.

Bibliography

ABBAS, A. K., LICHTMAN, A. H. & PILLAI, S. 2012. *Cellular and molecular immunology,* Philadelphia, Elsevier/Saunders.

ACHARYA, S. H., AVENELL, A., PHILIP, S., BURR, J., BEVAN, J. S. & ABRAHAM, P. 2008. Radioiodine therapy (RAI) for Graves' disease (GD) and the effect on ophthalmopathy: a systematic review. *Clin Endocrinol (Oxf),* 69**,** 943-50.

ADAMS, D. D. 1958. The presence of an abnormal thyroid-stimulating hormone in the serum of some thyrotoxic patients. *J Clin Endocrinol Metab,* 18**,** 699-712.

ADAMS, D. D. & PURVES, H. D. 1956a. Abnormal responses to the assay of thyrotrophin. *Proc Univ Otago Med Sch,* 34**,** 11-12.

ADAMS, D. D. & PURVES, H. D. 1956b. The assessment of thyroid function by tracer tests with radioactive iodine. *N Z Med J,* 55**,** 36-41.

AICHINGER, G., KOFLER, H., DIAZ-MERIDA, O. & WICK, G. 1984. Nonthyroid autoantibodies in obese strain (OS) chickens. *Clin Immunol Immunopathol,* 32**,** 57-69.

AJJAN, R. A., KAMARUDDIN, N. A., CRISP, M., WATSON, P. F., LUDGATE, M. & WEETMAN, A. P. 1998a. Regulation and tissue distribution of the human sodium iodide symporter gene. *Clin Endocrinol (Oxf),* 49**,** 517-23.

AJJAN, R. A., KEMP, E. H., WATERMAN, E. A., WATSON, P. F., ENDO, T., ONAYA, T. & WEETMAN, A. P. 2000. Detection of binding and blocking autoantibodies to the human sodium-iodide symporter in patients with autoimmune thyroid disease. *J Clin Endocrinol Metab,* 85**,** 2020-7.

AJJAN, R. A., WATSON, P. F., FINDLAY, C., METCALFE, R. A., CRISP, M., LUDGATE, M. & WEETMAN, A. P. 1998b. The sodium iodide symporter gene and its regulation by cytokines found in autoimmunity. *J Endocrinol,* 158**,** 351-8.

AL-ADHAMI, A., CRAIG, W. & KRUKOWSKI, Z. H. 2012. Quality of life after surgery for Graves' disease: comparison of those having surgery intended to preserve thyroid function with those having ablative surgery. *Thyroid,* 22**,** 494-500.

ALIESKY, H., COURTNEY, C. L., RAPOPORT, B. & MCLACHLAN, S. M. 2013. Thyroid autoantibodies are rare in non-human great apes and hypothyroidism cannot be attributed to thyroid autoimmunity. *Endocrinology*.

ALLAHABADIA, A., DAYKIN, J., HOLDER, R. L., SHEPPARD, M. C., GOUGH, S. C. & FRANKLYN, J. A. 2000. Age and gender predict the outcome of treatment for Graves' hyperthyroidism. *J Clin Endocrinol Metab,* 85**,** 1038-42.

ALLAHABADIA, A., HEWARD, J. M., NITHIYANANTHAN, R., GIBSON, S. M., REUSER, T. T., DODSON, P. M., FRANKLYN, J. A. & GOUGH, S. C. 2001. MHC class II region, CTLA4 gene, and ophthalmopathy in patients with Graves' disease. *Lancet,* 358**,** 984-5.

ALLEN, E. M., RAJATANAVIN, R., NOGIMORI, T., CUSHING, G., INGBAR, S. H. & BRAVERMAN, L. E. 1986. The effect of methimazole on the development of spontaneous lymphocytic thyroiditis in the diabetes-prone BB/W rat. *Am J Med Sci,* 292**,** 267-71.

ANDO, T., LATIF, R., PRITSKER, A., MORAN, T., NAGAYAMA, Y. & DAVIES, T. F. 2002. A monoclonal thyroid-stimulating antibody. *J Clin Invest,* 110**,** 1667-74.

ANDRAE, J., GALLINI, R. & BETSHOLTZ, C. 2008. Role of platelet-derived growth factors in physiology and medicine. *Genes Dev,* 22**,** 1276-312.

ANISZEWSKI, J. P., VALYASEVI, R. W. & BAHN, R. S. 2000. Relationship between disease duration and predominant orbital T cell subset in Graves' ophthalmopathy. *J Clin Endocrinol Metab,* 85**,** 776-80.

ANNERBO, M., STALBERG, P. & HELLMAN, P. 2012. Management of Grave's disease is improved by total thyroidectomy. *World J Surg,* 36**,** 1943-6.

ANVARI, M., KHALILZADEH, O., ESTEGHAMATI, A., ESFAHANI, S. A., RASHIDI, A., ETEMADI, A., MAHMOUDI, M. & AMIRZARGAR, A. A. 2010. Genetic susceptibility to Graves'

ophthalmopathy: the role of polymorphisms in proinflammatory cytokine genes. *Eye (Lond),* 24**,** 1058-63.

ARNOLD, K., TANDON, N., MCINTOSH, R. S., ELISEI, R., LUDGATE, M. & WEETMAN, A. P. 1994. T cell responses to orbital antigens in thyroid-associated ophthalmopathy. *Clin Exp Immunol,* 96**,** 329-34.

ASVOLD, B. O., BJORO, T., NILSEN, T. I. & VATTEN, L. J. 2007. Tobacco smoking and thyroid function: a population-based study. *Arch Intern Med,* 167**,** 1428-32.

AUDET, M. & BOUVIER, M. 2012. Restructuring G-protein- coupled receptor activation. *Cell,* 151**,** 14-23.

AYDIN, K., GUVEN, K., SENCER, S., CIKIM, A., GUL, N. & MINARECI, O. 2003. A new MRI method for the quantitative evaluation of extraocular muscle size in thyroid ophthalmopathy. *Neuroradiology,* 45**,** 184-7.

BACH, J. F. 2002. The effect of infections on susceptibility to autoimmune and allergic diseases. *N Engl J Med,* 347**,** 911-20.

BAHN, R. S. 2003. Clinical review 157: Pathophysiology of Graves' ophthalmopathy: the cycle of disease. *J Clin Endocrinol Metab,* 88**,** 1939-46.

BAHN, R. S. 2010. Graves' ophthalmopathy. *New England Journal of Medicine,* 362**,** 726-738.

BAHN, R. S. 2012a. Autoimmunity and Graves' disease. *Clin Pharmacol Ther,* 91**,** 577-9.

BAHN, R. S. 2012b. Emerging pharmacotherapy for treatment of Graves' disease. *Expert Rev Clin Pharmacol,* 5**,** 605-7.

BAHN, R. S. 2013. News and views: at long last, an animal model of graves' orbitopathy. *Endocrinology,* 154**,** 2989-91.

BAHN, R. S., BURCH, H. B., COOPER, D. S., GARBER, J. R., GREENLEE, M. C., KLEIN, I., LAURBERG, P., MCDOUGALL, I. R., MONTORI, V. M., RIVKEES, S. A., ROSS, D. S., SOSA, J. A., STAN, M. N., AMERICAN THYROID, A. & AMERICAN ASSOCIATION OF CLINICAL, E. 2011. Hyperthyroidism and other causes of thyrotoxicosis: management guidelines of the American Thyroid Association and American Association of Clinical Endocrinologists. *Endocr Pract,* 17**,** 456-520.

BAHN, R. S., DUTTON, C. M., NATT, N., JOBA, W., SPITZWEG, C. & HEUFELDER, A. E. 1998. Thyrotropin receptor expression in Graves' orbital adipose/connective tissues: potential autoantigen in Graves' ophthalmopathy. *J Clin Endocrinol Metab,* 83**,** 998-1002.

BAKER, G., MAZZIOTTI, G., VON RUHLAND, C. & LUDGATE, M. 2005. Reevaluating thyrotropin receptor-induced mouse models of graves' disease and ophthalmopathy. *Endocrinology,* 146**,** 835-44.

BAN, Y., DAVIES, T. F., GREENBERG, D. A., CONCEPCION, E. S., OSMAN, R., OASHI, T. & TOMER, Y. 2004. Arginine at position 74 of the HLA-DR beta1 chain is associated with Graves' disease. *Genes Immun,* 5**,** 203-8.

BAN, Y., TOZAKI, T., TANIYAMA, M., TOMITA, M. & BAN, Y. 2006. Association of a C/T single-nucleotide polymorphism in the 5' untranslated region of the CD40 gene with Graves' disease in Japanese. *Thyroid,* 16**,** 443-6.

BARRETT, J. C., CLAYTON, D. G., CONCANNON, P., AKOLKAR, B., COOPER, J. D., ERLICH, H. A., JULIER, C., MORAHAN, G., NERUP, J., NIERRAS, C., PLAGNOL, V., POCIOT, F., SCHUILENBURG, H., SMYTH, D. J., STEVENS, H., TODD, J. A., WALKER, N. M., RICH, S. S. & TYPE 1 DIABETES GENETICS, C. 2009. Genome-wide association study and meta-analysis find that over 40 loci affect risk of type 1 diabetes. *Nat Genet,* 41**,** 703-7.

BARRON, L. & WYNN, T. A. 2011. Fibrosis is regulated by Th2 and Th17 responses and by dynamic interactions between fibroblasts and macrophages. *Am J Physiol Gastrointest Liver Physiol,* 300**,** G723-8.

BARTALENA, L. 2013. Diagnosis and management of Graves disease: a global overview. *Nat Rev Endocrinol,* 9**,** 724-34.

BARTALENA, L., BALDESCHI, L., DICKINSON, A. J., ECKSTEIN, A., KENDALL-TAYLOR, P., MARCOCCI, C., MOURITS, M. P., PERROS, P., BOBORIDIS, K., BOSCHI, A., CURRO, N., DAUMERIE, C., KAHALY, G. J., KRASSAS, G., LANE, C. M., LAZARUS, J. H., MARINO, M., NARDI, M., NEOH, C., ORGIAZZI, J., PEARCE, S., PINCHERA, A., PITZ, S., SALVI, M., SIVELLI, P., STAHL, M., VON ARX, G. & WIERSINGA, W. M. 2008. Consensus statement of the European group on Graves' orbitopathy (EUGOGO) on management of Graves' orbitopathy. *Thyroid,* 18**,** 333-46.

BARTALENA, L., MARCOCCI, C., BOGAZZI, F., MANETTI, L., TANDA, M. L., DELL'UNTO, E., BRUNO-BOSSIO, G., NARDI, M., BARTOLOMEI, M. P., LEPRI, A., ROSSI, G., MARTINO, E. & PINCHERA, A. 1998. Relation between therapy for hyperthyroidism and the course of Graves' ophthalmopathy. *N Engl J Med,* 338**,** 73-8.

BARTALENA, L., MARCOCCI, C., CHIOVATO, L., LADDAGA, M., LEPRI, G., ANDREANI, D., CAVALLACCI, G., BASCHIERI, L. & PINCHERA, A. 1983. Orbital cobalt irradiation combined with systemic corticosteroids for Graves' ophthalmopathy: comparison with systemic corticosteroids alone. *J Clin Endocrinol Metab,* 56**,** 1139-44.

BARTH, P. J. & WESTHOFF, C. C. 2007. CD34+ fibrocytes: morphology, histogenesis and function. *Curr Stem Cell Res Ther,* 2**,** 221-7.

BASU, R., HATTON, R. D. & WEAVER, C. T. 2013. The Th17 family: flexibility follows function. *Immunol Rev,* 252**,** 89-103.

BATEMAN, J. M. & MCNEILL, H. 2006. Insulin/IGF signalling in neurogenesis. *Cell Mol Life Sci,* 63**,** 1701-5.

BECH, K., LARSEN, J. H., HANSEN, J. M. & NERUP, J. 1974. Letter: Yersinia enterocolitica infection and thyroid disorders. *Lancet,* 2**,** 951-2.

BECH, K., LUMHOLTZ, B., NERUP, J., THOMSEN, M., PLATZ, P., RYDER, L. P., SVEJGAARD, A., SIERSBAEK-NIELSEN, K., HANSEN, J. M. & LARSEN, J. H. 1977. HLA antigens in Graves' disease. *Acta Endocrinol (Copenh),* 86**,** 510-6.

BEN-SKOWRONEK, I., SIEROCINSKA-SAWA, J., SZEWCZYK, L. & KOROBOWICZ, E. 2009. Interaction of lymphocytes and thyrocytes in Graves' disease and nonautoimmune thyroid diseases in immunohistochemical and ultrastructural investigations. *Horm Res,* 71**,** 350-8.

BENNING, H., LIEB, W., KAHALY, G. & GREHN, F. 1994. [Color duplex ultrasound findings in patients with endocrine orbitopathy]. *Ophthalmologe,* 91**,** 20-5.

BENVENGA, S., SANTARPIA, L., TRIMARCHI, F. & GUARNERI, F. 2006. Human thyroid autoantigens and proteins of Yersinia and Borrelia share amino acid sequence homology that includes binding motifs to HLA-DR molecules and T-cell receptor. *Thyroid,* 16**,** 225-36.

BERNARD, N. F., BOUCHER, A., ZHANG, Z. G., SALVI, M. & WALL, J. R. 1991. Nature of a 64 kDa eye muscle membrane autoantigen as determined from immunoprecipitation and immunoblotting. *Exp Clin Endocrinol,* 97**,** 191-6.

BERNARD, N. F., ERTUG, F. & MARGOLESE, H. 1992. High incidence of thyroiditis and anti-thyroid autoantibodies in NOD mice. *Diabetes,* 41**,** 40-6.

BERTHOUT, A., VIGNAL, C., JACOMET, P. V., GALATOIRE, O. & MORAX, S. 2010. [Intraorbital pressure measured before, during, and after surgical decompression in Graves' orbitopathy]. *J Fr Ophtalmol,* 33**,** 623-9.

BETTELLI, E., CARRIER, Y., GAO, W., KORN, T., STROM, T. B., OUKKA, M., WEINER, H. L. & KUCHROO, V. K. 2006. Reciprocal developmental pathways for the generation of pathogenic effector TH17 and regulatory T cells. *Nature,* 441**,** 235-8.

BLAKESLEY, V. A., KATO, H., ROBERTS, C. T., JR. & LEROITH, D. 1995. Mutation of a conserved amino acid residue (tryptophan 1173) in the tyrosine kinase domain of the IGF-I receptor abolishes autophosphorylation but does not eliminate biologic function. *J Biol Chem,* 270**,** 2764-9.

BLANDER, J. M., TORCHINSKY, M. B. & CAMPISI, L. 2012. Revisiting the old link between infection and autoimmune disease with commensals and T helper 17 cells. *Immunol Res,* 54**,** 50-68.

BLOCK, S. R., WINFIELD, J. B., LOCKSHIN, M. D., D'ANGELO, W. A. & CHRISTIAN, C. L. 1975. Studies of twins with systemic lupus erythematosus. A review of the literature and presentation of 12 additional sets. *Am J Med,* 59**,** 533-52.

BNF 2010. *British National Formulary 60*, BMJ Group and Pharmaceutical Press.

BOEHM, B. O., KUHNL, P., MANFRAS, B. J., CHEN, M., LEE, J. C., HOLZBERGER, G., SEIDL, S., SCHIFFERDECKER, E., SCHUMM-DRAEGER, P. M. & USADEL, K. H. 1992. HLA-DRB3 gene alleles in Caucasian patients with Graves' disease. *Clin Investig,* 70**,** 956-60.

BONIFACIO, E., YU, L., WILLIAMS, A. K., EISENBARTH, G. S., BINGLEY, P. J., MARCOVINA, S. M., ADLER, K., ZIEGLER, A. G., MUELLER, P. W., SCHATZ, D. A., KRISCHER, J. P., STEFFES, M. W. & AKOLKAR, B. 2010. Harmonization of glutamic acid decarboxylase and islet antigen-2 autoantibody assays for national institute of diabetes and digestive and kidney diseases consortia. *J Clin Endocrinol Metab,* 95**,** 3360-7.

BOSCHI, A., DAUMERIE, C., SPIRITUS, M., BEGUIN, C., SENOU, M., YUKSEL, D., DUPLICY, M., COSTAGLIOLA, S., LUDGATE, M. & MANY, M. C. 2005. Quantification of cells expressing the thyrotropin receptor in extraocular muscles in thyroid associated orbitopathy. *Br J Ophthalmol,* 89**,** 724-9.

BOSSINI-CASTILLO, L., MARTIN, J. E., BROEN, J., GORLOVA, O., SIMEON, C. P., BERETTA, L., VONK, M. C., CALLEJAS, J. L., CASTELLVI, I., CARREIRA, P., GARCIA-HERNANDEZ, F. J., FERNANDEZ CASTRO, M., SPANISH SCLERODERMA, G., COENEN, M. J., RIEMEKASTEN, G., WITTE, T., HUNZELMANN, N., KREUTER, A., DISTLER, J. H., KOELEMAN, B. P., VOSKUYL, A. E., SCHUERWEGH, A. J., PALM, O., HESSELSTRAND, R., NORDIN, A., AIRO, P., LUNARDI, C., SCORZA, R., SHIELS, P., VAN LAAR, J. M., HERRICK, A., WORTHINGTON, J., DENTON, C., TAN, F. K., ARNETT, F. C., AGARWAL, S. K., ASSASSI, S., FONSECA, C., MAYES, M. D., RADSTAKE, T. R. & MARTIN, J. 2012. A GWAS follow-up study reveals the association of the IL12RB2 gene with systemic sclerosis in Caucasian populations. *Hum Mol Genet,* 21**,** 926-33.

BOSSOWSKI, A., MONIUSZKO, M., DABROWSKA, M., SAWICKA, B., RUSAK, M., JEZNACH, M., WOJTOWICZ, J., BODZENTA-LUKASZYK, A. & BOSSOWSKA, A. 2013. Lower proportions of CD4+CD25(high) and CD4+FoxP3, but not CD4+CD25+CD127(low) FoxP3+ T cell levels in children with autoimmune thyroid diseases. *Autoimmunity,* 46**,** 222-30.

BOTTAZZO, G. F., PUJOL-BORRELL, R., HANAFUSA, T. & FELDMANN, M. 1983. Role of aberrant HLA-DR expression and antigen presentation in induction of endocrine autoimmunity. *Lancet,* 2**,** 1115-9.

BRAND, O. J., BARRETT, J. C., SIMMONDS, M. J., NEWBY, P. R., MCCABE, C. J., BRUCE, C. K., KYSELA, B., CARR-SMITH, J. D., BRIX, T., HUNT, P. J., WIERSINGA, W. M., HEGEDUS, L., CONNELL, J., WASS, J. A., FRANKLYN, J. A., WEETMAN, A. P., HEWARD, J. M. & GOUGH, S. C. 2009. Association of the thyroid stimulating hormone receptor gene (TSHR) with Graves' disease. *Hum Mol Genet,* 18**,** 1704-13.

BRAND, O. J. & GOUGH, S. C. 2010. Genetics of thyroid autoimmunity and the role of the TSHR. *Mol Cell Endocrinol,* 322**,** 135-43.

BRAND, O. J., LOWE, C. E., HEWARD, J. M., FRANKLYN, J. A., COOPER, J. D., TODD, J. A. & GOUGH, S. C. 2007. Association of the interleukin-2 receptor alpha (IL-2Ralpha)/CD25 gene region with Graves' disease using a multilocus test and tag SNPs. *Clin Endocrinol (Oxf),* 66**,** 508-12.

BRENT, G. A. 2008. Clinical practice. Graves' disease. *N Engl J Med,* 358**,** 2594-605.

BRENT, G. A. 2010. Environmental exposures and autoimmune thyroid disease. *Thyroid,* 20**,** 755-61.

BRIX, T. H. & HEGEDUS, L. 2011. Twins as a tool for evaluating the influence of genetic susceptibility in thyroid autoimmunity. *Ann Endocrinol (Paris),* 72**,** 103-7.

BRIX, T. H. & HEGEDUS, L. 2012. Twin studies as a model for exploring the aetiology of autoimmune thyroid disease. *Clin Endocrinol (Oxf),* 76**,** 457-64.

BRIX, T. H., HEGEDUS, L., GARDAS, A., BANGA, J. P. & NIELSEN, C. H. 2011. Monozygotic twin pairs discordant for Hashimoto's thyroiditis share a high proportion of thyroid peroxidase autoantibodies to the immunodominant region A. Further evidence for genetic transmission of epitopic "fingerprints". *Autoimmunity,* 44**,** 188-94.

BRIX, T. H., HEGEDUS, L., WEETMAN, A. P. & KEMP, H. E. 2014. Pendrin and NIS antibodies are absent in healthy individuals and are rare in autoimmune thyroid disease: evidence from a Danish twin study. *Clin Endocrinol (Oxf)*.

BRIX, T. H., KNUDSEN, G. P., KRISTIANSEN, M., KYVIK, K. O., ORSTAVIK, K. H. & HEGEDUS, L. 2005. High frequency of skewed X-chromosome inactivation in females with autoimmune thyroid disease: a possible explanation for the female predisposition to thyroid autoimmunity. *J Clin Endocrinol Metab,* 90**,** 5949-53.

BRIX, T. H., KYVIK, K. O., CHRISTENSEN, K. & HEGEDUS, L. 2001. Evidence for a major role of heredity in Graves' disease: a population-based study of two Danish twin cohorts. *J Clin Endocrinol Metab,* 86**,** 930-4.

BRIX, T. H., KYVIK, K. O. & HEGEDUS, L. 1998. What is the evidence of genetic factors in the etiology of Graves' disease? A brief review. *Thyroid,* 8**,** 727-34.

BUDINGER, T. F. & LAUTERBUR, P. C. 1984. Nuclear magnetic resonance technology for medical studies. *Science,* 226**,** 288-98.

BURN, G. L., SVENSSON, L., SANCHEZ-BLANCO, C., SAINI, M. & COPE, A. P. 2011. Why is PTPN22 a good candidate susceptibility gene for autoimmune disease? *FEBS Lett,* 585**,** 3689-98.

CARAYANNIOTIS, G., HUANG, G. C., NICHOLSON, L. B., SCOTT, T., ALLAIN, P., MCGREGOR, A. M. & BANGA, J. P. 1995. Unaltered thyroid function in mice responding to a highly immunogenic thyrotropin receptor: implications for the establishment of a mouse model for Graves' disease. *Clin Exp Immunol,* 99**,** 294-302.

CARIDADE, M., OLIVEIRA, V. G., AGUA-DOCE, A., GRACA, L. & RIBEIRO, R. M. 2013. The fate of CD4+ T cells under tolerance-inducing stimulation: a modeling perspective. *Immunol Cell Biol,* 91**,** 652-60.

CASS, L. A. & MEINKOTH, J. L. 1998. Differential effects of cyclic adenosine 3',5'-monophosphate on p70 ribosomal S6 kinase. *Endocrinology,* 139**,** 1991-8.

CAWOOD, T. J., MORIARTY, P., O'FARRELLY, C. & O'SHEA, D. 2006. The effects of tumour necrosis factor-alpha and interleukin1 on an in vitro model of thyroid-associated ophthalmopathy; contrasting effects on adipogenesis. *Eur J Endocrinol,* 155**,** 395-403.

CAWOOD, T. J., MORIARTY, P., O'FARRELLY, C. & O'SHEA, D. 2007. Smoking and thyroid-associated ophthalmopathy: A novel explanation of the biological link. *J Clin Endocrinol Metab,* 92**,** 59-64.

CHANCE, B. 1989. What are the goals of magnetic resonance research? *NMR Biomed,* 2**,** 179-87.

CHAVELE, K. M. & EHRENSTEIN, M. R. 2011. Regulatory T-cells in systemic lupus erythematosus and rheumatoid arthritis. *FEBS Lett,* 585**,** 3603-10.

CHAZENBALK, G. D., PICHURIN, P., CHEN, C. R., LATROFA, F., JOHNSTONE, A. P., MCLACHLAN, S. M. & RAPOPORT, B. 2002. Thyroid-stimulating autoantibodies in Graves disease preferentially recognize the free A subunit, not the thyrotropin holoreceptor. *J Clin Invest,* 110**,** 209-17.

CHEN, C. R., MCLACHLAN, S. M. & RAPOPORT, B. 2007. Suppression of thyrotropin receptor constitutive activity by a monoclonal antibody with inverse agonist activity. *Endocrinology,* 148**,** 2375-82.

CHEN, C. R., PICHURIN, P., CHAZENBALK, G. D., ALIESKY, H., NAGAYAMA, Y., MCLACHLAN, S. M. & RAPOPORT, B. 2004. Low-dose immunization with adenovirus expressing the thyroid-stimulating hormone receptor A-subunit deviates the antibody response toward that of autoantibodies in human Graves' disease. *Endocrinology,* 145**,** 228-33.

CHEN, C. R., PICHURIN, P., NAGAYAMA, Y., LATROFA, F., RAPOPORT, B. & MCLACHLAN, S. M. 2003. The thyrotropin receptor autoantigen in Graves disease is the culprit as well as the victim. *J Clin Invest,* 111**,** 1897-904.

CHEN, H., MESTER, T., RAYCHAUDHURI, N., KAUH, C. Y., GUPTA, S., SMITH, T. J. & DOUGLAS, R. S. 2014. Teprotumumab, an IGF-1R Blocking Monoclonal Antibody Inhibits TSH and IGF-1 Action in Fibrocytes. *J Clin Endocrinol Metab***,** jc20141580.

CHEN, J., WANG, Q., CHEN, S., WICKLINE, S. A. & SONG, S. K. 2011. In vivo diffusion tensor MRI of the mouse retina: a noninvasive visualization of tissue organization. *NMR Biomed,* 24**,** 447-51.

CHEN, J., WANG, Q., ZHANG, H., YANG, X., WANG, J., BERKOWITZ, B. A., WICKLINE, S. A. & SONG, S. K. 2008a. In vivo quantification of T1, T2, and apparent diffusion coefficient in the mouse retina at 11.74T. *Magn Reson Med,* 59**,** 731-8.

CHEN, M. H., LIAO, S. L., CHEN, M. H., TSOU, P. L., SHIH, M. J., CHANG, T. C. & CHUANG, L. M. 2008b. Lysosome-related genes are regulated in the orbital fat of patients with graves' ophthalmopathy. *Invest Ophthalmol Vis Sci,* 49**,** 4760-4.

CHEN, Y., JIN, Z. Y., ZHANG, Z. H., XU, D. D., MENG, W., JIANG, B., FANG, H. Y., SUN, Z. Y., CHEN, Y., SUN, H. Y. & FENG, F. 2012. Quantitative evaluation of extraocular muscle with high-field magnetic resonance in patients with Graves' ophthalmopathy with upper-lid retraction. *Zhongguo Yi Xue Ke Xue Yuan Xue Bao,* 34**,** 461-7.

CHENG, W., PING, Y., ZHANG, Y., CHUANG, K. H. & LIU, Y. 2013. Magnetic resonance imaging (MRI) contrast agents for tumor diagnosis. *J Healthc Eng,* 4**,** 23-45.

CHESNEY, J., BACHER, M., BENDER, A. & BUCALA, R. 1997. The peripheral blood fibrocyte is a potent antigen-presenting cell capable of priming naive T cells in situ. *Proc Natl Acad Sci U S A,* 94**,** 6307-12.

CHESNEY, J., METZ, C., STAVITSKY, A. B., BACHER, M. & BUCALA, R. 1998. Regulated production of type I collagen and inflammatory cytokines by peripheral blood fibrocytes. *J Immunol,* 160**,** 419-25.

CHNG, C. L., LAI, O. F., CHEW, C. S., PEH, Y. P., FOOK-CHONG, S. M., SEAH, L. L. & KHOO, D. H. 2014. Hypoxia increases adipogenesis and affects adipocytokine production in orbital fibroblasts-a possible explanation of the link between smoking and Graves' ophthalmopathy. *Int J Ophthalmol,* 7**,** 403-7.

CHO, B. Y., SHONG, Y. K., LEE, H. K., KOH, C. S. & MIN, H. K. 1989. Graves' hyperthyroidism following primary hypothyroidism: sequential changes in various activities of thyrotropin receptor antibodies. *Acta Endocrinol (Copenh),* 120**,** 447-50.

CHO, J. H. & FELDMAN, M. 2015. Heterogeneity of autoimmune diseases: pathophysiologic insights from genetics and implications for new therapies. *Nat Med,* 21**,** 730-8.

CHO, J. H. & GREGERSEN, P. K. 2011. Genomics and the multifactorial nature of human autoimmune disease. *N Engl J Med,* 365**,** 1612-23.

CHRISTEN, U., BENDER, C. & VON HERRATH, M. G. 2012. Infection as a cause of type 1 diabetes? *Curr Opin Rheumatol,* 24**,** 417-23.

CHU, X., PAN, C. M., ZHAO, S. X., LIANG, J., GAO, G. Q., ZHANG, X. M., YUAN, G. Y., LI, C. G., XUE, L. Q., SHEN, M., LIU, W., XIE, F., YANG, S. Y., WANG, H. F., SHI, J. Y., SUN, W. W., DU, W. H., ZUO, C. L., SHI, J. X., LIU, B. L., GUO, C. C., ZHAN, M., GU, Z. H., ZHANG, X. N., SUN, F., WANG, Z. Q., SONG, Z. Y., ZOU, C. Y., SUN, W. H., GUO, T., CAO, H. M., MA, J. H., HAN, B., LI, P., JIANG, H., HUANG, Q. H., LIANG, L., LIU, L. B., CHEN, G., SU, Q., PENG, Y. D., ZHAO, J. J., NING, G., CHEN, Z., CHEN, J. L., CHEN, S. J., HUANG, W., SONG, H. D. & CHINA CONSORTIUM FOR GENETICS OF AUTOIMMUNE THYROID, D. 2011. A

genome-wide association study identifies two new risk loci for Graves' disease. *Nat Genet,* 43**,** 897-901.

COHN, S. A. 1955. Histochemical observations on the Harderian gland of the albino mouse. *J Histochem Cytochem,* 3**,** 342-53.

COLOBRAN, R., ARMENGOL MDEL, P., FANER, R., GARTNER, M., TYKOCINSKI, L. O., LUCAS, A., RUIZ, M., JUAN, M., KYEWSKI, B. & PUJOL-BORRELL, R. 2011. Association of an SNP with intrathymic transcription of TSHR and Graves' disease: a role for defective thymic tolerance. *Hum Mol Genet,* 20**,** 3415-23.

COOPER, D. S. 2005. Antithyroid drugs. *N Engl J Med,* 352**,** 905-17.

COOPER, J. D., SIMMONDS, M. J., WALKER, N. M., BURREN, O., BRAND, O. J., GUO, H., WALLACE, C., STEVENS, H., COLEMAN, G., WELLCOME TRUST CASE CONTROL, C., FRANKLYN, J. A., TODD, J. A. & GOUGH, S. C. 2012. Seven newly identified loci for autoimmune thyroid disease. *Hum Mol Genet,* 21**,** 5202-8.

CORAPCIOGLU, D., TONYUKUK, V., KIYAN, M., YILMAZ, A. E., EMRAL, R., KAMEL, N. & ERDOGAN, G. 2002. Relationship between thyroid autoimmunity and Yersinia enterocolitica antibodies. *Thyroid,* 12**,** 613-7.

COSTAGLIOLA, S., ALCALDE, L., RUF, J., VASSART, G. & LUDGATE, M. 1994. Overexpression of the extracellular domain of the thyrotrophin receptor in bacteria; production of thyrotrophin-binding inhibiting immunoglobulins. *J Mol Endocrinol,* 13**,** 11-21.

COSTAGLIOLA, S., BONOMI, M., MORGENTHALER, N. G., VAN DURME, J., PANNEELS, V., REFETOFF, S. & VASSART, G. 2004. Delineation of the discontinuous-conformational epitope of a monoclonal antibody displaying full in vitro and in vivo thyrotropin activity. *Mol Endocrinol,* 18**,** 3020-34.

COSTAGLIOLA, S., FRANSSEN, J. D., BONOMI, M., URIZAR, E., WILLNICH, M., BERGMANN, A. & VASSART, G. 2002. Generation of a mouse monoclonal TSH receptor antibody with stimulating activity. *Biochem Biophys Res Commun,* 299**,** 891-6.

COSTAGLIOLA, S., MANY, M. C., DENEF, J. F., POHLENZ, J., REFETOFF, S. & VASSART, G. 2000. Genetic immunization of outbred mice with thyrotropin receptor cDNA provides a model of Graves' disease. *J Clin Invest,* 105**,** 803-11.

COSTAGLIOLA, S., MANY, M. C., STALMANS-FALYS, M., VASSART, G. & LUDGATE, M. 1995. The autoimmune response induced by immunising female mice with recombinant human thyrotropin receptor varies with the genetic background. *Mol Cell Endocrinol,* 115**,** 199-206.

COSTAGLIOLA, S., MORGENTHALER, N. G., HOERMANN, R., BADENHOOP, K., STRUCK, J., FREITAG, D., POERTL, S., WEGLOHNER, W., HOLLIDT, J. M., QUADBECK, B., DUMONT, J. E., SCHUMM-DRAEGER, P. M., BERGMANN, A., MANN, K., VASSART, G. & USADEL, K. H. 1999. Second generation assay for thyrotropin receptor antibodies has superior diagnostic sensitivity for Graves' disease. *J Clin Endocrinol Metab,* 84**,** 90-7.

COSTAGLIOLA, S., RODIEN, P., MANY, M. C., LUDGATE, M. & VASSART, G. 1998. Genetic immunization against the human thyrotropin receptor causes thyroiditis and allows production of monoclonal antibodies recognizing the native receptor. *J Immunol,* 160**,** 1458-65.

COUET, J., DE BERNARD, S., LOOSFELT, H., SAUNIER, B., MILGROM, E. & MISRAHI, M. 1996a. Cell surface protein disulfide-isomerase is involved in the shedding of human thyrotropin receptor ectodomain. *Biochemistry,* 35**,** 14800-5.

COUET, J., SAR, S., JOLIVET, A., HAI, M. T., MILGROM, E. & MISRAHI, M. 1996b. Shedding of human thyrotropin receptor ectodomain. Involvement of a matrix metalloprotease. *J Biol Chem,* 271**,** 4545-52.

CRISP, M., STARKEY, K. J., LANE, C., HAM, J. & LUDGATE, M. 2000. Adipogenesis in thyroid eye disease. *Invest Ophthalmol Vis Sci,* 41**,** 3249-55.

CUNNINGHAM, M. W. 2012. Streptococcus and rheumatic fever. *Curr Opin Rheumatol,* 24**,** 408-16.

CUSICK, M. F., LIBBEY, J. E. & FUJINAMI, R. S. 2012. Molecular mimicry as a mechanism of autoimmune disease. *Clin Rev Allergy Immunol,* 42**,** 102-11.

CZARNOCKA, B. 2011. Thyroperoxidase, thyroglobulin, Na(+)/I(-) symporter, pendrin in thyroid autoimmunity. *Front Biosci (Landmark Ed),* 16**,** 783-802.

DAĞDELEN, S. U., KONG, Y.-C. M. & BANGA, J. P. 2009. Toward Better Models of Hyperthyroid Graves' Disease. *Endocrinology & Metabolism Clinics of North America,* 38**,** 343-354.

DAI, G., LEVY, O. & CARRASCO, N. 1996. Cloning and characterization of the thyroid iodide transporter. *Nature,* 379**,** 458-60.

DAUMERIE, C., LUDGATE, M., COSTAGLIOLA, S. & MANY, M. C. 2002. Evidence for thyrotropin receptor immunoreactivity in pretibial connective tissue from patients with thyroid-associated dermopathy. *Eur J Endocrinol,* 146**,** 35-8.

DAVIES, T. F. 1978. The impact of peptide hormone receptor research on clinical medicine. *J R Coll Physicians Lond,* 12**,** 379-97.

DAVIES, T. F., ALI, M. R. & LATIF, R. 2014. Allosteric modulators hit the TSH receptor. *Endocrinology,* 155**,** 1-5.

DAVIES, T. F., LATIF, R. & YIN, X. 2012. New genetic insights from autoimmune thyroid disease. *J Thyroid Res,* 2012**,** 623852.

DAVIES, T. F., MARTIN, A., CONCEPCION, E. S., GRAVES, P., COHEN, L. & BEN-NUN, A. 1991. Evidence of limited variability of antigen receptors on intrathyroidal T cells in autoimmune thyroid disease. *N Engl J Med,* 325**,** 238-44.

DAVIES, T. F., MARTIN, A., CONCEPCION, E. S., GRAVES, P., LAHAT, N., COHEN, W. L. & BEN-NUN, A. 1992. Evidence for selective accumulation of intrathyroidal T lymphocytes in human autoimmune thyroid disease based on T cell receptor V gene usage. *J Clin Invest,* 89**,** 157-62.

DAYAN, C. M., LONDEI, M., CORCORAN, A. E., GRUBECK-LOEBENSTEIN, B., JAMES, R. F., RAPOPORT, B. & FELDMANN, M. 1991. Autoantigen recognition by thyroid-infiltrating T cells in Graves disease. *Proc Natl Acad Sci U S A,* 88**,** 7415-9.

DE FORTEZA, R., SMITH, C. U., AMIN, J., MCKENZIE, J. M. & ZAKARIJA, M. 1994. Visualization of the thyrotropin receptor on the cell surface by potent autoantibodies. *J Clin Endocrinol Metab,* 78**,** 1271-3.

DE HAAN, S., LAHOOTI, H., MORRIS, O. & WALL, J. R. 2010. Epitopes, immunoglobulin classes and immunoglobulin G subclasses of calsequestrin antibodies in patients with thyroid eye disease. *Autoimmunity,* 43**,** 698-703.

DECHAIRO, B. M., ZABANEH, D., COLLINS, J., BRAND, O., DAWSON, G. J., GREEN, A. P., MACKAY, I., FRANKLYN, J. A., CONNELL, J. M., WASS, J. A., WIERSINGA, W. M., HEGEDUS, L., BRIX, T., ROBINSON, B. G., HUNT, P. J., WEETMAN, A. P., CAREY, A. H. & GOUGH, S. C. 2005. Association of the TSHR gene with Graves' disease: the first disease specific locus. *Eur J Hum Genet,* 13**,** 1223-30.

DIANA, T., BROWN, R., BOSSOWSKI, A., SEGNI, M., NIEDZIELA, M., KONIG, J., BOSSOWSKA, A., ZIORA, K., HALE, A., SMITH, J., PITZ, S., KANITZ, M. & KAHALY, G. 2014. Clinical Relevance of Thyroid-Stimulating Autoantibodies in Pediatric Graves' Disease - a Multicenter Study. *J Clin Endocrinol Metab***,** jc20134026.

DICKINSON, A. J. 2010a. Clinical Manifestation. *In:* WIERSINGA, W. M. & KAHALY, G. J. (eds.) *Graves' orbitopathy : a multidisciplinary approach - questions and answers.* 2nd, rev. ed. Basel etc.: S. Karger.

DICKINSON, A. J. 2010b. Clinical manifestations. *In:* WIERSINGA, W. M. & KAHALY, G. J. (eds.) *Graves' orbitopathy : a multidisciplinary approach - questions and answers.* 2nd, rev. ed. Basel etc.: S. Karger.

DINARELLO, C. A. 2000. The role of the interleukin-1-receptor antagonist in blocking inflammation mediated by interleukin-1. *N Engl J Med,* 343**,** 732-4.

DOUGLAS, R. S., AFIFIYAN, N. F., HWANG, C. J., CHONG, K., HAIDER, U., RICHARDS, P., GIANOUKAKIS, A. G. & SMITH, T. J. 2010. Increased generation of fibrocytes in thyroid-associated ophthalmopathy. *J Clin Endocrinol Metab,* 95**,** 430-8.

DOUGLAS, R. S., BRIX, T. H., HWANG, C. J., HEGEDUS, L. & SMITH, T. J. 2009. Divergent frequencies of IGF-I receptor-expressing blood lymphocytes in monozygotic twin pairs discordant for Graves' disease: evidence for a phenotypic signature ascribable to nongenetic factors. *J Clin Endocrinol Metab,* 94**,** 1797-802.

DOUGLAS, R. S., GIANOUKAKIS, A. G., KAMAT, S. & SMITH, T. J. 2007. Aberrant expression of the insulin-like growth factor-1 receptor by T cells from patients with Graves' disease may carry functional consequences for disease pathogenesis. *J Immunol,* 178**,** 3281-7.

DOUGLAS, R. S., NAIK, V., HWANG, C. J., AFIFIYAN, N. F., GIANOUKAKIS, A. G., SAND, D., KAMAT, S. & SMITH, T. J. 2008. B cells from patients with Graves' disease aberrantly express the IGF-1 receptor: implications for disease pathogenesis. *J Immunol,* 181**,** 5768-74.

DUNTAS, L. H. 2010. Selenium and the thyroid: a close-knit connection. *J Clin Endocrinol Metab,* 95**,** 5180-8.

DURRANI, O. M., REUSER, T. Q. & MURRAY, P. I. 2005. Infliximab: a novel treatment for sight-threatening thyroid associated ophthalmopathy. *Orbit,* 24**,** 117-9.

DUTTON, C. M., JOBA, W., SPITZWEG, C., HEUFELDER, A. E. & BAHN, R. S. 1997. Thyrotropin receptor expression in adrenal, kidney, and thymus. *Thyroid,* 7**,** 879-84.

ECKSTEIN, A., QUADBECK, B., MUELLER, G., RETTENMEIER, A. W., HOERMANN, R., MANN, K., STEUHL, P. & ESSER, J. 2003. Impact of smoking on the response to treatment of thyroid associated ophthalmopathy. *Br J Ophthalmol,* 87**,** 773-6.

ECKSTEIN, A., SCHITTKOWSKI, M. & ESSER, J. 2012. Surgical treatment of Graves' ophthalmopathy. *Best Pract Res Clin Endocrinol Metab,* 26**,** 339-58.

ECKSTEIN, A. K., JOHNSON, K. T., THANOS, M., ESSER, J. & LUDGATE, M. 2009. Current insights into the pathogenesis of Graves' orbitopathy. *Horm Metab Res,* 41**,** 456-64.

ECKSTEIN, A. K., QUADBECK, B., TEWS, S., MANN, K., KRUGER, C., MOHR, C. H., STEUHL, K. P., ESSER, J. & GIESELER, R. K. 2004. Thyroid associated ophthalmopathy: evidence for CD4(+) gammadelta T cells; de novo differentiation of RFD7(+) macrophages, but not of RFD1(+) dendritic cells; and loss of gammadelta and alphabeta T cell receptor expression. *Br J Ophthalmol,* 88**,** 803-8.

EFFRAIMIDIS, G., TIJSSEN, J. G., STRIEDER, T. G. & WIERSINGA, W. M. 2011. No causal relationship between Yersinia enterocolitica infection and autoimmune thyroid disease: evidence from a prospective study. *Clin Exp Immunol,* 165**,** 38-43.

EFFRAIMIDIS, G., TIJSSEN, J. G. & WIERSINGA, W. M. 2009. Discontinuation of smoking increases the risk for developing thyroid peroxidase antibodies and/or thyroglobulin antibodies: a prospective study. *J Clin Endocrinol Metab,* 94**,** 1324-8.

EFFRAIMIDIS, G. & WIERSINGA, W. M. 2014. Mechanisms in endocrinology: autoimmune thyroid disease: old and new players. *Eur J Endocrinol,* 170**,** R241-52.

EL-KAISSI, S., FRAUMAN, A. G. & WALL, J. R. 2004. Thyroid-associated ophthalmopathy: a practical guide to classification, natural history and management. *Intern Med J,* 34**,** 482-91.

EL FASSI, D., BANGA, J. P., GILBERT, J. A., PADOA, C., HEGEDUS, L. & NIELSEN, C. H. 2009. Treatment of Graves' disease with rituximab specifically reduces the production of thyroid stimulating autoantibodies. *Clin Immunol,* 130**,** 252-8.

EL FASSI, D., NIELSEN, C. H., BONNEMA, S. J., HASSELBALCH, H. C. & HEGEDUS, L. 2007. B lymphocyte depletion with the monoclonal antibody rituximab in Graves' disease: a controlled pilot study. *J Clin Endocrinol Metab,* 92**,** 1769-72.

EL FASSI, D., NIELSEN, C. H., HASSELBALCH, H. C. & HEGEDUS, L. 2006. Treatment-resistant severe, active Graves' ophthalmopathy successfully treated with B lymphocyte depletion. *Thyroid,* 16**,** 709-10.

ENDO, T., OHNO, M., KOTANI, S., GUNJI, K. & ONAYA, T. 1993. Thyrotropin receptor in non-thyroid tissues. *Biochem Biophys Res Commun,* 190**,** 774-9.

ENGERING, A. J., CELLA, M., FLUITSMA, D., BROCKHAUS, M., HOEFSMIT, E. C., LANZAVECCHIA, A. & PIETERS, J. 1997. The mannose receptor functions as a high capacity and broad specificity antigen receptor in human dendritic cells. *Eur J Immunol,* 27**,** 2417-25.

ERIKSSON, N., TUNG, J. Y., KIEFER, A. K., HINDS, D. A., FRANCKE, U., MOUNTAIN, J. L. & DO, C. B. 2012. Novel associations for hypothyroidism include known autoimmune risk loci. *PLoS One,* 7**,** e34442.

EVANS, M., SANDERS, J., TAGAMI, T., SANDERS, P., YOUNG, S., ROBERTS, E., WILMOT, J., HU, X., KABELIS, K., CLARK, J., HOLL, S., RICHARDS, T., COLLYER, A., FURMANIAK, J. & SMITH, B. R. 2010. Monoclonal autoantibodies to the TSH receptor, one with stimulating activity and one with blocking activity, obtained from the same blood sample. *Clin Endocrinol (Oxf),* 73**,** 404-12.

EWINS, D. L., BARNETT, P. S., TOMLINSON, R. W., MCGREGOR, A. M. & BANGA, J. P. 1992. Mapping epitope specificities of monoclonal antibodies to thyroid peroxidase using recombinant antigen preparations. *Autoimmunity,* 11**,** 141-9.

EZRA, D. G., KRELL, J., ROSE, G. E., BAILLY, M., STEBBING, J. & CASTELLANO, L. 2012. Transcriptome-level microarray expression profiling implicates IGF-1 and Wnt signalling dysregulation in the pathogenesis of thyroid-associated orbitopathy. *J Clin Pathol,* 65**,** 608-13.

FATOURECHI, V. 2012. Thyroid dermopathy and acropachy. *Best Pract Res Clin Endocrinol Metab,* 26**,** 553-65.

FEGER, U., LUTHER, C., POESCHEL, S., MELMS, A., TOLOSA, E. & WIENDL, H. 2007. Increased frequency of CD4+ CD25+ regulatory T cells in the cerebrospinal fluid but not in the blood of multiple sclerosis patients. *Clin Exp Immunol,* 147**,** 412-8.

FELDMANN, M. 2002. Development of anti-TNF therapy for rheumatoid arthritis. *Nat Rev Immunol,* 2**,** 364-71.

FELDON, S. E. 1990. Graves' ophthalmopathy. Is it really thyroid disease? *Arch Intern Med,* 150**,** 948-50.

FELDON, S. E., O'LOUGHLIN C, W., RAY, D. M., LANDSKRONER-EIGER, S., SEWERYNIAK, K. E. & PHIPPS, R. P. 2006. Activated human T lymphocytes express cyclooxygenase-2 and produce proadipogenic prostaglandins that drive human orbital fibroblast differentiation to adipocytes. *Am J Pathol,* 169**,** 1183-93.

FELDON, S. E., PARK, D. J., O'LOUGHLIN, C. W., NGUYEN, V. T., LANDSKRONER-EIGER, S., CHANG, D., THATCHER, T. H. & PHIPPS, R. P. 2005. Autologous T-lymphocytes stimulate proliferation of orbital fibroblasts derived from patients with Graves' ophthalmopathy. *Invest Ophthalmol Vis Sci,* 46**,** 3913-21.

FELICIELLO, A., PORCELLINI, A., CIULLO, I., BONAVOLONTA, G., AVVEDIMENTO, E. V. & FENZI, G. 1993. Expression of thyrotropin-receptor mRNA in healthy and Graves' disease retro-orbital tissue. *Lancet,* 342**,** 337-8.

FERNANDO, R., ATKINS, S., RAYCHAUDHURI, N., LU, Y., LI, B., DOUGLAS, R. S. & SMITH, T. J. 2012. Human fibrocytes coexpress thyroglobulin and thyrotropin receptor. *Proc Natl Acad Sci U S A,* 109**,** 7427-32.

FERNANDO, R., VONBERG, A., ATKINS, S. J., PIETROPAOLO, S., PIETROPAOLO, M. & SMITH, T. J. 2014. Human fibrocytes express multiple antigens associated with autoimmune endocrine diseases. *J Clin Endocrinol Metab***,** jc20133072.

FIRTH, S. M. & BAXTER, R. C. 2002. Cellular actions of the insulin-like growth factor binding proteins. *Endocr Rev,* 23**,** 824-54.

FLYNN, J. C., RAO, P. V., GORA, M., ALSHARABI, G., WEI, W., GIRALDO, A. A., DAVID, C. S., BANGA, J. P. & KONG, Y. M. 2004. Graves' hyperthyroidism and thyroiditis in HLA-DRB1*0301 (DR3) transgenic mice after immunization with thyrotropin receptor DNA. *Clin Exp Immunol,* 135**,** 35-40.

FORSTER, G. J., KRUMMENAUER, F., NICKEL, O. & KAHALY, G. J. 2000. Somatostatin-receptor scintigraphy in Graves' disease: reproducibility and variance of orbital activity. *Cancer Biother Radiopharm,* 15**,** 517-25.

FOUNTOULAKIS, S., VARTHOLOMATOS, G., KOLAITIS, N., FRILLINGOS, S., PHILIPPOU, G. & TSATSOULIS, A. 2008. HLA-DR expressing peripheral T regulatory cells in newly diagnosed patients with different forms of autoimmune thyroid disease. *Thyroid,* 18**,** 1195-200.

FOUSTERI, G., LIOSSIS, S. N. & BATTAGLIA, M. 2013. Roles of the protein tyrosine phosphatase PTPN22 in immunity and autoimmunity. *Clin Immunol,* 149**,** 556-65.

FRAZIER, A. L., ROBBINS, L. S., STORK, P. J., SPRENGEL, R., SEGALOFF, D. L. & CONE, R. D. 1990. Isolation of TSH and LH/CG receptor cDNAs from human thyroid: regulation by tissue specific splicing. *Mol Endocrinol,* 4**,** 1264-76.

FUJINAMI, R. S., OLDSTONE, M. B., WROBLEWSKA, Z., FRANKEL, M. E. & KOPROWSKI, H. 1983. Molecular mimicry in virus infection: crossreaction of measles virus phosphoprotein or of herpes simplex virus protein with human intermediate filaments. *Proc Natl Acad Sci U S A,* 80**,** 2346-50.

GALLI, L., CHIAPPINI, E. & DE MARTINO, M. 2012. Infections and autoimmunity. *Pediatr Infect Dis J,* 31**,** 1295-7.

GARCIA-ROJAS, L., ADAME-OCAMPO, G., MENDOZA-VAZQUEZ, G., ALEXANDERSON, E. & TOVILLA-CANALES, J. L. 2013. Orbital positron emission tomography/computed tomography (PET/CT) imaging findings in graves ophthalmopathy. *BMC Res Notes,* 6**,** 353.

GARRITY, J. A. & BAHN, R. S. 2006. Pathogenesis of graves ophthalmopathy: implications for prediction, prevention, and treatment. *Am J Ophthalmol,* 142**,** 147-153.

GASTALDI, R., POGGI, E., MUSSA, A., WEBER, G., VIGONE, M. C., SALERNO, M., DELVECCHIO, M., PERONI, E., PISTORIO, A. & CORRIAS, A. 2014. Graves Disease in Children: Thyroid-Stimulating Hormone Receptor Antibodies as Remission Markers. *J Pediatr*.

GENOVESE, B., NOURELDINE, S., GLEESON, E., TUFANO, R. & KANDIL, E. 2013. What Is the Best Definitive Treatment for Graves' Disease? A Systematic Review of the Existing Literature. *Annals of Surgical Oncology,* 20**,** 660-667.

GERDING, M. N., VAN DER ZANT, F. M., VAN ROYEN, E. A., KOORNNEEF, L., KRENNING, E. P., WIERSINGA, W. M. & PRUMMEL, M. F. 1999. Octreotide-scintigraphy is a disease-activity parameter in Graves' ophthalmopathy. *Clin Endocrinol (Oxf),* 50**,** 373-9.

GESSL, A., LEMMENS-GRUBER, R. & KAUTZKY-WILLER, A. 2012. Thyroid Disorders. *In:* REGITZ-ZAGROSEK, V. (ed.) *Sex and Gender Differences in Pharmacology.* Springer Berlin Heidelberg.

GETTS, D. R., CHASTAIN, E. M., TERRY, R. L. & MILLER, S. D. 2013. Virus infection, antiviral immunity, and autoimmunity. *Immunol Rev,* 255**,** 197-209.

GIANOUKAKIS, A. G., KHADAVI, N. & SMITH, T. J. 2008. Cytokines, Graves' disease, and thyroid-associated ophthalmopathy. *Thyroid,* 18**,** 953-8.

GILBERT, J. A. & BANGA, J. P. 2006. King's College London.

GILBERT, J. A., GIANOUKAKIS, A. G., SALEHI, S., MOORHEAD, J., RAO, P. V., KHAN, M. Z., MCGREGOR, A. M., SMITH, T. J. & BANGA, J. P. 2006. Monoclonal pathogenic antibodies to the thyroid-stimulating hormone receptor in Graves' disease with potent thyroid-stimulating activity but differential blocking activity activate multiple signaling pathways. *J Immunol,* 176**,** 5084-92.

GILLESPIE, E. F., PAPAGEORGIOU, K. I., FERNANDO, R., RAYCHAUDHURI, N., COCKERHAM, K. P., CHARARA, L. K., GONCALVES, A. C., ZHAO, S. X., GINTER, A., LU, Y., SMITH, T. J. & DOUGLAS, R. S. 2012. Increased Expression of TSH Receptor by Fibrocytes in Thyroid-Associated Ophthalmopathy Leads to Chemokine Production. *J Clin Endocrinol Metab,* 97**,** E740-6.

GIMENEZ-BARCONS, M., COLOBRAN, R., GOMEZ-PAU, A., MARIN-SANCHEZ, A., CASTERAS, A., OBIOLS, G., ABELLA, R., FERNANDEZ-DOBLAS, J., TONACCHERA, M., LUCAS-MARTIN, A. & PUJOL-BORRELL, R. 2015. Graves' disease TSHR-stimulating antibodies (TSAbs) induce the activation of immature thymocytes: a clue to the riddle of TSAbs generation? *J Immunol,* 194**,** 4199-206.

GLAS, J., SEIDERER, J., NAGY, M., FRIES, C., BEIGEL, F., WEIDINGER, M., PFENNIG, S., KLEIN, W., EPPLEN, J. T., LOHSE, P., FOLWACZNY, M., GOKE, B., OCHSENKUHN, T., DIEGELMANN, J., MULLER-MYHSOK, B., ROESKE, D. & BRAND, S. 2010. Evidence for STAT4 as a common autoimmune gene: rs7574865 is associated with colonic Crohn's disease and early disease onset. *PLoS One,* 5**,** e10373.

GLINOER, D., DE NAYER, P., BEX, M. & BELGIAN COLLABORATIVE STUDY GROUP ON GRAVES, D. 2001. Effects of l-thyroxine administration, TSH-receptor antibodies and smoking on the risk of recurrence in Graves' hyperthyroidism treated with antithyroid drugs: a double-blind prospective randomized study. *Eur J Endocrinol,* 144**,** 475-83.

GONCALVES, A. C., GEBRIM, E. M. & MONTEIRO, M. L. 2012. Imaging studies for diagnosing Graves' orbitopathy and dysthyroid optic neuropathy. *Clinics (Sao Paulo),* 67**,** 1327-34.

GOPINATH, B., MUSSELMAN, R., BEARD, N., EL-KAISSI, S., TANI, J., ADAMS, C. L. & WALL, J. R. 2006. Antibodies targeting the calcium binding skeletal muscle protein calsequestrin are specific markers of ophthalmopathy and sensitive indicators of ocular myopathy in patients with Graves' disease. *Clin Exp Immunol,* 145**,** 56-62.

GOUGH, S. C., WALKER, L. S. & SANSOM, D. M. 2005. CTLA4 gene polymorphism and autoimmunity. *Immunol Rev,* 204**,** 102-15.

GRUBECK-LOEBENSTEIN, B., TRIEB, K., SZTANKAY, A., HOLTER, W., ANDERL, H. & WICK, G. 1994. Retrobulbar T cells from patients with Graves' ophthalmopathy are CD8+ and specifically recognize autologous fibroblasts. *J Clin Invest,* 93**,** 2738-43.

GUO, N., BAGLOLE, C. J., O'LOUGHLIN, C. W., FELDON, S. E. & PHIPPS, R. P. 2010. Mast cell-derived prostaglandin D2 controls hyaluronan synthesis in human orbital fibroblasts via DP1 activation: implications for thyroid eye disease. *J Biol Chem,* 285**,** 15794-804.

GUO, N., WOELLER, C. F., FELDON, S. E. & PHIPPS, R. P. 2011. Peroxisome proliferator-activated receptor gamma ligands inhibit transforming growth factor-beta-induced, hyaluronan-dependent, T cell adhesion to orbital fibroblasts. *J Biol Chem,* 286**,** 18856-67.

HAAK, S., GYULVESZI, G. & BECHER, B. 2009. Th17 cells in autoimmune disease: changing the verdict. *Immunotherapy,* 1**,** 199-203.

HAAS, A. K., KLEINAU, G., HOYER, I., NEUMANN, S., FURKERT, J., RUTZ, C., SCHULEIN, R., GERSHENGORN, M. C. & KRAUSE, G. 2011. Mutations that silence constitutive signaling activity in the allosteric ligand-binding site of the thyrotropin receptor. *Cell Mol Life Sci,* 68**,** 159-67.

HAAS, J., HUG, A., VIEHOVER, A., FRITZSCHING, B., FALK, C. S., FILSER, A., VETTER, T., MILKOVA, L., KORPORAL, M., FRITZ, B., STORCH-HAGENLOCHER, B., KRAMMER, P. H., SURI-PAYER, E. & WILDEMANN, B. 2005. Reduced suppressive effect of CD4+CD25high regulatory T cells on the T cell immune response against myelin oligodendrocyte glycoprotein in patients with multiple sclerosis. *Eur J Immunol,* 35**,** 3343-52.

HAMIDI, S., ALIESKY, H., CHEN, C. R., RAPOPORT, B. & MCLACHLAN, S. M. 2010. Variable suppression of serum thyroxine in female mice of different inbred strains by triiodothyronine administered in drinking water. *Thyroid,* 20**,** 1157-62.

HANSSON, H. A. 1989. Aspects on growth factors in exophthalmos. *Acta Endocrinologica*, 107-111.

HANSSON, H. A., PETRUSON, B. & SKOTTNER, A. 1986. Somatomedin C in pathogenesis of malignant exophthalmos of endocrine origin. *Lancet,* 1, 218-9.

HAO, D., AI, T., GOERNER, F., HU, X., RUNGE, V. M. & TWEEDLE, M. 2012. MRI contrast agents: basic chemistry and safety. *J Magn Reson Imaging,* 36, 1060-71.

HARA, T., TAMAI, H., MUKUTA, T., FUKATA, S., KUMA, K. & SUGAWARA, M. 1990. Transient postpartum hypothyroidism caused by thyroid-stimulation-blocking antibody. *Lancet,* 336, 946.

HARFST, E., JOHNSTONE, A. P. & NUSSEY, S. S. 1992. Characterization of the extracellular region of the human thyrotrophin receptor expressed as a recombinant protein. *J Mol Endocrinol,* 9, 227-36.

HARFST, E., ROSS, M. S., NUSSEY, S. S. & JOHNSTONE, A. P. 1994. Production of antibodies to the human thyrotropin receptor and their use in characterising eukaryotically expressed functional receptor. *Mol Cell Endocrinol,* 102, 77-84.

HARGREAVES, C. E., GRASSO, M., HAMPE, C. S., STENKOVA, A., ATKINSON, S., JOSHUA, G. W., WREN, B. W., BUCKLE, A. M., DUNN-WALTERS, D. & BANGA, J. P. 2013. Yersinia enterocolitica provides the link between thyroid-stimulating antibodies and their germline counterparts in Graves' disease. *J Immunol,* 190, 5373-81.

HAY, F. C., WESTWOOD, O. M. R., NELSON, P. N. & HUDSON, L. P. I. 2001. *Practical immunology,* Malden, MA, Blackwell Science.

HEEMSTRA, K. A., TOES, R. E., SEPERS, J., PEREIRA, A. M., CORSSMIT, E. P., HUIZINGA, T. W., ROMIJN, J. A. & SMIT, J. W. 2008. Rituximab in relapsing Graves' disease, a phase II study. *Eur J Endocrinol,* 159, 609-15.

HEGEDIUS, L., BRIX, T. H. & VESTERGAARD, P. 2004. Relationship between cigarette smoking and Graves' ophthalmopathy. *J Endocrinol Invest,* 27, 265-71.

HEGEDUS, L. 2009. Treatment of Graves' hyperthyroidism: evidence-based and emerging modalities. *Endocrinol Metab Clin North Am,* 38, 355-71, ix.

HEGEDUS, L., SMITH, T. J., DOUGLAS, R. S. & NIELSEN, C. H. 2011. Targeted biological therapies for Graves' disease and thyroid-associated ophthalmopathy. Focus on B-cell depletion with Rituximab. *Clin Endocrinol (Oxf),* 74, 1-8.

HEMMINKI, K., LI, X., SUNDQUIST, J. & SUNDQUIST, K. 2010. The epidemiology of Graves' disease: evidence of a genetic and an environmental contribution. *J Autoimmun,* 34, J307-13.

HEUFELDER, A. E. 2000. Pathogenesis of ophthalmopathy in autoimmune thyroid disease. *Rev Endocr Metab Disord,* 1, 87-95.

HEUFELDER, A. E. & BAHN, R. S. 1992. Graves' immunoglobulins and cytokines stimulate the expression of intercellular adhesion molecule-1 (ICAM-1) in cultured Graves' orbital fibroblasts. *Eur J Clin Invest,* 22, 529-37.

HEUFELDER, A. E. & BAHN, R. S. 1993a. Detection and localization of cytokine immunoreactivity in retro-ocular connective tissue in Graves' ophthalmopathy. *Eur J Clin Invest,* 23, 10-7.

HEUFELDER, A. E. & BAHN, R. S. 1993b. Elevated expression in situ of selectin and immunoglobulin superfamily type adhesion molecules in retroocular connective tissues from patients with Graves' ophthalmopathy. *Clin Exp Immunol,* 91, 381-9.

HEUFELDER, A. E., BAHN, R. S. & SCRIBA, P. C. 1995a. Analysis of T-cell antigen receptor variable region gene usage in patients with thyroid-related pretibial dermopathy. *J Invest Dermatol,* 105, 372-8.

HEUFELDER, A. E., DUTTON, C. M., SARKAR, G., DONOVAN, K. A. & BAHN, R. S. 1993. Detection of TSH receptor RNA in cultured fibroblasts from patients with Graves' ophthalmopathy and pretibial dermopathy. *Thyroid,* 3, 297-300.

HEUFELDER, A. E., HERTERICH, S., ERNST, G., BAHN, R. S. & SCRIBA, P. C. 1995b. Analysis of retroorbital T cell antigen receptor variable region gene usage in patients with Graves' ophthalmopathy. *Eur J Endocrinol,* 132**,** 266-77.

HEUFELDER, A. E., JOBA, W. & MORGENTHALER, N. G. 2001. Autoimmunity involving the human sodium/iodide symporter: fact or fiction? *Exp Clin Endocrinol Diabetes,* 109**,** 35-40.

HEUFELDER, A. E., SCHWORM, H. D., WENZEL, B. E., GARRITY, J. A. & BAHN, R. S. 1996a. Molecular analysis of antigen receptor variable region repertoires in T lymphocytes infiltrating the intrathyroidal and extrathyroidal manifestations in patients with Graves' disease. *Exp Clin Endocrinol Diabetes,* 104 Suppl 4**,** 84-7.

HEUFELDER, A. E., WENZEL, B. E. & SCRIBA, P. C. 1996b. Antigen receptor variable region repertoires expressed by T cells infiltrating thyroid, retroorbital, and pretibial tissue in Graves' disease. *J Clin Endocrinol Metab,* 81**,** 3733-9.

HIRATANI, H., BOWDEN, D. W., IKEGAMI, S., SHIRASAWA, S., SHIMIZU, A., IWATANI, Y. & AKAMIZU, T. 2005. Multiple SNPs in intron 7 of thyrotropin receptor are associated with Graves' disease. *J Clin Endocrinol Metab,* 90**,** 2898-903.

HIROMATSU, Y., SATO, M., INOUE, Y., KOGA, M., MIYAKE, I., KAMEO, J., TOKISAWA, S., YANG, D. & NONAKA, K. 1996. Localization and clinical significance of thyrotropin receptor mRNA expression in orbital fat and eye muscle tissues from patients with thyroid-associated ophthalmopathy. *Thyroid,* 6**,** 553-62.

HIROMATSU, Y., YANG, D., BEDNARCZUK, T., MIYAKE, I., NONAKA, K. & INOUE, Y. 2000. Cytokine profiles in eye muscle tissue and orbital fat tissue from patients with thyroid-associated ophthalmopathy. *J Clin Endocrinol Metab,* 85**,** 1194-9.

HOLLOWELL, J. G., STAEHLING, N. W., FLANDERS, W. D., HANNON, W. H., GUNTER, E. W., SPENCER, C. A. & BRAVERMAN, L. E. 2002. Serum TSH, T(4), and thyroid antibodies in the United States population (1988 to 1994): National Health and Nutrition Examination Survey (NHANES III). *J Clin Endocrinol Metab,* 87**,** 489-99.

HONG, K. M., BELPERIO, J. A., KEANE, M. P., BURDICK, M. D. & STRIETER, R. M. 2007. Differentiation of human circulating fibrocytes as mediated by transforming growth factor-beta and peroxisome proliferator-activated receptor gamma. *J Biol Chem,* 282**,** 22910-20.

HSIAO, J. Y., TIEN, K. J., HSIAO, C. T. & HSIEH, M. C. 2008. A C/T polymorphism in CD40 gene is not associated with susceptibility and phenotype of Graves' disease in Taiwanese. *Endocr J,* 55**,** 477-84.

HUBER, A. K., FINKELMAN, F. D., LI, C. W., CONCEPCION, E., SMITH, E., JACOBSON, E., LATIF, R., KEDDACHE, M., ZHANG, W. & TOMER, Y. 2012. Genetically driven target tissue overexpression of CD40: a novel mechanism in autoimmune disease. *J Immunol,* 189**,** 3043-53.

HUBER, A. K., JACOBSON, E. M., JAZDZEWSKI, K., CONCEPCION, E. S. & TOMER, Y. 2008. Interleukin (IL)-23 receptor is a major susceptibility gene for Graves' ophthalmopathy: the IL-23/T-helper 17 axis extends to thyroid autoimmunity. *J Clin Endocrinol Metab,* 93**,** 1077-81.

HUNT, P. J., MARSHALL, S. E., WEETMAN, A. P., BELL, J. I., WASS, J. A. & WELSH, K. I. 2000. Cytokine gene polymorphisms in autoimmune thyroid disease. *J Clin Endocrinol Metab,* 85**,** 1984-8.

HWANG, C. J., AFIFIYAN, N., SAND, D., NAIK, V., SAID, J., POLLOCK, S. J., CHEN, B., PHIPPS, R. P., GOLDBERG, R. A., SMITH, T. J. & DOUGLAS, R. S. 2009. Orbital fibroblasts from patients with thyroid-associated ophthalmopathy overexpress CD40: CD154 hyperinduces IL-6, IL-8, and MCP-1. *Invest Ophthalmol Vis Sci,* 50**,** 2262-8.

IMAI, Y., IBARAKI, K., ODAJIMA, R. & SHISHIBA, Y. 1994. Effects of dibutyryl cyclic AMP on hyaluronan and proteoglycan synthesis by retroocular tissue fibroblasts in culture. *Endocr J,* 41**,** 645-54.

IYER, S. & BAHN, R. 2012. Immunopathogenesis of Graves' ophthalmopathy: the role of the TSH receptor. *Best Pract Res Clin Endocrinol Metab,* 26**,** 281-9.

JACOBSON, D. L., GANGE, S. J., ROSE, N. R. & GRAHAM, N. M. 1997. Epidemiology and estimated population burden of selected autoimmune diseases in the United States. *Clin Immunol Immunopathol,* 84**,** 223-43.

JACOBSON, E. M., CONCEPCION, E., OASHI, T. & TOMER, Y. 2005. A Graves' disease-associated Kozak sequence single-nucleotide polymorphism enhances the efficiency of CD40 gene translation: a case for translational pathophysiology. *Endocrinology,* 146**,** 2684-91.

JACOBSON, E. M., HUBER, A. & TOMER, Y. 2008. The HLA gene complex in thyroid autoimmunity: from epidemiology to etiology. *J Autoimmun,* 30**,** 58-62.

JACOBSON, E. M., HUBER, A. K., AKENO, N., SIVAK, M., LI, C. W., CONCEPCION, E., HO, K. & TOMER, Y. 2007. A CD40 Kozak sequence polymorphism and susceptibility to antibody-mediated autoimmune conditions: the role of CD40 tissue-specific expression. *Genes Immun,* 8**,** 205-14.

JACOBSON, E. M. & TOMER, Y. 2007. The CD40, CTLA-4, thyroglobulin, TSH receptor, and PTPN22 gene quintet and its contribution to thyroid autoimmunity: back to the future. *J Autoimmun,* 28**,** 85-98.

JADIDI-NIARAGH, F. & MIRSHAFIEY, A. 2011. Regulatory T-cell as orchestra leader in immunosuppression process of multiple sclerosis. *Immunopharmacol Immunotoxicol,* 33**,** 545-67.

JAUME, J. C., KAKINUMA, A., CHAZENBALK, G. D., RAPOPORT, B. & MCLACHLAN, S. M. 1997. Thyrotropin receptor autoantibodies in serum are present at much lower levels than thyroid peroxidase autoantibodies: analysis by flow cytometry. *J Clin Endocrinol Metab,* 82**,** 500-7.

JEFFREYS, J., DEPRAETERE, H., SANDERS, J., ODA, Y., EVANS, M., KIDDIE, A., RICHARDS, T., FURMANIAK, J. & REES SMITH, B. 2002. Characterization of the thyrotropin binding pocket. *Thyroid,* 12**,** 1051-61.

JI, J. D., LEE, W. J., KONG, K. A., WOO, J. H., CHOI, S. J., LEE, Y. H. & SONG, G. G. 2010. Association of STAT4 polymorphism with rheumatoid arthritis and systemic lupus erythematosus: a meta-analysis. *Mol Biol Rep,* 37**,** 141-7.

JIA, H., TAO, F., LIU, C., GUO, T., ZHU, W., WANG, S., CUI, B. & NING, G. 2015. Both interleukin-23A polymorphism and serum interlukin-23 expression are associated with Graves' disease risk. *Cell Immunol,* 294**,** 39-43.

JOHNSON, G. A., BENVENISTE, H., BLACK, R. D., HEDLUND, L. W., MARONPOT, R. R. & SMITH, B. R. 1993. Histology by magnetic resonance microscopy. *Magn Reson Q,* 9**,** 1-30.

JOHNSON, K. T., WIESWEG, B., SCHOTT, M., EHLERS, M., MULLER, M., MINICH, W. B., NAGAYAMA, Y., GULBINS, E., ECKSTEIN, A. K. & BERCHNER-PFANNSCHMIDT, U. 2013. Examination of orbital tissues in murine models of Graves' disease reveals expression of UCP-1 and the TSHR in retrobulbar adipose tissues. *Horm Metab Res,* 45**,** 401-7.

JONAS, H. A. & HARRISON, L. C. 1985. The human placenta contains two distinct binding and immunoreactive species of insulin-like growth factor-I receptors. *J Biol Chem,* 260**,** 2288-94.

JYONOUCHI, S. C., VALYASEVI, R. W., HARTENECK, D. A., DUTTON, C. M. & BAHN, R. S. 2001. Interleukin-6 stimulates thyrotropin receptor expression in human orbital preadipocyte fibroblasts from patients with Graves' ophthalmopathy. *Thyroid,* 11**,** 929-34.

KAHALY, G., DIAZ, M., HAHN, K., BEYER, J. & BOCKISCH, A. 1995a. Indium-111-pentetreotide scintigraphy in Graves' ophthalmopathy. *J Nucl Med,* 36**,** 550-4.

KAHALY, G., DIAZ, M., JUST, M., BEYER, J. & LIEB, W. 1995b. Role of octreoscan and correlation with MR imaging in Graves' ophthalmopathy. *Thyroid,* 5**,** 107-11.

KAHALY, G., GORGES, R., DIAZ, M., HOMMEL, G. & BOCKISCH, A. 1998. Indium-111-pentetreotide in Graves' disease. *J Nucl Med,* 39**,** 533-6.

KAHALY, G., HANSEN, C., FELKE, B. & DIENES, H. P. 1994. Immunohistochemical staining of retrobulbar adipose tissue in Graves' ophthalmopathy. *Clin Immunol Immunopathol,* 73**,** 53-62.

KAHALY, G. J. 1996. New imaging procedures in thyroid-associated ophthalmopathy. *Orbit,* 15**,** 165-175.

KAHALY, G. J. 2001. Imaging in thyroid-associated orbitopathy. *Eur J Endocrinol,* 145**,** 107-18.

KAHALY, G. J. 2004. Recent developments in Graves' ophthalmopathy imaging. *J Endocrinol Invest,* 27**,** 254-8.

KAHALY, G. J., PITZ, S., HOMMEL, G. & DITTMAR, M. 2005. Randomized, single blind trial of intravenous versus oral steroid monotherapy in Graves' orbitopathy. *J Clin Endocrinol Metab,* 90**,** 5234-40.

KAITHAMANA, S., FAN, J., OSUGA, Y., LIANG, S. G. & PRABHAKAR, B. S. 1999. Induction of experimental autoimmune Graves' disease in BALB/c mice. *J Immunol,* 163**,** 5157-64.

KAJITA, Y., RICKARDS, C. R., BUCKLAND, P. R., HOWELLS, R. D. & REES SMITH, B. 1985. Analysis of thyrotropin receptors by photoaffinity labelling. Orientation of receptor subunits in the cell membrane. *Biochem J,* 227**,** 413-20.

KANEDA, T., HONDA, A., HAKOZAKI, A., FUSE, T., MUTO, A. & YOSHIDA, T. 2007. An improved Graves' disease model established by using in vivo electroporation exhibited long-term immunity to hyperthyroidism in BALB/c mice. *Endocrinology,* 148**,** 2335-44.

KAVVOURA, F. K., AKAMIZU, T., AWATA, T., BAN, Y., CHISTIAKOV, D. A., FRYDECKA, I., GHADERI, A., GOUGH, S. C., HIROMATSU, Y., PLOSKI, R., WANG, P. W., BAN, Y., BEDNARCZUK, T., CHISTIAKOVA, E. I., CHOJM, M., HEWARD, J. M., HIRATANI, H., JUO, S. H., KARABON, L., KATAYAMA, S., KURIHARA, S., LIU, R. T., MIYAKE, I., OMRANI, G. H., PAWLAK, E., TANIYAMA, M., TOZAKI, T. & IOANNIDIS, J. P. 2007. Cytotoxic T-lymphocyte associated antigen 4 gene polymorphisms and autoimmune thyroid disease: a meta-analysis. *J Clin Endocrinol Metab,* 92**,** 3162-70.

KEMP, E. H., SANDHU, H. K., WATSON, P. F. & WEETMAN, A. P. 2013. Low frequency of pendrin autoantibodies detected using a radioligand binding assay in patients with autoimmune thyroid disease. *J Clin Endocrinol Metab,* 98**,** E309-13.

KEYMEULEN, B., VANDEMEULEBROUCKE, E., ZIEGLER, A. G., MATHIEU, C., KAUFMAN, L., HALE, G., GORUS, F., GOLDMAN, M., WALTER, M., CANDON, S., SCHANDENE, L., CRENIER, L., DE BLOCK, C., SEIGNEURIN, J. M., DE PAUW, P., PIERARD, D., WEETS, I., REBELLO, P., BIRD, P., BERRIE, E., FREWIN, M., WALDMANN, H., BACH, J. F., PIPELEERS, D. & CHATENOUD, L. 2005. Insulin needs after CD3-antibody therapy in new-onset type 1 diabetes. *N Engl J Med,* 352**,** 2598-608.

KHALILZADEH, O., ANVARI, M., ESTEGHAMATI, A., MAHMOUDI, M., TAHVILDARI, M., RASHIDI, A., KHOSRAVI, F. & AMIRZARGAR, A. 2009. Graves' ophthalmopathy and gene polymorphisms in interleukin-1alpha, interleukin-1beta, interleukin-1 receptor and interleukin-1 receptor antagonist. *Clin Experiment Ophthalmol,* 37**,** 614-9.

KHALILZADEH, O., ANVARI, M., ESTEGHAMATI, A., MOMEN-HERAVI, F., RASHIDI, A., AMIRI, H. M., TAHVILDARI, M., MAHMOUDI, M. & AMIRZARGAR, A. 2010. Genetic susceptibility to Graves' ophthalmopathy: The role of polymorphisms in anti-inflammatory cytokine genes. *Ophthalmic Genet,* 31**,** 215-20.

KHOO, T. K. & BAHN, R. S. 2007. Pathogenesis of Graves' ophthalmopathy: the role of autoantibodies. *Thyroid,* 17**,** 1013-8.

KIKUOKA, S., SHIMOJO, N., YAMAGUCHI, K. I., WATANABE, Y., HOSHIOKA, A., HIRAI, A., SAITO, Y., TAHARA, K., KOHN, L. D., MARUYAMA, N., KOHNO, Y. & NIIMI, H. 1998. The

formation of thyrotropin receptor (TSHR) antibodies in a Graves' animal model requires the N-terminal segment of the TSHR extracellular domain. *Endocrinology,* 139**,** 1891-8.

KIMBALL, L. E., KULINSKAYA, E., BROWN, B., JOHNSTON, C. & FARID, N. R. 2002. Does smoking increase relapse rates in Graves' disease? *J Endocrinol Invest,* 25**,** 152-7.

KIRSCH, E., VON ARX, G. & HAMMER, B. 2009. Imaging in Graves' orbitopathy. *Orbit,* 28**,** 219-25.

KIRSCH, E. C., KAIM, A. H., DE OLIVEIRA, M. G. & VON ARX, G. 2010. Correlation of signal intensity ratio on orbital MRI-TIRM and clinical activity score as a possible predictor of therapy response in Graves' orbitopathy--a pilot study at 1.5 T. *Neuroradiology,* 52**,** 91-7.

KITA, M., AHMAD, L., MARIANS, R. C., VLASE, H., UNGER, P., GRAVES, P. N. & DAVIES, T. F. 1999. Regulation and transfer of a murine model of thyrotropin receptor antibody mediated Graves' disease. *Endocrinology,* 140**,** 1392-8.

KOHLER, G. & MILSTEIN, C. 1975. Continuous cultures of fused cells secreting antibody of predefined specificity. *Nature,* 256**,** 495-7.

KOHN, L. D., ALVAREZ, F., MARCOCCI, C., KOHN, A. D., CORDA, D., HOFFMAN, W. E., TOMBACCINI, D., VALENTE, W. A., DE LUCA, M., SANTISTEBAN, P. & ET AL. 1986. Monoclonal antibody studies defining the origin and properties of autoantibodies in Graves' disease. *Ann N Y Acad Sci,* 475**,** 157-73.

KOUMAS, L., SMITH, T. J., FELDON, S., BLUMBERG, N. & PHIPPS, R. P. 2003. Thy-1 expression in human fibroblast subsets defines myofibroblastic or lipofibroblastic phenotypes. *Am J Pathol,* 163**,** 1291-300.

KOUMAS, L., SMITH, T. J. & PHIPPS, R. P. 2002. Fibroblast subsets in the human orbit: Thy-1+ and Thy-1- subpopulations exhibit distinct phenotypes. *Eur J Immunol,* 32**,** 477-85.

KRAIEM, Z., BARON, E., KAHANA, L., SADEH, O. & SHEINFELD, M. 1992. Changes in stimulating and blocking TSH receptor antibodies in a patient undergoing three cycles of transition from hypo to hyper-thyroidism and back to hypothyroidism. *Clin Endocrinol (Oxf),* 36**,** 211-4.

KRASSAS, G. E. & KAHALY, G. J. 1999. The role of octreoscan in thyroid eye disease. *Eur J Endocrinol,* 140**,** 373-5.

KRETOWSKI, A., WAWRUSIEWICZ, N., MIRONCZUK, K., MYSLIWIEC, J., KRETOWSKA, M. & KINALSKA, I. 2003. Intercellular adhesion molecule 1 gene polymorphisms in Graves' disease. *J Clin Endocrinol Metab,* 88**,** 4945-9.

KRISS, J. P., PLESHAKOV, V. & CHIEN, J. R. 1964. Isolation and Identification of the Long-Acting Thyroid Stimulator and Its Relation to Hyperthyroidism and Circumscribed Pretibial Myxedema. *J Clin Endocrinol Metab,* 24**,** 1005-28.

KRISS, J. P., PLESHAKOV, V., ROSENBLUM, A. L., HOLDERNESS, M., SHARP, G. & UTIGER, R. 1967. Studies on the pathogenesis of the ophthalmopathy of Graves' disease. *J Clin Endocrinol Metab,* 27**,** 582-93.

KUCHROO, V. K., OHASHI, P. S., SARTOR, R. B. & VINUESA, C. G. 2012. Dysregulation of immune homeostasis in autoimmune diseases. *Nat Med,* 18**,** 42-7.

KUMAR, S., COENEN, M. J., SCHERER, P. E. & BAHN, R. S. 2004. Evidence for enhanced adipogenesis in the orbits of patients with Graves' ophthalmopathy. *J Clin Endocrinol Metab,* 89**,** 930-5.

KUMAR, S., IYER, S., BAUER, H., COENEN, M. & BAHN, R. S. 2012. A stimulatory thyrotropin receptor antibody enhances hyaluronic Acid synthesis in graves' orbital fibroblasts: inhibition by an igf-I receptor blocking antibody. *J Clin Endocrinol Metab,* 97**,** 1681-7.

KUMAR, S., LEONTOVICH, A., COENEN, M. J. & BAHN, R. S. 2005. Gene expression profiling of orbital adipose tissue from patients with Graves' ophthalmopathy: a potential role for

secreted frizzled-related protein-1 in orbital adipogenesis. *J Clin Endocrinol Metab,* 90**,** 4730-5.

KUMAR, S., NADEEM, S., STAN, M. N., COENEN, M. & BAHN, R. S. 2011. A stimulatory TSH receptor antibody enhances adipogenesis via phosphoinositide 3-kinase activation in orbital preadipocytes from patients with Graves' ophthalmopathy. *J Mol Endocrinol,* 46**,** 155-63.

KUMAR, S., SCHIEFER, R., COENEN, M. J. & BAHN, R. S. 2010. A stimulatory thyrotropin receptor antibody (M22) and thyrotropin increase interleukin-6 expression and secretion in Graves' orbital preadipocyte fibroblasts. *Thyroid,* 20**,** 59-65.

KUNG, A. W. & JONES, B. M. 1998. A change from stimulatory to blocking antibody activity in Graves' disease during pregnancy. *J Clin Endocrinol Metab,* 83**,** 514-8.

KUNG, A. W., YAU, C. C. & CHENG, A. 1994. The incidence of ophthalmopathy after radioiodine therapy for Graves' disease: prognostic factors and the role of methimazole. *J Clin Endocrinol Metab,* 79**,** 542-6.

KURIYAN, A. E., WOELLER, C. F., O'LOUGHLIN, C. W., PHIPPS, R. P. & FELDON, S. E. 2013. Orbital fibroblasts from thyroid eye disease patients differ in proliferative and adipogenic responses depending on disease subtype. *Invest Ophthalmol Vis Sci,* 54**,** 7370-7.

KURMASHEVA, R. T. & HOUGHTON, P. J. 2006. IGF-I mediated survival pathways in normal and malignant cells. *Biochim Biophys Acta,* 1766**,** 1-22.

KUSADA, Y., MORIZONO, T., MATSUMOTO-TAKASAKI, A., SAKAI, K., SATO, S., ASANUMA, H., TAKAYANAGI, A. & FUJITA-YAMAGUCHI, Y. 2008. Construction and characterization of single-chain antibodies against human insulin-like growth factor-I receptor from hybridomas producing 1H7 or 3B7 monoclonal antibody. *J Biochem,* 143**,** 9-19.

KVETNY, J., PUHAKKA, K. B. & ROHL, L. 2006. Magnetic resonance imaging determination of extraocular eye muscle volume in patients with thyroid-associated ophthalmopathy and proptosis. *Acta Ophthalmol Scand,* 84**,** 419-23.

LAHOOTI, H., PARMAR, K. R. & WALL, J. R. 2010. Pathogenesis of thyroid-associated ophthalmopathy: does autoimmunity against calsequestrin and collagen XIII play a role? *Clin Ophthalmol,* 4**,** 417-25.

LAND, K. J., GUDAPATI, P., KAPLAN, M. H. & SEETHARAMAIAH, G. S. 2006. Differential requirement of signal transducer and activator of transcription-4 (Stat4) and Stat6 in a thyrotropin receptor-289-adenovirus-induced model of Graves' hyperthyroidism. *Endocrinology,* 147**,** 111-9.

LANTZ, M., VONDRICHOVA, T., PARIKH, H., FRENANDER, C., RIDDERSTRALE, M., ASMAN, P., ABERG, M., GROOP, L. & HALLENGREN, B. 2005. Overexpression of immediate early genes in active Graves' ophthalmopathy. *J Clin Endocrinol Metab,* 90**,** 4784-91.

LAUER, S. A., SILKISS, R. Z. & MCCORMICK, S. A. 2008. Oral montelukast and cetirizine for thyroid eye disease. *Ophthal Plast Reconstr Surg,* 24**,** 257-61.

LAURBERG, P., CERQUEIRA, C., OVESEN, L., RASMUSSEN, L. B., PERRILD, H., ANDERSEN, S., PEDERSEN, I. B. & CARLE, A. 2010. Iodine intake as a determinant of thyroid disorders in populations. *Best Pract Res Clin Endocrinol Metab,* 24**,** 13-27.

LAURBERG, P., NOHR, S. B., PEDERSEN, K. M., HREIDARSSON, A. B., ANDERSEN, S., BULOW PEDERSEN, I., KNUDSEN, N., PERRILD, H., JORGENSEN, T. & OVESEN, L. 2000. Thyroid disorders in mild iodine deficiency. *Thyroid,* 10**,** 951-63.

LEE, Y. K., MUKASA, R., HATTON, R. D. & WEAVER, C. T. 2009. Developmental plasticity of Th17 and Treg cells. *Curr Opin Immunol,* 21**,** 274-80.

LEHMANN, G. M., FELDON, S. E., SMITH, T. J. & PHIPPS, R. P. 2008. Immune mechanisms in thyroid eye disease. *Thyroid,* 18**,** 959-65.

LEHMANN, P. V., FORSTHUBER, T., MILLER, A. & SERCARZ, E. E. 1992. Spreading of T-cell autoimmunity to cryptic determinants of an autoantigen. *Nature,* 358**,** 155-7.

LEVY-SHRAGA, Y., TAMIR-HOSTOVSKY, L., BOYKO, V., LERNER-GEVA, L. & PINHAS-HAMIEL, O. 2014. Follow-Up of Newborns of Mothers with Graves' Disease. *Thyroid*.

LI, H., FITCHETT, C., KOZDON, K., JAYARAM, H., ROSE, G. E., BAILLY, M. & EZRA, D. G. 2014. Independent adipogenic and contractile properties of fibroblasts in Graves' orbitopathy: an in vitro model for the evaluation of treatments. *PLoS One,* 9**,** e95586.

LI, H. S. & CARAYANNIOTIS, G. 2007. Induction of goitrous hypothyroidism by dietary iodide in SJL mice. *Endocrinology,* 148**,** 2747-52.

LI, M. O., WAN, Y. Y. & FLAVELL, R. A. 2007. T cell-produced transforming growth factor-beta1 controls T cell tolerance and regulates Th1- and Th17-cell differentiation. *Immunity,* 26**,** 579-91.

LIANG, S. C., TAN, X. Y., LUXENBERG, D. P., KARIM, R., DUNUSSI-JOANNOPOULOS, K., COLLINS, M. & FOUSER, L. A. 2006. Interleukin (IL)-22 and IL-17 are coexpressed by Th17 cells and cooperatively enhance expression of antimicrobial peptides. *J Exp Med,* 203**,** 2271-9.

LIAO, W. L., CHEN, R. H., LIN, H. J., LIU, Y. H., CHEN, W. C., TSAI, Y., WAN, L. & TSAI, F. J. 2010. Toll-like receptor gene polymorphisms are associated with susceptibility to Graves' ophthalmopathy in Taiwan males. *BMC Med Genet,* 11**,** 154.

LIAO, W. L., CHEN, R. H., LIN, H. J., LIU, Y. H., CHEN, W. C., TSAI, Y., WAN, L. & TSAI, F. J. 2011. The association between polymorphisms of B7 molecules (CD80 and CD86) and Graves' ophthalmopathy in a Taiwanese population. *Ophthalmology,* 118**,** 553-7.

LIBERT, F., LEFORT, A., GERARD, C., PARMENTIER, M., PERRET, J., LUDGATE, M., DUMONT, J. E. & VASSART, G. 1989. Cloning, sequencing and expression of the human thyrotropin (TSH) receptor: evidence for binding of autoantibodies. *Biochem Biophys Res Commun,* 165**,** 1250-5.

LIDMAN, K., ERIKSSON, U., FAGRAEUS, A. & NORBERG, R. 1974. Letter: Antibodies against thyroid cells in Yersinia enterocolitica infection. *Lancet,* 2**,** 1449.

LIN, T. H., CHIANG, C. W., TRINKAUS, K., SPEES, W. M., SUN, P. & SONG, S. K. 2014. Manganese-enhanced MRI (MEMRI) via topical loading of Mn significantly impairs mouse visual acuity: a comparison with intravitreal injection. *NMR Biomed*.

LINDSEY, J. D., SCADENG, M., DUBOWITZ, D. J., CROWSTON, J. G. & WEINREB, R. N. 2007. Magnetic resonance imaging of the visual system in vivo: transsynaptic illumination of V1 and V2 visual cortex. *Neuroimage,* 34**,** 1619-26.

LO, S. S., TUN, R. Y., HAWA, M. & LESLIE, R. D. 1991. Studies of diabetic twins. *Diabetes Metab Rev,* 7**,** 223-38.

LOOSFELT, H., PICHON, C., JOLIVET, A., MISRAHI, M., CAILLOU, B., JAMOUS, M., VANNIER, B. & MILGROM, E. 1992. Two-subunit structure of the human thyrotropin receptor. *Proc Natl Acad Sci U S A,* 89**,** 3765-9.

LU, R., BURMAN, K. D. & JONKLAAS, J. 2005. Transient Graves' hyperthyroidism during pregnancy in a patient with Hashimoto's hypothyroidism. *Thyroid,* 15**,** 725-9.

LUDGATE, M. 2000. Animal models of Graves' disease. *Eur J Endocrinol,* 142**,** 1-8.

LUTTRELL, L. M., VAN BIESEN, T., HAWES, B. E., KOCH, W. J., TOUHARA, K. & LEFKOWITZ, R. J. 1995. G beta gamma subunits mediate mitogen-activated protein kinase activation by the tyrosine kinase insulin-like growth factor 1 receptor. *J Biol Chem,* 270**,** 16495-8.

LYTTON, S. D. & KAHALY, G. J. 2010. Bioassays for TSH-receptor autoantibodies: an update. *Autoimmun Rev,* 10**,** 116-22.

MACLENNAN, A. C. 1995. Radiation dose to the lens from CT brain scans in general radiology departments. *Br J Radiol,* 68**,** 219.

MACLENNAN, A. C. & HADLEY, D. M. 1995. Radiation dose to the lens from computed tomography scanning in a neuroradiology department. *Br J Radiol,* 68**,** 19-22.

MADDUR, M. S., MIOSSEC, P., KAVERI, S. V. & BAYRY, J. 2012. Th17 cells: biology, pathogenesis of autoimmune and inflammatory diseases, and therapeutic strategies. *Am J Pathol,* 181**,** 8-18.

MAJOS, A., PAJAK, M., GRZELAK, P. & STEFANCZYK, L. 2007. Magnetic Resonance evaluation of disease activity in Graves' ophthalmopathy: T2-time and signal intensity of extraocular muscles. *Med Sci Monit,* 13 Suppl 1**,** 44-8.

MANGALAM, A. K., TANEJA, V. & DAVID, C. S. 2013. HLA class II molecules influence susceptibility versus protection in inflammatory diseases by determining the cytokine profile. *J Immunol,* 190**,** 513-8.

MANGAN, P. R., HARRINGTON, L. E., O'QUINN, D. B., HELMS, W. S., BULLARD, D. C., ELSON, C. O., HATTON, R. D., WAHL, S. M., SCHOEB, T. R. & WEAVER, C. T. 2006. Transforming growth factor-beta induces development of the T(H)17 lineage. *Nature,* 441**,** 231-4.

MANLEY, S. W., BOURKE, J. R. & HAWKER, R. W. 1974. The thyrotrophin receptor in guinea-pig thyroid homogenate: interaction with the long-acting thyroid stimulator. *J Endocrinol,* 61**,** 437-45.

MANY, M.-C., COSTAGLIOLA, S., DETRAIT, M., DENEF, J.-F., VASSART, G. & LUDGATE, M. 1999. Development of an Animal Model of Autoimmune Thyroid Eye Disease. *The Journal of Immunology,* 162**,** 4966-4974.

MAO, C., WANG, S., XIAO, Y., XU, J., JIANG, Q., JIN, M., JIANG, X., GUO, H., NING, G. & ZHANG, Y. 2011. Impairment of regulatory capacity of CD4+CD25+ regulatory T cells mediated by dendritic cell polarization and hyperthyroidism in Graves' disease. *J Immunol,* 186**,** 4734-43.

MARAZUELA, M., GARCIA-LOPEZ, M. A., FIGUEROA-VEGA, N., DE LA FUENTE, H., ALVARADO-SANCHEZ, B., MONSIVAIS-URENDA, A., SANCHEZ-MADRID, F. & GONZALEZ-AMARO, R. 2006. Regulatory T cells in human autoimmune thyroid disease. *J Clin Endocrinol Metab,* 91**,** 3639-46.

MARCOCCI, C., BARTALENA, L., BOGAZZI, F., BRUNO-BOSSIO, G., LEPRI, A. & PINCHERA, A. 1991. Orbital radiotherapy combined with high dose systemic glucocorticoids for Graves' ophthalmopathy is more effective than radiotherapy alone: results of a prospective randomized study. *J Endocrinol Invest,* 14**,** 853-60.

MARCOCCI, C., BARTALENA, L., PANICUCCI, M., MARCONCINI, C., CARTEI, F., CAVALLACCI, G., LADDAGA, M., CAMPOBASSO, G., BASCHIERI, L. & PINCHERA, A. 1987. Orbital cobalt irradiation combined with retrobulbar or systemic corticosteroids for Graves' ophthalmopathy: a comparative study. *Clin Endocrinol (Oxf),* 27**,** 33-42.

MARCOCCI, C., BARTALENA, L., ROCCHI, R., MARINO, M., MENCONI, F., MORABITO, E., MAZZI, B., MAZZEO, S., SARTINI, M. S., NARDI, M., CARTEI, F., CIONINI, L. & PINCHERA, A. 2003. Long-term safety of orbital radiotherapy for Graves' ophthalmopathy. *J Clin Endocrinol Metab,* 88**,** 3561-6.

MARCOCCI, C., BARTALENA, L., TANDA, M. L., MANETTI, L., DELL'UNTO, E., ROCCHI, R., BARBESINO, G., MAZZI, B., BARTOLOMEI, M. P., LEPRI, P., CARTEI, F., NARDI, M. & PINCHERA, A. 2001. Comparison of the effectiveness and tolerability of intravenous or oral glucocorticoids associated with orbital radiotherapy in the management of severe Graves' ophthalmopathy: results of a prospective, single-blind, randomized study. *J Clin Endocrinol Metab,* 86**,** 3562-7.

MARCOCCI, C., KAHALY, G. J., KRASSAS, G. E., BARTALENA, L., PRUMMEL, M., STAHL, M., ALTEA, M. A., NARDI, M., PITZ, S., BOBORIDIS, K., SIVELLI, P., VON ARX, G., MOURITS, M. P., BALDESCHI, L., BENCIVELLI, W., WIERSINGA, W. & EUROPEAN GROUP ON GRAVES, O. 2011. Selenium and the course of mild Graves' orbitopathy. *N Engl J Med,* 364**,** 1920-31.

MARINO, M., MORABITO, E., BRUNETTO, M. R., BARTALENA, L., PINCHERA, A. & MAROCCI, C. 2004. Acute and severe liver damage associated with intravenous glucocorticoid pulse therapy in patients with Graves' ophthalmopathy. *Thyroid,* 14**,** 403-6.

MARION, S., BRAUN, J. M., ROPARS, A., KOHN, L. D. & CHARREIRE, J. 1994. Induction of autoimmunity by immunization of mice with human thyrotropin receptor. *Cell Immunol,* 158**,** 329-41.

MARQUEZ, S. D., LUM, B. L., MCDOUGALL, I. R., KATKURI, S., LEVIN, P. S., MACMANUS, M. & DONALDSON, S. S. 2001. Long-term results of irradiation for patients with progressive Graves' ophthalmopathy. *Int J Radiat Oncol Biol Phys,* 51**,** 766-74.

MARTIN, A., NAKASHIMA, M., ZHOU, A., ARONSON, D., WERNER, A. J. & DAVIES, T. F. 1997. Detection of major T cell epitopes on human thyroid stimulating hormone receptor by overriding immune heterogeneity in patients with Graves' disease. *J Clin Endocrinol Metab,* 82**,** 3361-6.

MCBEATH, R., PIRONE, D. M., NELSON, C. M., BHADRIRAJU, K. & CHEN, C. S. 2004. Cell shape, cytoskeletal tension, and RhoA regulate stem cell lineage commitment. *Dev Cell,* 6**,** 483-95.

MCCORQUODALE, T., LAHOOTI, H., GOPINATH, B. & WALL, J. R. 2012. Long-term follow-up of seven patients with ophthalmopathy not associated with thyroid autoimmunity: heterogeneity of autoimmune ophthalmopathy. *Clin Ophthalmol,* 6**,** 1063-71.

MCKENZIE, J. 1958. Delayed thyroid response to serum from thyrotoxic patients. *Endocrinology,* 62**,** 865-8.

MCKENZIE, J. M. 1962. Fractionation of plasma containing the long acting thyroid stimulator. *J Biol Chem,* 237**,** 3571-2.

MCLACHLAN, S. M., ALIESKY, H. A., CHEN, C. R. & RAPOPORT, B. 2012. Role of self-tolerance and chronic stimulation in the long-term persistence of adenovirus-induced thyrotropin receptor antibodies in wild-type and transgenic mice. *Thyroid,* 22**,** 931-7.

MCLACHLAN, S. M., ALPI, K. & RAPOPORT, B. 2011. Review and hypothesis: does Graves' disease develop in non-human great apes? *Thyroid,* 21**,** 1359-66.

MCLACHLAN, S. M., NAGAYAMA, Y. & RAPOPORT, B. 2005. Insight into Graves' hyperthyroidism from animal models. *Endocr Rev,* 26**,** 800-32.

MCLACHLAN, S. M. & RAPOPORT, B. 2004. Thyroid stimulating monoclonal antibodies: overcoming the road blocks and the way forward. *Clin Endocrinol (Oxf),* 61**,** 10-8.

MCLACHLAN, S. M. & RAPOPORT, B. 2013. Thyrotropin-blocking autoantibodies and thyroid-stimulating autoantibodies: potential mechanisms involved in the pendulum swinging from hypothyroidism to hyperthyroidism or vice versa. *Thyroid,* 23**,** 14-24.

MCLACHLAN, S. M. & RAPOPORT, B. 2014. Breaking tolerance to thyroid antigens: changing concepts in thyroid autoimmunity. *Endocr Rev,* 35**,** 59-105.

MEDICI, M., PORCU, E., PISTIS, G., TEUMER, A., BROWN, S. J., JENSEN, R. A., RAWAL, R., ROEF, G. L., PLANTINGA, T. S., VERMEULEN, S. H., LAHTI, J., SIMMONDS, M. J., HUSEMOEN, L. L., FREATHY, R. M., SHIELDS, B. M., PIETZNER, D., NAGY, R., BROER, L., CHAKER, L., KOREVAAR, T. I., PLIA, M. G., SALA, C., VOLKER, U., RICHARDS, J. B., SWEEP, F. C., GIEGER, C., CORRE, T., KAJANTIE, E., THUESEN, B., TAES, Y. E., VISSER, W. E., HATTERSLEY, A. T., KRATZSCH, J., HAMILTON, A., LI, W., HOMUTH, G., LOBINA, M., MARIOTTI, S., SORANZO, N., COCCA, M., NAUCK, M., SPIELHAGEN, C., ROSS, A., ARNOLD, A., VAN DE BUNT, M., LIYANARACHCHI, S., HEIER, M., GRABE, H. J., MASCIULLO, C., GALESLOOT, T. E., LIM, E. M., REISCHL, E., LEEDMAN, P. J., LAI, S., DELITALA, A., BREMNER, A. P., PHILIPS, D. I., BEILBY, J. P., MULAS, A., VOCALE, M., ABECASIS, G., FORSEN, T., JAMES, A., WIDEN, E., HUI, J., PROKISCH, H., RIETZSCHEL, E. E., PALOTIE, A., FEDDEMA, P., FLETCHER, S. J., SCHRAMM, K., ROTTER, J. I., KLUTTIG, A., RADKE, D., TRAGLIA, M., SURDULESCU, G. L., HE, H., FRANKLYN, J. A., TILLER, D., VAIDYA, B., DE MEYER, T., JORGENSEN, T., ERIKSSON, J. G., O'LEARY, P. C., WICHMANN,

E., HERMUS, A. R., PSATY, B. M., ITTERMANN, T., HOFMAN, A., BOSI, E., SCHLESSINGER, D., WALLASCHOFSKI, H., PIRASTU, N., AULCHENKO, Y. S., DE LA CHAPELLE, A., NETEA-MAIER, R. T., GOUGH, S. C., MEYER ZU SCHWABEDISSEN, H., FRAYLING, T. M., KAUFMAN, J. M., et al. 2014. Identification of novel genetic Loci associated with thyroid peroxidase antibodies and clinical thyroid disease. *PLoS Genet,* 10**,** e1004123.

MEHDI, S. Q. & NUSSEY, S. S. 1975. A radio-ligand receptor assay for the long-acting thyroid stimulator. Inhibition by the long-acting thyroid stimulator of the binding of radioiodinated thyroid-stimulating hormone to human thyroid membranes. *Biochem J,* 145**,** 105-11.

MENCONI, F., HASHAM, A. & TOMER, Y. 2011. Environmental triggers of thyroiditis: hepatitis C and interferon-alpha. *J Endocrinol Invest,* 34**,** 78-84.

MENCONI, F., MONTI, M. C., GREENBERG, D. A., OASHI, T., OSMAN, R., DAVIES, T. F., BAN, Y., JACOBSON, E. M., CONCEPCION, E. S., LI, C. W. & TOMER, Y. 2008. Molecular amino acid signatures in the MHC class II peptide-binding pocket predispose to autoimmune thyroiditis in humans and in mice. *Proc Natl Acad Sci U S A,* 105**,** 14034-9.

MENCONI, F., OSMAN, R., MONTI, M. C., GREENBERG, D. A., CONCEPCION, E. S. & TOMER, Y. 2010. Shared molecular amino acid signature in the HLA-DR peptide binding pocket predisposes to both autoimmune diabetes and thyroiditis. *Proc Natl Acad Sci U S A,* 107**,** 16899-903.

MENCONI, F., PROFILO, M. A., LEO, M., SISTI, E., ALTEA, M. A., ROCCHI, R., LATROFA, F., NARDI, M., VITTI, P., MARCOCCI, C. & MARINO, M. 2014. Spontaneous improvement of untreated mild graves' ophthalmopathy: Rundle's curve revisited. *Thyroid,* 24**,** 60-6.

MENGISTU, M., LUKES, Y. G., NAGY, E. V., BURCH, H. B., CARR, F. E., LAHIRI, S. & BURMAN, K. D. 1994. TSH receptor gene expression in retroocular fibroblasts. *J Endocrinol Invest,* 17**,** 437-41.

METCALFE, R., JORDAN, N., WATSON, P., GULLU, S., WILTSHIRE, M., CRISP, M., EVANS, C., WEETMAN, A. & LUDGATE, M. 2002. Demonstration of immunoglobulin G, A, and E autoantibodies to the human thyrotropin receptor using flow cytometry. *J Clin Endocrinol Metab,* 87**,** 1754-61.

MILLER, F. W., POLLARD, K. M., PARKS, C. G., GERMOLEC, D. R., LEUNG, P. S., SELMI, C., HUMBLE, M. C. & ROSE, N. R. 2012. Criteria for environmentally associated autoimmune diseases. *J Autoimmun,* 39**,** 253-8.

MILLS, K. H. 2011. TLR-dependent T cell activation in autoimmunity. *Nat Rev Immunol,* 11**,** 807-22.

MINICH, W. B., DEHINA, N., WELSINK, T., SCHWIEBERT, C., MORGENTHALER, N. G., KOHRLE, J., ECKSTEIN, A. & SCHOMBURG, L. 2013. Autoantibodies to the IGF1 receptor in Graves' orbitopathy. *J Clin Endocrinol Metab,* 98**,** 752-60.

MINUTO, F., BARRECA, A., DEL MONTE, P., CARIOLA, G., TORRE, G. C. & GIORDANO, G. 1989. Immunoreactive insulin-like growth factor I (IGF-I) and IGF-I-binding protein content in human thyroid tissue. *J Clin Endocrinol Metab,* 68**,** 621-6.

MIOSSEC, P., KORN, T. & KUCHROO, V. K. 2009. Interleukin-17 and type 17 helper T cells. *N Engl J Med,* 361**,** 888-98.

MISRAHI, M., GHINEA, N., SAR, S., SAUNIER, B., JOLIVET, A., LOOSFELT, H., CERUTTI, M., DEVAUCHELLE, G. & MILGROM, E. 1994. Processing of the precursors of the human thyroid-stimulating hormone receptor in various eukaryotic cells (human thyrocytes, transfected L cells and baculovirus-infected insect cells). *Eur J Biochem,* 222**,** 711-9.

MISRAHI, M., LOOSFELT, H., ATGER, M., SAR, S., GUIOCHON-MANTEL, A. & MILGROM, E. 1990. Cloning, sequencing and expression of human TSH receptor. *Biochem Biophys Res Commun,* 166**,** 394-403.

MIZOKAMI, T., SALVI, M. & WALL, J. R. 2004. Eye muscle antibodies in Graves' ophthalmopathy: pathogenic or secondary epiphenomenon? *J Endocrinol Invest,* 27**,** 221-9.

MIZUTORI, Y., CHEN, C. R., LATROFA, F., MCLACHLAN, S. M. & RAPOPORT, B. 2009. Evidence that shed thyrotropin receptor A subunits drive affinity maturation of autoantibodies causing Graves' disease. *J Clin Endocrinol Metab,* 94**,** 927-35.

MIZUTORI, Y., SAITOH, O., EGUCHI, K. & NAGAYAMA, Y. 2006. Adenovirus encoding the thyrotropin receptor A-subunit improves the efficacy of dendritic cell-induced Graves' hyperthyroidism in mice. *J Autoimmun,* 26**,** 32-6.

MOELLER, A., GILPIN, S. E., ASK, K., COX, G., COOK, D., GAULDIE, J., MARGETTS, P. J., FARKAS, L., DOBRANOWSKI, J., BOYLAN, C., O'BYRNE, P. M., STRIETER, R. M. & KOLB, M. 2009. Circulating fibrocytes are an indicator of poor prognosis in idiopathic pulmonary fibrosis. *Am J Respir Crit Care Med,* 179**,** 588-94.

MOLNAR, I., HORVATH, S. & BALAZS, C. 1996. Detectable serum IgE levels in Graves' ophthalmopathy. *Eur J Med Res,* 1**,** 543-6.

MORSHED, S. A., ANDO, T., LATIF, R. & DAVIES, T. F. 2010. Neutral antibodies to the TSH receptor are present in Graves' disease and regulate selective signaling cascades. *Endocrinology,* 151**,** 5537-49.

MORSHED, S. A., LATIF, R. & DAVIES, T. F. 2009. Characterization of thyrotropin receptor antibody-induced signaling cascades. *Endocrinology,* 150**,** 519-29.

MORSHED, S. A., LATIF, R. & DAVIES, T. F. 2012. Delineating the autoimmune mechanisms in Graves' disease. *Immunol Res,* 54**,** 191-203.

MOSHKELGOSHA, S., SO, P. W., DEASY, N., DIAZ-CANO, S. & BANGA, J. P. 2013. Cutting Edge: Retrobulbar Inflammation, Adipogenesis, and Acute Orbital Congestion in a Preclinical Female Mouse Model of Graves' Orbitopathy Induced by Thyrotropin Receptor Plasmid-in Vivo Electroporation. *Endocrinology,* 154**,** 3008-15.

MUIR, E. R. & DUONG, T. Q. 2011. MRI of retinal and choroidal blood flow with laminar resolution. *NMR Biomed,* 24**,** 216-23.

MULLER-FORELL, W. & KAHALY, G. J. 2012. Neuroimaging of Graves' orbitopathy. *Best Pract Res Clin Endocrinol Metab,* 26**,** 259-71.

MULLER-FORELL, W., PITZ, S., MANN, W. & KAHALY, G. J. 1999. Neuroradiological diagnosis in thyroid-associated orbitopathy. *Exp Clin Endocrinol Diabetes,* 107 Suppl 5**,** S177-83.

MULLIN, B. R., LEE, G., LEDLEY, F. D., WINLAND, R. J. & KOHN, L. D. 1976. Thyrotropin interactions with human fat cell membrane preparations and the finding of soluble thyrotropin binding component. *Biochem Biophys Res Commun,* 69**,** 55-62.

MURPHY, K. M. & STOCKINGER, B. 2010. Effector T cell plasticity: flexibility in the face of changing circumstances. *Nat Immunol,* 11**,** 674-80.

NAGAYAMA, Y. 2005. Animal models of Graves' hyperthyroidism. *Endocr J,* 52**,** 385-94.

NAGAYAMA, Y., HORIE, I., SAITOH, O., NAKAHARA, M. & ABIRU, N. 2007. CD4+CD25+ naturally occurring regulatory T cells and not lymphopenia play a role in the pathogenesis of iodide-induced autoimmune thyroiditis in NOD-H2h4 mice. *J Autoimmun,* 29**,** 195-202.

NAGAYAMA, Y., KITA-FURUYAMA, M., ANDO, T., NAKAO, K., MIZUGUCHI, H., HAYAKAWA, T., EGUCHI, K. & NIWA, M. 2002. A novel murine model of Graves' hyperthyroidism with intramuscular injection of adenovirus expressing the thyrotropin receptor. *J Immunol,* 168**,** 2789-94.

NAIK, V. M., NAIK, M. N., GOLDBERG, R. A., SMITH, T. J. & DOUGLAS, R. S. 2010. Immunopathogenesis of thyroid eye disease: emerging paradigms. *Surv Ophthalmol,* 55**,** 215-26.

NAKAHARA, M., JOHNSON, K., ECKSTEIN, A., TAGUCHI, R., YAMADA, M., ABIRU, N. & NAGAYAMA, Y. 2012. Adoptive transfer of antithyrotropin receptor (TSHR)

autoimmunity from TSHR knockout mice to athymic nude mice. *Endocrinology,* 153**,** 2034-42.

NAKAHARA, M., MITSUTAKE, N., SAKAMOTO, H., CHEN, C. R., RAPOPORT, B., MCLACHLAN, S. M. & NAGAYAMA, Y. 2010. Enhanced response to mouse thyroid-stimulating hormone (TSH) receptor immunization in TSH receptor-knockout mice. *Endocrinology,* 151**,** 4047-54.

NAKAMURA, Y., WATANABE, M., MATSUZUKA, F., MARUOKA, H., MIYAUCHI, A. & IWATANI, Y. 2004. Intrathyroidal CD4+ T lymphocytes express high levels of Fas and CD4+ CD8+ macrophages/dendritic cells express Fas ligand in autoimmune thyroid disease. *Thyroid,* 14**,** 819-24.

NEUMANN, S., ELISEEVA, E., MCCOY, J. G., NAPOLITANO, G., GIULIANI, C., MONACO, F., HUANG, W. & GERSHENGORN, M. C. 2011. A new small-molecule antagonist inhibits Graves' disease antibody activation of the TSH receptor. *J Clin Endocrinol Metab,* 96**,** 548-54.

NEUMANN, S., NIR, E. A., ELISEEVA, E., HUANG, W., MARUGAN, J., XIAO, J., DULCEY, A. E. & GERSHENGORN, M. C. 2014. A selective TSH receptor antagonist inhibits stimulation of thyroid function in female mice. *Endocrinology,* 155**,** 310-4.

NG, C. M., YUEN, H. K., CHOI, K. L., CHAN, M. K., YUEN, K. T., NG, Y. W. & TIU, S. C. 2005. Combined orbital irradiation and systemic steroids compared with systemic steroids alone in the management of moderate-to-severe Graves' ophthalmopathy: a preliminary study. *Hong Kong Med J,* 11**,** 322-30.

NISHIMOTO, N. & KISHIMOTO, T. 2006. Interleukin 6: from bench to bedside. *Nat Clin Pract Rheumatol,* 2**,** 619-26.

NIU, Q., HUANG, Z. C., CAI, B., WANG, L. L. & FENG, W. H. 2010. [Study on ratio imbalance of peripheral blood Th17/Treg cells in patients with rheumatoid arthritis]. *Xi Bao Yu Fen Zi Mian Yi Xue Za Zhi,* 26**,** 267-9, 272.

NUNEZ MIGUEL, R., SANDERS, J., CHIRGADZE, D. Y., FURMANIAK, J. & REES SMITH, B. 2009. Thyroid stimulating autoantibody M22 mimics TSH binding to the TSH receptor leucine rich domain: a comparative structural study of protein-protein interactions. *J Mol Endocrinol,* 42**,** 381-95.

NYSTROM, H. F., JANSSON, S. & BERG, G. 2013. Incidence rate and clinical features of hyperthyroidism in a long-term iodine sufficient area of Sweden (Gothenburg) 2003-2005. *Clin Endocrinol (Oxf),* 78**,** 768-76.

ODA, Y., SANDERS, J., EVANS, M., KIDDIE, A., MUNKLEY, A., JAMES, C., RICHARDS, T., WILLS, J., FURMANIAK, J. & SMITH, B. R. 2000. Epitope analysis of the human thyrotropin (TSH) receptor using monoclonal antibodies. *Thyroid,* 10**,** 1051-9.

OHKURA, N. & SAKAGUCHI, S. 2010. Regulatory T cells: roles of T cell receptor for their development and function. *Semin Immunopathol,* 32**,** 95-106.

OHNESORGE, B., FLOHR, T., SCHALLER, S., KLINGENBECK-REGN, K., BECKER, C., SCHOPF, U. J., BRUNING, R. & REISER, M. F. 1999. [The technical bases and uses of multi-slice CT]. *Radiologe,* 39**,** 923-31.

ORGIAZZI, J. & LUDGATE, M. 2010. Pathogenesis. *In:* WIERSINGA, W. M. & KAHALY, G. J. (eds.) *Graves' orbitopathy: a multidisciplinary apptoach* Karger.

OTTO, E. A., OCHS, K., HANSEN, C., WALL, J. R. & KAHALY, G. J. 1996. Orbital tissue-derived T lymphocytes from patients with Graves' ophthalmopathy recognize autologous orbital antigens. *J Clin Endocrinol Metab,* 81**,** 3045-50.

OWENS, G. P. & BENNETT, J. L. 2012. Trigger, pathogen, or bystander: the complex nexus linking Epstein- Barr virus and multiple sclerosis. *Mult Scler,* 18**,** 1204-8.

PACHTER, B. R., DAVIDOWITZ, J. & BREININ, G. M. 1976. Morphological fiber types of retractor bulbi muscle in mouse and rat. *Invest Ophthalmol,* 15**,** 654-7.

PADOA, C. J., LARSEN, S. L., HAMPE, C. S., GILBERT, J. A., DAGDAN, E., HEGEDUS, L., DUNN-WALTERS, D. & BANGA, J. P. 2010. Clonal relationships between thyroid-stimulating hormone receptor-stimulating antibodies illustrate the effect of hypermutation on antibody function. *Immunology,* 129**,** 300-308.

PAN, D., SHIN, Y. H., GOPALAKRISHNAN, G., HENNESSEY, J. & DE GROOT, L. J. 2009. Regulatory T cells in Graves' disease. *Clin Endocrinol (Oxf),* 71**,** 587-93.

PAPANASTASIOU, L., VATALAS, I. A., KOUTRAS, D. A. & MASTORAKOS, G. 2007. Thyroid autoimmunity in the current iodine environment. *Thyroid,* 17**,** 729-39.

PAPPA, A., LAWSON, J. M., CALDER, V., FELLS, P. & LIGHTMAN, S. 2000. T cells and fibroblasts in affected extraocular muscles in early and late thyroid associated ophthalmopathy. *Br J Ophthalmol,* 84**,** 517-22.

PARIDAENS, D., VAN DEN BOSCH, W. A., VAN DER LOOS, T. L., KRENNING, E. P. & VAN HAGEN, P. M. 2005. The effect of etanercept on Graves' ophthalmopathy: a pilot study. *Eye (Lond),* 19**,** 1286-9.

PARK, E. S., KIM, H., SUH, J. M., PARK, S. J., KWON, O. Y., KIM, Y. K., RO, H. K., CHO, B. Y., CHUNG, J. & SHONG, M. 2000a. Thyrotropin induces SOCS-1 (suppressor of cytokine signaling-1) and SOCS-3 in FRTL-5 thyroid cells. *Mol Endocrinol,* 14**,** 440-8.

PARK, E. S., KIM, H., SUH, J. M., PARK, S. J., YOU, S. H., CHUNG, H. K., LEE, K. W., KWON, O. Y., CHO, B. Y., KIM, Y. K., RO, H. K., CHUNG, J. & SHONG, M. 2000b. Involvement of JAK/STAT (Janus kinase/signal transducer and activator of transcription) in the thyrotropin signaling pathway. *Mol Endocrinol,* 14**,** 662-70.

PARK, Y. J., KIM, T. Y., LEE, S. H., KIM, H., KIM, S. W., SHONG, M., YOON, Y. K., CHO, B. Y. & PARK, D. J. 2005. p66Shc expression in proliferating thyroid cells is regulated by thyrotropin receptor signaling. *Endocrinology,* 146**,** 2473-80.

PASCHKE, R., METCALFE, A., ALCALDE, L., VASSART, G., WEETMAN, A. & LUDGATE, M. 1994. Presence of nonfunctional thyrotropin receptor variant transcripts in retroocular and other tissues. *J Clin Endocrinol Metab,* 79**,** 1234-8.

PATERSON, J. A. & KAISERMAN-ABRAMOF, I. R. 1981. The oculomotor nucleus and extraocular muscles in a mutant anophthalmic mouse. *Anat Rec,* 200**,** 239-51.

PATIBANDLA, S. A., DALLAS, J. S., SEETHARAMAIAH, G. S., TAHARA, K., KOHN, L. D. & PRABHAKAR, B. S. 1997. Flow cytometric analyses of antibody binding to Chinese hamster ovary cells expressing human thyrotropin receptor. *J Clin Endocrinol Metab,* 82**,** 1885-93.

PEDERSEN, I. B., LAURBERG, P., KNUDSEN, N., JORGENSEN, T., PERRILD, H., OVESEN, L. & RASMUSSEN, L. B. 2008. Smoking is negatively associated with the presence of thyroglobulin autoantibody and to a lesser degree with thyroid peroxidase autoantibody in serum: a population study. *Eur J Endocrinol,* 158**,** 367-73.

PERRET, J., LUDGATE, M., LIBERT, F., GERARD, C., DUMONT, J. E., VASSART, G. & PARMENTIER, M. 1990. Stable Expression of the Human Tsh Receptor in Cho Cells and Characterization of Differentially Expressing Clones. *Biochem Biophys Res Commun,* 171**,** 1044-1050.

PERROS, P. & DICKINSON, A. J. 2005. Ophthalmopathy. *Werner & Ingbar's the thyroid : a fundamental and clinical text.* 9th ed. Philadelphia: Lippincott Williams & Wilkins.

PERROS, P. & KENDALL-TAYLOR, P. 1992. Biological activity of autoantibodies from patients with thyroid-associated ophthalmopathy: in vitro effects on porcine extraocular myoblasts. *Q J Med,* 84**,** 691-706.

PERROS, P. & KENDALL-TAYLOR, P. 1998. Natural history of thyroid eye disease. *Thyroid,* 8**,** 423-5.

PETERS, A. L., STUNZ, L. L. & BISHOP, G. A. 2009. CD40 and autoimmunity: the dark side of a great activator. *Semin Immunol,* 21**,** 293-300.

PEYSTER, R. G., GINSBERG, F., SILBER, J. H. & ADLER, L. P. 1986. Exophthalmos caused by excessive fat: CT volumetric analysis and differential diagnosis. *AJR Am J Roentgenol,* 146**,** 459-64.

PIANTANIDA, E., TANDA, M. L., LAI, A., SASSI, L. & BARTALENA, L. 2013. Prevalence and natural history of Graves' orbitopathy in the XXI century. *J Endocrinol Invest,* 36**,** 444-9.

PICHURIN, P., PICHURINA, O., CHAZENBALK, G. D., PARAS, C., CHEN, C. R., RAPOPORT, B. & MCLACHLAN, S. M. 2002. Immune deviation away from Th1 in interferon-gamma knockout mice does not enhance TSH receptor antibody production after naked DNA vaccination. *Endocrinology,* 143**,** 1182-9.

PICHURIN, P., YAN, X. M., FARILLA, L., GUO, J., CHAZENBALK, G. D., RAPOPORT, B. & MCLACHLAN, S. M. 2001. Naked TSH receptor DNA vaccination: A TH1 T cell response in which interferon-gamma production, rather than antibody, dominates the immune response in mice. *Endocrinology,* 142**,** 3530-6.

PITZ, S. 2010. Orbital imaging. *In:* WIERSINGA, W. M. & KAHALY, G. J. (eds.) *Graves' orbitopathy : a multidisciplinary approach - questions and answers.* 2nd, rev. ed. Basel etc.: S. Karger.

PLANCK, T., PARIKH, H., BRORSON, H., MARTENSSON, T., ASMAN, P., GROOP, L., HALLENGREN, B. & LANTZ, M. 2011. Gene expression in Graves' ophthalmopathy and arm lymphedema: similarities and differences. *Thyroid,* 21**,** 663-74.

PLOSKI, R., BRAND, O. J., JURECKA-LUBIENIECKA, B., FRANASZCZYK, M., KULA, D., KRAJEWSKI, P., KARAMAT, M. A., SIMMONDS, M. J., FRANKLYN, J. A., GOUGH, S. C., JARZAB, B. & BEDNARCZUK, T. 2010. Thyroid stimulating hormone receptor (TSHR) intron 1 variants are major risk factors for Graves' disease in three European Caucasian cohorts. *PLoS One,* 5**,** e15512.

POHLENZ, J., MAQUEEM, A., CUA, K., WEISS, R. E., VAN SANDE, J. & REFETOFF, S. 1999. Improved radioimmunoassay for measurement of mouse thyrotropin in serum: strain differences in thyrotropin concentration and thyrotroph sensitivity to thyroid hormone. *Thyroid,* 9**,** 1265-71.

POLITI, L. S., GODI, C., CAMMARATA, G., AMBROSI, A., IADANZA, A., LANZI, R., FALINI, A. & BIANCHI MARZOLI, S. 2014. Magnetic resonance imaging with diffusion-weighted imaging in the evaluation of thyroid-associated orbitopathy: getting below the tip of the iceberg. *Eur Radiol,* 24**,** 1118-26.

PONTO, K. A., KANITZ, M., OLIVO, P. D., PITZ, S., PFEIFFER, N. & KAHALY, G. J. 2011. Clinical relevance of thyroid-stimulating immunoglobulins in graves' ophthalmopathy. *Ophthalmology,* 118**,** 2279-85.

PRABHAKAR, B. S., BAHN, R. S. & SMITH, T. J. 2003. Current perspective on the pathogenesis of Graves' disease and ophthalmopathy. *Endocr Rev,* 24**,** 802-35.

PRITCHARD, J., HAN, R., HORST, N., CRUIKSHANK, W. W. & SMITH, T. J. 2003. Immunoglobulin activation of T cell chemoattractant expression in fibroblasts from patients with Graves' disease is mediated through the insulin-like growth factor I receptor pathway. *J Immunol,* 170**,** 6348-54.

PRITCHARD, J., HORST, N., CRUIKSHANK, W. & SMITH, T. J. 2002. Igs from patients with Graves' disease induce the expression of T cell chemoattractants in their fibroblasts. *J Immunol,* 168**,** 942-50.

PRUMMEL, M. F., MOURITS, M. P., BERGHOUT, A., KRENNING, E. P., VAN DER GAAG, R., KOORNNEEF, L. & WIERSINGA, W. M. 1989. Prednisone and cyclosporine in the treatment of severe Graves' ophthalmopathy. *N Engl J Med,* 321**,** 1353-9.

PRUMMEL, M. F., SUTTORP-SCHULTEN, M. S., WIERSINGA, W. M., VERBEEK, A. M., MOURITS, M. P. & KOORNNEEF, L. 1993. A new ultrasonographic method to detect disease activity and predict response to immunosuppressive treatment in Graves ophthalmopathy. *Ophthalmology,* 100**,** 556-61.

PUJOL-BORRELL, R., GIMÉNEZ-BARCONS, M., SÁNCHEZ, A. M. & COLOBRAN, R. 2015. Genetics of Graves' disease: Special focus on the role of TSHR gene. *Hormone and Metabolic Research*.

QUADBECK, B., ECKSTEIN, A. K., TEWS, S., WALZ, M., HOERMANN, R., MANN, K. & GIESELER, R. 2002. Maturation of thyroidal dendritic cells in Graves' disease. *Scand J Immunol,* 55**,** 612-20.

QUAN, T. E., COWPER, S., WU, S. P., BOCKENSTEDT, L. K. & BUCALA, R. 2004. Circulating fibrocytes: collagen-secreting cells of the peripheral blood. *Int J Biochem Cell Biol,* 36**,** 598-606.

QUARATINO, S., BADAMI, E., PANG, Y. Y., BARTOK, I., DYSON, J., KIOUSSIS, D., LONDEI, M. & MAIURI, L. 2004. Degenerate self-reactive human T-cell receptor causes spontaneous autoimmune disease in mice. *Nat Med,* 10**,** 920-6.

RAIKOW, R. B., DALBOW, M. H., KENNERDELL, J. S., COMPHER, K., MACHEN, L., HILLER, W. & BLENDERMANN, D. 1990. Immunohistochemical evidence for IgE involvement in Graves' orbitopathy. *Ophthalmology,* 97**,** 629-35.

RAO, P. V., WATSON, P. F., WEETMAN, A. P., CARAYANNIOTIS, G. & BANGA, J. P. 2003. Contrasting activities of thyrotropin receptor antibodies in experimental models of Graves' disease induced by injection of transfected fibroblasts or deoxyribonucleic acid vaccination. *Endocrinology,* 144**,** 260-6.

RAPOPORT, B., CHAZENBALK, G. D., JAUME, J. C. & MCLACHLAN, S. M. 1998. The thyrotropin (TSH) receptor: interaction with TSH and autoantibodies. *Endocr Rev,* 19**,** 673-716.

RASOOLY, L., BUREK, C. L. & ROSE, N. R. 1996. Iodine-induced autoimmune thyroiditis in NOD-H-2h4 mice. *Clin Immunol Immunopathol,* 81**,** 287-92.

RASPE, E., COSTAGLIOLA, S., RUF, J., MARIOTTI, S., DUMONT, J. E. & LUDGATE, M. 1995. Identification of the thyroid Na+/I- cotransporter as a potential autoantigen in thyroid autoimmune disease. *Eur J Endocrinol,* 132**,** 399-405.

REES SMITH, B., MCLACHLAN, S. M. & FURMANIAK, J. 1988. Autoantibodies to the thyrotropin receptor. *Endocr Rev,* 9**,** 106-21.

REGE, T. A. & HAGOOD, J. S. 2006. Thy-1 as a regulator of cell-cell and cell-matrix interactions in axon regeneration, apoptosis, adhesion, migration, cancer, and fibrosis. *FASEB J,* 20**,** 1045-54.

REGENSBURG, N. I., WIERSINGA, W. M., BERENDSCHOT, T. T., SAEED, P. & MOURITS, M. P. 2011. Effect of smoking on orbital fat and muscle volume in Graves' orbitopathy. *Thyroid,* 21**,** 177-81.

RIEMANN, C. D., FOSTER, J. A. & KOSMORSKY, G. S. 1999a. Direct orbital manometry in healthy patients. *Ophthal Plast Reconstr Surg,* 15**,** 121-5.

RIEMANN, C. D., FOSTER, J. A. & KOSMORSKY, G. S. 1999b. Direct orbital manometry in patients with thyroid-associated orbitopathy. *Ophthalmology,* 106**,** 1296-302.

RIGANTE, D., MAZZONI, M. B. & ESPOSITO, S. 2014. The cryptic interplay between systemic lupus erythematosus and infections. *Autoimmun Rev,* 13**,** 96-102.

ROMO-TENA, J., GOMEZ-MARTIN, D. & ALCOCER-VARELA, J. 2013. CTLA-4 and autoimmunity: new insights into the dual regulator of tolerance. *Autoimmun Rev,* 12**,** 1171-6.

ROOT-BERNSTEIN, R. & FAIRWEATHER, D. 2014. Complexities in the relationship between infection and autoimmunity. *Curr Allergy Asthma Rep,* 14**,** 407.

ROSE, N. R. 2012. Infection and autoimmunity: theme and variations. *Curr Opin Rheumatol,* 24**,** 380-2.

ROSEN, N. & BEN SIMON, G. J. 2010. Orbital decompression in thyroid related orbitopathy. *Pediatr Endocrinol Rev,* 7 Suppl 2**,** 217-21.

ROSENFELD, R. G. & DOLLAR, L. A. 1982. Characterization of the somatomedin-C/insulin-like growth factor I (SM-C/IGF-I) receptor on cultured human fibroblast monolayers:

regulation of receptor concentrations by SM-C/IGF-I and insulin. *J Clin Endocrinol Metab,* 55**,** 434-40.

ROSS, D. S. 2011. Radioiodine therapy for hyperthyroidism. *N Engl J Med,* 364**,** 542-50.

ROTELLA, C. M., ALVAREZ, F., KOHN, L. D. & TOCCAFONDI, R. 1987. Graves' autoantibodies to extrathyroidal TSH receptor: their role in ophthalmopathy and pretibial myxedema. *Acta Endocrinol Suppl (Copenh),* 281**,** 344-7.

ROTELLA, C. M., ZONEFRATI, R., TOCCAFONDI, R., VALENTE, W. A. & KOHN, L. D. 1986. Ability of monoclonal antibodies to the thyrotropin receptor to increase collagen synthesis in human fibroblasts: an assay which appears to measure exophthalmogenic immunoglobulins in Graves' sera. *J Clin Endocrinol Metab,* 62**,** 357-67.

ROTONDI, M., PIRALI, B., LODIGIANI, S., BRAY, S., LEPORATI, P., CHYTIRIS, S., BALZANO, S., MAGRI, F. & CHIOVATO, L. 2008. The post partum period and the onset of Graves' disease: an overestimated risk factor. *Eur J Endocrinol,* 159**,** 161-5.

RUNDLE, F. F. 1957. Management of exophthalmos and related ocular changes in Graves' disease. *Metabolism,* 6**,** 36-48.

RUNDLE, F. F. & WILSON, C. W. 1945. Development and course of exophthalmos and ophthalmoplegia in Graves' disease with special reference to the effect of thyroidectomy. *Clin Sci,* 5**,** 177-94.

SAITOH, O., ABIRU, N., NAKAHARA, M. & NAGAYAMA, Y. 2007. CD8+CD122+ T cells, a newly identified regulatory T subset, negatively regulate Graves' hyperthyroidism in a murine model. *Endocrinology,* 148**,** 6040-6.

SALVI, M., VANNUCCHI, G. & BECK-PECCOZ, P. 2013. Potential utility of rituximab for Graves' orbitopathy. *J Clin Endocrinol Metab,* 98**,** 4291-9.

SALVI, M., VANNUCCHI, G., CAMPI, I., CURRO, N., DAZZI, D., SIMONETTA, S., BONARA, P., ROSSI, S., SINA, C., GUASTELLA, C., RATIGLIA, R. & BECK-PECCOZ, P. 2007. Treatment of Graves' disease and associated ophthalmopathy with the anti-CD20 monoclonal antibody rituximab: an open study. *Eur J Endocrinol,* 156**,** 33-40.

SALVI, M., VANNUCCHI, G., CAMPI, I., ROSSI, S., BONARA, P., SBROZZI, F., GUASTELLA, C., AVIGNONE, S., PIROLA, G., RATIGLIA, R. & BECK-PECCOZ, P. 2006. Efficacy of rituximab treatment for thyroid-associated ophthalmopathy as a result of intraorbital B-cell depletion in one patient unresponsive to steroid immunosuppression. *Eur J Endocrinol,* 154**,** 511-7.

SALVI, M., VANNUCCHI, G., CURRO, N., CAMPI, I., COVELLI, D., DAZZI, D., SIMONETTA, S., GUASTELLA, C., PIGNATARO, L., AVIGNONE, S. & BECK-PECCOZ, P. 2015. Efficacy of B-cell targeted therapy with rituximab in patients with active moderate to severe Graves' orbitopathy: a randomized controlled study. *J Clin Endocrinol Metab,* 100**,** 422-31.

SANDERS, J., ALLEN, F., JEFFREYS, J., BOLTON, J., RICHARDS, T., DEPRAETERE, H., NAKATAKE, N., EVANS, M., KIDDIE, A., PREMAWARDHANA, L. D., CHIRGADZE, D. Y., MIGUEL, R. N., BLUNDELL, T. L., FURMANIAK, J. & SMITH, B. R. 2005. Characteristics of a monoclonal antibody to the thyrotropin receptor that acts as a powerful thyroid-stimulating autoantibody antagonist. *Thyroid,* 15**,** 672-82.

SANDERS, J., CHIRGADZE, D. Y., SANDERS, P., BAKER, S., SULLIVAN, A., BHARDWAJA, A., BOLTON, J., REEVE, M., NAKATAKE, N., EVANS, M., RICHARDS, T., POWELL, M., MIGUEL, R. N., BLUNDELL, T. L., FURMANIAK, J. & SMITH, B. R. 2007. Crystal structure of the TSH receptor in complex with a thyroid-stimulating autoantibody. *Thyroid,* 17**,** 395-410.

SANDERS, J., EVANS, M., BETTERLE, C., SANDERS, P., BHARDWAJA, A., YOUNG, S., ROBERTS, E., WILMOT, J., RICHARDS, T., KIDDIE, A., SMALL, K., PLATT, H., SUMMERHAYES, S., HARRIS, R., REEVE, M., COCO, G., ZANCHETTA, R., CHEN, S., FURMANIAK, J. & SMITH, B. R. 2008. A human monoclonal autoantibody to the thyrotropin receptor with thyroid-stimulating blocking activity. *Thyroid,* 18**,** 735-46.

SANDERS, J., EVANS, M., PREMAWARDHANA, L. D., DEPRAETERE, H., JEFFREYS, J., RICHARDS, T., FURMANIAK, J. & REES SMITH, B. 2003. Human monoclonal thyroid stimulating autoantibody. *Lancet,* 362**,** 126-8.

SANDERS, J., JEFFREYS, J., DEPRAETERE, H., RICHARDS, T., EVANS, M., KIDDIE, A., BRERETON, K., GROENEN, M., ODA, Y., FURMANIAK, J. & REES SMITH, B. 2002. Thyroid-stimulating monoclonal antibodies. *Thyroid,* 12**,** 1043-50.

SANDERS, P., YOUNG, S., SANDERS, J., KABELIS, K., BAKER, S., SULLIVAN, A., EVANS, M., CLARK, J., WILMOT, J., HU, X., ROBERTS, E., POWELL, M., NUNEZ MIGUEL, R., FURMANIAK, J. & REES SMITH, B. 2011. Crystal structure of the TSH receptor (TSHR) bound to a blocking-type TSHR autoantibody. *J Mol Endocrinol,* 46**,** 81-99.

SARESELLA, M., MARVENTANO, I., LONGHI, R., LISSONI, F., TRABATTONI, D., MENDOZZI, L., CAPUTO, D. & CLERICI, M. 2008. CD4+CD25+FoxP3+PD1- regulatory T cells in acute and stable relapsing-remitting multiple sclerosis and their modulation by therapy. *FASEB J,* 22**,** 3500-8.

SATO, A., TAKEMURA, Y., YAMADA, T., OHTSUKA, H., SAKAI, H., MIYAHARA, Y., AIZAWA, T., TERAO, A., ONUMA, S., JUNEN, K., KANAMORI, A., NAKAMURA, Y., TEJIMA, E., ITO, Y. & KAMIJO, K. 1999. A possible role of immunoglobulin E in patients with hyperthyroid Graves' disease. *J Clin Endocrinol Metab,* 84**,** 3602-5.

SCHNEIDER, M. J., FIERING, S. N., PALLUD, S. E., PARLOW, A. F., ST GERMAIN, D. L. & GALTON, V. A. 2001. Targeted disruption of the type 2 selenodeiodinase gene (DIO2) results in a phenotype of pituitary resistance to T4. *Mol Endocrinol,* 15**,** 2137-48.

SEETHARAMAIAH, G. S. 2003. Animal models of Graves' hyperthyroidism. *Autoimmunity,* 36**,** 381-7.

SEISSLER, J., WAGNER, S., SCHOTT, M., LETTMANN, M., FELDKAMP, J., SCHERBAUM, W. A. & MORGENTHALER, N. G. 2000. Low frequency of autoantibodies to the human Na(+)/I(-) symporter in patients with autoimmune thyroid disease. *J Clin Endocrinol Metab,* 85**,** 4630-4.

SELMI, C., LU, Q. & HUMBLE, M. C. 2012. Heritability versus the role of the environment in autoimmunity. *J Autoimmun,* 39**,** 249-52.

SELVA, D., CHEN, C. & KING, G. 2004. Late reactivation of thyroid orbitopathy. *Clin Experiment Ophthalmol,* 32**,** 46-50.

SHAN, S. J. & DOUGLAS, R. S. 2014. The pathophysiology of thyroid eye disease. *J Neuroophthalmol,* 34**,** 177-85.

SHEN, X., XI, G., MAILE, L. A., WAI, C., ROSEN, C. J. & CLEMMONS, D. R. 2012. Insulin-like growth factor (IGF) binding protein 2 functions coordinately with receptor protein tyrosine phosphatase beta and the IGF-I receptor to regulate IGF-I-stimulated signaling. *Mol Cell Biol,* 32**,** 4116-30.

SHENKMAN, L. & BOTTONE, E. J. 1976. Antibodies to Yersinia enterocolitica in thyroid disease. *Ann Intern Med,* 85**,** 735-9.

SHEPHERD, P. S., DA COSTA, C. R., CRIDLAND, J. C., GILMORE, K. S. & JOHNSTONE, A. P. 1999. Identification of an important thyrotrophin binding site on the human thyrotrophin receptor using monoclonal antibodies. *Mol Cell Endocrinol,* 149**,** 197-206.

SHIBUSAWA, N., YAMADA, M., HIRATO, J., MONDEN, T., SATOH, T. & MORI, M. 2000. Requirement of thyrotropin-releasing hormone for the postnatal functions of pituitary thyrotrophs: ontogeny study of congenital tertiary hypothyroidism in mice. *Mol Endocrinol,* 14**,** 137-46.

SHIMOJO, N., KOHNO, Y., YAMAGUCHI, K., KIKUOKA, S., HOSHIOKA, A., NIIMI, H., HIRAI, A., TAMURA, Y., SAITO, Y., KOHN, L. D. & TAHARA, K. 1996. Induction of Graves-like disease in mice by immunization with fibroblasts transfected with the thyrotropin receptor and a class II molecule. *Proc Natl Acad Sci U S A,* 93**,** 11074-9.

SIMMONDS, M. J. 2013. GWAS in autoimmune thyroid disease: redefining our understanding of pathogenesis. *Nat Rev Endocrinol,* 9**,** 277-87.

SIMMONDS, M. J. & GOUGH, S. C. 2004. Unravelling the genetic complexity of autoimmune thyroid disease: HLA, CTLA-4 and beyond. *Clin Exp Immunol,* 136**,** 1-10.

SIMMONDS, M. J. & GOUGH, S. C. 2011. The search for the genetic contribution to autoimmune thyroid disease: the never ending story? *Brief Funct Genomics,* 10**,** 77-90.

SIMMONDS, M. J., KAVVOURA, F. K., BRAND, O. J., NEWBY, P. R., JACKSON, L. E., HARGREAVES, C. E., FRANKLYN, J. A. & GOUGH, S. C. 2014. Skewed X chromosome inactivation and female preponderance in autoimmune thyroid disease: an association study and meta-analysis. *J Clin Endocrinol Metab,* 99**,** E127-31.

SMITH, B. R. & HALL, R. 1974. Thyroid-stimulating immunoglobulins in Graves' disease. *Lancet,* 2**,** 427-31.

SMITH, R. S. 2002. *Systematic evaluation of the mouse eye : anatomy, pathology, and biomethods,* Boca Raton ; London, CRC Press.

SMITH, T. J. 2010a. Insulin-like growth factor-I regulation of immune function: a potential therapeutic target in autoimmune diseases? *Pharmacol Rev,* 62**,** 199-236.

SMITH, T. J. 2010b. Potential role for bone marrow-derived fibrocytes in the orbital fibroblast heterogeneity associated with thyroid-associated ophthalmopathy. *Clin Exp Immunol,* 162**,** 24-31.

SMITH, T. J. 2013. Is IGF-I receptor a target for autoantibody generation in Graves' disease? *J Clin Endocrinol Metab,* 98**,** 515-8.

SMITH, T. J. 2015. TSH-receptor-expressing fibrocytes and thyroid-associated ophthalmopathy. *Nat Rev Endocrinol,* 11**,** 171-81.

SMITH, T. J., BAHN, R. S., GORMAN, C. A. & CHEAVENS, M. 1991. Stimulation of glycosaminoglycan accumulation by interferon gamma in cultured human retroocular fibroblasts. *J Clin Endocrinol Metab,* 72**,** 1169-71.

SMITH, T. J., HEGEDUS, L. & DOUGLAS, R. S. 2012. Role of insulin-like growth factor-1 (IGF-1) pathway in the pathogenesis of Graves' orbitopathy. *Best Pract Res Clin Endocrinol Metab,* 26**,** 291-302.

SMITH, T. J. & HOA, N. 2004. Immunoglobulins from Patients with Graves' Disease Induce Hyaluronan Synthesis in Their Orbital Fibroblasts through the Self-Antigen, Insulin-Like Growth Factor-I Receptor. *Journal of Clinical Endocrinology & Metabolism,* 89**,** 5076-5080.

SMITH, T. J., KOUMAS, L., GAGNON, A., BELL, A., SEMPOWSKI, G. D., PHIPPS, R. P. & SORISKY, A. 2002. Orbital fibroblast heterogeneity may determine the clinical presentation of thyroid-associated ophthalmopathy. *J Clin Endocrinol Metab,* 87**,** 385-92.

SMITH, T. J. & PARIKH, S. J. 1999. HMC-1 mast cells activate human orbital fibroblasts in coculture: evidence for up-regulation of prostaglandin E2 and hyaluronan synthesis. *Endocrinology,* 140**,** 3518-25.

SMITH, T. J., SEMPOWSKI, G. D., WANG, H. S., DEL VECCHIO, P. J., LIPPE, S. D. & PHIPPS, R. P. 1995a. Evidence for cellular heterogeneity in primary cultures of human orbital fibroblasts. *J Clin Endocrinol Metab,* 80**,** 2620-5.

SMITH, T. J., TSAI, C. C., SHIH, M. J., TSUI, S., CHEN, B., HAN, R., NAIK, V., KING, C. S., PRESS, C., KAMAT, S., GOLDBERG, R. A., PHIPPS, R. P., DOUGLAS, R. S. & GIANOUKAKIS, A. G. 2008. Unique attributes of orbital fibroblasts and global alterations in IGF-1 receptor signaling could explain thyroid-associated ophthalmopathy. *Thyroid,* 18**,** 983-8.

SMITH, T. J., WANG, H. S. & EVANS, C. H. 1995b. Leukoregulin is a potent inducer of hyaluronan synthesis in cultured human orbital fibroblasts. *Am J Physiol,* 268**,** C382-8.

SMYK, D., RIGOPOULOU, E. I., ZEN, Y., ABELES, R. D., BILLINIS, C., PARES, A. & BOGDANOS, D. P. 2012. Role for mycobacterial infection in pathogenesis of primary biliary cirrhosis? *World J Gastroenterol,* 18**,** 4855-65.

SOARES, R. M., DIAS, A. T., CASTRO, S. B., ALVES, C. C., EVANGELISTA, M. G., SILVA, L. C., FARIAS, R. E., CASTANON, M. C., JULIANO, M. A. & FERREIRA, A. P. 2013. Optical neuritis induced by different concentrations of myelin oligodendrocyte glycoprotein presents different profiles of the inflammatory process. *Autoimmunity,* 46**,** 480-485.

SOLIMAN, M., KAPLAN, E., STRAUS, F., FISFALEN, M. E., HIDAKA, Y., GUIMARAES, V. & DEGROOT, L. J. 1995. Graves' disease in severe combined immunodeficient mice. *J Clin Endocrinol Metab,* 80**,** 2848-55.

SOOS, M. A., FIELD, C. E., LAMMERS, R., ULLRICH, A., ZHANG, B., ROTH, R. A., ANDERSEN, A. S., KJELDSEN, T. & SIDDLE, K. 1992. A panel of monoclonal antibodies for the type I insulin-like growth factor receptor. Epitope mapping, effects on ligand binding, and biological activity. *J Biol Chem,* 267**,** 12955-63.

SORISKY, A., PARDASANI, D., GAGNON, A. & SMITH, T. J. 1996. Evidence of adipocyte differentiation in human orbital fibroblasts in primary culture. *J Clin Endocrinol Metab,* 81**,** 3428-31.

STAHL, P. & GORDON, S. 1982. Expression of a mannosyl-fucosyl receptor for endocytosis on cultured primary macrophages and their hybrids. *J Cell Biol,* 93**,** 49-56.

STAN, M. N. & BAHN, R. S. 2010. Risk factors for development or deterioration of Graves' ophthalmopathy. *Thyroid,* 20**,** 777-83.

STAN, M. N., GARRITY, J. A., CARRANZA LEON, B. G., PRABIN, T., BRADLEY, E. A. & BAHN, R. S. 2015. Randomized controlled trial of rituximab in patients with Graves' orbitopathy. *J Clin Endocrinol Metab,* 100**,** 432-41.

STAN, M. N., GARRITY, J. A., THAPA, P., BRADLEY, E. A. & BAHN, R. 2013. (Abs Highlighted Oral 3) RANDOMIZED DOUBLE-BLIND PLACEBO-CONTROLLED TRIAL OF RITUXIMAB FOR TREATMENT OF GRAVES' OPHTHALMOPATHY. *83rd Annual Meeting of the American Thyroid Association.* Puerto Rico.

STANKOV, K., BENC, D. & DRASKOVIC, D. 2013. Genetic and epigenetic factors in etiology of diabetes mellitus type 1. *Pediatrics,* 132**,** 1112-22.

STARKEY, K. J., JANEZIC, A., JONES, G., JORDAN, N., BAKER, G. & LUDGATE, M. 2003. Adipose thyrotrophin receptor expression is elevated in Graves' and thyroid eye diseases ex vivo and indicates adipogenesis in progress in vivo. *J Mol Endocrinol,* 30**,** 369-80.

STEFAN, M., WEI, C., LOMBARDI, A., LI, C. W., CONCEPCION, E. S., INABNET, W. B., 3RD, OWEN, R., ZHANG, W. & TOMER, Y. 2014. Genetic-epigenetic dysregulation of thymic TSH receptor gene expression triggers thyroid autoimmunity. *Proc Natl Acad Sci U S A,* 111**,** 12562-7.

STIEBEL-KALISH, H., ROBENSHTOK, E., HASANREISOGLU, M., EZRACHI, D., SHIMON, I. & LEIBOVICI, L. 2009. Treatment modalities for Graves' ophthalmopathy: systematic review and metaanalysis. *J Clin Endocrinol Metab,* 94**,** 2708-16.

STRIEDER, T. G., PRUMMEL, M. F., TIJSSEN, J. G., ENDERT, E. & WIERSINGA, W. M. 2003. Risk factors for and prevalence of thyroid disorders in a cross-sectional study among healthy female relatives of patients with autoimmune thyroid disease. *Clin Endocrinol (Oxf),* 59**,** 396-401.

SUN, S. W., CAMPBELL, B., LUNDERVILLE, C., WON, E. & LIANG, H. F. 2011. Noninvasive topical loading for manganese-enhanced MRI of the mouse visual system. *Invest Ophthalmol Vis Sci,* 52**,** 3914-20.

SZYPOWSKA, A., STELMASZCZYK-EMMEL, A., DEMKOW, U. & LUCZYNSKI, W. 2012. Low frequency of regulatory T cells in the peripheral blood of children with type 1 diabetes diagnosed under the age of five. *Arch Immunol Ther Exp (Warsz),* 60**,** 307-13.

TAKASU, N. & MATSUSHITA, M. 2012. Changes of TSH-Stimulation Blocking Antibody (TSBAb) and Thyroid Stimulating Antibody (TSAb) Over 10 Years in 34 TSBAb-Positive Patients with Hypothyroidism and in 98 TSAb-Positive Graves' Patients with Hyperthyroidism:

Reevaluation of TSBAb and TSAb in TSH-Receptor-Antibody (TRAb)-Positive Patients. *J Thyroid Res,* 2012**,** 182176.

TAKASU, N., YAMADA, T., SATO, A., NAKAGAWA, M., KOMIYA, I., NAGASAWA, Y. & ASAWA, T. 1990. Graves' disease following hypothyroidism due to Hashimoto's disease: studies of eight cases. *Clin Endocrinol (Oxf),* 33**,** 687-98.

TAKEDA, K., TAKAMATSU, J., KASAGI, K., SAKANE, S., IKEGAMI, Y., ISOTANI, H., MAJIMA, T., MAJIMA, M., KITAOKA, H., IIDA, Y. & ET AL. 1988. Development of hyperthyroidism following primary hypothyroidism: a case report with changes in thyroid-related antibodies. *Clin Endocrinol (Oxf),* 28**,** 341-4.

TALLA, V., YANG, C., SHAW, G., PORCIATTI, V., KOILKONDA, R. D. & GUY, J. 2013. Noninvasive assessments of optic nerve neurodegeneration in transgenic mice with isolated optic neuritis. *Invest Ophthalmol Vis Sci,* 54**,** 4440-50.

TALLSTEDT, L., LUNDELL, G., TORRING, O., WALLIN, G., LJUNGGREN, J. G., BLOMGREN, H. & TAUBE, A. 1992. Occurrence of ophthalmopathy after treatment for Graves' hyperthyroidism. The Thyroid Study Group. *N Engl J Med,* 326**,** 1733-8.

TAN, G. H., DUTTON, C. M. & BAHN, R. S. 1996. Interleukin-1 (IL-1) receptor antagonist and soluble IL-1 receptor inhibit IL-1-induced glycosaminoglycan production in cultured human orbital fibroblasts from patients with Graves' ophthalmopathy. *J Clin Endocrinol Metab,* 81**,** 449-52.

TANAKA, K., CHAZENBALK, G. D., MCLACHLAN, S. M. & RAPOPORT, B. 1999a. The shed thyrotropin receptor is primarily a carboxyl terminal truncated form of the A subunit, not the entire A subunit. *Mol Cell Endocrinol,* 150**,** 113-9.

TANAKA, K., CHAZENBALK, G. D., MCLACHLAN, S. M. & RAPOPORT, B. 1999b. Thyrotropin receptor cleavage at site 1 involves two discontinuous segments at each end of the unique 50-amino acid insertion. *J Biol Chem,* 274**,** 2093-6.

TANDA, M. L., PIANTANIDA, E., LAI, A., LOMBARDI, V., DALLE MULE, I., LIPARULO, L., PARIANI, N. & BARTALENA, L. 2009. Thyroid autoimmunity and environment. *Horm Metab Res,* 41**,** 436-42.

TANDA, M. L., PIANTANIDA, E., LIPARULO, L., VERONESI, G., LAI, A., SASSI, L., PARIANI, N., GALLO, D., AZZOLINI, C., FERRARIO, M. & BARTALENA, L. 2013. Prevalence and natural history of Graves' orbitopathy in a large series of patients with newly diagnosed graves' hyperthyroidism seen at a single center. *J Clin Endocrinol Metab,* 98**,** 1443-9.

TANDON, R., SHARMA, M., CHANDRASHEKHAR, Y., KOTB, M., YACOUB, M. H. & NARULA, J. 2013. Revisiting the pathogenesis of rheumatic fever and carditis. *Nat Rev Cardiol,* 10**,** 171-7.

TEFT, W. A., KIRCHHOF, M. G. & MADRENAS, J. 2006. A molecular perspective of CTLA-4 function. *Annu Rev Immunol,* 24**,** 65-97.

TELGMANN, L., SPERLING, M. & KARST, U. 2013. Determination of gadolinium-based MRI contrast agents in biological and environmental samples: a review. *Anal Chim Acta,* 764**,** 1-16.

TENG, M. W., BOWMAN, E. P., MCELWEE, J. J., SMYTH, M. J., CASANOVA, J. L., COOPER, A. M. & CUA, D. J. 2015. IL-12 and IL-23 cytokines: from discovery to targeted therapies for immune-mediated inflammatory diseases. *Nat Med,* 21**,** 719-29.

THEOHARIDES, T. C., KEMPURAJ, D., TAGEN, M., CONTI, P. & KALOGEROMITROS, D. 2007. Differential release of mast cell mediators and the pathogenesis of inflammation. *Immunol Rev,* 217**,** 65-78.

TOLLEFSEN, S. E., THOMPSON, K. & PETERSEN, D. J. 1987. Separation of the high affinity insulin-like growth factor I receptor from low affinity binding sites by affinity chromatography. *J Biol Chem,* 262**,** 16461-9.

TOMER, Y. 2010. Genetic susceptibility to autoimmune thyroid disease: past, present, and future. *Thyroid,* 20**,** 715-25.

TOMER, Y. 2014. Mechanisms of autoimmune thyroid diseases: from genetics to epigenetics. *Annu Rev Pathol,* 9**,** 147-56.

TOMER, Y. & DAVIES, T. F. 2003. Searching for the autoimmune thyroid disease susceptibility genes: from gene mapping to gene function. *Endocr Rev,* 24**,** 694-717.

TOMER, Y., HASHAM, A., DAVIES, T. F., STEFAN, M., CONCEPCION, E., KEDDACHE, M. & GREENBERG, D. A. 2013. Fine mapping of loci linked to autoimmune thyroid disease identifies novel susceptibility genes. *J Clin Endocrinol Metab,* 98**,** E144-52.

TOMER, Y. & HUBER, A. 2009. The etiology of autoimmune thyroid disease: a story of genes and environment. *J Autoimmun,* 32**,** 231-9.

TONACCHERA, M. & PINCHERA, A. 2000. Thyrotropin receptor polymorphisms and thyroid diseases. *J Clin Endocrinol Metab,* 85**,** 2637-9.

TRAISK, F., TALLSTEDT, L., ABRAHAM-NORDLING, M., ANDERSSON, T., BERG, G., CALISSENDORFF, J., HALLENGREN, B., HEDNER, P., LANTZ, M., NYSTROM, E., PONJAVIC, V., TAUBE, A., TORRING, O., WALLIN, G., ASMAN, P., LUNDELL, G. & THYROID STUDY GROUP OF, T. T. 2009. Thyroid-associated ophthalmopathy after treatment for Graves' hyperthyroidism with antithyroid drugs or iodine-131. *J Clin Endocrinol Metab,* 94**,** 3700-7.

TRAMONTANO, D., CUSHING, G. W., MOSES, A. C. & INGBAR, S. H. 1986. Insulin-like growth factor-I stimulates the growth of rat thyroid cells in culture and synergizes the stimulation of DNA synthesis induced by TSH and Graves'-IgG. *Endocrinology,* 119**,** 940-2.

TRAMONTANO, D., MOSES, A. C. & INGBAR, S. H. 1988a. The role of adenosine 3',5'-monophosphate in the regulation of receptors for thyrotropin and insulin-like growth factor I in the FRTL5 rat thyroid follicular cell. *Endocrinology,* 122**,** 133-6.

TRAMONTANO, D., MOSES, A. C., PICONE, R. & INGBAR, S. H. 1987. Characterization and regulations of the receptor for insulin-like growth factor-I in the FRTL-5 rat thyroid follicular cell line. *Endocrinology,* 120**,** 785-90.

TRAMONTANO, D., MOSES, A. C., VENEZIANI, B. M. & INGBAR, S. H. 1988b. Adenosine 3',5'-monophosphate mediates both the mitogenic effect of thyrotropin and its ability to amplify the response to insulin-like growth factor I in FRTL5 cells. *Endocrinology,* 122**,** 127-32.

TREE, T. I., MORGENTHALER, N. G., DUHINDAN, N., HICKS, K. E., MADEC, A. M., SCHERBAUM, W. A. & BANGA, J. P. 2000. Two amino acids in glutamic acid decarboxylase act in concert for maintenance of conformational determinants recognised by Type I diabetic autoantibodies. *Diabetologia,* 43**,** 881-9.

TSAI, S. & SANTAMARIA, P. 2013. MHC Class II Polymorphisms, Autoreactive T-Cells, and Autoimmunity. *Front Immunol,* 4**,** 321.

TSUI, S., NAIK, V., HOA, N., HWANG, C. J., AFIFIYAN, N. F., SINHA HIKIM, A., GIANOUKAKIS, A. G., DOUGLAS, R. S. & SMITH, T. J. 2008. Evidence for an Association between Thyroid-Stimulating Hormone and Insulin-Like Growth Factor 1 Receptors: A Tale of Two Antigens Implicated in Graves' Disease. *The Journal of Immunology,* 181**,** 4397-4405.

TUCKER, W. E., JR. 1962. Thyroiditis in a group of laboratory dogs. A study of 167 beagles. *Am J Clin Pathol,* 38**,** 70-4.

TURCU, A. F., KUMAR, S., NEUMANN, S., COENEN, M., IYER, S., CHIRIBOGA, P., GERSHENGORN, M. C. & BAHN, R. S. 2013. A small molecule antagonist inhibits thyrotropin receptor antibody-induced orbital fibroblast functions involved in the pathogenesis of Graves ophthalmopathy. *J Clin Endocrinol Metab,* 98**,** 2153-9.

UNO, H., SASAZUKI, T., TAMAI, H. & MATSUMOTO, H. 1981. Two major genes, linked to HLA and Gm, control susceptibility to Graves' disease. *Nature,* 292**,** 768-70.

VAIDYA, B., WILLIAMS, G. R., ABRAHAM, P. & PEARCE, S. H. 2008. Radioiodine treatment for benign thyroid disorders: results of a nationwide survey of UK endocrinologists. *Clin Endocrinol (Oxf),* 68**,** 814-20.

VALYASEVI, R. W., ERICKSON, D. Z., HARTENECK, D. A., DUTTON, C. M., HEUFELDER, A. E., JYONOUCHI, S. C. & BAHN, R. S. 1999. Differentiation of human orbital preadipocyte fibroblasts induces expression of functional thyrotropin receptor. *J Clin Endocrinol Metab,* 84**,** 2557-62.

VALYASEVI, R. W., HARTENECK, D. A., DUTTON, C. M. & BAHN, R. S. 2002. Stimulation of adipogenesis, peroxisome proliferator-activated receptor-gamma (PPARgamma), and thyrotropin receptor by PPARgamma agonist in human orbital preadipocyte fibroblasts. *J Clin Endocrinol Metab,* 87**,** 2352-8.

VALYASEVI, R. W., JYONOUCHI, S. C., DUTTON, C. M., MUNSAKUL, N. & BAHN, R. S. 2001. Effect of tumor necrosis factor-alpha, interferon-gamma, and transforming growth factor-beta on adipogenesis and expression of thyrotropin receptor in human orbital preadipocyte fibroblasts. *J Clin Endocrinol Metab,* 86**,** 903-8.

VAN DER VEEKEN, J., OLIVEIRA, S., SCHIFFELERS, R. M., STORM, G., VAN BERGEN EN HENEGOUWEN, P. M. & ROOVERS, R. C. 2009. Crosstalk between epidermal growth factor receptor- and insulin-like growth factor-1 receptor signaling: implications for cancer therapy. *Curr Cancer Drug Targets,* 9**,** 748-60.

VAN KOPPEN, C. J., DE GOOYER, M. E., KARSTENS, W. J., PLATE, R., CONTI, P. G., VAN ACHTERBERG, T. A., VAN AMSTEL, M. G., BRANDS, J. H., WAT, J., BERG, R. J., LANE, J. R., MILTENBURG, A. M. & TIMMERS, C. M. 2012. Mechanism of action of a nanomolar potent, allosteric antagonist of the thyroid-stimulating hormone receptor. *Br J Pharmacol,* 165**,** 2314-24.

VAN SANDE, J., SWILLENS, S., GERARD, C., ALLGEIER, A., MASSART, C., VASSART, G. & DUMONT, J. E. 1995. In Chinese hamster ovary K1 cells dog and human thyrotropin receptors activate both the cyclic AMP and the phosphatidylinositol 4,5-bisphosphate cascades in the presence of thyrotropin and the cyclic AMP cascade in its absence. *Eur J Biochem,* 229**,** 338-43.

VAN STEENSEL, L., PARIDAENS, D., DINGJAN, G. M., VAN DAELE, P. L., VAN HAGEN, P. M., KUIJPERS, R. W., VAN DEN BOSCH, W. A., DREXHAGE, H. A., HOOIJKAAS, H. & DIK, W. A. 2010. Platelet-derived growth factor-BB: a stimulus for cytokine production by orbital fibroblasts in Graves' ophthalmopathy. *Invest Ophthalmol Vis Sci,* 51**,** 1002-7.

VAN STEENSEL, L., PARIDAENS, D., SCHRIJVER, B., DINGJAN, G. M., VAN DAELE, P. L., VAN HAGEN, P. M., VAN DEN BOSCH, W. A., DREXHAGE, H. A., HOOIJKAAS, H. & DIK, W. A. 2009. Imatinib mesylate and AMN107 inhibit PDGF-signaling in orbital fibroblasts: a potential treatment for Graves' ophthalmopathy. *Invest Ophthalmol Vis Sci,* 50**,** 3091-8.

VAN STEENSEL, L., PARIDAENS, D., VAN MEURS, M., VAN HAGEN, P. M., VAN DEN BOSCH, W. A., KUIJPERS, R. W., DREXHAGE, H. A., HOOIJKAAS, H. & DIK, W. A. 2012. Orbit-infiltrating mast cells, monocytes, and macrophages produce PDGF isoforms that orchestrate orbital fibroblast activation in Graves' ophthalmopathy. *J Clin Endocrinol Metab,* 97**,** E400-8.

VAN STEENSEL, L., VAN HAGEN, P. M., PARIDAENS, D., KUIJPERS, R. W., VAN DEN BOSCH, W. A., DREXHAGE, H. A., HOOIJKAAS, H. & DIK, W. A. 2011. Whole orbital tissue culture identifies imatinib mesylate and adalimumab as potential therapeutics for Graves' ophthalmopathy. *Br J Ophthalmol,* 95**,** 735-8.

VAN ZEIJL, C. J., FLIERS, E., VAN KOPPEN, C. J., SUROVTSEVA, O. V., DE GOOYER, M. E., MOURITS, M. P., WIERSINGA, W. M., MILTENBURG, A. M. & BOELEN, A. 2010. Effects of thyrotropin and thyrotropin-receptor-stimulating Graves' disease immunoglobulin G

on cyclic adenosine monophosphate and hyaluronan production in nondifferentiated orbital fibroblasts of Graves' ophthalmopathy patients. *Thyroid,* 20**,** 535-44.

VAN ZEIJL, C. J., FLIERS, E., VAN KOPPEN, C. J., SUROVTSEVA, O. V., DE GOOYER, M. E., MOURITS, M. P., WIERSINGA, W. M., MILTENBURG, A. M. & BOELEN, A. 2011. Thyrotropin receptor-stimulating Graves' disease immunoglobulins induce hyaluronan synthesis by differentiated orbital fibroblasts from patients with Graves' ophthalmopathy not only via cyclic adenosine monophosphate signaling pathways. *Thyroid,* 21**,** 169-76.

VAN ZEIJL, C. J., VAN KOPPEN, C. J., SUROVTSEVA, O. V., DE GOOYER, M. E., PLATE, R., CONTI, P., KARSTENS, W. J., TIMMERS, M., SAEED, P., WIERSINGA, W. M., MILTENBURG, A. M., FLIERS, E. & BOELEN, A. 2012. Complete inhibition of rhTSH-, Graves' disease IgG-, and M22-induced cAMP production in differentiated orbital fibroblasts by a low-molecular-weight TSHR antagonist. *J Clin Endocrinol Metab,* 97**,** E781-5.

VANG, T., MILETIC, A. V., BOTTINI, N. & MUSTELIN, T. 2007. Protein tyrosine phosphatase PTPN22 in human autoimmunity. *Autoimmunity,* 40**,** 453-61.

VAREWIJCK, A. J., BOELEN, A., LAMBERTS, S. W., FLIERS, E., HOFLAND, L. J., WIERSINGA, W. M. & JANSSEN, J. A. 2013. Circulating IgGs may modulate IGF-I receptor stimulating activity in a subset of patients with Graves' ophthalmopathy. *J Clin Endocrinol Metab,* 98**,** 769-76.

VELAGA, M. R., WILSON, V., JENNINGS, C. E., OWEN, C. J., HERINGTON, S., DONALDSON, P. T., BALL, S. G., JAMES, R. A., QUINTON, R., PERROS, P. & PEARCE, S. H. 2004. The codon 620 tryptophan allele of the lymphoid tyrosine phosphatase (LYP) gene is a major determinant of Graves' disease. *J Clin Endocrinol Metab,* 89**,** 5862-5.

VERON, P., LEBORGNE, C., MONTEILHET, V., BOUTIN, S., MARTIN, S., MOULLIER, P. & MASURIER, C. 2012. Humoral and cellular capsid-specific immune responses to adeno-associated virus type 1 in randomized healthy donors. *J Immunol,* 188**,** 6418-24.

VESTERGAARD, P., REJNMARK, L., WEEKE, J., HOECK, H. C., NIELSEN, H. K., RUNGBY, J., LAURBERG, P. & MOSEKILDE, L. 2002. Smoking as a risk factor for Graves' disease, toxic nodular goiter, and autoimmune hypothyroidism. *Thyroid,* 12**,** 69-75.

VIRAKUL, S., DALM, V. A., PARIDAENS, D., VAN DEN BOSCH, W. A., HIRANKARN, N., VAN HAGEN, P. M. & DIK, W. A. 2014. The tyrosine kinase inhibitor dasatinib effectively blocks PDGF-induced orbital fibroblast activation. *Graefes Arch Clin Exp Ophthalmol,* 252**,** 1101-9.

VITTI, P., RAGO, T., CHIOVATO, L., PALLINI, S., SANTINI, F., FIORE, E., ROCCHI, R., MARTINO, E. & PINCHERA, A. 1997. Clinical features of patients with Graves' disease undergoing remission after antithyroid drug treatment. *Thyroid,* 7**,** 369-75.

VLAEMINCK-GUILLEM, V., HO, S. C., RODIEN, P., VASSART, G. & COSTAGLIOLA, S. 2002. Activation of the cAMP pathway by the TSH receptor involves switching of the ectodomain from a tethered inverse agonist to an agonist. *Mol Endocrinol,* 16**,** 736-46.

VOLPE, R., KASUGA, Y., AKASU, F., MORITA, T., YOSHIKAWA, N., RESETKOVA, E. & ARREAZA, G. 1993. The use of the severe combined immunodeficient mouse and the athymic "nude" mouse as models for the study of human autoimmune thyroid disease. *Clin Immunol Immunopathol,* 67**,** 93-9.

WAGLE, N. M., DALLAS, J. S., SEETHARAMAIAH, G. S., FAN, J. L., DESAI, R. K., MEMAR, O., RAJARAMAN, S. & PRABHAKAR, B. S. 1994. Induction of hyperthyroxinemia in BALB/C but not in several other strains of mice. *Autoimmunity,* 18**,** 103-12.

WAKELKAMP, I. M., BAKKER, O., BALDESCHI, L., WIERSINGA, W. M. & PRUMMEL, M. F. 2003. TSH-R expression and cytokine profile in orbital tissue of active vs. inactive Graves' ophthalmopathy patients. *Clin Endocrinol (Oxf),* 58**,** 280-7.

WAKELKAMP, I. M., TAN, H., SAEED, P., SCHLINGEMANN, R. O., VERBRAAK, F. D., BLANK, L. E., PRUMMEL, M. F. & WIERSINGA, W. M. 2004. Orbital irradiation for Graves'

ophthalmopathy: Is it safe? A long-term follow-up study. *Ophthalmology,* 111**,** 1557-62.

WALENKAMP, M. J. & WIT, J. M. 2006. Genetic disorders in the growth hormone - insulin-like growth factor-I axis. *Horm Res,* 66**,** 221-30.

WALL, J. R. 2014. Thyroid function. Pathogenesis of Graves ophthalmopathy--a role for TSH-R? *Nat Rev Endocrinol,* 10**,** 256-8.

WALL, J. R. & LAHOOTI, H. 2011. [Pathogenesis of thyroid eye disease - does autoimmunity against the TSH receptor explain all cases?]. *Endokrynol Pol,* 62 Suppl 1**,** 1-7.

WALL, J. R., TRILLER, H., BOUCHER, A., BERNARD, N. F., SALVI, M. & LUDGATE, M. 1993. Antibodies reactive with an intracellular epitope of a recombinant 64 kDa thyroid and eye muscle protein in patients with thyroid autoimmunity and ophthalmopathy. *J Endocrinol Invest,* 16**,** 863-8.

WANG, Q., VLKOLINSKY, R., XIE, M., OBENAUS, A. & SONG, S. K. 2012. Diffusion tensor imaging detected optic nerve injury correlates with decreased compound action potentials after murine retinal ischemia. *Invest Ophthalmol Vis Sci,* 53**,** 136-42.

WANG, S. H., CARAYANNIOTIS, G., ZHANG, Y., GUPTA, M., MCGREGOR, A. M. & BANGA, J. P. 1998. Induction of thyroiditis in mice with thyrotropin receptor lacking serologically dominant regions. *Clin Exp Immunol,* 113**,** 119-25.

WANG, S. H., MEZOSI, E., WOLF, J. M., CAO, Z., UTSUGI, S., GAUGER, P. G., DOHERTY, G. M. & BAKER, J. R., JR. 2004. IFNgamma sensitization to TRAIL-induced apoptosis in human thyroid carcinoma cells by upregulating Bak expression. *Oncogene,* 23**,** 928-35.

WANG, Y. & SMITH, T. J. 2014. Current concepts in the molecular pathogenesis of thyroid-associated ophthalmopathy. *Invest Ophthalmol Vis Sci,* 55**,** 1735-48.

WARD, C. W., GARRETT, T. P., MCKERN, N. M., LOU, M., COSGROVE, L. J., SPARROW, L. G., FRENKEL, M. J., HOYNE, P. A., ELLEMAN, T. C., ADAMS, T. E., LOVRECZ, G. O., LAWRENCE, L. J. & TULLOCH, P. A. 2001. The three dimensional structure of the type I insulin-like growth factor receptor. *Mol Pathol,* 54**,** 125-32.

WATANABE, Y., TAHARA, K., HIRAI, A., TADA, H., KOHN, L. D. & AMINO, N. 1997. Subtypes of anti-TSH receptor antibodies classified by various assays using CHO cells expressing wild-type or chimeric human TSH receptor. *Thyroid,* 7**,** 13-9.

WEAVER, C. T., HARRINGTON, L. E., MANGAN, P. R., GAVRIELI, M. & MURPHY, K. M. 2006. Th17: an effector CD4 T cell lineage with regulatory T cell ties. *Immunity,* 24**,** 677-88.

WEETMAN, A. P. 1992. How antithyroid drugs work in Graves' disease. *Clin Endocrinol (Oxf),* 37**,** 317-8.

WEETMAN, A. P. 2000. Graves' disease. *N Engl J Med,* 343**,** 1236-48.

WEETMAN, A. P. 2001. Determinants of autoimmune thyroid disease. *Nat Immunol,* 2**,** 769-70.

WEETMAN, A. P. 2003. Grave's disease 1835-2002. *Horm Res,* 59 Suppl 1**,** 114-8.

WEETMAN, A. P. 2009. The genetics of autoimmune thyroid disease. *Horm Metab Res,* 41**,** 421-5.

WEETMAN, A. P. 2010. Immunity, thyroid function and pregnancy: molecular mechanisms. *Nat Rev Endocrinol,* 6**,** 311-8.

WEETMAN, A. P. 2012. Thyroid disease in pregnancy in 2011: Thyroid function--effects on mother and baby unraveled. *Nat Rev Endocrinol,* 8**,** 69-70.

WEETMAN, A. P., COHEN, S., GATTER, K. C., FELLS, P. & SHINE, B. 1989. Immunohistochemical analysis of the retrobulbar tissues in Graves' ophthalmopathy. *Clin Exp Immunol,* 75**,** 222-7.

WEGELIUS, O., ASBOE-HANSEN, G. & LAMBERG, B. A. 1957. Retrobulbar connective tissue changes in malignant exophthalmos. *Acta Endocrinol (Copenh),* 25**,** 452-6.

WEIGHTMAN, D. R., PERROS, P., SHERIF, I. H. & KENDALL-TAYLOR, P. 1993. Autoantibodies to IGF-1 binding sites in thyroid associated ophthalmopathy. *Autoimmunity,* 16**,** 251-7.

WEISSEL, M. & HAUFF, W. 2000. Fatal liver failure after high-dose glucocorticoid pulse therapy in a patient with severe thyroid eye disease. *Thyroid,* 10**,** 521.

WESCOMBE, L., LAHOOTI, H., GOPINATH, B. & WALL, J. R. 2010. The cardiac calsequestrin gene (CASQ2) is up-regulated in the thyroid in patients with Graves' ophthalmopathy-- support for a role of autoimmunity against calsequestrin as the triggering event. *Clin Endocrinol (Oxf),* 73**,** 522-8.

WESTBROOK, C. & KAUT ROTH, C. 1998. *MRI in Practice,* Oxford, Blackwell.

WHITTEN, A. E., SMITH, B. J., MENTING, J. G., MARGETTS, M. B., MCKERN, N. M., LOVRECZ, G. O., ADAMS, T. E., RICHARDS, K., BENTLEY, J. D., TREWHELLA, J., WARD, C. W. & LAWRENCE, M. C. 2009. Solution structure of ectodomains of the insulin receptor family: the ectodomain of the type 1 insulin-like growth factor receptor displays asymmetry of ligand binding accompanied by limited conformational change. *J Mol Biol,* 394**,** 878-92.

WICHMANN, W. 2002. Magnetic resonance imaging (MRI). *In:* MÜLLER-FORELL, W. (ed.) *Imaging of orbital and visual pathway*

pathology. Heidelberg: Springer.

WIERSINGA, W. M. 1992. Immunosuppressive treatment of Graves' ophthalmopathy. *Thyroid,* 2**,** 229-33.

WIERSINGA, W. M. 2011. Autoimmunity in Graves' ophthalmopathy: the result of an unfortunate marriage between TSH receptors and IGF-1 receptors? *J Clin Endocrinol Metab,* 96**,** 2386-94.

WIERSINGA, W. M. 2013. Smoking and thyroid. *Clin Endocrinol (Oxf),* 79**,** 145-51.

WIERSINGA, W. M. & BARTALENA, L. 2002. Epidemiology and prevention of Graves' ophthalmopathy. *Thyroid,* 12**,** 855-60.

WIESWEG, B., JOHNSON, K. T., ECKSTEIN, A. K. & BERCHNER-PFANNSCHMIDT, U. 2013. Current Insights into Animal Models of Graves' Disease and Orbitopathy. *Horm Metab Res*.

WILKE, C. M., BISHOP, K., FOX, D. & ZOU, W. 2011. Deciphering the role of Th17 cells in human disease. *Trends Immunol,* 32**,** 603-11.

WRIGHT, G. P., EHRENSTEIN, M. R. & STAUSS, H. J. 2011. Regulatory T-cell adoptive immunotherapy: potential for treatment of autoimmunity. *Expert Rev Clin Immunol,* 7**,** 213-25.

WU, L., XUN, L., YANG, J., XU, L., TIAN, Z., GAO, S., ZHANG, Y., HOU, P. & SHI, B. 2011. Induction of murine neonatal tolerance against Graves' disease using recombinant adenovirus expressing the TSH receptor A-subunit. *Endocrinology,* 152**,** 1165-71.

XU, J., SUN, S. W., NAISMITH, R. T., SNYDER, A. Z., CROSS, A. H. & SONG, S. K. 2008. Assessing optic nerve pathology with diffusion MRI: from mouse to human. *NMR Biomed,* 21**,** 928-40.

YAMADA, M., LI, A. W., WEST, K. A., CHANG, C. H. & WALL, J. R. 2002. Experimental model for ophthalmopathy in BALB/c and outbred (CD-1) mice genetically immunized with G2s and the thyrotropin receptor. *Autoimmunity,* 35**,** 403-13.

YAMADA, T., SATO, A., AIZAWA, T., OOTSUKA, H., MIYAHARA, Y., SAKAI, H., TERAO, A., ONUMA, S., ITO, Y., KANAMORI, A., NAKAMURA, Y. & TEJIMA, E. 1998. An elevation of stem cell factor in patients with hyperthyroid Graves' disease. *Thyroid,* 8**,** 499-504.

YAMAGUCHI, K., SHIMOJO, N., KIKUOKA, S., HOSHIOKA, A., HIRAI, A., TAHARA, K., KOHN, L. D., KOHNO, Y. & NIIMI, H. 1997. Genetic control of anti-thyrotropin receptor antibody generation in H-2K mice immunized with thyrotropin receptor-transfected fibroblasts. *J Clin Endocrinol Metab,* 82**,** 4266-9.

YE, F., HOU, P., WU, X., MA, X., GAO, L., WU, L., XU, L. & SHI, B. 2012. The significance of immune-related molecule expression profiles in an animal model of Graves' disease. *Autoimmunity,* 45**,** 143-52.

YE, F., SHI, B., WU, X., HOU, P., GAO, L., MA, X., XU, L. & WU, L. 2011. Experience with lentivirus-mediated CD40 gene silencing in a mouse model of Graves' disease. *J Endocrinol,* 208**,** 285-91.

YIN, K. C., CHEN, D., BAKHTIAR, R. & VERCH, T. 2011. Evaluation of two ELISA methods to detect therapeutic anti-IGF1R antibodies in clinical study samples of dalotuzumab. *Bioanalysis,* 3**,** 2107-17.

YIN, X., LATIF, R., BAHN, R. & DAVIES, T. F. 2012. Genetic profiling in Graves' disease: further evidence for lack of a distinct genetic contribution to Graves' ophthalmopathy. *Thyroid,* 22**,** 730-6.

YIN, X., LATIF, R., BAHN, R., TOMER, Y. & DAVIES, T. F. 2008. Influence of the TSH receptor gene on susceptibility to Graves' disease and Graves' ophthalmopathy. *Thyroid,* 18**,** 1201-6.

YOUNG, D. A., EVANS, C. H. & SMITH, T. J. 1998. Leukoregulin induction of protein expression in human orbital fibroblasts: evidence for anatomical site-restricted cytokine-target cell interactions. *Proc Natl Acad Sci U S A,* 95**,** 8904-9.

ZAKARIJA, M., MCKENZIE, J. M. & EIDSON, M. S. 1990. Transient neonatal hypothyroidism: characterization of maternal antibodies to the thyrotropin receptor. *J Clin Endocrinol Metab,* 70**,** 1239-46.

ZELANTE, T., DE LUCA, A., BONIFAZI, P., MONTAGNOLI, C., BOZZA, S., MORETTI, S., BELLADONNA, M. L., VACCA, C., CONTE, C., MOSCI, P., BISTONI, F., PUCCETTI, P., KASTELEIN, R. A., KOPF, M. & ROMANI, L. 2007. IL-23 and the Th17 pathway promote inflammation and impair antifungal immune resistance. *Eur J Immunol,* 37**,** 2695-706.

ZHANG, J., HUANG, Z., SUN, R., TIAN, Z. & WEI, H. 2012. IFN-gamma induced by IL-12 administration prevents diabetes by inhibiting pathogenic IL-17 production in NOD mice. *J Autoimmun,* 38**,** 20-8.

ZHANG, L., BOWEN, T., GRENNAN-JONES, F., PADDON, C., GILES, P., WEBBER, J., STEADMAN, R. & LUDGATE, M. 2009. Thyrotropin receptor activation increases hyaluronan production in preadipocyte fibroblasts: contributory role in hyaluronan accumulation in thyroid dysfunction. *J Biol Chem,* 284**,** 26447-55.

ZHANG, L., GRENNAN-JONES, F., DRAMAN, M. S., LANE, C., MORRIS, D., DAYAN, C. M., TEE, A. R. & LUDGATE, M. 2014. Possible targets for nonimmunosuppressive therapy of graves' orbitopathy. *J Clin Endocrinol Metab,* 99**,** E1183-90.

ZHANG, M., TONG, K. P., FREMONT, V., CHEN, J., NARAYAN, P., PUETT, D., WEINTRAUB, B. D. & SZKUDLINSKI, M. W. 2000. The extracellular domain suppresses constitutive activity of the transmembrane domain of the human TSH receptor: implications for hormone-receptor interaction and antagonist design. *Endocrinology,* 141**,** 3514-7.

ZHANG, X., SUN, P., WANG, J., WANG, Q. & SONG, S. K. 2011. Diffusion tensor imaging detects retinal ganglion cell axon damage in the mouse model of optic nerve crush. *Invest Ophthalmol Vis Sci,* 52**,** 7001-6.

ZHAO, L. Q., WEI, R. L., CHENG, J. W., CAI, J. P. & LI, Y. 2010. The expression of intercellular adhesion molecule-1 induced by CD40-CD40L ligand signaling in orbital fibroblasts in patients with Graves' ophthalmopathy. *Invest Ophthalmol Vis Sci,* 51**,** 4652-60.

ZHAO, S.-X., TSUI, S., CHEUNG, A., DOUGLAS, R. S., SMITH, T. J. & BANGA, J. P. 2011. Orbital fibrosis in a mouse model of Graves' disease induced by genetic immunization of thyrotropin receptor cDNA. *Journal of Endocrinology,* 210**,** 369-377.

ZHENG, L., WANG, X., XU, L., WANG, N., CAI, P., LIANG, T. & HU, L. 2015. Foxp3 gene polymorphisms and haplotypes associate with susceptibility of Graves' disease in Chinese Han population. *Int Immunopharmacol,* 25**,** 425-431.

ZHOU, X., KONG, N., ZOU, H., BRAND, D., LI, X., LIU, Z. & ZHENG, S. G. 2011. Therapeutic potential of TGF-beta-induced CD4(+) Foxp3(+) regulatory T cells in autoimmune diseases. *Autoimmunity,* 44**,** 43-50.

ZHU, X. G., KANESHIGE, M., PARLOW, A. F., CHEN, E., HUNZIKER, R. D., MCDONALD, M. P. & CHENG, S. Y. 1999. Expression of the mutant thyroid hormone receptor PV in the pituitary of transgenic mice leads to weight reduction. *Thyroid,* 9**,** 1137-45.

ZIMMERMANN, M. B. & BOELAERT, K. 2015. Iodine deficiency and thyroid disorders. *Lancet Diabetes Endocrinol,* 3**,** 286-295.

Appendices

Appendix 1 Summary of individual immune mice in 4 groups of immunisations

Weeks after end of immunisation	Animal code	Immunisation Plasmid	*Thyroid histology	TSHR Abs	IGF-1R Abs	# Orbital histology	**IHC on orbital tissues	
							CD3	F4/80
6 Weeks (Group 1)	59/0	pTriEx-TSHR	hypo	TSBAbs	+ve	EOM	+	+
	59/L	pTriEx-TSHR	hypo	TSBAbs	-ve	EOM	+	+
	59/R	pTriEx-TSHR	hypo	TSBAbs	+ve	EOM	+	+
	59/2	pTriEx-TSHR	hyper	TSAbs	+ve	EOM	+	+
	60/0	pTriEx-TSHR	✝ hypo	TSAbs	ND	intense infiltration	+++	+
	60/L	pTriEx-TSHR	hypo	TSBAbs	+ve	adipose expansion	+	+
	60/R	pTriEx-TSHR	hypo	TSBAbs	+ve	EOM	+	+
	60/2	pTriEx-TSHR	hypo	TSBAbs	+ve	EOM	+	+
	61/0	pTriEx-IGF-1Rα	normal	None	+ve	normal	-	-
	61/L	pTriEx-IGF-1Rα	normal	None	+ve	normal	-	-
	61/R	pTriEx-IGF-1Rα	normal	None	+ve	normal	-	-
	62/0	pTriEx-β-Gal	normal	None	-ve	normal	-	-
	62/L	pTriEx-β-Gal	normal	None	-ve	normal	-	-
	62/R	pTriEx-β-Gal	normal	None	-ve	normal	-	-
longitudinal study, 9 Weeks (Group 2)	63/0	pTriEx-TSHR	hypo	TSBAbs	-ve	EOM	+	+
	63/L	pTriEx-TSHR	hyper	TSBAbs	-ve	EOM	+	+
	63/R	pTriEx-TSHR	hypo	TSBAbs	-ve	EOM	+	+
	63/2	pTriEx-TSHR	hyper	TSBAbs	-ve	EOM	+	+
	64/0	pTriEx-TSHR	hypo	TSBAbs	-ve	EOM	+	+
	64/L	pTriEx-TSHR	hypo	TSBAbs	-ve	adipose expansion	+	+
	64/R	pTriEx-TSHR	hypo	TSAbs	-ve	EOM	+	+
	64/2	pTriEx-TSHR	hypo	TSAbs	-ve	EOM	+	+
long term study, 15 Weeks (Group3)	57/0	pTriEx-TSHR	hypo	TSBAbs	-ve	Fibrosis/EOM	+	+
	57/L	pTriEx-TSHR	hypo	TSAbs	-ve	Fibrosis/EOM	+	+
	57/R	pTriEx-TSHR	hypo	TSBAbs	-ve	adipose expansion	+	+
	58/0	pTriEx-TSHR	hypo	TSBAbs	-ve	Fibrosis/EOM	+	+
	58/L	pTriEx-TSHR	normal	TSAbs	-ve	Fibrosis/EOM	+	+
	58/R	pTriEx-TSHR	hypo	TSBAbs	-ve	intense infiltration	+++	+
	56/0	pTriEx-IGF-1Rα	normal	None	+ve	normal	-	-
	56/L	pTriEx-IGF-1Rα	normal	None	+ve	normal	-	-
	56/R	pTriEx-IGF-1Rα	normal	None	+ve	normal	-	-
	55/0	pTriEx-β-Gal	normal	None	-ve	normal	-	-
	55/L	pTriEx-β-Gal	normal	None	-ve	normal	-	-
	55/R	pTriEx-β-Gal	normal	None	-ve	normal	-	-
mAbs study, 6 Weeks (Group 4)	65/0	pTriEx-TSHR	hypo	ND	-ve	EOM	+	+
	65/L	pTriEx-TSHR	normal	ND	-ve	EOM	+	+
	65/R	pTriEx-TSHR	hypo	ND	-ve	EOM	+	+
	65/2	pTriEx-TSHR	normal	ND	-ve	EOM	+	+
	66/0	pTriEx-TSHR	hypo	ND	-ve	EOM	+	+
	66/L	pTriEx-TSHR	hypo	ND	-ve	EOM	+	+
	66/R	pTriEx-TSHR	hypo	ND	-ve	EOM	+	+
	66/2	pTriEx-TSHR	hypo	ND	-ve	EOM	+	+

Appendix 2 Flow cytometry intra-assay and inter-assay CV

	Samples	Intra-assay CV Test 1	Intra-assay CV Test 2	Intra-assay CV Test 3	**Interassay CV**
1	1H7 mAb 1µl	8.16	9.12	8.18	**24.77**
2	1H7 mAb 0.3µl	7.43	8.43	8.03	**19.93**
3	1H7 mAb 0.1µl	7.17	8.79	6.95	**22.37**
	Total	**7.58**	**8.78**	**7.69**	

Appendix 3 Calculations for competition assay; displacement of LUMI-IGF-1 with unlabelled IGF-1

The plan was to make IGF-1 at 'double' the concentration and then mix with an equal volume of LUMI-IGF-1 at 'double' the concentration to achieve the final working concentrations of IGF-1 at 10^{-6}M and LUMI-IGF-1 at 5×10^5 RLU/µl.

LUMI-IGF-1

Stock $\quad\quad\quad$ 10^8 RLU/µl

Required $\quad\quad$ 10^6 RLU/µl (double working dilution)

So do 1:100 dilution of LUMI-IGF-1 at 10^8 RLU/µl in PBS/1% BSA to achieve 10^6 RLU/µl

IGF-1 (Molecular weight 7649 Daltons)

7649 g/L	1 M	
7.7 g/L	1 mM	10^{-3} M
7.7 mg/L	1 µM	10^{-6} M
7.7 µg/L	1 nM	10^{-9} M
7.7 ng/ml	1 nM	10^{-9} M

To make calculations easier, instead of working with 7.7 µg/ml, we decided to work with

10 µg/ml (10mg/L).

Stock solution of IGF-1 = 10 mg/ml or 1 mg/ml aliquots

Do 1:10 dilution of IGF-1 at 1 mg/ml in PBS/1% BSA to achieve 0.1 mg/ml = 100 µg/ml [a]

Take [a] and do 1:5 dilution in PBS/1% BSA to achieve 20 µg/ml = 2×10^{-6}M [b]

Take [b] and do 10 fold dilutions to achieve 2×10^{-7}–2×10^{-11}M

Finally, add equal volumes of LUMI-IGF-1 and IGF-1 to achieve: LUMI-IGF-1 at 5×10^5 RLU/µl and IGF-1 at 10^XM (where X is -11 to -6)

Appendix 4 Calculations for comparison of competition assay in this study with Weightman et al,1993

Cold IGF-1 cocentration:
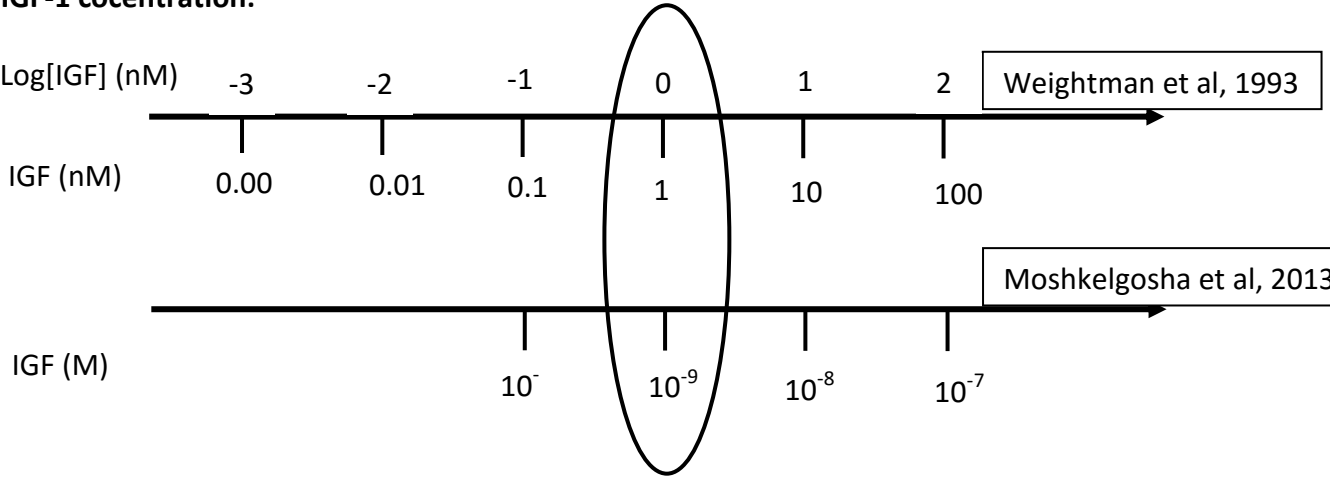
IGF concentration (M)	IGF concentration (nM)
10^{-7}	100
10^{-8}	10
10^{-9}	1
10^{-10}	0.1
10^{-11}	0.01
10^{-12}	0.001

Appendix 5 ELISA intra-assay and inter-assay CV

	Samples	Intra-assay CV Test 1	Intra-assay CV Test 2	Intra-assay CV Test 3	Intra-assay CV Test 4	Intra-assay CV Test 5	Inter-assay CV
1	E8/0	1.56	1.12	3.1	4.04	1.56	**4.77**
2	E8/L	1.46	1.43	1.03	1.37	1.46	**5.93**
3	E8/R	1.17	0.79	2.95	2.95	2.11	**3.37**
4	E8/2	6.13	4.22	3.84	4.53	4.96	**6.02**
5	E9/0	2.08	2.39	1.26	1.82	2.08	**5.28**
6	E9/L	0.88	0.49	2.43	1.83	1.28	**4.90**
7	E9/R	0.67	1.62	1.29	2.32	4.41	**4.61**
8	E9/02	4.07	1.47	2.40	0.39	1.07	**5.50**
9	E11/0	3.15	4.04	3.16	3.1	4.89	**4.12**
10	E11/L	1.03	1.83	0.53	1.56	1.03	**5.89**
11	E11/R	2.95	2.77	1.33	1.46	2.12	**4.64**
12	E11/2	3.84	2.53	4.17	3.17	4.50	**5.47**
13	E12/0	1.26	1.82	1.26	2.13	1.92	**4.67**
14	E12/L	2.43	1.03	2.43	2.08	3.14	**6.53**
15	E12/R	3.62	2.32	2.90	0.88	3.55	**6.36**
16	E12/2	4.40	3.79	5.21	3.67	2.58	**5.69**
	Total	**2.08**	**2.60**	**3.19**	**2.24**	**2.82**	

Appendix 6 Cutting Edge publication accompanied with "News and Views"

CUTTING EDGE

Cutting Edge: Retrobulbar Inflammation, Adipogenesis, and Acute Orbital Congestion in a Preclinical Female Mouse Model of Graves' Orbitopathy Induced by Thyrotropin Receptor Plasmid-in Vivo Electroporation

Sajad Moshkelgosha, Po-Wah So, Neil Deasy, Salvador Diaz-Cano, and J Paul Banga

Division of Diabetes and Nutritional Sciences (S.M., J.P.B.), King's College London School of Medicine, London, United Kingdom SE5 9NU; Preclinical Imaging Unit (P.-W.S.), Department of Neuroimaging, Department of Neuroradiology (N.D.), Institute of Psychiatry, King's College London, London, United Kingdom SE5 9NU; and King's College Hospital NHS Trust (S.D.-C.), Department of Pathology, London, United Kingdom SE5 9RS

Graves' orbitopathy (GO) is a complication in Graves' disease (GD) but mechanistic insights into pathogenesis remain unresolved, hampered by lack of animal model. The TSH receptor (TSHR) and perhaps IGF-1 receptor (IGF-1R) are considered relevant antigens. We show that genetic immunization of human TSHR (hTSHR) A-subunit plasmid leads to extensive remodeling of orbital tissue, recapitulating GO. Female BALB/c mice immunized with hTSHR A-subunit or control plasmids by in vivo muscle electroporation were evaluated for orbital remodeling by histopathology and magnetic resonance imaging (MRI). Antibodies to TSHR and IGF-1R were present in animals challenged with hTSHR A-subunit plasmid, with predominantly TSH blocking antibodies and were profoundly hypothyroid. Orbital pathology was characterized by interstitial inflammation of extraocular muscles with CD3+ T cells, F4/80+ macrophages, and mast cells, accompanied by glycosaminoglycan deposition with resultant separation of individual muscle fibers. Some animals showed heterogeneity in orbital pathology with 1) large infiltrate surrounding the optic nerve or 2) extensive adipogenesis with expansion of retrobulbar adipose tissue. A striking finding that underpins the new model were the in vivo MRI scans of mouse orbital region that provided clear and quantifiable evidence of orbital muscle hypertrophy with protrusion (proptosis) of the eye. Additionally, eyelid manifestations of chemosis, including dilated and congested orbital blood vessels, were visually apparent. Immunization with control plasmids failed to show any orbital pathology. Overall, these findings support TSHR as the pathogenic antigen in GO. Development of a new preclinical model will facilitate molecular investigations on GO and evaluation of new therapeutic interventions. (*Endocrinology* 154: 3008–3015, 2013)

Graves' disease (GD) is an antibody-mediated autoimmune condition targeting the TSH receptor (TSHR) in the thyroid gland resulting in hyperthyroidism (1). Antibodies to TSHR modulate thyroid function and are responsible for GD, with thyroid stimulating antibodies (TSAbs) and TSH stimulating blocking antibodies (TSBAbs), which stimulate or inhibit TSHR signaling, respectively. Antibodies to TSHR with neutral properties are also present, which may also induce receptor signaling (2). A complication of GD is the extrathyroidal condition of

News and Views: At Long Last, an Animal Model of Graves' Orbitopathy

Rebecca S. Bahn

Division of Endocrinology, Metabolism and Diabetes, Mayo Clinic, Rochester, Minnesota 55905

Patients with Graves' disease (GD) are classically hyperthyroid due to excess production of thyroid hormones. They often have a goiter and may experience weight loss, sensitivity to heat, tremor, and nervousness. Some 30% to 60% of these patients also have signs and symptoms of Graves' orbitopathy (GO; also termed Graves' ophthalmopathy or thyroid eye disease). Although the majority experience only mild eye irritation and redness, some 3% to 5% of GO patients suffer from more severe disease that presents variably as painful soft tissue swelling and redness of the eyes and lids, forward protrusion of the globes (proptosis), and/or debilitating double vision. Some patients risk sight loss due to compressive optic neuropathy or breakdown of the cornea. Orbital imaging generally shows extraocular muscle enlargement and, in some patients, increased orbital fat volume. The former is caused by deposition of hydrophilic glycosaminoglycans (GAGs) between the muscle fibers, and the latter develops as a result of de novo adipogenesis within the orbit. Also evident on histologic examination is an infiltration of mononuclear cells including predominately $CD4^+$ T cells with occasional populations of $CD8^+$ cells, B cells, and macrophages (1).

Although it is well known that the hyperthyroidism of GD is caused by stimulation of the TSH receptor (TSHR) on thyroid follicular cells by autoantibodies directed against the receptor (TSHR antibodies [TRAbs]), the pathogenesis of GO is less clear. The clinical observation that GO is frequently diagnosed concurrent with or shortly after the diagnosis of Graves' hyperthyroidism led early on to the concept that these conditions comprise a syndrome and share a common etiology. It wasn't, however, until after the cloning of TSHR that circulating TRAb could be reliably measured and the possible expression of TSHR within the orbit explored. Studies followed demonstrating that prognosis can be predicted from the TRAb level (2) and activity and severity assessed using a sensitive bioassay that detects IgG stimulation of TSHR in a reporter cell line (3). Although some patients with GO have never been hyperthyroid or may even be hypothyroid, very sensitive TRAb assays can measure circulating antibody in essentially all patients diagnosed with GO (4). The demonstration by several laboratories of TSHR expression in the orbit and specifically on orbital fibroblasts further connected the ocular and thyroidal manifestations of GD. In addition, in response to GD patients' IgGs or a monoclonal stimulatory TRAb, orbital fibroblasts differentiate into mature adipocytes (5) and produce excessive GAGs (6). Furthermore, these processes can be blocked using a small-molecule antagonist of TSHR activation (7). However, although these and other lines of circumstantial evidence supported a central role for TSHR in the pathogenesis of GO, confirmatory in vivo data were not available owing primarily to the lack of a spontaneous or inducible animal model of the disease.

Several animal models of the hyperthyroidism of GD have been developed over the past 2 decades using various vectors to deliver TSHR (8, 9). Although no convincing evidence of GO was reported in any of these models, in most, the orbits were not carefully examined. The earliest animal models involved conventional immunization with human TSHR protein expressed in bacteria or insect cells. Although antibodies reacting with the receptor were induced, the animals did not produce thyroid stimulating antibodies (TSAbs) or develop hyperthyroidism. In contrast, transient TSAb activity was measured in severe combined immunodeficient (SCID) mice engrafted with human Graves' thyroid tissue, with some also receiving

identity is achieved mainly by variation in the expression levels of a common set of miRNAs rather than by tissue-especific miRNA expression. We observed that mir-146b was by far the most highly overexpressed miRNA in thyroid tumors followed by mir-21, mir-221, mir-222 and mir-31 (in order of abundance). These miRNAs have been previously associated with thyroid cancer. Additionally, we observed at least four miRNAs consistently overexpressed in thyroid cancer and not previously described. Based on computational prediction of potential targets, we identify a set of miRNAs that target genes essential for thyroid differentiation such as NIS, TPO, TG, TSHR, PAX8 and TTF1. Among these miRNAs, we found mir-146b to have one of the best scores in the predictions. We validated mir-146b through functional studies using the differentiated rat thyroid follicular cells PCCl3 and MDCK cells stably transfected with human NIS. Mir-146b is strongly downregulated by TSH in PCCl3 and its expression is recovered by TGFbeta, a strong repressor of thyroid differentiation. We demonstrate that mir-146b binds to the 3'UTR of NIS, destabilizing the mRNA and leading to an impaired translation of the protein and subsequently decreasing the iodide uptake of the cells. In conclusion, our work expands the number of known microRNAs in thyroid cancer and highlights the importance of microRNAs in thyroid differentiation.

OP2 Young Investigators Session

OP07

LOW BIRTH WEIGHT IN CHILDREN BORN TO MOTHERS WITH HYPERTHYROIDISM AND HIGH BIRTH WEIGHT IN HYPOTHYROIDISM, WHEREAS PRETERM BIRTH IS COMMON IN BOTH CONDITIONS: A DANISH NATIONAL HOSPITAL STUDY OF 1,638,338 CHILDREN AND THEIR MOTHERS

Andersen SL[1], Olsen J[2], Wu CS[2], Laurberg P[1]
[1]Aalborg University Hospital, Department of Endocrinology, Aalborg, Denmark, [2]Aarhus University, Section for Epidemiology, Department of Public Health, Aarhus, Denmark

Objectives: Maternal hyper- and hypothyroidism have been associated with increased risk of adverse pregnancy outcomes, but studies have led to inconsistent results. We identified children born to mothers with a hospital recorded diagnosis of thyroid dysfunction in Denmark and studied the association with gestational age at delivery and birth weight of the child.

Methods: Population-based cohort study using Danish nationwide registers. All singleton live births in Denmark, 1978–2006, were identified and stratified by maternal first time diagnosis of hyper- or hypothyroidism registered in a Danish hospital after January 1, 1977 and before January 1, 2007. Information on gestational age at delivery and birth weight of the child was obtained from the Medical Birth Registry. Multivariate logistic regression models including potential confounders were used to estimate odds ratio (OR) with 95% confidence interval (95% CI).

Results: Maternal thyroid dysfunction was first time diagnosed before (n = 6,268), during (n = 2,503) or after (n = 24,038) the pregnancy in 2.0% of the singleton live births (n = 1,638,338). Maternal hyperthyroidism and hypothyroidism were associated with increased risk of preterm birth (hyperthyroidism: adjusted OR when diagnosed *before* 1.36 (95% CI 1.20–1.54), *during* 1.43 (1.14–1.79), *after* 1.17 (1.09–1.25) the pregnancy, hypothyroid-

OP08

GRAVES' ORBITOPATHY IN MICE WITH THYROTROPIN RECEPTOR PLASMID ELECTROPORATION, CHARACTERISED BY RETROBULBAR INFLAMMATION, ADIPOGENESIS, FIBROSIS AND OCULAR MANIFESTATIONS OF ACUTE CONGESTIVE OPHTHALMOPATHY

Moshkelgosha S[1], So P-W[2], Deasy N[3], Diaz-Cano S[4], Banga JP[1]
[1]King's College London School of Medicine, Diabetes and Endocrinology, London, UK, [2]King's College London School of Medicine, Institute of Psychiatry, Preclinical Imaging Unit, London, UK, [3]Institute of Psychiatry, Neuroradiology, London, UK, [4]King's College Hospital NHS Trust, Pathology, London, UK

Objectives: Graves' orbitopathy (GO) is a complication in Graves' disease (GD), but the nature of autoantigen(s) and mechanistic insights into pathogenesis remain unresolved, hampered by lack of an animal model. The thyrotropin receptor (TSHR) is considered likely primary antigen, with insulin growth factor-1 receptor 1 (IGF-1R) as second relevant antigen. While experimental models of GD induced by genetic delivery of TSHR are well established, all models universally fail in remodelling of orbital tissues. Following our studies on experimental GD, we show modulation of genetic delivery of TSHR provides a faithful model of human GO.

Methods: Genetic immunisation of BALB/c mice with hTSHR A-subunit (n = 22) or control plasmids (n = 12) by *in-vivo* muscle electroporation. Immune animals evaluated for immunological, thyroid function and orbital histology and small animal Magnetic Resonance Imaging (MRI).

Results: Antibodies to TSHR detected in all animals challenged with hTSHR A-subunit. Surprisingly, thyroid stimulating blocking antibodies dominate, with established hypothyroidism confirmed by depressed serum T4, significant weight gain and thyroid histology. Two types of orbital pathology (i) inflammation around optic nerve and orbital muscle, characterised by infiltration of CD3+ T cells and F4/80+ macrophages in extraocular muscles, accompanied by extensive fibrosis and hyaluronan deposition, extending into the muscle isolating individual fibers and (ii) adipogenesis, characterised by expansion of retrobulbar adipose tissue. Antibodies to IGF-1R were detectable by ELISA and flow cytometry. MRI showed clear evidence of orbital muscle hypertrophy. Importantly, manifestations characteristic of orbital congestion associated with orbitopathy were apparent, which appear to resolve spontaneously with time.

Conclusions: Data provides unambiguous evidence for TSHR as pathogenic antigen in GO. Histopathological findings reproduce those reported in human GO, including disease heterogeneity. Development of new model will facilitate studies on inflammatory T cells, cytokines and role of antibodies to TSHR and IGF-1R in GO pathology and for evaluating new therapeutic interventions.

OP09

MATERNAL HYPOTHYROXINEMIA AND TPO ANTIBODIES, BUT NOT HIGH TSH LEVELS, ARE RISK FACTORS FOR PREMATURITY: THE GENERATION R STUDY

Korevaar TIM[1], Medici M[1], de Rijke YB[2], Visser W[3], de Muinck Keizer-Schrama SMPF[4], Jaddoe VWV[4], Hofman A[4], Visser WE[1], Hooijkaas H[5], Steegers EAP[3], Tiemeier H[4], Bongers-Schokking JJ[4], Visser TJ[1], Peeters RP[1]
[1]Erasmus Medical Center, Endocrinology, Rotterdam, Netherlands

Appendix 8 Young Investigator Award certificate, 37th ETA conference 2013, Lieden, The Netherlands

http://www.eta2013.org/_downloads/Prize-Winners-2013.pdf